

THEORETICAL INVESTIGATION OF UNIMOLECULAR REACTIONS OF
CYCLIC C₃H₆ COMPOUNDS BY AB INITIO QUANTUM CHEMICAL
METHODS

A THESIS SUBMITTED TO
THE GRADUATE SCHOOL OF NATURAL AND APPLIED SCIENCES
OF
MIDDLE EAST TECHNICAL UNIVERSITY

BY

ARMAĞAN KINAL

IN PARTIAL FULFILLMENT OF THE REQUIREMENTS FOR THE DEGREE OF
DOCTOR OF PHILOSOPHY

IN
DEPARTMENT OF CHEMISTRY

JULY 2004

Approval of the Graduate School of Natural and Applied Sciences

Prof. Dr. Canan ÖZGEN
Director

I certify that this thesis satisfies all the requirements as a thesis for the degree of
Doctor of Philosophy.

Prof. Dr. Hüseyin İŞÇİ
Head of Chemistry Department

This is to certify that we have read this thesis and that in our opinion it is fully
adequate, in scope and quality, as a thesis for the degree of Doctor of Philosophy.

Prof. Dr. Metin BALCI
Co-Supervisor

Prof. Dr. İlker ÖZKAN
Supervisor

Examining Committee Members

| | | |
|---------------------------|--------|-------|
| Prof. Dr. Ersin YURTSEVER | KOÇ U. | _____ |
| Prof. Dr. İlker ÖZKAN | METU | _____ |
| Prof. Dr. Metin BALCI | METU | _____ |
| Prof. Dr. Şakir ERKOÇ | METU | _____ |
| Prof. Dr. Ali GÖKMEN | METU | _____ |

I hereby declare that all information in this document has been obtained and presented in accordance with academic rules and ethical conduct. I also declare that, as required by these rules and conduct, I have fully cited and referenced all material and results that are not original to this work.

Name, Last name : Armağan KINAL

Signature :

ABSTRACT

THEORETICAL INVESTIGATION OF UNIMOLECULAR REACTIONS OF CYCLIC C₅H₆ COMPOUNDS BY AB INITIO QUANTUM CHEMICAL METHODS

KINAL, Armağan

Ph.D., Department of Chemistry

Supervisor: Prof. Dr. İlker Özkan

Co-Advisor: Prof. Dr. Metin Balcı

July 2004, 158 pages

Thermodynamic stabilities of eighteen cyclic C₅H₆ isomers were explored computationally both on singlet and triplet state potential energy surfaces (PES). All isomers have singlet ground states except for bicyclo[2.1.0]pent-5-ylidene (**B5**) having no stable geometry on the singlet C₅H₆ PES. Cyclopenta-1,3-diene (**M1**) is the most stable cyclic C₅H₆ isomer while cyclopent-1,4-diylidene is the least stable one among all. Cyclopenta-1,2-diene (**M2**) and cyclopentyne (**M3**) have biradical characters of 46.9 and 21.5%, respectively.

Seven unimolecular isomerization reactions occurring among several of these molecules were investigated by DFT and ab initio methods. The conversion of bicyclo[2.1.0]pent-2-ene (**B1**) and tricyclo[2.1.0.0^{2,5}]-pentane (**T1**) into 1,3-

cyclopentadiene (**M1**) are shown to be concerted processes whose reaction paths pass through TSs with a high degree of biradical character. The reaction enthalpies (ΔH_0) are predicted to be -47.7 kcal/mol for **B1** and -63.8 kcal/mol for **T1** at UB3LYP/6-31G(d) level. The activation enthalpy (ΔH_0^\ddagger) for the ring opening of **B1** was calculated by the CR-CCSD(T) method to be 25.2 kcal/mol, in good agreement with experiment. Furthermore, the ΔH_0^\ddagger for the ring opening of **T1** was obtained by the CR-CCSD(T) method to be 48.2 kcal/mol. The self-conversion of **M1** via 1,5-hydrogen shift is a facile and concerted reaction with aromatic TS. The ΔH_0^\ddagger estimations of B3LYP and CC methods are 25.24 and 28.78 kcal/mol, respectively. For 1,2-hydrogen shift reactions of cyclopent-3-enylidene (**M4**) and cyclopenten-2-ylidene (**M5**), the single point CC calculations predicted the ΔH_0^\ddagger values of 3.13 and 10.12 kcal/mol, as well as, the ΔH_0 values of -71.28 and -64.05 kcal/mol, respectively. The reason of **M5** being more stable than **M4** is due to the conjugation of the carbene carbon and the double bond in **M5**. The reaction path of cyclobutylidene methylene to cyclopentyne rearrangement is found to be rather shallow. The ΔH_0^\ddagger and ΔH_0 values predicted by the RCCSD(T) method to be 3.65 and -5.72 kcal/mol, respectively. Finally, triplet state isomerization of bicyclo[2.1.0]pent-5-ylidene to cyclopenta-1,2-diene, as well as, its parent reaction, cyclopropylidene to 1,2-propadiene were investigated at several levels of theory including DFT, CASSCF and CC methods. The UCCSD(T) method estimated a moderate barrier whose value is 8.12 kcal/mol for the isomerization of $^3\text{B5}$ with the reaction enthalpy of -44.63 kcal/mol.

Keywords: Cyclic C_5H_6 Compounds, Singlet and Triplet Potential Energy Surfaces (PES), Transition State Structure (TS), Unimolecular Rearrangements, Hydrogen Shift Reactions, Density functional theory (DFT).

ÖZ

HALKALI C₅H₆ BİLEŞİKLERİNİN ÜNİMOLKÜLER REAKSİYONLARININ AB İNİTIO KUANTUM KİMYASAL YÖNTEMLERLE TEORİK ÇALIŞMASI

KINAL, Armağan

Doktora, Kimya Bölümü

Tez Yöneticisi: Prof. Dr. İlker Özkan

Ortak Tez Yöneticisi: Prof. Dr. Metin Balcı

Temmuz 2004, 158 sayfa

Halkalı C₅H₆ izomerlerinden onsekizinin termodinamik kararlılıkları tekli (S=0) ve üçlü hal (S=1) potansiyel enerji yüzeylerinde hesapsal olarak araştırıldı. Tekli C₅H₆ potansiyel enerji yüzeyinde kararlı bir yapıya sahip olmayan bisiklo[2.1.0]pent-5-yiliden (**B5**) hariç, tüm izomerlerin temel halleri teklidir. Tüm izomerlerin içinde, en kararlı izomer siklopenta-1,3-dien (**M1**) iken en kararsız izomer siklopent-1,4-diyiliden'dir. Siklopenta-1,2-dien (**M2**) ve siklopentin (**M3**) sırasıyla % 46.9 ve % 21.5 çift radikalik karaktere sahiptir.

Bu moleküllerden bazıları arasında meydana gelen yedi ünimoleküler izomerleşme tepkimesi yoğunluk fonksiyon teorisi (DFT) ve ab initio metotlar kullanılarak incelendi. Bisiklo[2.1.0]pent-2-en (**B1**) ve trisiklo[2.1.0.0^{2,5}]pentan'ın

(**T1**) siklopentadien' e (**M1**) dönüşümleri “concerted” tepkimeler olduğu ve her ikisinin de yüksek biradikalik karakterli geçiş hali yapılarından geçtikleri gösterilmiştir. UB3LYP/6-31G(d) seviyesinde, reaksiyon entalpileri **B1** için -47.7 kcal/mol **T1** için -63.8 kcal/mol olarak bulundu. **B1**'in halka açılma aktifleşme entalpisi CR-CCSD(T) metodu ile 25.2 kcal/mol olarak hesaplandı ve bu değerin deneysel değer ile uyum içerisinde olduğu görüldü. Ek olarak, **T1**'in halka açılması aktifleşme entalpisi CR-CCSD(T) metodu ile 48.2 kcal/mol olarak hesaplandı. 1,5-Hidrojen kayması yoluyla **M1**'in kendine dönüşümü aromatik bir geçiş hal yapısına sahip, kolay ve “concerted” bir tepkimedir. B3LYP ve CC metotlarının aktifleşme enerjisi bulguları sırasıyla 25.24 and 28.78 kcal/mol'dür. 3-Siklopenteniliden (**M4**) ve 2-siklopenteniliden' in(**M5**) 1,2-hidrojen kayma tepkimeleri için, ΔH_0^\ddagger değerleri CC metodu sırasıyla 3.13 and 10.12 kcal/mol ve ΔH_0 değerlerini ise -71.28 and -64.05 kcal/mol olarak hesaplamıştır. **M5** izomerinin **M4**'den daha kararlı olmasının sebebi **M5**'deki çift bağ ile karben karbonu arasındaki konjugasyondur. Siklobütilden metilenin siklopentine dönüşmesinin reaksiyon yolu oldukça sık olarak bulunmuştur. RCCSD(T) metodu aracılığı ile bu reaksiyonun ΔH_0^\ddagger and ΔH_0 değerlerini sırasıyla 3.65 ve -5.72 kcal/mol olarak belirlendi. Son olarak, bisiklo[2.1.0]pent-5-yilidenin üçlü durumda ve siklopropilidenin 1,2-propadiene üçlü durumda izomerleşmeleri; DFT, CASSCF ve CC metotlarını içeren çeşitli seviyelerde araştırıldı. UCCSD(T) metodu, reaksiyon entalpisini -44.63 kcal/mol olarak belirlediği **³B5** molekülünün izomerleşmesinin 8.12 kcal/mol'ük ortalama bir bariyere sahip olduğunu tahmin etmiştir.

Anahtar Kelimeler: Halkalı C_5H_6 Bileşikleri, Tekli ve Üçlü Hal Potansiyel Enerji Yüzeyleri (PES), Geçiş Hal Yapısı (TS), Ünimoleküler Dönüşümler, Hidrojen Kayma Reaksiyonları, Yoğunluk Fonksiyoneli Teorisi (DFT).

*to Sanem, my dear wife
and
to Fikri Kerem, my lovely son*

ACKNOWLEDGEMENTS

I would like to express my sincere appreciation to Prof. Dr. İlker ÖZKAN for his continuous advice, criticism, support and guidance throughout the research.

I would like to thank to Prof. Dr. Metin BALCI for his helps, suggestions and comments.

I would like to thank to Assoc. Prof. Dr. Metin ZORA for his helps and moral support.

I would like to thank to my wife, Sanem Ezgi KINAL, and whole KINAL and BİLGİN families for their ceaseless helps and moral support. I owe them a great deal.

Finally, I would like to thank all old and new my roommates, Nevin ÖKSÜZ, M. Fatih DANIŞMAN, Mehrdad GHOLAMI and Yavuz DEDE for their moral support.

TABLE OF CONTENTS

| | |
|--|-------|
| ABSTRACT..... | iv |
| ÖZ..... | vi |
| ACKNOWLEDGMENTS..... | ix |
| TABLE OF CONTENTS..... | x |
| LIST OF TABLES..... | xii |
| LIST OF FIGURES..... | xv |
| LIST OF ABBREVIATIONS | xviii |
| CHAPTER | |
| 1. INTRODUCTION..... | 1 |
| 2. THEORETICAL CALCULATION METHODS | 12 |
| 2.1. Introduction..... | 12 |
| 2.2. The Schrödinger Equation | 13 |
| 2.2.1. The Born-Oppenheimer Approximation..... | 14 |
| 2.3. The Hartree-Fock Theory | 15 |
| 2.3.1. Restricted and Unrestricted Hartree-Fock Wave Functions..... | 19 |
| 2.4. The Basis Set Approximation | 20 |
| 2.4.1. Classification and types of basis sets..... | 21 |
| 2.5. Electron Correlation Methods | 24 |
| 2.5.1. Configuration Interaction (CI)..... | 25 |
| 2.5.2. Multi-configuration Self-consistent Field (MCSCF) Theory..... | 26 |
| 2.5.2.1. Complete Active Space SCF theory (CASSCF)..... | 27 |
| 2.5.3. Many Body Perturbation Theory (MBPT)..... | 28 |
| 2.5.3.1. Møller Plesset Perturbation Theory | 29 |
| 2.5.4. Coupled Cluster (CC) Theory | 31 |
| 2.5.5. Density Functional Theory (DFT) | 32 |

| | |
|--|-----|
| 2.5.5.1. Local spin density approximation (LSDA) | 34 |
| 2.5.5.2. Generalized gradient approximation (GGA) | 35 |
| 2.5.5.3. Hybrid methods..... | 35 |
| 2.5.6. The Computational Chemistry Suites Employed | 36 |
| 3. RESULTS AND DISCUSSION | 37 |
| 3.1. Stable Cyclic C ₅ H ₆ Structures | 38 |
| 3.1.1. Minima on Singlet and Triplet Potential Energy Surfaces of C ₅ H ₆ | 38 |
| 3.2. Unimolecular rearrangements of several cyclic C ₅ H ₆ isomers | 54 |
| 3.2.1. Isomerizations of Bicyclo[2.1.0]pent-2-ene and Tricyclo[2.1.0.0 ^{2,5}]- pentane into Cyclopenta-1,3-diene | 54 |
| 3.2.2. 1,5-Sigmatropic Hydrogen Shift Reaction of Cyclopentadiene (M1) | 66 |
| 3.2.3. 1,2-Hydrogen Shift Reactions of 3-cyclopentenylidene (M4) and 2- cyclopentenylidene (M5) yielding cyclopentadiene (M1) | 69 |
| 3.2.4. Formation of Cyclopentyne (M3) from cyclobutylidenemethylene (M7) .. | 74 |
| 3.2.5. Triplet State Isomerization of Bicyclo[2.1.0]pent-5-ylidene (B5) to cyclopenta-1,2-diene (M2) | 84 |
| 4. CONCLUSION | 93 |
| REFERENCES..... | 97 |
| APPENDICES | |
| A. Electronic Energies of All Stable and Transition State Structures..... | 107 |
| B. Cartesian Coordinates of All Stable Isomers..... | 111 |
| C. Cartesian Coordinates of TS Structures..... | 147 |
| CURICULUM VITAE..... | 157 |

LIST OF TABLES

| | |
|---|----|
| Table 1.1 The IUPAC nomenclature and the nature of the cyclic C ₅ H ₆ isomers. | 3 |
| Table 2.1 Common <i>k-nm/G</i> type basis sets and their representations. | 23 |
| Table 2.2 Acronyms for some popular functionals in DFT..... | 35 |
| Table 3.1 Energies and ZPVE ^a (in kcal/mol) relative to those of singlet cyclopenta-1,3-diene (¹ M1), <S ² > values, point group symmetries, electronic states and configurations of singlet states of all isomers at (U)B3LYP/cc-pVTZ level. Last column includes the vertical S-T energy splittings, $\Delta E_{S-T}^{ver} = E_{Triplet} - E_{Singlet}$, at singlet geometries. | 39 |
| Table 3.2 Energies and ZPVE ^a (in kcal/mol) relative to those of singlet cyclopenta-1,3-diene (¹ M1), <S ² > values, point group symmetries, electronic states and electronic configurations of triplet states of all isomers at UB3LYP/cc-pVTZ level. Last column includes the adiabatic S-T energy splittings, ΔE_{S-T} | 39 |
| Table 3.3 Energies and ZPVE ^a (in kcal/mol) relative to those of singlet cyclopenta-1,3-diene (¹ M1), point group symmetries, electronic states and configurations of singlet states of all isomers at CASSCF(4,4)/6-31G(d) level. Last column includes the vertical S-T energy splittings, $\Delta E_{S-T}^{ver} = E_{Triplet} - E_{Singlet}$, at singlet optimized geometries. | 40 |
| Table 3.4 Energies and ZPVE ^a (in kcal/mol) relative to those of singlet cyclopenta-1,3-diene (¹ M1), point group symmetries, electronic states and electronic configurations of triplet states of all isomers at CASSCF(4,4)/6-31G(d) level. Last column includes the adiabatic S-T energy splittings, ΔE_{S-T} | 40 |
| Table 3.5 Occupation numbers (n _i) of natural orbitals in each active space and percent biradical characters (BR%) for M2 – M6 at CASSCF(4,4)/6-311G(d,p) level. | 53 |

| | |
|--|----|
| Table 3.6 Vertical Singlet-Triplet State Energy Differences, ΔE_{S-T}^{ver} , of M2 – M6 in kcal/mol | 53 |
| Table 3.7 Electronic ^a and zero-point vibrational energies ^b (kcal/mol) of various species relative to M1 calculated by different methods using the 6-31G(d) basis set..... | 57 |
| Table 3.8 Correlation energies of various species at (U)B3LYP/6-3G(d) optimized structures as predicted by the ab initio methods ^a | 60 |
| Table 3.9 Relative ^a correlation energies (kcal/mol) of various species at (U)B3LYP/6-31G(d) optimized geometries predicted by different methods.... | 60 |
| Table 3.10 Activation and reaction energies (kcal/mol) for the rearrangement of B1 into M1 at 0 K at different levels of theory using the 6-31G(d) basis set | 61 |
| Table 3.11 Activation and reaction energies (kcal/mol) for the rearrangement of T1 into M1 at 0 K at different levels of theory using the 6-31G(d) basis set | 61 |
| Table 3.12 Vertical singlet-triplet splitting energies ^a in kcal/mol, and spin contaminations ($\langle S^2 \rangle$ for singlets in parentheses) in DFT methods of the transition structures | 62 |
| Table 3.13 CAS88 ^a Mulliken Effectively Unpaired Electron Populations and Biradical Indices ^{b,c} | 63 |
| Table 3.14 Electronic ^a and zero-point vibrational energies ^b (kcal/mol) of the species involved in the 1,5-H shift reaction relative to M1. | 67 |
| Table 3.15 Activation and reaction enthalpies (kcal/mol) of the 1,5-H shift reaction of cyclopentadiene Electronic ^a and zero-point vibrational energies ^b (kcal/mol) of the species involved in the 1,5-H shift reaction relative to M1. | 67 |
| Table 3.16 Electronic and zero point vibrational energies (kcal/mol) of M4, M5, [TS_M4-M1] and [TS_M5-M1] relative to the energy (Hartrees) and ZPVE of M1 calculated at different levels of theory. ZPVEs are given in parenthesis.... | 71 |
| Table 3.17 Activation barriers and reaction enthalpies at absolute zero for 1,2-hydrogen shift reactions of M4 and M5 calculated with DFT and RCCSD(T) methods..... | 71 |
| Table 3.18 Electronic and zero point vibrational energies (kcal/mol) of M3, [TS_M7-M3], [TS_inv_M7-M7'] and [TS_inv_M3-M3'] relative to the energy | |

| | |
|--|----|
| (Hartrees) and ZPVE of M7 calculated at different levels of theory. ZPVEs are given in parenthesis. | 79 |
| Table 3.19 Activation barriers and reaction enthalpies at absolute zero for the M7 to M3 rearrangement calculated at various levels of theory..... | 80 |
| Table 3.20 Vertical S – T energy differences, ΔE_{S-T}^{ver} , and $\langle S^2 \rangle$ values (in parenthesis) obtained from UB3LYP calculations for all species involved in the reaction... | 81 |
| Table 3.21 Electronic and zero point vibrational energies (kcal/mol) of $^3\text{M2}$, $^3[\text{TS_B5-M2}]$ relative to the energy (Hartrees) and ZPVE of $^3\text{B2}$ calculated at different levels of theory. ZPVEs are given in parenthesis. | 87 |
| Table 3.22 Electronic and zero point vibrational energies (kcal/mol) of ^3ppd and $^3[\text{TS_cppy-ppd}]$ relative to the energy (Hartrees) and ZPVE of $^3\text{cppy}$ calculated at different levels of theory. ZPVEs are given in parenthesis..... | 87 |
| Table 3.23 Activation barriers and reaction enthalpies at absolute zero for the $^3\text{B5}$ to $^3\text{M2}$ rearrangement calculated with various methods. | 88 |
| Table 3.24 Activation barriers and reaction enthalpies at absolute zero for the $^3\text{cppy}$ to ^3ppd rearrangement calculated with DFT and CCSD(T) methods..... | 88 |

LIST OF FIGURES

| | |
|---|----|
| Figure 1.1 Structures of the cyclic C ₅ H ₆ isomers constituting the scope of this thesis. The molecules starting with M, B and T letters are monocyclic, bicyclic and tricyclic structures, respectively..... | 2 |
| Figure 1.2 Geometrical structure and π molecular orbital diagram of cyclopentadiene..... | 5 |
| Figure 1.3 The Diels-Alder reaction between cyclopenta-1,3-diene and ethylene..... | 5 |
| Figure 1.4 (a) chiral, (b) diradical singlet, (c) diradical triplet and (d) zwitterionic, states of 1,2-cyclopentadiene | 6 |
| Figure 1.5 Reaction of atomic carbon with cyclobutene resulting isomer M2..... | 7 |
| Figure 1.6 Synthesis mechanism of tricyclo[2.1.0.0 ^{1,3}]pentane (T3)..... | 10 |
| Figure 3.1 Relative energies of all singlet state isomers at (U)B3LYP/cc-pVTZ level. | 41 |
| Figure 3.2 The vertical (ΔE_{S-T}^{ver}) and adiabatic (ΔE_{S-T}) S–T energy separations of all isomers at (U)B3LYP/cc-pVTZ level. | 41 |
| Figure 3.3 Geometrical parameters of cyclopenta-1,3-diene (M1) in both singlet and triplet (in parenthesis) states at RB3LYP/cc-pVTZ level..... | 42 |
| Figure 3.4 Ground state geometrical parameters of 3-methylenecyclobutene (M8) at RB3LYP/cc-pVTZ level. The values in square brackets belong to ref [34] | 43 |
| Figure 3.5 Selected triplet state geometrical parameters of bicyclo[2.1.0]pent-2-ene (B1) found at UHF/6-31G*, UMP2/6-31G* (bold face) and CASSCF(4,4)/6-31G* (in square brackets) levels. | 44 |
| Figure 3.6 Selected ground state geometrical parameters of [1.1.1]propellane (T2) found at (U)B3LYP/cc-pVTZ level. The experimental values [] are given in square brackets. | 45 |

| | |
|--|----|
| Figure 3.7 Selected singlet and triplet state geometrical parameters of cyclopenta-1,2-diene (M2) found at (U)B3LYP/cc-pVTZ level. | 46 |
| Figure 3.8 Selected singlet and triplet state geometrical parameters of spiropentene (B7) found at (U)B3LYP/cc-pVTZ level. The schematic representation of ³ B7 is also shown. | 47 |
| Figure 3.9 Selected singlet and triplet state geometrical parameters of tricyclo[2.1.1.0 ^{1,3}]pentane (T3) found at (U)B3LYP/cc-pVTZ level. The parameters in parenthesis belong to the TS structure of T3 to M4 isomerization optimized at UMP2/6-31G(d) level [61]. The values in square brackets are also taken from ref. [61]. | 49 |
| Figure 3.10 Selected singlet and triplet state geometrical parameters of bicyclo[2.1.0]pent-1(4)-ene (B2) found at (U)B3LYP/cc-pVTZ level. | 51 |
| Figure 3.11 Schematic representation of conversions of B1 and T1 into M1. | 55 |
| Figure 3.12 Selected interatomic distances (Å), points groups and electronic states shown in Figure 3.11. The uppermost values refer to UB3LYP geometry. The corresponding CAS88 values are indicated in parentheses, and the experimental values (when available) are shown in square brackets (ref [39] for B1, ref [] for M1). | 58 |
| Figure 3.13 Qualitative behavior of the minimum energy path in the isomerization of T1, showing the intersystem crossing. | 64 |
| Figure 3.14 1,5-sigmatropic hydrogen shift in cyclopentadiene. | 66 |
| Figure 3.15 Selected geometrical parameters of [TS_M1-M1] optimized by RB3LYP method. | 68 |
| Figure 3.16 Reaction of 1,1-dibromo-2-vinyl-cyclopropane with methyllithium yielding cyclopenta-1,3-diene and penta-1,2,4-triene. | 69 |
| Figure 3.17 Reaction of 1,1-dibromo-2-vinyl-cyclopropane with methyllithium yielding cyclopenta-1,3-diene via (path A) M4 and (path B) M5 intermediates. | 70 |
| Figure 3.18 Selected geometrical parameters of M4, [TS_M4-M1], M5 and [TS_M5-M1] obtained by DFT optimizations. | 73 |
| Figure 3.19 The proposed synthesis mechanism of cyclopentyne from different cyclobutane derivatives. | 75 |

| | |
|---|----|
| Figure 3.20 Schematic representation of M7 to M3 path resulted in UB3LYP method. | 78 |
| Figure 3.21 Schematic representation of M7 to M3 path resulted in CAS66 method. | 78 |
| Figure 3.22 Selected geometrical parameters of all stationary points on M7 to M3 path optimized by CASSCF/6-31G(d) level. | 82 |
| Figure 3.23 Selected geometrical parameters of all stationary points on M7 to M3 path optimized by (U)B3LYP/6-31G(d) level. | 83 |
| Figure 3.24 The structures of bicyclo[2.1.0]pent-5-ylidene (B5), 1,2-cyclopentadiene (M2), cyclopropylidene (cppy) and 1,2-propadiene (ppd). | 84 |
| Figure 3.25 The proposed mechanism for synthesis of 1,2-cyclohexadiene. | 85 |
| Figure 3.26 Selected geometrical parameters for ³ B5, ³ M2 and ³ [TS_B5-M2] geometries optimized by DFT and CASSCF methods. | 89 |
| Figure 3.27 Selected geometrical parameters for ³ cppy, ³ ppd and ³ [TS_cppy-ppd] geometries optimized by UB3LYP method. | 89 |
| Figure 3.28 IRC pathway of ³ B5 to ³ M2 isomerization calculated at UB3LYP/6-31G(d) level. | 91 |

LIST OF ABBREVIATIONS

| | |
|-----------------------|---|
| ΔH_f^0 | Standard enthalpy of formation |
| ΔH_f^{298} | Enthalpy of formation at 298 K |
| ΔH_0 | Reaction enthalpy at 0 K |
| ΔH_0^\ddagger | Activation enthalpy at 0 K |
| (U) | Unrestricted methodology where necessary otherwise restricted methodology |
| $\langle S^2 \rangle$ | Average value of S^2 operator |
| Å | Angstrom |
| AO | Atomic orbital |
| B3LYP | Becke' s three parameter exchange hybrid functional with Lee, Yang, Parr (LYP) correlation functional |
| BR | Jensen' s biradical index |
| BR% | Percent biradical character |
| CASnm | n-electron m-orbital complete active space self consistent field theory |
| CASnm-MP2 | Single-state multireference Moller-Plesset second-order perturbation theory based on CASnm wave function |
| CASSCF | Complete active space self consistent field theory |
| CC | Coupled cluster theory |
| CCSD(T) | Coupled cluster theory with single and double excitations and noniterative inclusion of triples |
| CGTO | Contracted gaussian type orbital |
| CI | Configuration interaction |
| CISD(T) | Configuration interaction with single and double excitations and noniterative inclusion of triples |
| CR-CCSD(T) | Completely renormalized coupled cluster theory with single and double excitations and noniterative inclusion of triples |

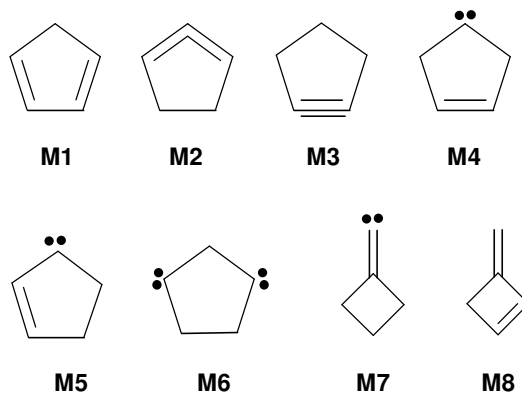
| | |
|------------------------|--|
| CSF | Configuration state function |
| ΔE_{S-T} | Adiabatic singlet - triplet energy difference |
| ΔE_{S-T}^{ver} | Vertical singlet - triplet energy difference |
| DFT | Density functional theory |
| FORS | Full optimized reaction space |
| GTO | Gaussian type orbital |
| HF | Hartree-Fock theory |
| HOMO | Highest occupied molecular orbital |
| IRC | Intrinsic reaction coordinate |
| LUMO | Lowest unoccupied molecular orbital |
| MBPT | Many body perturbation theory |
| MCSCF | Multi-configurational self consistent field theory |
| MO | Molecular orbital |
| MPn | Mollet-Plesset n th order perturbation theory |
| NMR | Nuclear magnetic resonance spectroscopy |
| PES | Potential energy surface |
| PGTO | Primitive gaussian type orbital |
| ψ | Wave function (state function) |
| PT | Perturbation theory |
| rxn | Reaction coordinate |
| STO | Slater type orbital |
| TS | Transition state structure |
| ZPVE | Zero point vibrational energy |

CHAPTER I

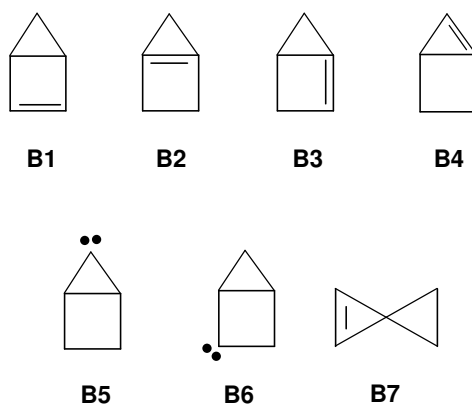
INTRODUCTION

A fundamental goal in both the experimental and theoretical chemistry has been the search for ultimate restrictions in the geometrical structures of hydrocarbons. A challenging problem in this respect is the stability of small-sized ring structures. Such a compound has generally low thermodynamic stability and high reactivity due to its inherent strain. These types of structures are called reactive intermediates. Identification of such compounds either includes indirect methods or requires rather sophisticated techniques, in other words, they are either trapped with other reagents in the reaction medium or identified with spectroscopic methods before decomposition. Computational investigations of reactive intermediates are most of the time preferable because of saving time and money. In this thesis, we are interested in several mono-, bi- and tricyclic isomers having C_5H_6 chemical formula that contain alkene, diene, alkyne, allene and carbene units (Figure 1.1). The most prominent and common feature of these structures is their strain caused by small ring size and incomplete valence. Accordingly, ten of these isomers have been stated as the reactive intermediates in the previous studies and five of them are only hypothetical compounds, whose existences are unknown. Only three isomers are relatively stable so that they can be isolated in appreciable amounts. The IUPAC nomenclature and the nature of these isomers are listed in Table 1.1.

Monocyclic C_5H_6 isomers



Bicyclic C_5H_6 isomers



Tricyclic C_5H_6 isomers

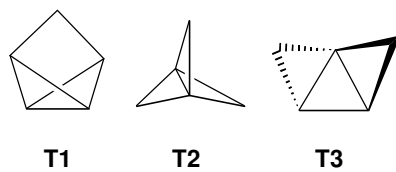


Figure 1.1 Structures of the cyclic C_5H_6 isomers constituting the scope of this thesis. The molecules starting with M, B and T letters are monocyclic, bicyclic and tricyclic structures, respectively.

Table 1.1 The IUPAC nomenclature and the nature of the cyclic C₅H₆ isomers.

| Isomer | IUPAC Name | Nature | ΔH_f^0 (kcal/mol) |
|--------|--|-----------------------|---------------------------|
| M1 | Cyclopenta-1,3-diene | Stable | 32.1 ± 0.4[11] |
| M2 | Cyclopenta-1,2-diene | Reactive intermediate | |
| M3 | Cyclopentyne | Reactive intermediate | |
| M4 | 3-cyclopentenylidene | Reactive intermediate | |
| M5 | 2-cyclopentenylidene | Reactive intermediate | |
| M6 | Cyclopent-1,4-diylidene | Elusive | |
| M7 | Cyclobutylidene methylene | Reactive intermediate | |
| M8 | 3-Methylenecyclobutene | Stable | |
| B1 | Bicyclo[2.1.0]pent-2-ene | Reactive intermediate | 79.1 [126] |
| B2 | Bicyclo[2.1.0]pent-1(4)-ene | Reactive intermediate | |
| B3 | Bicyclo[2.1.0]pent-1-ene | Elusive | |
| B4 | Bicyclo[2.1.0]pent-1(5)-ene | Elusive | |
| B5 | Bicyclo[2.1.0]pent-5-ylidene | Elusive | |
| B6 | Bicyclo[2.1.0]pent-2-ylidene | Elusive | |
| B7 | Spiro[2.2]pent-1-ene | Reactive intermediate | |
| T1 | Tricyclo[2.1.0.0 ^{2,5}]pentane | Reactive intermediate | 84± 1 [127] |
| T2 | Tricyclo[1.1.1.0 ^{1,3}]pentane | Stable | |
| T3 | Tricyclo[2.1.0.0 ^{1,3}]pentane | Reactive intermediate | |

Mostly the structural characteristics and some significant properties of these cyclic C_5H_6 isomers are going to be discussed here.

The most remarkable molecule among cyclic isomers of C_5H_6 is cyclopenta-1,3-diene (**M1**) since it is the most widely studied conjugated cyclic diene in the history of organic chemistry [1]. Its importance originates from the following reasons;

- It is a stable, well-established and versatile chemical compound, which is available in dimer form [2].
- Due to having conjugated double bonds and an active methylene group, it can undergo a Diels-Alder diene addition reaction with almost any unsaturated compound, e.g., olefins, acetylene, maleic anhydride, etc. [3].
- It is widely used in industry; some of its usage fields are polyesters, hydrocarbon resins, elastomers, polychlorinated pesticides, flame retardants, etc. [1].
- It reacts with some metals to give metallocenes [4, 5], hence, play an important role in organometallic chemistry. Thousands of complexes of **M1** have been characterized, and several of these form the basis for important industrial processes.

Cyclopenta-1,3-diene is a member of cyclic conjugated dienes that have two conjugated double bonds. Its geometrical structure and π -molecular orbital diagram are depicted in Figure 1.2. As seen from the π -molecular orbital diagram, **M1** has four π -electrons. The orbitals on the $C5$ do not participate in the π bonding because of being sp^3 hybridized. For that reason, **M1** is not an aromatic molecule in spite of its planarity. Furthermore, it is unusually acidic for a hydrocarbon so that it can easily be converted into its anion, cyclopentadienyl, by treatment with a moderately strong base. This anion is unusually stable and NMR spectroscopy shows that all five hydrogen atoms in cyclopentadienyl anion are equivalent, leading to its aromatic character.

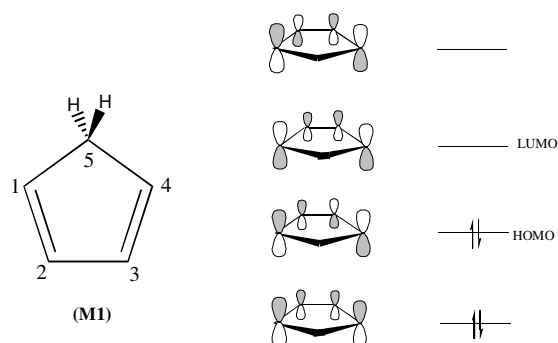


Figure 1.2 Geometrical structure and π molecular orbital diagram of cyclopentadiene.

The chemistry of conjugated dienes is interesting because it has been realized that double bonds interact with each other and this leads to unexpected properties and reactions. Diels-Alder reaction [6-8], the most important one of these reactions and in which **M1** is used heavily, is a powerful tool employed frequently for the synthesis of six-membered ring systems with excellent stereoselective control. This reaction is also called 1,4-cycloaddition of dienes. A representative example is the reaction between **M1** as diene and ethylene [9, 10] as dienophile (Figure 1.3). Moreover, **M1** also reacts with itself to form its dimer and behaves like both diene and dienophile in this 1,4-cycloaddition reaction.

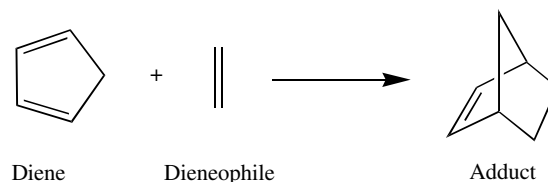


Figure 1.3 The Diels-Alder reaction between cyclopenta-1,3-diene and ethylene

From energetical point of view, **M1** is the most stable cyclic isomer ($\Delta H_f^0 = 32.1 \pm 0.4$ kcal/mol [11]) on the C_5H_6 PES, therefore it is the end product of a lot of isomerization reactions, five of which will be presented in sections 3.2.1 - 3.2.3.

Allenes [12] are the compounds that contain two adjacent double bonds. The equilibrium geometry of the simplest allene, 1,2-propadiene, is linear in its singlet state with orthogonal pair of substituents since the planes of π -bonds are

perpendicular to each other. In the cyclic allenes [13], ring constraints bend the allene and exert torsion toward a planar rearrangement of substituents. Nine and more membered carbocyclic allenes are relatively unstrained [14]. However, the stability of cyclic allenes decreases rapidly as the ring size diminishes [15], cyclonona-1,2-diene is a distillable liquid [16], while cycloocta-1,2-diene [17] rapidly dimerizes at room temperature showing that it is less stable. Cyclohepta-1,2-diene [17], the smaller cyclic allene, has proved too reactive to be isolated or even to be observed spectroscopically [18, 19]. Six membered ring, cyclohexa-1,2-diene was only trapped chemically as dimer or tetramer in the reaction between 1-bromocyclohexene and t-BuOK/DMSO [20]. In addition, trapping it with diphenylbenzofuran afforded two stereoisomeric cyclic adducts [21]. A bicyclic derivative of cyclopenta-1,2-diene has recently been achieved by the trapping experiments [22] even though the parent molecule has not been synthesized, yet. This structure has a great importance because it is the smallest cyclic allene that has ever been observed. In fact, it constitutes the lower limit of cyclic allenes. Obviously, it is a reactive intermediate and it immediately reacts with the reagents in the reaction medium. Owing to its very short-living nature, its structural features have been obtained from ab initio quantum chemical calculations by Johnson *et al.* [15]. They focused on chiral, diradical singlet, diradical triplet, and further excited (zwitterionic) states of **M2** and concluded that the chiral allenic structure is slightly favored (Figure 1.4).

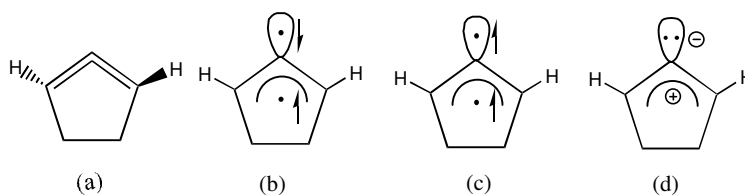


Figure 1.4 (a) chiral, (b) diradical singlet, (c) diradical triplet and (d) zwitterionic, states of 1,2-cyclopentadiene

In recent years, atomic carbon has become rather important due to its easy production and ability to react with a variety of organic molecules. It is generated by two ways. One method is the production of carbon vapor as a result of high temperature attained by the arc applied on graphite electrodes [23], and the other one

is the production of a pulsed supersonic carbon beam via laser ablation of graphite [24]. Mostly, the reactions of atomic carbon with organic molecules [25-29] have drawn the attention of chemists, and it became a synthetically important reactant. For example, formation of the smallest cyclic carbene, cyclopropylidene, is observed in the reaction of atomic carbon with ethylene and the simplest allene was synthesized within the same reaction [30]. In the light of this information about atomic carbon, it is logical to propose a reaction between atomic carbon and cyclobutene for the synthesis of **M2** via ring opening of bicyclo[2.1.0]pent-5-ylidene, **B5** (Figure 1.5). The rearrangement of ³**B5**, which might be experimentally produced from the reaction of atomic carbon and cyclobutene, to ³**M2** is presented in section 3.2.5.

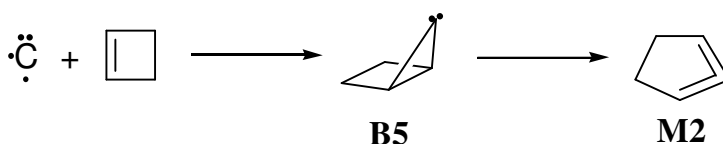


Figure 1.5 Reaction of atomic carbon with cyclobutene resulting isomer **M2**

Cyclopentyne (**M3**) is an alkyne structure integrated in a five membered ring. Cycloalkynes have been studied over the years in an attempt to understand molecular strain. The incorporation of a triple bond into a small and medium sized carbocycle can only be achieved by the deviation of C-C≡C-C group from the linear geometry. This leads to an increase in the destabilization of the system as the ring size decreases. While alkynes having eight- and more than eight-membered ring size are stable and isolable compounds, seven-, six- and five-membered cyclic alkynes have been either trapped or observed spectroscopically at low temperature matrices. Cyclobutyne and cyclopropyne are the elusive compounds because of having incredible ring strain. Therefore, **M3** is the smallest experimentally observed cyclic alkyne, a limiting structure among cyclic alkynes, similar to **M2**. The ground state geometry of **M3** was computationally predicted as having C_s symmetry with a slightly puckered ring structure [31]. The formation reaction of cyclopentyne from its corresponding carbene, cyclobutylidene methylene (**M7**), on C₅H₆ PES will be discussed in section 3.2.4.

3-cyclopentenylidene (**M4**) and 2-cyclopentenylidene (**M5**) are the carbene structures having a double bond in five-membered ring. They are proposed to form in

the reaction of 1,1-dibromo-2-vinylcyclopropane with methyllithium at very low temperatures (as low as $-78\text{ }^{\circ}\text{C}$) but not in equal amounts [32]. Neither of them has been isolated up to nowadays, indicating that they are also reactive intermediates. Finally, both are converted into **M1** via 1,2-hydrogen shifts in the course of mentioned reaction, on which the results of our computational study are presented in section 3.2.3.

Another conjugated diene structure, methylene cyclobut-3-ene (**M8**), has been synthesized by thermolysis of [1.1.1]propellane (**T2**) via formation of a carbene intermediate, 3-methylenecyclobutylidene, followed by 1,2-hydrogen migration. Wiberg and Walker [33] conducted this reaction for the first time, and they observed that **T2** rearranged to **M8** within five minutes at $114\text{ }^{\circ}\text{C}$ in the gas phase. The heat of formation (ΔH_f^{298}) of **M8** has a value of 58.1 kcal/mol calculated by G2(MP2,SVP) methodology [34], which is not much higher than heat of formation of **M1**. Interestingly, semi-empirical MNDO calculations [35] underestimated the heat of formation of this molecule only 4 kcal/mol comparing to G2(MP2,SVP) method. From these thermodynamic data, it can be predicted that **M8** is a moderately stable C_5H_6 isomer.

Bicyclo[2.1.0]pent-2-ene (**B1**), first prepared by photolysis of cyclopentadiene (**M1**) in 1966 [36], has withdrawn considerable interest in the past due to its facile thermal reactions. **B1** has two main thermal reactions i) walk rearrangement [37] and ii) electrocyclic ring opening to **M1** [38, 39]. In the walk rearrangement reaction, **B1** is converted into a different arrangement of itself in a concerted manner through a biradical transition state [37]. The mechanism of electrocyclic ring opening reaction of **B1** was found to be a disrotatory biradical process [40], so thermally disallowed according to Woodward - Hoffmann [41] rules. A detailed discussion and our results related to this reaction are given in section 3.2.1.

One of the first detailed examinations on bicyclo[2.1.0]pent-1(4)-ene (**B2**) structure is a theoretical study by Wagner *et al.* [42], and they found that its preferred geometry is non-planar with pyramidalized π -bonds. Due to its strained structure, this molecule is also another reactive intermediate among C_5H_6 isomers. It has been prepared only in the form of the substituted derivatives and characterized by trapping

experiments [43]. However, the preparation of parent compound (**B2**) is found to be unlikely [44] because of having high olefinic strain energy [45], which is defined as the difference in strain between the alkene and the corresponding alkane.

Spiro[2.2]pent-2-ene (**B7**) containing one cyclopropane and one cyclopropene rings in spiro conjugation is another known strained molecule of cyclic C_5H_6 compounds that polymerizes in the condensed phase at low temperature. Its first isolation was reported by Jones and Stowe [46] in 1964. Later, Bloch and Denis [47] characterized this molecule by NMR spectroscopy at 0°C and trapped it with cyclopentadiene and furan. Recently, Dodziuk *et al.* [48] have performed a theoretical study on **B7** by using high level ab initio and DFT methods and they claimed that the assignment of one of the signals in experimental NMR spectrum of **B7** is in error.

The first derivatives of tricyclo[2.1.0.0^{2,5}]pentane (**T1**) were reported in 1964 [49, 50], and the identification of parent **T1**, which is stable below -20 °C, [51] was achieved fifteen years later. Very recently, a review article illuminating its structure, properties and reactions of this molecule have been published by Levin *et al.* [52]. A comprehensive discussion and the results of our computational study on the conversion of **T1** to **M1** are presented in section 3.2.1

[1.1.1]propellane (tricyclo[1.1.1.0^{1,3}]pentane) (**T2**) is also one of the most interesting isomers among C_5H_6 compounds. Despite its huge strain, it is stable for several minutes in the gas phase at 110 °C and there are indications that **T2** and its derivatives may be stable at even higher temperatures in the absence of electrophiles [52]. This molecule contains three fused cyclopropane rings with structural parameters similar to those of the parent cyclopropane. It has a relatively high strain energy of 98 kcal/mol [52-54]. In spite of its high strain, the stability of the molecule has excited the scientists to explore the reason. Finally, it is found that there is no easy way of releasing the strain. Breaking of the central C-C bond releases only less than one third of the strain energy. In other words, the product obtained after breaking the central C-C bond, (bicyclo[1.1.1]pentane), has a strain energy of 65-68 kcal/mol [52]. Moreover, **T2** is also the most fascinating of the small-ring propellanes [52, 56, 57]. Having an “inverted” tetrahedral geometry at the bridgehead carbons and its stability are the most prominent features of this molecule

that were first theoretically predicted, later experimentally confirmed by preparing it from 1,3-dibromobicyclo[1.1.1]pentane [33].

Owing to deviation of the central bond from normal sp^3 hybridization, **T2** is brittle against nucleophilic attacks breaking the central C-C bond. Therefore, it reacts with a variety of molecules such as alkenes, alkynes [58], free radicals [59], etc. Sella *et al.* [60] claimed that its reactivity not only comes from strain relief at the transition state but also, and more significantly, from the orbital rehybridization.

Another exciting isomer of C_5H_6 compounds is tricyclo[2.1.0.0^{1,3}]pentane (**T3**) having three cyclopropane rings attaching to each other from different edges. This molecule has never been isolated, but there are evidences that it may be an intermediate structure. Wiberg *et al.* [61, 62] suggested that the formation of this isomer is possible within the reaction of 1,1-dibromo-2,3-bis(chloromethyl) cyclopropane with methyl lithium according to following mechanism (Figure 1.6).

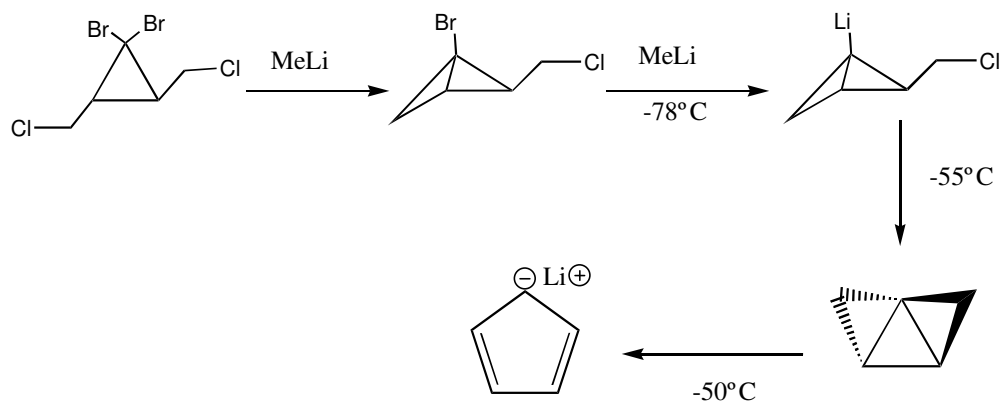


Figure 1.6 Synthesis mechanism of tricyclo[2.1.0.0^{1,3}]pentane (**T3**)

Wiberg and his colleagues [61] have performed low temperature NMR studies in order to find evidences about formation of **T3**. In this study, the NMR data provided good evidence that **T3** is formed as an intermediate in the reaction. In addition, they have done some ab initio calculations on the rearrangement of **T3** to **M1** via cyclopentenyl carbene (**M4**) as an intermediate and they found reasonable agreement between experiment and theory. Moreover, the heat of formation and strain energy of **T3** was calculated as 132 kcal/mol and 143 kcal/mol, respectively.

Thus, on a per carbon basis **T3** is one of the most highly strained molecules among organic compounds (29 kcal/mol/carbon).

A comprehensive theoretical investigation on the stabilities, electronic and geometrical characteristics, and several unimolecular rearrangements of the cyclic C_5H_6 isomers is to be presented within this thesis. The singlet and triplet electronic potential energy surface (PES) of C_5H_6 system pertaining to these structures was thoroughly explored by high-level ab initio and DFT methods. Details of the theoretical methods employed are provided in chapter II. While the minima on the PES that correspond to the stable structures are given in section 3.1, the transition states involved in mentioned unimolecular rearrangements of these species are discussed in section 3.2.

CHAPTER II

THEORETICAL CALCULATION METHODS

2.1. Introduction

“The underlying physical laws necessary for the mathematical theory of a large part of physics and the whole of chemistry are thus completely known, and the difficulty is only that exact application of these laws leads to equations much too complicated to be soluble.”

P. A. M. Dirac

Chemistry is the science dealing with the constructions, transformations and properties of molecules. Traditionally, molecules are considered as being “composed” of atoms. In fact, they are a collection of nuclei and electrons. The only physical force for the chemical phenomena is the Coulombic interaction between nuclei and electrons. There are huge amounts of different molecules in nature because they have different nuclei, different nuclear positions and different number of electrons.

Theoretical chemistry is a subfield of chemistry in which the elementary laws of physics are employed to explain chemical processes with the help of mathematical methods. In theoretical chemistry, it is intended to find out the most stable spatial arrangement of the nuclei in a molecule and to calculate relative energies, properties such as dipole moment, polarizability, etc. and transformations of molecules, as well as the time dependence of the molecular structures and properties.

Unfortunately, one- or two-particle systems can exactly be solved. For many body systems, only the numerical solutions (to a given accuracy) can be found by performing a very large number of mathematical operations. After development of fast and powerful computers, a new field in chemistry has arisen, “computational chemistry” where these vast numbers of mathematical operations are performed via computers. The computational chemistry can be regarded as an experimental tool, because the main objective in this field is to obtain results of chemical problems, not to develop new theoretical methods. There is certainly a strong interaction between computational and theoretical chemistry. While some improvements might be performed in theory due to results obtained from computational calculations, new theories may enable new computational problems to be studied.

Nowadays, depending on the desired accuracy, one can computationally obtain valuable information for a system containing several thousands of atoms. However, the most challenging problem in computational chemistry is the choice of appropriate level of theory for the studied system, and to be able to assess the quality of the obtained results. In the following, the methods of computational chemistry are going to be explained from the basic ideas to the sophisticated techniques.

2.2. The Schrödinger Equation

In quantum mechanics, the state of a system is fully described by the wave function $\Psi(\mathbf{r},t)$, where \mathbf{r} are spatial coordinates of the particles that constitute the system and t is the time. The product of wave function with its complex conjugate is defined as the probability distribution of the particle, i.e. the probability of finding a particle in its volume element $d\mathbf{r}$ around its point \mathbf{r} at the time t . The dynamical evolution of the wave function with time is described by the time-dependent Schrödinger equation [63]

$$i\hbar \frac{\partial \Psi(\mathbf{r},t)}{\partial t} = \hat{H}\Psi(\mathbf{r},t) = E\Psi(\mathbf{r},t) \quad (2.1)$$

where \hat{H} is the Hamiltonian operator for the system, corresponding to the total energy.

In most cases, time-dependent interaction of atoms and molecules can be neglected. The Schrödinger equation is thus separated into equations for time and space variation of the wave function using the variable separation $\Psi(\mathbf{r}, t) = \Psi(\mathbf{r})\Psi(t)$. The time-independent Schrödinger equation is therefore given as;

$$\hat{H} \Psi(\mathbf{r}) = E \Psi(\mathbf{r}) \quad (2.2)$$

where

$$\hat{H} = -\sum_{i=1}^N \frac{1}{2} \nabla_i^2 - \sum_{a=1}^M \frac{1}{2M_a} \nabla_a^2 - \sum_i \sum_a \frac{Z_a}{r_{ia}} + \sum_i \sum_{j>i} \frac{1}{r_{ij}} + \sum_{a=1}^M \sum_{b>a} \frac{Z_a Z_b}{R_{ab}} \quad (2.3)$$

Here i and j are indices of N electrons whereas a and b are indices of M atomic nuclei. Atomic units are used throughout. M_a is the ratio of the mass of nucleus a to an electron, and Z_a is the atomic number of nucleus a . The distance between the i^{th} and the j^{th} electron is r_{ij} ; the distance between the a^{th} nucleus and the b^{th} nucleus is R_{ab} ; r_{ia} specifies the distance between electron i and nucleus a . The first and second terms in Equation 2.3 are the kinetic energy operators of the electrons (T_e) and the nuclei (T_n), respectively. The third term is the electron nucleus attraction energy operator (V_{ne}), whereas the fourth and fifth terms represent the repulsion energy operator of the electron-electron (V_{ee}) and the nucleus-nucleus repulsion (V_{nn}), respectively.

$$\hat{H} = T_e + T_n + V_{ne} + V_{ee} + V_{nn} \quad (2.4)$$

2.2.1. The Born-Oppenheimer Approximation

Perhaps the great disappointment of quantum chemistry is that, while the Schrödinger equation is powerful enough to describe almost all chemistry, it is too complex to solve for almost all systems except the simplest ones. Even the simplest molecule, H_2^+ , consists of three particles, thus producing a Schrödinger equation that is impossible to solve analytically. To overcome this difficulty a variety of approximations are made and the most common of which is the Born-Oppenheimer approximation [64].

The masses of the nuclei are much greater than the electrons, hence the electrons can respond almost instantaneously to any change in the nuclear positions.

Thus, to a good approximation, one can think of the electrons as moving in a field of fixed nuclei. Within this approximation, the nuclear kinetic energy term can be neglected and the nuclear-nuclear repulsion term can be considered a constant. These two terms can therefore be removed from the full Hamiltonian and, the remaining part is called the “electronic Hamiltonian”. For an isolated N-electron atomic or molecular system within the Born-Oppenheimer approximation, the electronic Schrödinger equation is given by

$$\hat{H}_{\text{elec}} \Psi_{\text{elec}} = E_{\text{elec}} \Psi_{\text{elec}} \quad (2.5)$$

where $E_{\text{elec}} = E_{\text{elec}}(\{\mathbf{R}_a\})$ is the electronic energy, $\Psi_{\text{elec}} = \Psi_{\text{elec}}(\{\mathbf{r}_i\}; \{\mathbf{R}_a\})$ is the wave function which describes the motion of the electrons and explicitly depends on the electronic coordinates but depends *parametrically* on the nuclear coordinates (3M-6 variables for a nonlinear molecule), as does the electronic energy. \hat{H}_{elec} is the electronic Hamiltonian operator:

$$\hat{H} = -\sum_{i=1}^N \frac{1}{2} \nabla_i^2 - \sum_i \sum_a^M \frac{Z_a}{r_{ia}} + \sum_i \sum_{j>i}^N \frac{1}{r_{ij}} + \sum_{a=1}^M \sum_{b>a}^M \frac{Z_a Z_b}{R_{ab}} \quad (2.6)$$

The electronic energy, E_{elec} , as a function of 3M-6 variables constitutes the potential energy surface (PES) of the molecule in the given electronic state. Since we will be concerned with electronic quantities only, in what follows the subscript elec will be dropped.

2.3. The Hartree-Fock Theory

Although the Born-Oppenheimer approximation considerably reduces the complexity of the Schrödinger equation, the resulting electronic Schrödinger equation is still extremely complex, due to the electron-electron interactions. A satisfying solution is to introduce the molecular orbital approximation, the simplest of which is the independent-particle, or Hartree approximation, wherein the total wavefunction is approximated by a product of orthonormal molecular orbitals (MOs). This idea closely follows the chemists' view of electrons occupying orbitals. The Hartree approximation assumes that each electron moves independently, and

sees only the *average* field generated by all the other electrons. The Hartree wavefunction (for an N electron system) is

$$\Psi = \phi_1(x_1)\phi_2(x_2)\dots\phi_N(x_N) \quad (2.7)$$

where each ϕ_i is a spin orbital assigned to one electron. The ϕ_i s are orthonormal, consisting of a spatial orbital $\chi_i(\vec{r})$ and one of the two spin functions, $\alpha(s)$ and $\beta(s)$ (where s is spin variable), representing spin up and spin down states. “ x ” is the space-spin coordinate, containing both positions, \vec{r} , and spin, s , of an electron.

Applying the variational method in this case implies that we will consider variations that will make the expectation value of the electronic Hamiltonian (equation 2.8) stationary,

$$\langle \Psi | H_{elec} | \Psi \rangle \quad (2.8)$$

under the constraints that all the individual orbitals are orthonormal, as specified,

$$\langle \phi_i | \phi_j \rangle = \delta_{ij} \quad (2.9)$$

The Hartree equations established after variation, in principle, determine the orbitals ϕ_i . However, this approximation suffers from a severe problem, so that it is considered too crude in the immense number of cases. The main problem of the Hartree wave function is that it does not take into account that the electrons are indistinguishable. It violates therefore one of the most fundamental principles of the quantum theory. It is the fact that the electrons are fermions so that the wave function must satisfy the antisymmetry condition, (equation 2.10),

$$\Psi(x_1, x_2, x_3, \dots, x_N) = -\Psi(x_2, x_1, x_3, \dots, x_N) \quad (2.10)$$

In order to satisfy the antisymmetry conditions, the approximate wave function must be improved. Slater [65] introduced an improvement on the approximate wave function by putting it into a determinantal form that makes it mutually antisymmetric upon exchange of any two electrons. This determinant is called “Slater determinant” (equation 2.11).

$$\Psi = \frac{1}{\sqrt{N!}} \begin{vmatrix} \phi_1(x_1) & \phi_2(x_1) & \dots & \phi_N(x_1) \\ \phi_1(x_2) & \phi_2(x_2) & \dots & \phi_N(x_2) \\ \dots & \dots & \dots & \dots \\ \phi_1(x_N) & \phi_2(x_N) & \dots & \phi_N(x_N) \end{vmatrix} \quad (2.11)$$

When the determinantal function (equation 2.11) is used in equation 2.8, the Hartree-Fock [66, 67] energy is obtained

$$E_{\text{HF}} = \sum_i^N h_{ii} + \frac{1}{2} \sum_i^N \sum_j^N (J_{ij} - K_{ij}) + V_{nn} \quad (2.12)$$

where the single electron integral h_{ii} , the Coulomb integral J_{ij} and the Exchange integral K_{ij} are defined as follows.

$$h_{ii} = \langle \phi_i | h | \phi_i \rangle = \langle \phi_i(x_1) | -\frac{1}{2} \nabla_1^2 - \sum_a \frac{Z_a}{|\mathbf{R}_a - \mathbf{r}_1|} | \phi_i(x_1) \rangle \quad (2.13)$$

$$J_{ij} = \langle \phi_i(x_1) \phi_j(x_2) | \frac{1}{|\mathbf{r}_1 - \mathbf{r}_2|} | \phi_i(x_1) \phi_j(x_2) \rangle \quad (2.14)$$

$$K_{ij} = \langle \phi_i(x_1) \phi_j(x_2) | \frac{1}{|\mathbf{r}_1 - \mathbf{r}_2|} | \phi_j(x_1) \phi_i(x_2) \rangle \quad (2.15)$$

The Coulomb integral, J_{ij} , represents a classical repulsion between two charge distributions described by $\phi_i^2(x_1)$ and $\phi_j^2(x_2)$. On the other hand, the Exchange integral, K_{ij} , has no classical analogy. It arises from the exchange of the electrons.

It is convenient to define the Coulomb and Exchange operators for the variation of the energy.

$$\mathbf{J}_i | \phi_j(x_2) \rangle = \left\langle \phi_i(x_1) | \frac{1}{|\mathbf{r}_1 - \mathbf{r}_2|} | \phi_i(x_1) \right\rangle | \phi_j(x_2) \rangle \quad (2.16)$$

$$\mathbf{K}_i | \phi_j(x_2) \rangle = \left\langle \phi_i(x_1) | \frac{1}{|\mathbf{r}_1 - \mathbf{r}_2|} | \phi_j(x_1) \right\rangle | \phi_i(x_2) \rangle \quad (2.17)$$

While the Coulomb operator, \mathbf{J} , involves multiplication by a matrix element with the same orbital on both sides of the repulsion operator, the Exchange operator, \mathbf{K} , exchanges the two functions on the right hand side of the $1/|\mathbf{r}_1 - \mathbf{r}_2|$. Then, the Hartree Fock energy can be rewritten in terms of these operators as shown in equation 2.18.

$$E_{\text{HF}} = \sum_i^N \langle \phi_i | h | \phi_i \rangle + \frac{1}{2} \sum_{ij}^N (\langle \phi_j | \mathbf{J}_i | \phi_j \rangle - \langle \phi_j | \mathbf{K}_i | \phi_j \rangle) + V_{nn} \quad (2.18)$$

Here, it is aimed to find a set of MOs that makes the energy stationary with respect to a change in the orbitals. Of course, the main desire is to obtain a minimum.

The variation of the energy will be a constrained optimization since the MOs must remain orthogonal and normalized. This can be handled by means of Lagrange multipliers method. The condition is that the Lagrange function must remain stationary with respect to an orbital variation.

$$L = E - \sum_{ij}^N \lambda_{ij} (\langle \phi_i | \phi_j \rangle - \delta_{ij}) \quad (2.19)$$

$$\delta L = \delta E - \sum_{ij}^N \lambda_{ij} (\langle \delta \phi_i | \phi_j \rangle + \langle \phi_i | \delta \phi_j \rangle) = 0 \quad (2.20)$$

$$\delta E = \sum_i^N (\langle \delta \phi_i | \mathbf{F}_i | \phi_i \rangle + \langle \phi_i | \mathbf{F}_i | \delta \phi_i \rangle) \quad (2.21)$$

$$\mathbf{F}_i = h + \sum_j^N (\mathbf{J}_j - \mathbf{K}_j) \quad (2.22)$$

The Fock operator, \mathbf{F}_i , is an effective one-electron energy operator, and it expresses the kinetic energy of an electron, the attraction to all the nuclei and the repulsion to all the other electrons. The sum of these operators does not give the Hamiltonian operator because they are obtained from the variation of the energy, not from the energy, itself. Thus, the final *Hartree-Fock equations* can be written as

$$\mathbf{F}_i \phi_i = \sum_j^N \lambda_{ij} \phi_j \quad (2.23)$$

The non-diagonal Lagrange multipliers, λ_{ij} where $i \neq j$, have nonzero values. These equations can be made simpler by means of a unitary transformation that makes the Lagrange multipliers' matrix diagonal. In other words, while all non-diagonal elements go to zero, the diagonal elements become molecular orbital energies, ϵ_i . Moreover, this special set of MOs is called canonical MOs (ϕ'), and they transform equation 2.23 into a set of pseudo-eigenvalue equations (equation 2.24).

$$\mathbf{F}_i \phi'_i = \epsilon_i \phi'_i \quad (2.24)$$

The equations in equation 2.24 are not ordinary eigenvalue equations, because the Fock operator depends on all the MOs (via the Coulomb and Exchange operators). Such equations can be solved iteratively. A suitable set of the spin orbitals is chosen as initial guess and the Fock operator is constructed via equation 2.22. The solutions of equation 2.24 result in an improved set of orbitals. The new orbitals thus found are used as the new guess in the Fock operator, and the procedure

is repeated until the solutions of equation 2.24 do not change within a prescribed tolerance. This iterative method of solving the Hartree-Fock equations is called the *Self-consistent Field* (SCF) method.

2.3.1. Restricted and Unrestricted Hartree-Fock Wave Functions

In equation 2.11, the Slater determinant is formed from spin molecular orbitals ϕ_i . Spin molecular orbitals are the product of space molecular orbitals with a spin part, namely α for $m_s = 1/2$ and β for $m_s = -1/2$. If the considered system is a closed shell, every space molecular orbital is doubly occupied and so the system is a singlet. By this way the number of integrals to be calculated is reduced, and the wave function for such a system is called Restricted Hartree-Fock (RHF) wave function.

If the considered system is an open shell then not every space molecular orbital is doubly occupied. For such a system, RHF wave function is impossible to use. Therefore, the wave function can be constructed by using a different space orbital for each spin orbital, namely no restrictions on the orbitals. The resulting wave function is called an unrestricted Hartree-Fock (UHF) wave function [68], and always gives lower (or equal) energies than the restricted function. One drawback of the UHF wave function is that it is not a spin eigenfunction as is the case for RHF. As a result, “singlet” UHF wave function may contain contributions from higher-lying triplet, quintet, etc. states, which is called spin contamination.

Another approach to employ in open-shell states is to assign one spatial orbital for each electron pair in the core, but assign different spatial orbital(s) for open shell electron(s). This treatment is called the restricted open-shell Hartree-Fock (ROHF) method. The ROHF wave function is a spin eigenfunction and commonly used for the doublet and triplet states.

2.4. The Basis Set Approximation

The usage of a basis set expansion to express the unknown MOs in terms of a set of known functions (equation 2.25) is a common feature of all calculations in computational chemistry [69].

$$\phi_i = \sum_{\alpha}^K c_{\alpha i} \chi_{\alpha} \quad (2.25)$$

In principle, any complete set of function can be used as a basis set, χ_{α} . There are two criteria in the choice of the function type. The first is that the set of functions chosen must have an appropriate behavior for the physics of the problem. For example, the functions should go towards zero as the distance between nucleus and electron becomes large for a bound atomic or molecular system. The second criterion is computational feasibility, i.e. the chosen function should let the easy calculation of all required integrals. There are two types of functions satisfying these criteria better than other types: Gaussian type orbitals (GTO) and Slater Type Orbitals (STO). Slater type orbitals have the form

$$\chi_{\zeta, n, l, m}(r, \theta, \varphi) = N Y_{l, m}(\theta, \varphi) r^{n-1} e^{-\zeta r} \quad (2.26)$$

whereas the Gaussian type orbitals have the form

$$\chi_{\zeta, n, l, m}(r, \theta, \varphi) = N Y_{l, m}(\theta, \varphi) r^{(2n-2-l)} e^{-\zeta r^2} \quad (2.27)$$

Both have some advantages and disadvantages. The exponential functions are physically appropriate because of their resemblance to the solutions of the hydrogen atom, but they produce integrals difficult to calculate. The Gaussian functions however are computationally much easier to manage, although they are not as efficient as the exponential ones in describing the electronic structure on a one-to-one basis. Since the computational feasibility is more important feature for a function type, the linear combinations of Gaussian functions are commonly used as basis sets.

The HF equations can be solved numerically according to the suggestion of Roothaan [70] and Hall [71]. A set of known spatial basis functions is introduced and the unknown molecular orbitals are expanded in the linear expansion (equation 2.25). If the set of χ_i is complete, the expansion would be exact. The problem of calculating

the HF molecular orbitals is then reduced to the problem of calculating a set of expansion coefficients. Substituting equation 2.25 into the HF equation (equation 2.24) therefore gives

$$F_i \sum_{\alpha}^M c_{\alpha i} \chi_{\alpha} = \epsilon_i \sum_{\alpha}^M c_{\alpha i} \chi_{\alpha} \quad (2.28)$$

In matrix notation 2.28 can be rewritten as:

$$\mathbf{FC} = \mathbf{SC}\epsilon \quad (2.29)$$

where $F_{\alpha\beta} = \langle \chi_{\alpha} | \mathbf{F} | \chi_{\beta} \rangle$ and $S_{\alpha\beta} = \langle \chi_{\alpha} | \chi_{\beta} \rangle$ are the matrix elements of Fock and overlap matrices, respectively, and ϵ is the diagonal matrix of MO energies.

This new form of the Hartree-Fock equation is more suitable for the SCF method. First of all an initial guess is made for the atomic orbital coefficients. Then by using these coefficients the Fock matrix is constructed, and a new set of atomic orbital coefficients is calculated. This operation goes on iteratively until the difference between consecutive results is under a certain limit.

2.4.1. Classification and types of basis sets

After deciding the type of basis set, the most significant issue is the number of functions to be used. If smallest number of functions is employed in the basis set definition, this is called minimum basis set. For example, a single s-function is used for a hydrogen atom or Li atom requires only two s-functions. In order to increase the accuracy in the computation, all basis functions in the minimum set could be doubled producing a *Double Zeta* (DZ) type basis. “Zeta” word comes from the exponent denoted by ζ in the GTO and STO type basis functions. A DZ basis set, for example, employs two s-functions with different ζ s (1s and 1s') for a hydrogen atom. Valence electrons play more important role than the core (inner) electrons in the chemical bonding, therefore a different type of DZ basis doubles only valence orbitals, producing a *split valence* basis set. Those sets reduce computation time giving reasonable accuracy. The next step in the basis set size is the introduction of *Triple Zeta* type basis. As its name implies, a TZ basis set has three times as many functions as in the minimum basis, i.e. three s-functions for H atom. Number of core

orbitals can be reduced by splitting only the valence orbitals. These types of TZ basis sets are called triple split valence basis sets.

In most cases higher angular momentum functions should be included in the basis in order to describe the charge polarization effects. If a set of p-orbitals is added to a hydrogen atom in a hydrocarbon molecule, the p_z component can be used for improving the description of the C-H bond. The p-function introduces a polarization of the s-orbital(s). Similarly, d- and f- functions increase the polarizabilities of p- and d-orbitals, respectively. If there are weakly bound electrons in the system of interest, small exponent functions are needed in the basis set. The functions having smaller exponents (they decay at longer distances) are called *diffuse* functions, and they can be added to the basis set.

The *contracted* basis set concept is introduced for more efficient description of core electrons being energetically important but chemically unimportant. Combining the full set of basis functions, known as the *primitive* GTOs (PGTOs), into a smaller set of functions by forming fixed linear combinations is known as the basis set *contraction* and the resulting functions are called *contracted* GTOs (CGTOs).

$$\chi(\text{CGTO}) = \sum_i^k a_i \chi_i(\text{PGTO}) \quad (2.30)$$

where a_i s are the contraction coefficients.

Contraction is especially helpful for orbitals describing the core electrons, since they require a relatively large number of functions for representing the wave function cusp near the nucleus, and largely independent of the environment. Furthermore, contracting a basis set always increases the energy and decreases its flexibility because of the restrictions in the number of variational parameters, but it drastically reduces computational cost. The choice of a contracted basis set depends on how much loss in accuracy is acceptable compared to the gain in computational efficiency.

The number of PGTOs forming CGTOs is called the degree of contraction. The specification of a basis set in terms of primitive and contracted functions is given by such a notation (10s4p1d/4s1p)→[3s2p1d/2s1p]. The basis in parentheses represents the number of PGTOs as the square brackets show CGTOs. The left side

of the slash belongs to heavy atoms (first row elements), while the functions belonging to hydrogen atom are put on right side in both representations. For example, 10 s-PTGOs are contracted into 3 s-functions (three CGTOs). This notation does not give any information on how the contraction is performed. There are many contacted basis sets available in the literature. Only thing that a computational chemist does is to choose an appropriate one and use. Short descriptions are given below related to the several important and commonly used basis sets, including the ones employed in this thesis.

STO-nG basis sets: Slater Type Orbital consisting of n PGTOs [72]. This is a minimum type basis and its PGTO exponents are determined by fitting to the STO. STO-3G is the most widely used minimum basis set. The notation for STO-3G basis is (6s3p/3s)→[2s1p/1s].

k-nlmG basis sets: These basis sets are of the split valence type, with *k* indicating the number of PGTOs used in the description of core orbitals. The *nlm* shows how many functions the valence orbitals split into, as well as, how many PGTOs are used for their representation. Two (*nl*) and three (*nlm*) values indicate split valence and triple split valence, respectively. The values before G illustrate the s- and p- functions while the polarization functions are added after that letter. Most common *k-nlmG* basis sets and their PGTO→CGTO contractions are listed in Table 2.1.

Table 2.1 Common *k-nlmG* type basis sets and their contractions.

| Basis set | Contraction |
|-------------|----------------------|
| 3-21G [73] | (6s3p/3s)→[3s2p/2s] |
| 6-31G [74] | (10s4p/4s)→[3s2p/2s] |
| 6-311G [75] | (11s5p/5s)→[4s3p/3s] |

Diffuse and/or polarization functions can be added to each of these basis sets. Diffuse functions are normally s- and p- functions and denoted by + (s- and p- functions are added to heavy atoms only) and ++ (s- and p- functions are added to heavy atoms, as well as s-functions added to hydrogen atoms). They come before the G letter. Polarization functions are indicated after the G, with a separate designation for heavy atoms and hydrogens. For example, in 6-31++G(d,p) basis set, diffusion functions are added to both heavy (s and p functions) and H (s function) atoms, in

addition, d- and p- polarization functions are added to heavy atoms and hydrogens, respectively. Sometimes, * and ** are put instead of (d) and (d,p) polarization functions, e.g. 6-31G* and 6-31G**.

Another type of basis set is the *correlation consistent* (cc-) basis sets designed for recovering the correlation energy of the valence electrons. Several different sizes of cc- basis sets are available in terms of final number of contracted functions. These are known by the acronyms, cc-pVDZ [76], cc-pVTZ [77], cc-pVQZ [78], etc. Correlation consistent polarized valence double zeta (cc-pVTZ) basis set, which is employed in the thesis, has a designation as follows;

$$(10s5p2d1f/5s2p1d) \rightarrow [4s3p2d1f/3s2p1d].$$

2.5. Electron Correlation Methods

The motion of the electrons is correlated due to the Coulomb repulsion. The difference between the exact non-relativistic energy and the Hartree-Fock energy in a given basis set is called the electron correlation energy.

The HF method determines the best one-determinant wave function in a given basis set. It is therefore obvious that in order to improve the HF results, the starting point must be a trial wave function which contains more than one Slater determinant

$$\Psi = a_0 \Phi_{\text{HF}} + \sum_{i=1} a_i \Phi_i \quad (2.31)$$

where Ψ is the total trial wave function, Φ_{HF} is the HF wave function and Φ_i are the wave functions represented by additional Slater determinants. The a_0 and a_i are the variational coefficients. By replacing occupied MOs in the HF determinant by unoccupied MOs, a whole series of determinants may be generated. These can be denoted according to how many occupied HF-MOs have been replaced, thus leading to Slater determinants which are singly, doubly, triply, quadruply etc. excited relative to the HF determinant. These determinants are often referred to as Singles (S), Doubles (D), Triples (T), Quadruples (Q) with a maximum excitation of N electrons (N- multiple).

The main methods for including electron correlation are Configuration Interaction (CI), Multi-configuration Self Consistent Field (MCSCF) Theory, Many

Body Perturbation Theory (MBPT), Coupled Cluster (CC) Theory, and Density Functional Theory (DFT).

2.5.1. Configuration Interaction (CI)

Conceptually, the simplest way of introducing the instantaneous interaction of electrons is via *Configuration Interaction* (CI) [79, 80]. The CI method uses a wavefunction which is a linear combination of the HF determinant and determinants from electron excitations given in equation 2.31.

The expansion coefficients of the trial wave functions for CI approach are determined under the requirement that energy should be minimum (or at least stationary). The MOs used for building the excited Slater determinants are taken from a HF calculation and are held fixed. The CI expansion, if the expansion is complete (full CI), gives the exact correlation energy within the basis set approximation. The number of determinants in full CI grows exponentially with the system size, making the method impractical for all but the smallest systems. In other words, very large number of configurations (determinants), as stated, is required to yield energies and wave functions approaching the exact many-body wavefunction. As the total number of determinants is

$$\text{\# of Slater Det} = \frac{M!}{N!(M-N)!} \quad (2.32)$$

where the length of the expansion is given in terms of the number of electrons, N , and the number of basis functions, M . For decreasing the size of the matrix to be diagonalized, the CI expansion is usually truncated at some order. First order expansion does not make any improvement on HF wave function since Brillouin's theorem states that singly excited determinants do not mix with the HF determinant [81]. Therefore CISD method [82-84] where only singly and doubly excited determinants are considered is the cheapest valuable form of CI method that is generally applicable for a large variety of systems. For computationally feasible systems (i.e. medium size molecules and basis sets), it typically recovers 80-90% of the available correlation energy. Triple-excitation (CISDT) and quadruple excitation (CISDTQ) calculations are done only when very-high-accuracy results are desired.

2.5.2. Multi-configuration Self-consistent Field (MCSCF) Theory

Multi-configuration self-consistent field (MCSCF) methods can be considered as a type of CI where not only the coefficients in front of the determinants are optimized by the variational principle, but also the MOs used for constructing the determinants are made optimum. MCSCF methods are hardly ever used for calculation of large fraction of correlation energy because orbital relaxations do not recover large part of correlation energy. Usually CI is employed for this purpose. MCSCF methods are mainly used for the systems of molecules whose electronic structures cannot be defined by single determinantal wave function i.e. it is used when RHF calculations of such systems fail. The most important and common examples of such systems are the molecules having biradical character. Although unrestricted formalism of HF theory (UHF) gives qualitative representation for biradicalic systems, the energy results of this theory are unreliable due to inclusion of high spin contamination, admixture of higher spin states (mostly triplet) to singlet state wave function. However, the configurational state functions (CSFs) entering into an MCSCF expansion are pure spin states therefore they do not suffer from the spin contamination problem. Hence, MCSCF methods are the best choice for obtaining descriptive electronic structures and reliable energy values of biradicalic structures.

The reference energy for electron correlation is defined as RHF energy. In MCSCF terminology, electron correlation is considered to have two parts. Energy lowering by adding enough flexibility in the wave function to be able to qualitatively describe the system is generally called the *static* electron correlation. This is essentially the effect of allowing the orbitals to become singly occupied instead of forcing double occupation. The remaining part, lowering the energy due to the electron motions, is called the *dynamic* correlation. The correlation recovered by MCSCF methods is mostly the static correlation, but they recover the dynamic correlation only by addition of more and more CSFs. Accordingly, there is no strict border between static and dynamic correlation.

2.5.2.1. Complete Active Space SCF theory (CASSCF)

The major problem in MCSCF methods is the choice of necessary configurations to include the property of interest. Complete Active Space SCF (CASSCF) method is one of the commonly used MCSCF methods. It is sometimes called Full Optimized Reaction Space (FORS). In this method, the configuration selection is performed by dividing the MOs into *active* and *inactive* spaces. The MOs in active space are generally some of highest occupied and lowest unoccupied MOs from a RHF calculation. The remaining MOs in inactive space are both core (doubly occupied) and virtual (empty) orbitals. A full CI is performed within the active space MOs and all symmetry-adapted configurations are included in the MCSCF optimization. All of the MOs in active space must be selected manually by taking the problem of interest into account.

Several notations have been proposed for the CASSCF methods like $[n,m]$ -CASSCF, CASSCF(n,m), etc. In all of these n,m part is common since they define constituents of active space. Here, n stands for the number of active electrons that are distributed in all possible ways in m orbitals defining the active space. The full CI expansion within the active space restricts the number of orbitals and electrons that can be treated by CASSCF methods. The exponential increase of CSFs with increasing constituents of active space limits its dimensions to less than 10-12 electron or orbitals. Therefore, the goal of CASSCF methods is to recover the changes occurring in the correlation energy for the given process, not recovering considerable amount of the correlation. All over the thesis, CAS44, CAS66 and CAS88 abbreviations emphasizing active spaces are used for CASSCF(4,4), CASSCF(6,6) and CASSCF(8,8) methods, respectively.

One drawback of CASSCF methods is their inherent tendency to give unbalanced descriptions for different parts of the system interested. Although all electron correlation energy for the active electrons is recovered, those arising from either inactive electrons or between active and inactive electrons are not calculated at all. For example, CASSCF methods probably overestimate biradicalic character of a system due to these unbalanced descriptions of the parts [85, 86].

2.5.3. Many Body Perturbation Theory (MBPT)

A different systematic procedure for evaluating the correlation energy, which is not variational in the sense that it does not give energies that are upper bounds to the exact energy but is size consistent at each level, is perturbation theory (PT). The application of PT to a system composed of many interacting particles is generally called many-body perturbation theory (MBPT). This perturbation method is based on a partitioning of the full Hamiltonian into two pieces,

$$\hat{H} = \hat{H}_0 + \lambda \hat{H}' \quad (2.33)$$

\hat{H}_0 is a reference or unperturbed part, \hat{H}' is a small perturbation to \hat{H}_0 , λ is a parameter defining the strength of the perturbation. The solutions for unperturbed Hamiltonian, \hat{H}_0 , is a complete orthonormal set (equation 2.34).

$$\hat{H}_0 \Phi_i = E_i \Phi_i, \quad i = 0, 1, 2, \dots, \infty \quad (2.34)$$

Here, we will assume the following conditions being hold, (i) the perturbation is time-independent, (ii) the reference wave function is non-degenerate, and (iii) it belongs to the lowest energy state. The perturbed equation is

$$\hat{H}\Psi = W\Psi \quad (2.35)$$

When $\lambda = 0$, then $H = H_0$, $\Psi = \Phi_0$ and $W = E_0$. If the perturbation is increased from zero to a finite value, the new energy and the wave function should change continuously, and they can be written as a Taylor series expansion in powers of the perturbation parameter, λ .

$$\begin{aligned} W &= \lambda^0 W_0 + \lambda^1 W_1 + \lambda^2 W_2 + \lambda^3 W_3 + \dots \\ \Psi &= \lambda^0 \Psi_0 + \lambda^1 \Psi_1 + \lambda^2 \Psi_2 + \lambda^3 \Psi_3 + \dots \end{aligned} \quad (2.36)$$

It is obvious that, $W_0 = E_0$ and $\Psi_0 = \Phi_0$ when λ is zero. These are unperturbed or zero order energy and wave function. W_1, W_2, \dots are first order, second order, and etc. order corrections to the unperturbed energy. Similarly, Ψ_1, Ψ_2, \dots are first order, second order, and etc. order corrections to the unperturbed wave function.

If the expansions in equation 2.36 are substituted into the Schrödinger equation given in equation 2.35, the resulting equation becomes

$$\begin{aligned}
&(\hat{H}_0 + \lambda \hat{H}')(\lambda^0 \Psi_0 + \lambda^1 \Psi_1 + \lambda^2 \Psi_2 + \dots) = \\
&(\lambda^0 W_0 + \lambda^1 W_1 + \lambda^2 W_2 + \dots)(\lambda^0 \Psi_0 + \lambda^1 \Psi_1 + \lambda^2 \Psi_2 + \dots)
\end{aligned} \tag{2.37}$$

The terms with the same power of λ in equation 2.37 can be assembled as shown in equation 2.38.

$$\begin{aligned}
\lambda^0 : \hat{H}_0 \Psi_0 &= W_0 \Psi_0 \\
\lambda^1 : \hat{H}_0 \Psi_1 + \hat{H}' \Psi_0 &= W_0 \Psi_1 + W_1 \Psi_0 \\
\lambda^2 : \hat{H}_0 \Psi_2 + \hat{H}' \Psi_1 &= W_0 \Psi_2 + W_1 \Psi_1 + W_2 \Psi_0 \\
&\dots\dots\dots \\
\lambda^n : \hat{H}_0 \Psi_n + \hat{H}' \Psi_{n-1} &= \sum_{i=0}^n W_i \Psi_{n-i}
\end{aligned} \tag{2.38}$$

These equations are zeroth-, first-, second- ... and nth -order perturbation equations. First is the Schrödinger equation of unperturbed system. W_1 and Ψ_1 are the unknowns in first order perturbation equation.

2.5.3.1. Møller Plesset Perturbation Theory

The zero-order Hamiltonian from the Fock operators of the HF-SCF method is adopted according to the Moller-Plesset [87] perturbation theory (MPPT) in order to obtain the correlation energy for the ground state. \hat{H}_0 is defined as the sum of the one electron Fock operator,

$$\hat{H}_0 = \sum_i F_i \tag{2.39}$$

and E_0 is the sum of the orbital energies, ϵ_i .

$$E_0 = \sum_i \epsilon_i \tag{2.40}$$

All Slater determinants are eigenfunctions of \hat{H}_0 , and the evaluation of matrix elements is greatly simplified. The perturbation, \hat{H}' , is defined as $H - H_0$. Although this supposition does not obey the main assumption that the perturbation should be small, it satisfies the other requirement that solutions of unperturbed Schrödinger equation should be known. Therefore, this is the only choice having the requested size extensivity property.

A correction of the electron correlation energy is achieved, if at least a 2nd order perturbation is considered. The inclusion of such a second-order energy correction involves only a sum over doubly occupied excited determinants. These can be generated by exciting the electrons from i and j orbitals to virtual a and b orbitals.

$$W_2 = \sum_{i < j}^{occ} \sum_{a < b}^{vir} \frac{\langle \Phi_0 | \hat{H}' | \Phi_{ij}^{ab} \rangle \langle \Phi_{ij}^{ab} | \hat{H}' | \Phi_0 \rangle}{E_0 - E_{ij}^{ab}} \quad (2.41)$$

The difference in total energy of two Slater determinants becomes a difference in MO energies, therefore a more explicit formula for second order Møller Pleset correction to energy, $E(\text{MP2})$, can be given as

$$E(\text{MP2}) = \sum_{i < j}^{occ} \sum_{a < b}^{vir} \frac{[\langle \phi_i \phi_j | \phi_a \phi_b \rangle - \langle \phi_i \phi_j | \phi_b \phi_a \rangle]^2}{\epsilon_i + \epsilon_j - (\epsilon_a + \epsilon_b)} \quad (2.42)$$

Supplementary explanations for PT and MPn theories, as well as, the formula of first and second order correction to wave function are available in most of the computational chemistry books [69, 88, 89].

The low cost compared to CI methods makes MP2 calculations one of the most economical methods for including electron correlation. If MPPT is extended to include third- and fourth-order energy correction, the procedures are referred to as MP3 and MP4, and the algebra involved becomes more and more complicated.

Perturbation theory (PT) can be applied to the references other than the solutions of HF-SCF method. The unperturbed wave function for example can be multi-configurational function obtained from an MCSCF calculation. As mentioned previously, MCSCF methods cannot recover the dynamic correlation well. Therefore, the application of PT to an MCSCF wave function introduces this type of electron correlation to total energy. There are several methodologies using MCSCF wave function as the reference for PT [90-93]. Single-state multireference second

order perturbation theory of Hirao and Nakano [94, 95] is one of the examples, which is employed within in this thesis.

2.5.4. Coupled Cluster (CC) Theory

Perturbation methods add all types of excitations (S, D, T, Q etc.) to the reference wave function to a given order (2, 3, 4 etc.). The idea in Coupled Cluster (CC) [96-98] methods is to include all corrections of a given type to infinite order. The coupled cluster wave function is written as

$$\Psi_{CC} = e^{\hat{T}} \Phi_0 \quad (2.43)$$

$$e^{\hat{T}} = 1 + \hat{T} + \frac{1}{2}\hat{T}^2 + \frac{1}{6}\hat{T}^3 + \dots = \sum_{k=0}^{\infty} \frac{1}{k!} \hat{T}^k \quad (2.44)$$

where the cluster operator T is given by

$$\hat{T} = \hat{T}_1 + \hat{T}_2 + \hat{T}_3 + \dots + \hat{T}_N \quad (2.45)$$

The \hat{T}_i operator acting on a HF reference wave function generates all i^{th} excited Slater determinants.

$$\hat{T}_1 \Phi_0 = \sum_i^{\text{occ}} \sum_a^{\text{vir}} t_i^a \Phi_i^a \quad (2.46a)$$

$$\hat{T}_2 \Phi_0 = \sum_{i < j}^{\text{occ}} \sum_{a < b}^{\text{vir}} t_{ij}^{ab} \Phi_{ij}^{ab} \quad (2.46b)$$

The expansion coefficients are called amplitudes. From equations 2.44 and 2.45 the exponential operator may be written as

$$e^{\hat{T}} = 1 + \hat{T}_1 + (\hat{T}_2 + \frac{1}{2}\hat{T}_1^2) + (\hat{T}_3 + \hat{T}_2\hat{T}_1 + \frac{1}{6}\hat{T}_1^3) + \dots \quad (2.47)$$

The first term generates the reference HF and the second all singly excited states. The first term in parenthesis generates all doubly excited states. The second parenthesis generates all triply excited states.

When coupled cluster wave function (equation 2.43) is used, the Schrödinger equation becomes

$$H e^{\hat{T}} \Phi_0 = E e^{\hat{T}} \Phi_0 \quad (2.48)$$

Multiplying this equation from the left by Φ_0^* and integrating gives

$$E_{CC} = \langle \Phi_0 | H e^{\hat{T}} | \Phi_0 \rangle \quad (2.49)$$

Expanding $e^{\hat{T}}$ and applying the fact that Hamiltonian contains only one- and two-electron operators as well as knowing that the matrix elements formed from singly excited Slater determinants are zero since HF orbitals are used, E_{CC} becomes [69]

$$E_{CC} = E_0 + \sum_{i < j}^{occ} \sum_{a < b}^{vir} (t_{ij}^{ab} + t_i^a t_j^b - t_i^b t_j^a) (\langle \phi_i \phi_j | \phi_a \phi_b \rangle - \langle \phi_i \phi_j | \phi_b \phi_a \rangle) \quad (2.50)$$

Truncated coupled cluster methods are used due to the limitations of computational resources. As stated earlier, inclusion of only the \hat{T}_1 operator does not yield any improvement over HF. The lowest level of approximation is therefore $\hat{T} = \hat{T}_2$, referred to as CCD [99]. Using $\hat{T} = \hat{T}_1 + \hat{T}_2$ gives the CCSD [97, 100-102] model. The contribution of triples can be evaluated by perturbation theory and added to the CCSD results thus resulting in a method abbreviated as CCSD(T) [103]. If all cluster operators up to \hat{T}_N are included in \hat{T} , all possible excited determinants are generated and the coupled cluster wave function is equivalent to full CI.

In this thesis, we employed both CCSD(T) theory implemented in GAUSSIAN 98 [104] and the completely renormalized (CR) coupled-cluster theory of Piecuch *et al.* [105] with single and double excitations and noniterative inclusion of triples. The latter method, denoted by CR-CCSD(T), is implemented in the GAMESS program [106]. Despite the fact that it is a single-reference method based on the closed-shell RHF determinant, it appears to yield excellent results even for biradical structures that normally require a multireference treatment.

2.5.5. Density Functional Theory (DFT)

Density functional theory (DFT) has its roots in the work of Thomas and Fermi in the 1920s [107, 108], but the real basis for this theory is the proof of Hohenberg and Kohn [109] stating that the ground state electronic energy is

determined completely by the electron density, $\rho(\mathbf{r})$, meaning that there is a one-to-one correspondence between the density of the system and its energy. DFT allows replacement of the complicated N-electron wave function Ψ (depends on 3N coordinates) and the associated Schrödinger equation by much simpler electron density (depends only on three coordinates). This is the reason that DFT has been growing in popularity over the past decade. Nevertheless, the “only” but “challenging” problem is that, although it has been proven that the density yielding the ground state energy is unique, the functional connecting these two quantities is still elusive. Therefore, the main aim of DFT methods is to achieve the correct functional connecting the electron density with the energy.

The procedure in DFT calculations is quite similar to that in HF theory. The HF energy for a single determinant wave function $\Phi = |\phi_1 \phi_2 \dots \phi_N|$ is obtained by equation 2.12. The last term before V_{nn} in equation 2.12 is the exchange contribution,

$$E_{\chi}^{\text{HF}} = -\frac{1}{2} \sum_i^N \sum_j^N K_{ij} \quad (2.51)$$

The orbitals are found by solving the HF equations (2.24). In DFT, the exchange term in the HF energy is replaced by the exchange-correlation energy functional

$$E^{\text{DFT}} = \sum_i^N h_{ii} + \frac{1}{2} \sum_i^N \sum_j^N J_{ij} + E_{\chi c}[\rho] \quad (2.52)$$

where the electron density ρ is assumed to have the form

$$\rho(\mathbf{r}) = \sum_{i=1}^N \phi_i^*(\mathbf{r}) \phi_i(\mathbf{r}) = \sum_{i=1}^{N_{\alpha}} \phi_i^{\alpha*} \phi_i^{\alpha} + \sum_{i=1}^{N_{\beta}} \phi_i^{\beta*} \phi_i^{\beta} = \rho_{\alpha} + \rho_{\beta} \quad (2.53)$$

As in the HF theory, for a closed-shell case $\phi_i^{\alpha} = \phi_i^{\beta}$ and $\rho_{\alpha} = \rho_{\beta}$; in the unrestricted DFT (for open shells), $\rho_{\alpha} \neq \rho_{\beta}$ and the α , β spin densities are independent.

The orbitals in DFT are found by solving the Kohn-Sham equations [110]

$$\left(-\frac{1}{2} \nabla^2 + V_{ne}(\mathbf{r}) + \int \frac{\rho(\mathbf{r}')}{|\mathbf{r} - \mathbf{r}'|} d\mathbf{r}' + v_{xc} \right) \phi_i = \epsilon_i \phi_i \quad (2.54)$$

where one electron (first two terms) and Coulomb (third term) parts are identical in form to Fock matrix and the one electron potential v_{xc} is obtained as the functional derivative of E_{xc} (for the closed-shell case)

$$v_{xc}(r) = \frac{\delta E_{xc}}{\delta \rho} \quad (2.55)$$

As stated in the beginning, the major problem in DFT is that an exact expression for $E_{xc}[\rho]$ (and therefore the potential v_{xc}) is not known. There are several commonly used approximate expressions for E_{xc} , all of which are based on a non-interacting, homogenous electron gas in the ground state. It is customary to split E_{xc} and v_{xc} into an exchange and a correlation part, in spite of its unknown validity.

$$E_{xc}[\rho] = E_x[\rho] + E_c[\rho] \quad (2.56a)$$

$$v_{xc} = v_x + v_c \quad (2.56b)$$

The functionals suggested in the literature can be grouped into three types that will be presented in the subsequent section.

2.5.5.1. Local spin density approximation (LSDA)

It is assumed that the density locally can be treated as a uniform electron gas, or equivalently that the density is a slowly varying function. The functionals E_x and E_c are those appropriate for a homogeneous electron gas, and contain only the density, ρ (ρ_α and ρ_β in the unrestricted case). The local exchange term is as follows

$$E_x^{LSDA}[\rho_\alpha, \rho_\beta] = -2^{1/3} C_x \int \left(\rho_\alpha^{4/3} + \rho_\beta^{4/3} \right) dr \quad (2.57)$$

where $C_x = \frac{3}{4} \left(\frac{3}{\pi} \right)^{1/3}$ in Thomas-Fermi-Dirac [111] model. The potential $v_x^\alpha(r)$ obtained from this expression is

$$v_x^\alpha(r) = \frac{\delta E_x^{LSDA}}{\delta \rho_\alpha} = -2^{1/3} C_x \rho_\alpha^{1/3} \quad (2.58)$$

and similarly for $v_x^\beta(r)$

$$v_x^\beta(r) = \frac{\delta E_x^{LSDA}}{\delta \rho_\beta} = -2^{1/3} C_x \rho_\beta^{1/3} \quad (2.59)$$

The correlation energy of a uniform electron gas, which has been found by Monte Carlo methods of different densities, has been put into a functional form, which can be employed in DFT calculations, by Vosko, Wilk and Nusair [112]. It is commonly denoted by E_c^{VWN} (or E_c^{LSDA}), and leads to v_c^{vwm} to be used in equation 2.54.

2.5.5.2. Generalized gradient approximation (GGA)

In order to improve LSDA, a non-uniform electron gas behavior should be taken into account. A step in this direction is to make the exchange and correlation energies depend on not only electron density, but also on derivatives of the density, $E_{\text{xc}}[\rho, \nabla\rho]$. Such methods are known as *Gradient Corrected* or *Generalized Gradient Approximation* (GGA) methods. The acronyms for the more popular functionals are given in Table 2.2. Any exchange functional in the table may be used with any correlation functional.

Table 2.2 Acronyms for some popular functionals in DFT.

| Exchange functionals, E_x^{GGA} | Correlation functionals, E_c^{GGA} |
|--|---|
| B88 (Becke 88) [113] | LYP (Lee-Yang-Parr) [114] |
| PW86 (Perdew-Wang 86) [115] | P86 (Perdew 86) [116] |
| PW91 (Perdew-Wang 91) [117] | PW91 (PerdewWang 91) [118, 119] |
| | B96 (Becke 96) [120] |

2.5.5.3. Hybrid methods

The functionals in the previous two groups contain electron density (in sections 2.5.5.1 and 2.5.5.2), and gradients of the density (in section 2.5.5.2). The Kohn-Sham orbitals ϕ_i do not explicitly enter into the expressions for E_{xc} except for the implicit dependence of ρ on ϕ_i through Equation 2.53. The exchange-correlation energy $E_{\text{xc}}[\rho]$ can be obtained by a suitable combination of exchange functionals of

LSDA and HF and a gradient corrected term (e.g. $E_x^{B88}, E_x^{PW91}, etc.$) with correlation functionals of LSDA plus a gradient corrected term (e.g. $E_c^{P86}, E_c^{P86}, etc.$). Such models including HF exchange (equation 2.52) are called *hybrid* methods. One of the most commonly used hybrid functional is B3LYP formed from the Becke's 3-parameter exchange hybrid functional [121] with Lee, Yang, Parr (LYP) correlation functional [114].

$$E_{xc}^{B3LYP} = aE_x^{LSDA} + (1-a)E_x^{HF} + b\Delta E_x^{B88} + c\Delta E_c^{LYP} \quad (2.60)$$

where $\Delta E_x^{B88} = E_x^{B88} - E_x^{LSDA}$, $\Delta E_c^{LYP} = E_c^{LYP} - E_c^{LSDA}$ and the empirical values of the parameters are: $a = 0.80$, $b = 0.72$, and $c = 0.81$.

2.5.6. The Computational Chemistry Suites Employed

The calculations in this work have mostly been performed by using Gaussian 98 [104]. Additionally, GAMESS [106] and HONDO [122] computational chemistry packages have been employed in section 3.2.1. A graphical interface program [123], which allows full integration of various packages including Gaussian 98, GAMESS, and HONDO, have been used for the processes of giving input and assessing output, as well as all kind of visualization jobs.

CHAPTER III

RESULTS AND DISCUSSION

The unimolecular rearrangements of cyclic C_5H_6 isomers have been studied by utilizing quantum chemical methods involving ab initio and density functional (DFT) theories. Initially, geometries and energies of minima on the singlet state (electronic) potential energy surface (PES) of C_5H_6 have been determined at (U)B3LYP/cc-pVTZ and CASSCF(4,4)/6-31G(d) levels of theory. Additionally, the energies of these isomers in triplet state have also been calculated at the same levels. The aim of locating triplet states is both to decide whether the ground state of each species is singlet or triplet, and to calculate their singlet – triplet state energy separations that has importance in understanding their overall reactivity. Finally, geometries and energies of the transition state structures (TSs) connecting these minima have been obtained at different levels of theory including mainly DFT methods. The details related to the levels used will be given in the appropriate places of the text. The nature of each stationary point on the PES was identified by harmonic vibrational analysis. A stationary point is a minimum if all of its vibrational frequencies have positive values and it is a TS i.e. first order saddle point if it has only one imaginary frequency. The most challenging stage of the study was the prediction of the TS geometries, because we do not have any straightforward method available for finding their geometries other than our chemical intuition and our ability of estimating the probable reaction coordinate. Furthermore, discovering and identifying a TS is not enough in some cases, it is also necessary to prove that the TS connects the desired reactant to the desired product. Fortunately, there is a convenient method, called intrinsic reaction coordinate (IRC) [124, 125], for this purpose. The IRC paths were traced in order to check the

energy profiles connecting each TS to the two associated minima of the proposed mechanism. Throughout the text, all distances are in Å and all angles are in degrees.

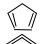
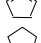

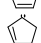
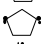
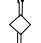




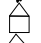




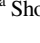


3.1. Stable Cyclic C₅H₆ Structures

3.1.1. Minima on Singlet and Triplet Potential Energy Surfaces of C₅H₆

The energetic and electronic properties of all stable isomers on both singlet and triplet PES of C₅H₆ are given in Tables 3.1 – 3.4, in which their relative energies and zero point vibrational energies (ZPVE), points group symmetries, electronic states and electronic configurations are commonly included. First two tables (3.1 and 3.2) show the results of (U)B3LYP/cc-pVTZ level optimizations, while last two (Tables 3.3 and 3.4) belong to those of CASSCF(4,4)/6-31G(d) level calculations. All energies reported in the tables are relative to singlet cyclopenta-1,3-diene (¹M1), thermodynamically the most stable cyclic isomer among all. The $\langle S^2 \rangle$ values are also included in the Tables 3.1 and 3.2 representing DFT results. Furthermore, Tables 3.1 and 3.3 include the vertical S–T energy separations, $\Delta E_{S-T}^{ver} = E_{Triplet} - E_{Singlet}$ calculated at singlet state optimized geometries, while Tables 3.2 and 3.4 contain the adiabatic S–T energy gaps, ΔE_{S-T} . Electronic energies (in Hartrees) and cartesian coordinates of all minima at both levels of theory are given in Appendices A and B, respectively.

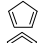
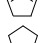
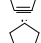
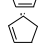
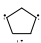
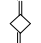
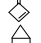








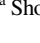


CASSCF method recover only a small portion of the electron correlation, which is very important for obtaining reliable energies of molecules, even though it gives more explicit results on their electronic structures. On the other hand, DFT methods (especially B3LYP functionals) cover appreciable amount of the electron correlation and give results that generally agree with experimental observations in terms of both energy and geometry. For these reasons, our discussion will mostly be based upon the results of (U)B3LYP/cc-pVTZ level calculations. The relative energies of all singlet state isomers at (U)B3LYP/cc-pVTZ level are depicted in Figure 3.1. Additionally, the vertical (ΔE_{S-T}^{ver}) and adiabatic (ΔE_{S-T}) S–T energy separations obtained from the same level of theory are given in Figure 3.2.

Table 3.1 Energies and ZPVE^a (in kcal/mol) relative to those of singlet cyclopenta-1,3-diene (¹M1), <S²> values, point group symmetries, electronic states and configurations of singlet states of all isomers at (U)B3LYP/cc-pVTZ level. Last column includes the vertical S-T energy splittings, $\Delta E_{S-T}^{ver} = E_{Triplet} - E_{Singlet}$, at singlet geometries.

| Isomer | (U)B3LYP/cc-pVTZ | <S ² > | Point Group | Electronic State | Configuration | ΔE_{S-T}^{ver} |
|---|----------------------------------|-------------------|-----------------|-------------------------------|---|------------------------|
|  M1 | -194.174117 ^b (57.93) | 0.000 | C _{2v} | ¹ A ₁ | ..(2b ₁) ² (1a ₂) ² | 74.39 |
|  M2 | 67.03 (-1.84) | 0.856 | C ₂ | ¹ A | ..(8b) ² (10a) ² | 4.88 |
|  M3 | 85.74 (-0.99) | 0.287 | C _s | ¹ A' | | 25.80 |
|  M4 | 71.48 (-2.50) | 0.216 | C _{2v} | ¹ A | | 16.34 |
|  M5 | 61.96 (-1.50) | 0.257 | C _s | ¹ A | | 10.97 |
|  M6 | 141.14 (-5.10) | 0.398 | C ₁ | ¹ A | | 12.81 |
|  M7 | 86.89 (-1.44) | 0.000 | C _s | ¹ A' | ..(12a') ² (13a') ² | 43.16 |
|  M8 | 26.80 (-0.82) | 0.000 | C _s | ¹ A' | ..(2a'') ² (3a'') ² | 78.78 |
|  B1 | 49.67 (-0.49) | 0.000 | C _s | ¹ A' | ..(6a'') ² (12a') ² | |
|  B2 | 96.85 (-1.27) | 0.000 | C _s | ¹ A' | ..(11a') ² (12a') ² | 48.04 |
|  B3 | 90.10 (-1.74) | 0.000 | C ₁ | ¹ A | | 41.31 |
|  B4 | 91.68 (-1.50) | 0.000 | C ₁ | ¹ A | | 52.91 |
|  B5 | | | | | | |
|  B6 | 85.26 (-1.09) | 0.000 | C ₁ | ¹ A | | 65.44 |
|  B7 | 67.65 (-1.93) | 0.000 | C _{2v} | ¹ A ₁ | ..(9a ₁) ² (4b ₁) ² | 89.31 |
|  T1 | 67.15 (-0.68) | 0.000 | C _{2v} | ¹ A ₁ | ..(1a ₂) ² (9a ₁) ² | 167.29 |
|  T2 | 61.29 (0.42) | 0.000 | D _{3h} | ¹ A ₁ ' | ..(2e'') ² (5a ₁ ') ² | 107.12 |
|  T3 | 93.25 (-1.09) | 0.000 | C ₁ | ¹ A | | 113.34 |



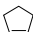


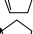

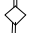







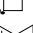


^a Shown in parenthesis. ^b Reference electronic energy in Hartrees.

Table 3.2 Energies and ZPVE^a (in kcal/mol) relative to those of singlet cyclopenta-1,3-diene (¹M1), <S²> values, point group symmetries, electronic states and electronic configurations of triplet states of all isomers at UB3LYP/cc-pVTZ level. Last column includes the adiabatic S-T energy splittings, ΔE_{S-T} .

| Isomer | UB3LYP/cc-pVTZ | <S ² > | Point Group | Electronic State | Configuration | ΔE_{S-T} |
|---|----------------|-------------------|-----------------|-------------------------------|--|------------------|
|  M1 | 57.04 (-2.85) | 2.007 | C _{2v} | ³ B ₂ | ..(2b ₁) ² (1a ₂)(3b ₁) | 54.19 |
|  M2 | 68.79 (-1.69) | 2.013 | C _{2v} | ³ A ₂ | ..(2b ₁) ² (9a ₁)(2a ₂) | 1.91 |
|  M3 | 103.80 (-0.51) | 2.004 | C _s | ³ A'' | ..(11a') ² (12a') ² (7a'') | 18.53 |
|  M4 | 78.77 (-1.25) | 2.006 | C _{2v} | ³ B ₁ | ..(2b ₁) ² (9a ₁)(3b ₁) | 8.54 |
|  M5 | 66.36 (-1.19) | 2.033 | C _s | ³ A'' | ..(3a') ² (15a') ² (4a'') | 4.71 |
|  M6 | 144.08 (-3.10) | 2.008 | C ₁ | ³ A | | 4.94 |
|  M7 | 128.82 (-2.71) | 2.009 | C _s | ³ A'' | ..(12a') ² (13a') ² (6a'') | 40.66 |
|  M8 | 87.18 (-3.75) | 2.015 | C ₁ | ³ A | | 57.44 |
|  B1 | | | | | | |
|  B2 | 122.86 (-1.50) | 2.006 | C _s | ³ A'' | ..(11a') ² (12a') ² (7a'') | 25.77 |
|  B3 | 112.10 (-2.16) | 2.006 | C ₁ | ³ A | | 21.59 |
|  B4 | 113.27 (-1.68) | 2.005 | C ₁ | ³ A | | 21.41 |
|  B5 | 117.07 (-1.45) | 2.005 | C _s | ³ A' | ..(7a') ² (11a') ² (12a') | |
|  B6 | 109.98 (-1.29) | 2.006 | C ₁ | ³ A | | 24.51 |
|  B7 | 120.85 (-3.21) | 2.007 | C ₂ | ³ B | ..(10a) ² (8b)(11a) | 51.93 |
|  T1 | 127.89 (-2.16) | 2.007 | C _{2v} | ³ B ₂ | ..(4b ₁) ² (5b ₂)(9a ₁) | 59.25 |
|  T2 | 154.02 (-0.77) | 2.004 | D _{3h} | ³ A ₂ ' | ..(1e') ² (2e') ² (3a') | 91.55 |
|  T3 | 110.71 (-2.32) | 2.007 | C ₁ | ³ A | | 16.24 |





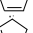
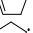
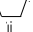
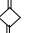
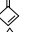






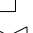


^a Shown in parenthesis

Table 3.3 Energies and ZPVE^a (in kcal/mol) relative to those of singlet cyclopenta-1,3-diene (¹M1), point group symmetries, electronic states and configurations of singlet states of all isomers at CASSCF(4,4)/6-31G(d) level. Last column includes the vertical S-T energy splittings, $\Delta E_{S-T}^{ver} = E_{Triplet} - E_{Singlet}$, at singlet optimized geometries.

| Isomer | CASSCF(4,4)/6-31G(d) | Point Group | Electronic State | Configuration | ΔE_{S-T}^{ver} |
|---|----------------------------------|-----------------|-------------------------------|---|------------------------|
|  M1 | -192.846625 ^b (61.30) | C _{2v} | ¹ A ₁ | ..(2b ₁) ² (1a ₂) ² | 76.75 |
|  M2 | 61.16 (-0.50) | C ₂ | ¹ A | ..(10a) ² (8b) ² | 16.07 |
|  M3 | 69.41 (0.83) | C _s | ¹ A' | ..(7a' ² 11a' ²) | 31.86 |
|  M4 | 68.42 (-1.46) | C _{2v} | ¹ A ₁ | ..(2b ₁) ² (9a ₁) ² | 8.78 |
|  M5 | 62.46 (-0.51) | C _s | ¹ A' | ..(3a' ² 15a' ²) | 6.50 |
|  M6 | 136.69 (-2.93) | C ₁ | ¹ A | | 9.20 |
|  M7 | 77.16 (-0.45) | C _s | ¹ A' | ..(12a' ² 13a' ²) | 115.55 |
|  M8 | 27.75 (-0.93) | C _s | ¹ A' | ..(2a' ² 3a' ²) | 80.51 |
|  B1 | 55.02 (0.02) | C _s | ¹ A' | ..(11a' ² 12a' ²) | 84.98 |
|  B2 | 96.23 (0.21) | C _s | ¹ A' | ..(11a' ² 12a' ²) | 46.29 |
|  B3 | 93.89 (-0.40) | C ₁ | ¹ A | | 40.60 |
|  B4 | 93.44 (-0.32) | C ₁ | ¹ A | | 52.77 |
|  B5 | | | | | |
|  B6 | 93.22 (0.10) | C ₁ | ¹ A | | 69.27 |
|  B7 | 69.56 (-1.37) | C _{2v} | ¹ A ₁ | ..(9a ₁) ² (4b ₁) ² | 100.57 |
|  T1 | 87.62 (0.41) | C _{2v} | ¹ A ₁ | ..(1a ₂) ² (9a ₁) ² | 58.59 |
|  T2 | 78.10 (1.83) | D _{3h} | ¹ A ₁ ' | ..(2e' ² 5a ₁ ' ²) | 103.74 |
|  T3 | 105.30 (0.17) | C ₁ | ¹ A | | 70.51 |

^a Shown in parenthesis. ^b Reference electronic energy in Hartrees.

Table 3.4 Energies and ZPVE^a (in kcal/mol) relative to those of singlet cyclopenta-1,3-diene (¹M1), point group symmetries, electronic states and electronic configurations of triplet states of all isomers at CASSCF(4,4)/6-31G(d) level. Last column includes the adiabatic S-T energy splittings, ΔE_{S-T} .

| Isomer | CASSCF(4,4)/6-31G(d) | Point Group | Electronic State | Configuration | ΔE_{S-T} |
|---|----------------------|-----------------|--------------------------------|--|------------------|
|  M1 | 58.36 (58.41) | C ₁ | ³ A | | 58.36 |
|  M2 | 68.95 (1.66) | C _{2v} | ³ A ₂ | ..(2b ₁) ² (9a ₁)(2a ₂) | 8.29 |
|  M3 | 94.09 (3.61) | C _s | ³ A'' | ..(11a' ² 7a'')(12a') | 23.85 |
|  M4 | 68.29 (2.63) | C _{2v} | ³ B ₁ | ..(2b ₁) ² (9a ₁)(3b ₁) | 1.34 |
|  M5 | 61.69 (2.51) | C _s | ³ A'' | ..(3a'') ² (15a') (4a'') | -0.25 |
|  M6 | 136.55 (1.03) | C ₁ | ³ A | | 2.79 |
|  M7 | 115.08 (2.36) | C _s | ³ A'' | ..(12a' ² 13a') (6a'') | 38.48 |
|  M8 | 87.58 (-0.53) | C ₁ | ³ A | | 60.76 |
|  B1 | 113.17 (1.69) | C ₁ | ³ A | | 58.13 |
|  B2 | 127.77 (3.07) | C _s | ³ A'' | ..(11a' ² 12a') (7a'') | 31.33 |
|  B3 | 117.81 (2.28) | C ₁ | ³ A | | 24.32 |
|  B4 | 127.86 (2.26) | C ₁ | ³ A | | 34.70 |
|  B5 | 132.67 (3.36) | C _s | ³ A' | ..(7a'') ² (11a') (12a') | |
|  B6 | 110.45 (3.18) | C ₁ | ³ A | | 17.24 |
|  B7 | 128.65 (1.20) | C ₂ | ³ B | ..(10a) ² (8b)(11a) | 60.46 |
|  T1 | 113.19 (2.76) | C _{2v} | ³ B ₂ | ..(4b ₁) ² (5b ₂)(9a ₁) | 53.62 |
|  T2 | 164.27 (4.13) | D _{3h} | ³ A ₂ '' | ..(1e' ² 2e') (3a') | 84.42 |
|  T3 | 117.39 (2.16) | C ₁ | ³ A | | 11.92 |

^a Shown in parenthesis

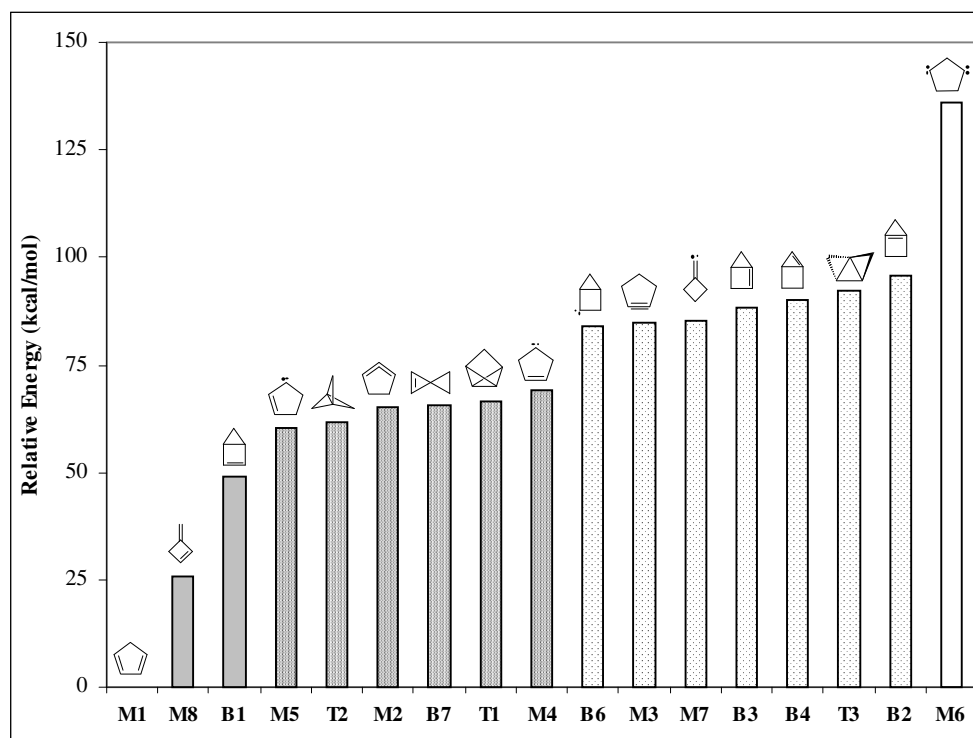


Figure 3.1 Relative energies of all singlet state isomers at (U)B3LYP/cc-pVTZ level.

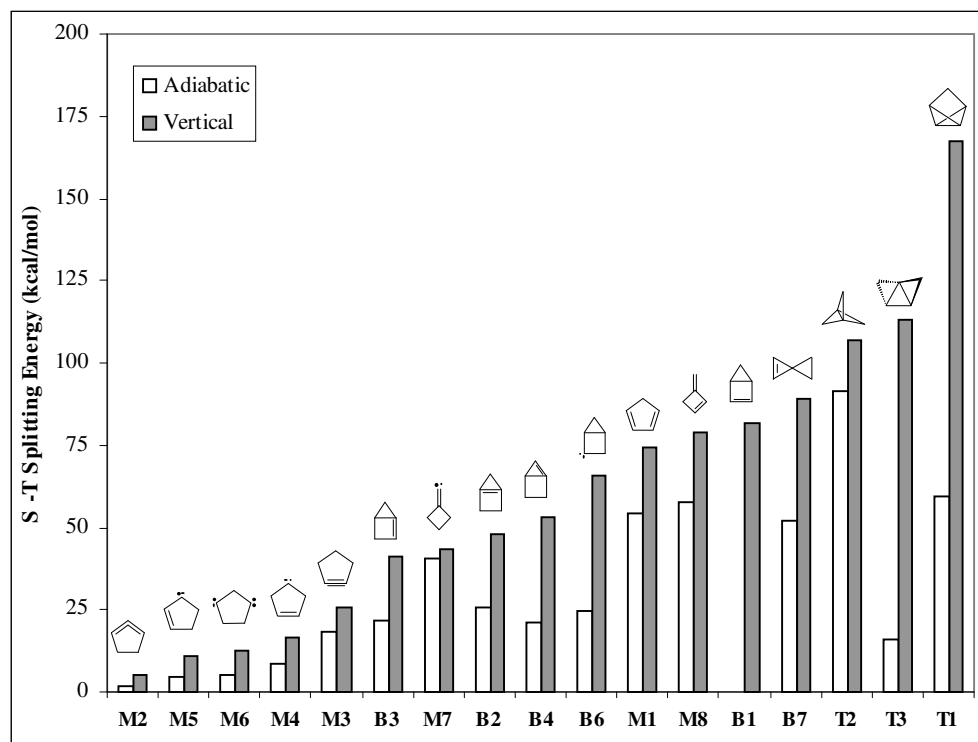


Figure 3.2 The vertical (ΔE_{S-T}^{ver}) and adiabatic (ΔE_{S-T}) S-T energy separations of all isomers at (U)B3LYP/cc-pVTZ level.

Cyclopenta-1,3-diene (**M1**) is the most stable cyclic isomer on C₅H₆ PES. Its stability is mostly originated from the conjugation of π -electrons, which are delocalized over π -molecular orbitals (π -MOs). Therefore, it is a well known and one of the most commonly used compounds in chemistry, especially in organic and organometallic chemistry.

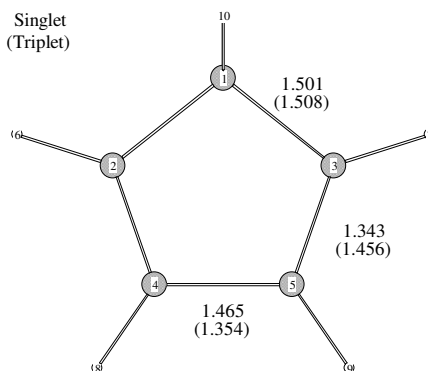


Figure 3.3 Geometrical parameters of cyclopenta-1,3-diene (**M1**) in both singlet and triplet (in parenthesis) states at RB3LYP/cc-pVTZ level.

Figure 3.3 depicts important parameters of the singlet and triplet state geometries of **M1**. The ground electronic state of this molecule is found to be 1A_1 with C_{2v} geometry. The C2-C4 and C3-C5 bonds are typical double bonds (1.343 Å), but the C4-C5 bond (1.465 Å) is considerably smaller than the usual single bond (1.54 Å), showing the delocalization of π -electrons over four carbon atoms. The situation is just the opposite in triplet state geometry having electronic state of 3B_2 . The C2-C4 and C3-C5 bonds are elongated to 1.456 Å and they lose the double bond characters while the C4-C5 bond gains a double bond character (1.354 Å). This state takes place almost 54 kcal/mol above the ground state since the π -electrons are not delocalized, anymore.

The second thermodynamically most stable cyclic isomer on C₅H₆ PES is 3-methylenecyclobutene (**M8**) lying ~26 kcal/mol above cyclopenta-1,3-diene. **M8** also owes its stability to the delocalization of π -electrons over conjugated double bonds. Its ground state has a planar C_s-symmetric structure with $^1A'$ electronic state. The geometrical parameters of **M8** obtained from DFT calculations are given in Figure 3.4, and the values in square brackets belong to the optimized structure at RMP2/6-311G+(3df,2p) level [34]. The geometries obtained from these two levels of

theory confirm each other quite well. The π bond in the ring (C3-C4) is a bit larger than the one outside (C1-C5) due to the ring constraints, and the bond between π -bonds (C1-C4) is considerably shorter than a typical single bond, indicating the π -electron delocalization. It is noteworthy that the corresponding single bonds located between π bonds in **M8** and **M1** have almost the same lengths.

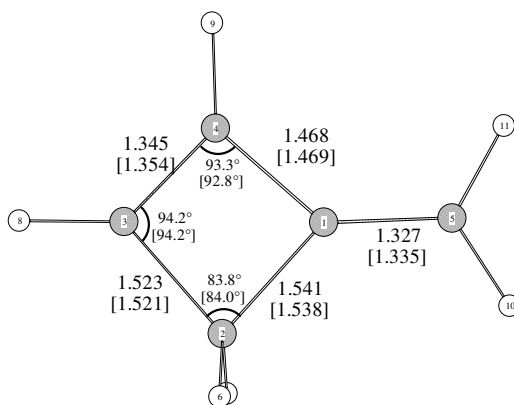


Figure 3.4 Ground state geometrical parameters of 3-methylenecyclobutene (**M8**) at RB3LYP/cc-pVTZ level. The values in square brackets belong to ref [34]

Bicyclo[2.1.0]pent-2-ene (**B1**) is the subsequent most stable cyclic C_5H_6 isomer (relative energy of ~ 49 kcal/mol) even though it has a strained bicyclic structure. Experimentally determined relative energy of **B1** is around 46 kcal/mol [126], accordingly the DFT level calculations overestimate the relative energy of **B1** only within 3 kcal/mol. The energy value obtained from CAS44 calculations, 10 kcal/mol above the experimental value, sustains our argument at the beginning. It has singlet ground state of C_s symmetry. This species is discussed in more detail in Section 3.2.1. The DFT calculations could not locate a stable triplet state geometry nearby the singlet structure. In contrast to DFT, CASSCF(4,4)/6-31G(d) level calculations found a stable triplet geometry. In order to remove this contradiction, triplet state geometry optimizations for **B1** isomer have also been performed by using UHF and UMP2 methods with standard 6-31G(d) basis set. These methods confirmed the CAS44 results. Figure 3.5 depicts the selected geometrical parameters of $^3\text{B1}$ found by UHF, UMP2 and CAS44 methods. Since three different methods

find a stationary point corresponding to **³B1**, we believe that bicyclo[2.1.0]pent-2-ene is stable at the geometry shown in Figure 3.5.

As is clear from Figure 3.5, the most prominent geometrical feature of **³B1** is that the double bond in the ground state geometry loses its character and turns into a single bond (~1.52 Å). The hydrogen atoms bound to C4 and C5 atoms have an anti arrangement implying that both carbon atoms have electron densities with parallel spins localized at the reverse sides of the hydrogen atoms.

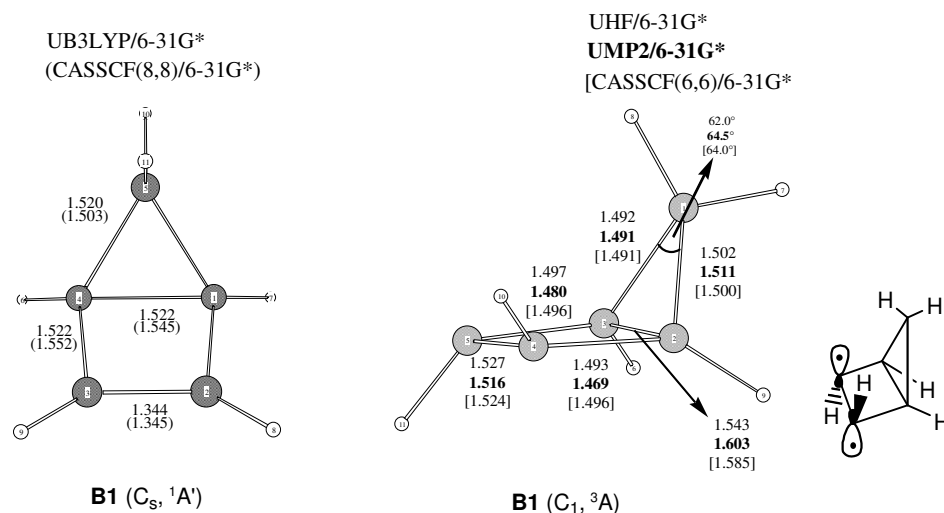


Figure 3.5 Selected singlet and triplet state geometrical parameters of bicyclo[2.1.0]pent-2-ene (**B1**) at various levels of theory.

The carbene structures **M4** and **M5**, tricyclic **T1** and **T2**, the allene **M2** and spiro-conjugated **B7** isomers lie in the relative energy range of 60 – 70 kcal/mol according to the (U)B3LYP/cc-pVTZ level calculations. The carbenes **M4** and **M5** are reactive intermediates (the details are in Section 3.2.3) whose relative energies predicted by DFT method are approximately 69 and 60 kcal/mol, respectively. **T1** is spectroscopically identified at low temperature [51], but it is converted into **M1** as the temperature is elevated. The **T2** isomer is a relatively stable compound, as well as it has relatively low reactivity. Wiberg *et al.* [127] predicted the experimental heat of formation value of **T2** as being 84 ± 1 kcal/mol in gas phase with an indirect method and hence it is calculated that the relative energy of **T2** with respect to **M1** is around 52 kcal/mol ($\Delta H_f^0 = 32.1 \pm 0.4$ kcal/mol [11] for **M1**). Although the DFT calculations (Table 3.1) ~9 kcal/mol overestimate this value, the geometry prediction

of this method is relatively reasonable. The largest deviations in calculated and experimental bond lengths and angles are 0.025 Å and 4.3°, respectively (Figure 3.6). The poor estimation of the energy is probably originated from the bridgehead bond that is slightly underestimated by the DFT calculations. The adiabatic singlet-triplet energy separation (ΔE_{S-T}) for **T2** has an empirical value of 94.3 kcal/mol [128]. The DFT method is rather successful in the estimation of ΔE_{S-T} of **T2**, which is only ~3 kcal/mol lower (Table 3.2) than the experimental value. This situation possibly indicates that the triplet state energy (relative to **M1**) predicted by DFT is overestimated, as well.

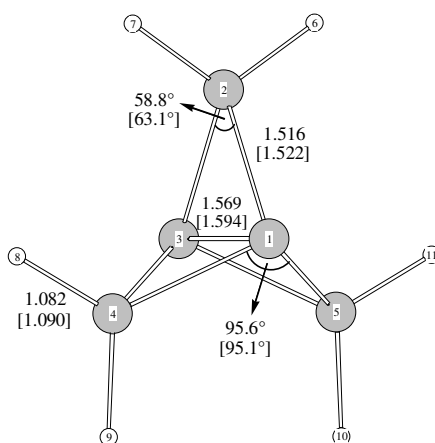


Figure 3.6 Selected ground state geometrical parameters of [1.1.1]propellane (**T2**) found at (U)B3LYP/cc-pVTZ level. The experimental values [129] are given in square brackets.

In 1985, Johnson *et al.* [15] performed ab initio calculations including HF, MP2 and MCSCF methods with extremely small STO-3G and 3-21G basis sets. They predicted that the ground state of **M2**, whose geometry has a chiral allenic structure with a very low racemization barrier, is the singlet state even though its S – T energy gap is rather low. In spite of their usage of very low level calculations comparing with the levels employed nowadays, both (U)B3LYP and CAS44 calculations completely confirm their predictions. Both methods predict that singlet spin state is the ground state of **M2**, and the singlet state geometries predicted by these methods have chiral allenic structures, as well. The relative energy of **M2** should be a value between 60 - 65 kcal/mol according to DFT and CAS44

calculations. Furthermore, they both agree with **M2** having a low-lying triplet state, hence it must have a considerable biradical character.

Several geometrical parameters of $^1\mathbf{M2}$ and $^3\mathbf{M2}$ are given in Figure 3.7. The singlet and triplet states have C_2 and C_{2v} point group symmetries, respectively. The most important difference between these geometries is observed in the spatial arrangement of allenic carbon atoms. In the singlet state, they are not in the same plane with the remaining two carbon atoms, on the other hand, the five carbon atoms of the triplet geometry are in the same plane. Moreover, the allenic angle is slightly smaller in singlet state. The calculations clearly indicate that the adiabatic S – T energy separation of **M2** is rather small (~ 2 kcal/mol in DFT and ~ 8 kcal/mol in CAS44).

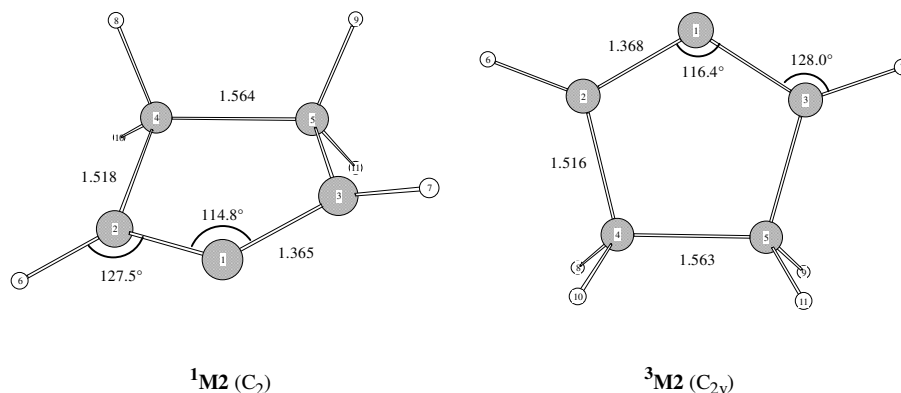


Figure 3.7 Selected singlet and triplet state geometrical parameters of cyclopenta-1,2-diene (**M2**) found at (U)B3LYP/cc-pVTZ level.

Spiropentene (**B7**) has a structure of cyclopropene put together with a cyclopropane ring through a spiro carbon atom. Due to lack of experimental formation enthalpy values for **B7**, our findings will be compared with high-level computational studies. In an earlier study, the formation enthalpy of **B7** was predicted to be 99.7 kcal/mol at RHF/4-31G level [130]. The recent estimations of high level G2(MP2) and G2(MP2, SVP) methods [131] for this parameter were 99.3 and 98.7 kcal/mol, respectively. When these values are compared with each other, it is seen that RHF/4-31G level calculations have surprisingly good predictions. Moreover, our CAS44 and DFT calculations have also very good performance. While the G2(MP2) and G2(MP2, SVP) energies of **B7** relative to **M1** are 67.7 and

67.9 kcal/mol, respectively, the DFT and CAS44 methods estimate its relative energy as ~66 kcal/mol.

We could not come across any spectroscopic data providing the geometrical parameters for this structure in the literature. Therefore, our discussion will be based on the singlet and triplet state (U)B3LYP/cc-pVTZ optimized geometries of spiropentene shown in Figure 3.8. Geometrical parameters of the singlet state predicted at several levels of theory including B3LYP/6-311++G(d,p) level calculations were previously presented by Dodziuk *et al.* [48]. As expected, (U)B3LYP/cc-pVTZ level geometry of **¹B7** almost exactly matches with B3LYP/6-311++G(d,p) since both basis sets have triple zeta character. The most intriguing feature of the triplet geometry, which is positioned ~50 kcal/mol above the singlet ground state in the energy scale, is the anti arrangement of the hydrogen atoms attached to the double bond carbons. The situation is very similar to the case of **³B1**. The two triplet structures have both electron densities with parallel spins located at the reverse sides of the hydrogen atoms and a carbon-carbon bond that loses its double bond character (Figure 3.8).

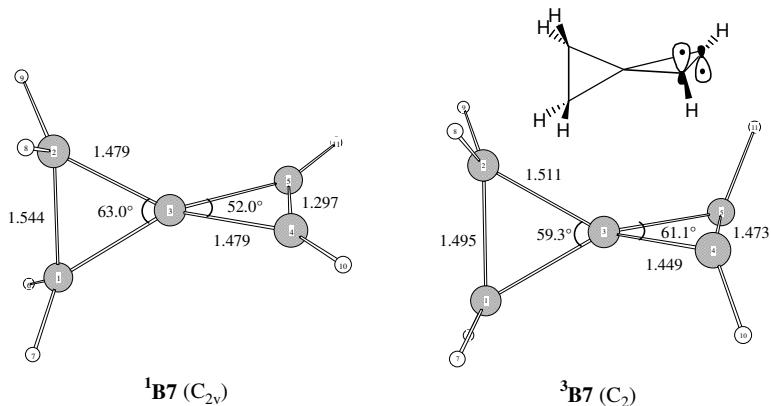


Figure 3.8 Selected singlet and triplet state geometrical parameters of spiropentene (**B7**) found at (U)B3LYP/cc-pVTZ level. The schematic representation of **³B7** is also shown.

In the 85 – 95 kcal/mol range, there are seven isomers including three bicyclic alkenes (**B2**, **B3**, **B4**), one bicyclic carbene (**B6**), cyclopentyne (**M3**) with its corresponding carbene (**M7**) and one tricyclic structure (**T3**). The existences of only two of them (**M3** and **T3**) are known as reactive intermediates. **M7** is the precursor

of cyclopentyne (the detailed information for isomerization of **M7** to **M3** is given in Section 3.2.4). Only a derivative of **B2** has been synthesized previously [43]. The remaining three isomers (**B3**, **B4** and **B6**) are hypothetical structures that have no experimental evidence for their existence. The DFT energy for the bicyclic carbene, **B6**, is almost 5 kcal/mol lower compared with those of other two isomers (~90 kcal/mol). On the other hand, the CAS44 method estimates that they all have almost equal relative energies (around 93 kcal/mol). At the first sight the CAS44 results may seem to be more plausible, because the higher stability of a carbene structure (**B6**) having incomplete valence shell with respect to the species **B3** and **B4** is not an expected situation. However, there is no spin contamination problem in **B6** structure since its lowest triplet state is energetically rather far away from the ground state, and it is known that electron correlation recovery of DFT methods, especially B3LYP functionals, is better than the CAS44 method. All of this information lead us to speculate that bicyclo[2.1.0]pent-2-ylidene have higher thermodynamical stability compared to **B3** and **B4**.

Cyclopentyne (**M3**) and its corresponding carbene (**M7**) are rather attractive C_5H_6 isomers because **M3** is the limiting structure (the smallest observed one) of a molecule group entitled cyclic alkynes, and **M7** is the major precursor of cyclopentyne. The comprehensive discussion of these isomers will be presented in section 3.2.4.

Tricyclo[2.1.0.0^{1,3}]pentane, **T3**, is structurally an interesting molecule due to being the first member of the bridged spiropentanes. Initially, its heat of formation (ΔH_f^0) was calculated as 132 kcal/mol by means of adding the experimental formation enthalpy of [1.1.1]propellane (**T2**) [127] to the energy of **T3** (relative to **T2**) found at MP2/6-31G(d) level [61]. Recently, ΔH_f^0 of **T3** has been recalculated as being 126 kcal/mol by means of “group equivalent approach” [132]. The calculated enthalpy of formation value of tricyclo[2.1.0.0^{1,3}]pentane by using DFT energies is 124.1 kcal/mol, which is the summation of the relative energy of **T3** isomer (~92 kcal/mol) and the experimental heat of formation value (32.1 kcal/mol) of **M1**. As the MP2 and B3LYP methods generally recover comparable amount of electron correlation, the formation enthalpy predictions of these methods corroborate each other reasonably good.

The ground singlet and the lowest triplet state **T3** geometries are shown in Figure 3.9 with their several geometrical parameters. The singlet DFT geometry contains deviations up to 0.07 Å in the bond lengths from that of MP2, so the geometries predicted by the two methods are significantly different. On the other hand, the singlet TS structure connecting **T3** to **M4** found by MP2 method [61] resembles the triplet **T3** geometry very much. It may be speculated that the triplet PES become very close to the singlet one at the point where the TS was reached. Another significant feature of **T3** molecule is that there is huge gap between the vertical and adiabatic S – T energy separations, around 97 kcal/mol. Such a high difference possibly arises from the very different singlet and triplet geometries. In the triplet geometry there is no bond between the C3 and C4 atoms (2.072 Å) while these carbons (1.507 Å) are bonded to each other in the singlet geometry.

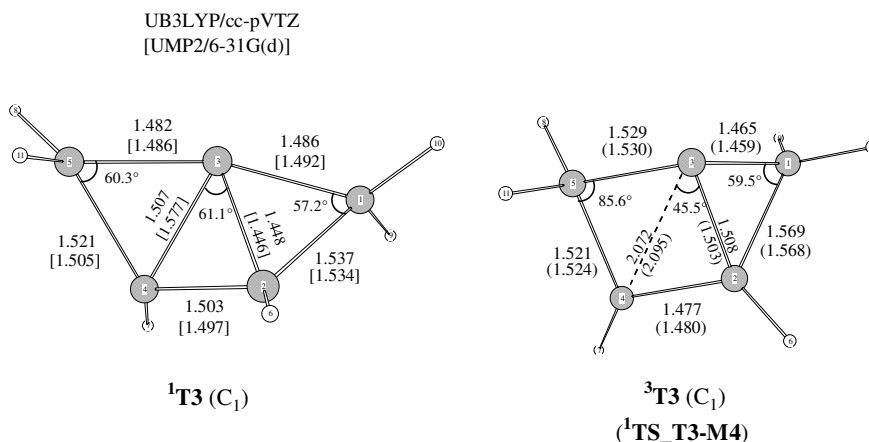


Figure 3.9 Selected singlet and triplet state geometrical parameters of tricyclo[2.1.1.0]^{1,3}pentane (**T3**) found at (U)B3LYP/cc-pVTZ level. The parameters in parenthesis belong to the TS structure of **T3** to **M4** isomerization optimized at UMP2/6-31G(d) level [61]. The values in square brackets are also taken from ref. [61].

Bicyclo[2.1.0]pent-1(4)-ene (**B2**) is the second most strained bicyclic cyclopropene derivative whose structures are bent rather than planar. Even though the double bonds have a tendency of being planar, the ring constraints tilt these bicyclic structures and they become pyramidalized olefins. The heat of formation for **B2** was predicted to be 133 kcal/mol via isodesmic reactions [133] at MP3/6-

31G(d,p)//MP2/6-31G(d) level of theory [44]. Our ΔH_f^0 prediction for this molecule (shown in equation 3.1) is ~128 kcal/mol at (U)B3LYP/cc-pVTZ level.

$$\Delta H_f^0(\mathbf{B2}) = E_{rel}(\mathbf{B2}) + \Delta H_f^0(\mathbf{M1})$$

$$\text{where } E_{rel}(\mathbf{B2}) = E_0^{B3LYP/cc-pVTZ}(\mathbf{B2}) - E_0^{B3LYP/cc-pVTZ}(\mathbf{M1}) \quad (3.1)$$

It can be accepted that these methods successfully confirm each other. It is a closed shell structure with no spin contamination problem. This is consistent with its vertical (ΔE_{S-T}^{ver}) and adiabatic (ΔE_{S-T}) S – T energy differences, ~48 and ~26 kcal/mol, respectively.

The DFT geometries and their selected geometrical parameters of $^1\mathbf{B2}$ and $^3\mathbf{B2}$ are given in Figure 3.10. The singlet state geometry almost matches the one found by MP2 method, especially both methods predict the angle between two rings, α , almost equal ($\alpha_{B3LYP} = 130.8^\circ$ and $\alpha_{MP2} = 128.9^\circ$). As expected, the double bond of $^1\mathbf{B2}$ geometry loses its character in the triplet state, i.e. C2-C3 bond distance elongates from 1.350 to 1.518 Å as the spin state changes from singlet to triplet.

M6, the only dicarbene structure, is the least stable one among all of the C_5H_6 isomers studied. Its existence is very unlikely because of having huge ground state energy, which is almost 135 kcal/mol above the ground state energy of **M1**. In other words, its heat of formation value is approximately 167 kcal/mol.

Although seventeen of the isomers have stable geometries on the singlet state PES of C_5H_6 , singlet state of bicyclo[2.1.0]pent-5-ylidene (**B5**) has no stable geometry at mentioned levels of theory. In order to check whether this structure is indeed unstable or not, additional optimizations were also performed at other levels (HF, MP2 with basis sets larger than the Pople's standard 6-31G(d) basis). None of these calculations resulted in a stable **B5** geometry, all of them distorted the structure to that of allene, **M2**. A recent study by Freemann *et al.* [134] supports our findings stating that B3LYP/6-31G(d) level optimization of **B5** relax to **M2** when there are no restrictions. Hence, it appears that the carbene structure (**B5**) containing three and four membered carbon rings fused to each other is not stable on singlet state PES in the gas phase.

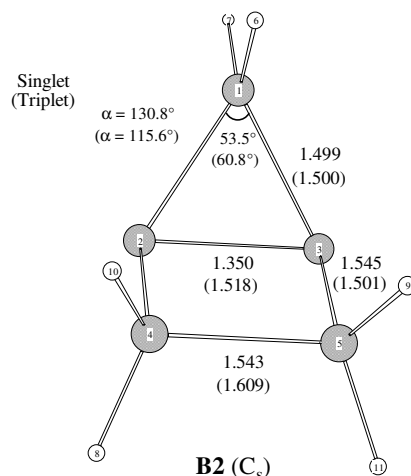


Figure 3.10 Selected singlet and triplet state geometrical parameters of bicyclo[2.1.0]pent-1(4)-ene (**B2**) found at (U)B3LYP/cc-pVTZ level.

Two important parameters in understanding the overall reactivity of a molecule are vertical (ΔE_{S-T}^{ver}) and adiabatic (ΔE_{S-T}) S – T energy differences. Usual closed shell molecules such as saturated hydrocarbons mostly do not have low-lying triplet states. On the other hand, some classes of molecules like carbenes, cyclic allenes, etc. have small singlet-triplet energy gaps. For example, CH_2 , the simplest carbene, has a triplet ground state [135]. When a singlet wavefunction calculated by a spin unrestricted methodology results in a nonzero $\langle S^2 \rangle$ value, the structure is expected to have some biradical character and a low-lying triplet state (or higher excited states) relative to closed shell structures ($\langle S^2 \rangle = 0$). Although DFT methods are not very fragile against "spin contamination", similar consequences are also valid for these methods in many cases. As seen from Table 3.1, five of the isomers have nonzero $\langle S^2 \rangle$ values for singlet state wave functions. When all isomers are arranged in increasing order of their vertical S - T energy gap values (Figure 3.2), those having nonzero $\langle S^2 \rangle$ values become the first five species. This situation clearly indicates the relationship between spin contamination and vertical S - T energy gap. The $\langle S^2 \rangle$ values for **M3**, **M4**, **M5** and **M6** are rather small compared with that of **M2**. Accordingly, it can be considered that latter isomer should have more biradical character than the other four. The quantitative determination of their biradical characters is not possible by taking only the $\langle S^2 \rangle$ values of those isomers into

account. One possible way of calculating the percent biradical character is the Jensen's biradical index [37], BR, defined as

$$BR = 2 - n_H \quad (3.2)$$

where n_H is the occupation number of the natural orbital corresponding to HOMO. Here, we have performed single point CASSCF(4,4)/6-311G(d,p) calculations on UB3LYP/cc-pVTZ level optimized geometries of **M2** – **M6** isomers to reveal their percent biradical natures via biradical index, BR. The occupation numbers of natural orbitals in four electron four orbital active space and BR values for these isomers are given in Table 3.5.

As mentioned, $\langle S^2 \rangle$ value for singlet state of a molecule obtained from DFT calculations does not quantitatively correspond to its percent biradical character (BR%). The following example evidently confirms this statement. The isomer **M3**, whose $\langle S^2 \rangle$ value is 0.287, has a biradical character of 21.5%, whereas **M6** is only 6.3%-biradicalic molecule having an $\langle S^2 \rangle$ value of 0.398. If the $\langle S^2 \rangle$ values were considered a quantitative measure of the biradical nature, the conclusion would be that **M6** has more biradical character than **M3**. However, the real situation is just the opposite proving the previous statement.

The isomers **M4**, **M5** and **M6** have so low BR% values that they can be considered as closed shell structures and, as expected, their $\langle S^2 \rangle$ values are smaller compared to that of **M2** isomer having a high biradical character. Cyclopentyne (**M3**) has a biradical character more than 20%, associated with the fact that in plane π^* natural orbital of **M3** contains appreciable amount of electron density. The allenic isomer, **M2**, has almost fifty percent biradical character in its ground state. It is seen from Table 3.6, triplet state of chiral allenic **M2** is low enough to create huge spin contamination. The ΔE_{S-T} values of **M3** and **T3** are very close to each other, 18.53 and 16.24 kcal/mol, respectively (Table 3.2). **T3** has no spin contamination while **M3** has considerably high $\langle S^2 \rangle$ value (0.287). Unlike ΔE_{S-T}^{ver} , smallness of ΔE_{S-T} value of a molecule does not necessarily indicate that it has a spin contamination or it has some biradical nature. The situation in **M3** and **T3** provides evidence for this statement.

Table 3.5 Occupation numbers (n_i) of natural orbitals in each active space and percent biradical characters (BR%) for **M2** – **M6** at CASSCF(4,4)/6-311G(d,p) level.

| Species | CASSCF(4,4)/6-311G(d,p) level ^a | | | | BR% ^b |
|-----------|--|-------|-------|-------|------------------|
| | n_1 | n_2 | n_3 | n_4 | |
| M2 | 1.889 | 1.532 | 0.477 | 0.102 | 46.9 |
| M3 | 1.920 | 1.785 | 0.216 | 0.079 | 21.5 |
| M4 | 1.938 | 1.919 | 0.081 | 0.062 | 8.1 |
| M5 | 1.944 | 1.919 | 0.090 | 0.046 | 8.1 |
| M6 | 1.939 | 1.937 | 0.065 | 0.059 | 6.3 |

^aSingle point energy calculation on UB3LYP/cc-pVTZ level optimized geometries.

^bBR%=(2- n_2)*100

Table 3.6 Vertical Singlet-Triplet State Energy Differences, ΔE_{S-T}^{ver} , of **M2** – **M6** in kcal/mol

| Species | ΔE_{S-T}^{ver} | | $\langle S^2 \rangle^b$ |
|-----------|-----------------------------------|-----------------------------|-------------------------|
| | CAS(4,4)/6-311G(d,p) ^a | UB3LYP/cc-pVTZ ^a | |
| M2 | 9.95 | 4.88 | 0.856 |
| M3 | 36.48 | 25.80 | 0.287 |
| M4 | 10.91 | 16.34 | 0.216 |
| M5 | 5.81 | 10.97 | 0.257 |
| M6 | 10.12 | 12.81 | 0.398 |

^aAll calculations were performed on singlet state optimized geometries at UB3LYP/cc-pVTZ level.

^b $\langle S^2 \rangle$ values are belong to singlet state UB3LYP/cc-pVTZ level calculations.

3.2. Unimolecular rearrangements of several cyclic C₅H₆ isomers

The cyclic C₅H₆ molecules on which we focused in this study isomerize via hydrogen shift, carbon shift and ring opening reactions. As indicated in the previous section, all of the isomers have singlet ground states, and therefore their rearrangements should take place on the singlet PES. Nevertheless, triplet states for several isomers (**M2** – **M6**) are so close to their singlet states that they may have some reactions taking place on triplet PES. As their relative energies are taken into account, a great number of the isomers are the reactive intermediates.

As already expressed, the most stable isomer is cyclopenta-1,3-diene molecule (**M1**) among cyclic C₅H₆ structures. In the previous studies, there are considerable amount of isomerization reactions in which **M1** involves as either reactant or product. Hence, we wish to begin our discussion with the reactions of several cyclic C₅H₆ isomers, all of whose products is cyclopentadiene. Particularly, we present the results of our computational studies on conversions of five isomers; cyclopentadiene (**M1**) itself, bicyclo[2.1.0]pent-2-ene (**B1**), tricyclo[2.1.0.0^{2,5}]-pentane (**T1**), 3-cyclopentenylidene (**M4**) and 2-cyclopentenylidene (**M5**) into the most stable cyclic C₅H₆ molecule (**M1**). The formation reaction of cyclopentyne (**M3**), the smallest cyclic alkyne ever synthesized, from its carbene isomer, cyclobutylidene methylene (**M7**) will be the next reaction to be discussed. Finally, we will present our finding on triplet state isomerization of bicyclo[2.1.0]pent-5-ylidene (³**B5**) into five membered ring allene, cyclopenta-1,2-diene (³**M2**). Electronic energies and cartesian coordinates of all TS structures of those reactions are given in Appendix C.

3.2.1. Isomerizations of Bicyclo[2.1.0]pent-2-ene and Tricyclo[2.1.0.0^{2,5}]-pentane into Cyclopenta-1,3-diene

Bicyclo[2.1.0]pent-2-ene (**B1**) is one of the strained C₅H₆ isomer that was first prepared in 1966 by Brauman, Ellis, and van Tamelen [36, 38, 39]. It was synthesized from the photolysis of cyclopentadiene (**M1**) by a method that was later sophisticated by Baldwin's group [40, 51, 126, 136-138] so that it could be obtained

in quantities adequate for synthetic utilization and other experimental work. The photolysis mixture was containing another C_5H_6 isomer, tricyclo[2.1.0.0^{2,5}]pentane (**T1**), which was later discovered by Andrews and Baldwin [51]. The proportions of **M1**:**B1**:**T1** in the photolysis mixture were approximately 14:7:1. Whether **M1** or **B1** is the source of **T1** was not recognized.

The fundamental importance of **B1** originates from its facile thermal conversion back to **M1**. The kinetics of the rearrangement at temperatures between 26.0 °C and 108.4 °C was studied by Brauman and Golden [38, 39], who reported $\log k(s^{-1}) = (14.2 \pm 0.2) - \frac{(26.9 \pm 0.3)}{2.303RT}$. They supposed that the reaction involved bridgehead bond cleavage in a disrotatory sense, which is forbidden according to Woodward-Hoffmann (W-H) rules of electrocyclic reactions [41]. The discussion about the reaction mode followed in the isomerization, [40, 51, 126, 137-139] has lasted almost a decade until the ¹³C labeling experiments of Andrews and Baldwin [40]. They proved that the reaction mechanism favors the disrotatory, disallowed biradical process that represents a counterexample to the W-H rules (Figure 3.11). While the molecular structure of **B1** has been determined by its microwave spectrum [138], the experimental reaction enthalpy of **B1** to **M1** conversion is also known, -47.8 ± 0.5 kcal/mol at 25 °C [141, 142].

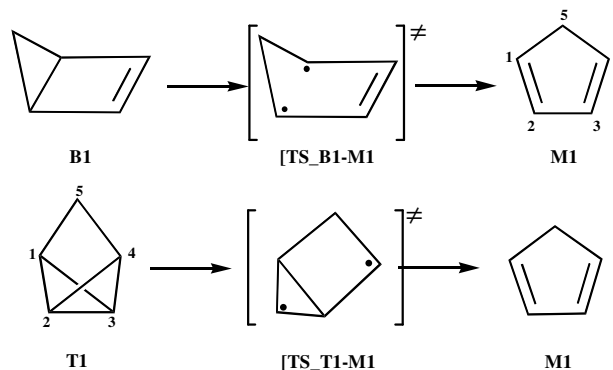


Figure 3.11 Schematic representation of conversions of **B1** and **T1** into **M1**

A limited number of computational studies on the ring opening of **B1** into **M1** are available in the literature. There are three semi empirical studies (MINDO/3)

[143-145] whose results are inconsistent with each other. Skancke, Yamashita, and Morokuma [146] have performed several ab initio calculations on the thermal reactions of **B1** including walk rearrangement and the ring opening to **M1**. They stated that the transition state structure of ring opening has considerable amount of biradical character. The activation barrier and reaction enthalpy values calculated at (U)MP4/6-31G(d)//(U)HF/3-21G level are in good agreement with the experiment. However, Jensen [37] criticized their result related to walk rearrangement in terms of use of spin contaminated UHF wave functions for the description of biradical states. Therefore, the closeness of Skancke, Yamashita, and Morokuma's results for the ring opening in **B1** to experiment might be fortuitous. The full reaction path has never been followed in the computational studies stated, but this is important because it has been suggested that forbidden pericyclic reactions cannot take place in a concerted manner; i.e. the reaction path must pass through intermediates [39, 143].

Although a lot of experimental studies of thermal reactions of **T1** and its derivatives [52, 147-156] are available in the literature, there is no data related to experimental reaction parameters of the ring opening of this molecule. To our knowledge, no high level computational study has been made on the isomerization of **T1** to **M1**. It is plausible to expect that **T1** molecule rearranges to cyclopentadiene via bicyclobutane to butadiene rearrangement [140, 157-162] since **T1** can be considered as a bicyclobutane derivative. Ring opening of **T1** should be more difficult than that in **B1** as the first process includes the homolytic cleavage of two σ bonds while the second has only one σ bond cleavage. The TS(s) and intermediate(s) (if any) are expected to have a considerable amount of biradical character. Furthermore, **T1** has C_{2v} symmetry, having four equivalent C-C σ bonds of which two are to be broken during the reaction. Although four electrons are actually involved in the process, the presence of four equivalent bonds makes the theoretical analysis complicated.

In this part of the thesis, we intended to find out the characteristic aspects of that piece of the potential energy surface regarding the three closed-shell species **M1**, **B1**, and **T1** shown in Figure 3.11. It is predictable that the TS structures have biradical characters. Therefore, usage of only one method (e.g. DFT or MCSCF) may not be able to handle all of the species with a comparable accuracy. Here,

calculations at a number of different levels of theory are reported to control the validity of the results predicted by these methods and evaluate the possible errors. Particularly, we tried to obtain reliable values for the reaction parameters by combining the predictions of DFT, CASSCF, multireference Moller Plesset perturbation theory (CASSCF-MP2), and coupled-clusters (CC) methods.

Table 3.7 Electronic^a and zero-point vibrational energies^b (kcal/mol) of various species relative to **M1** calculated by different methods using the 6-31G(d) basis set

| | M1 | B1 | T1 | [TS_B1-M1] | [TS_T1-M1] |
|-------------------------------|---------------------|---------------|---------------|-------------------|-------------------|
| (U)B3LYP^c | -194.101058 (58.29) | 48.12 (-0.43) | 64.47 (-0.62) | 73.95 (-2.96) | 106.63 (-3.26) |
| (U)BPW91^d | -194.071896 (56.77) | 44.54 (-0.41) | 58.18 (-0.57) | 72.04 (-3.01) | 102.75 (-3.16) |
| RHF^c | -192.790176 | 50.65 | 66.63 | 95.49 | 145.37 |
| CR-CCSD(T)^c | -193.486405 | 46.95 | 64.39 | 74.69 | 115.19 |
| CAS44^e | -192.846625 (61.30) | 55.02 (0.02) | 80.03 (0.41) | 70.31 (-2.04) | 114.98 (-1.99) |
| CAS44-MP2^e | -193.433949 | 50.18 | 71.85 | 72.25 | 113.75 |
| CAS88^f | -192.899439 (61.26) | 58.66 (-0.43) | 79.90 (-0.20) | 77.32 (-2.59) | 121.01 (-2.41) |
| CAS88-MP2^f | -193.426281 | 47.32 | 67.32 | 69.52 | 109.89 |

^aElectronic energies for the reference **M1** molecule are in hartrees. ^bZPVEs in kcal/mol are shown in parentheses. ZPVEs of species other than **M1** are relative to that in **M1**. ^cCalculated at the (U)B3LYP optimized geometries.

^dCalculated at the (U)BPW91 optimized geometries. ^eCalculated at the CAS44 optimized geometries.

^fCalculated at the CAS88 optimized geometries.

The electronic and zero-point vibrational energies (ZPVE) of all species calculated by different methods are conveniently summarized in Table 3.7. Coupled-clusters values in Table 3.7 refer to single-point calculations at the (U)B3LYP optimized geometries. Similarly, CAS44-MP2 and CAS88-MP2 calculations were carried out at the CAS44 and CAS88 optimized structures, respectively. The main geometrical parameters of the five stationary species (three minima and two TSs) optimized at the (U)B3LYP and CAS88 levels employing the 6-31G(d) basis set are shown in Figure 3.12. Density functional theory and CASSCF calculations agreed on the fact that both processes occur in a concerted manner as verified by following the complete IRCs; i.e. no intermediates were present along the reaction pathways.

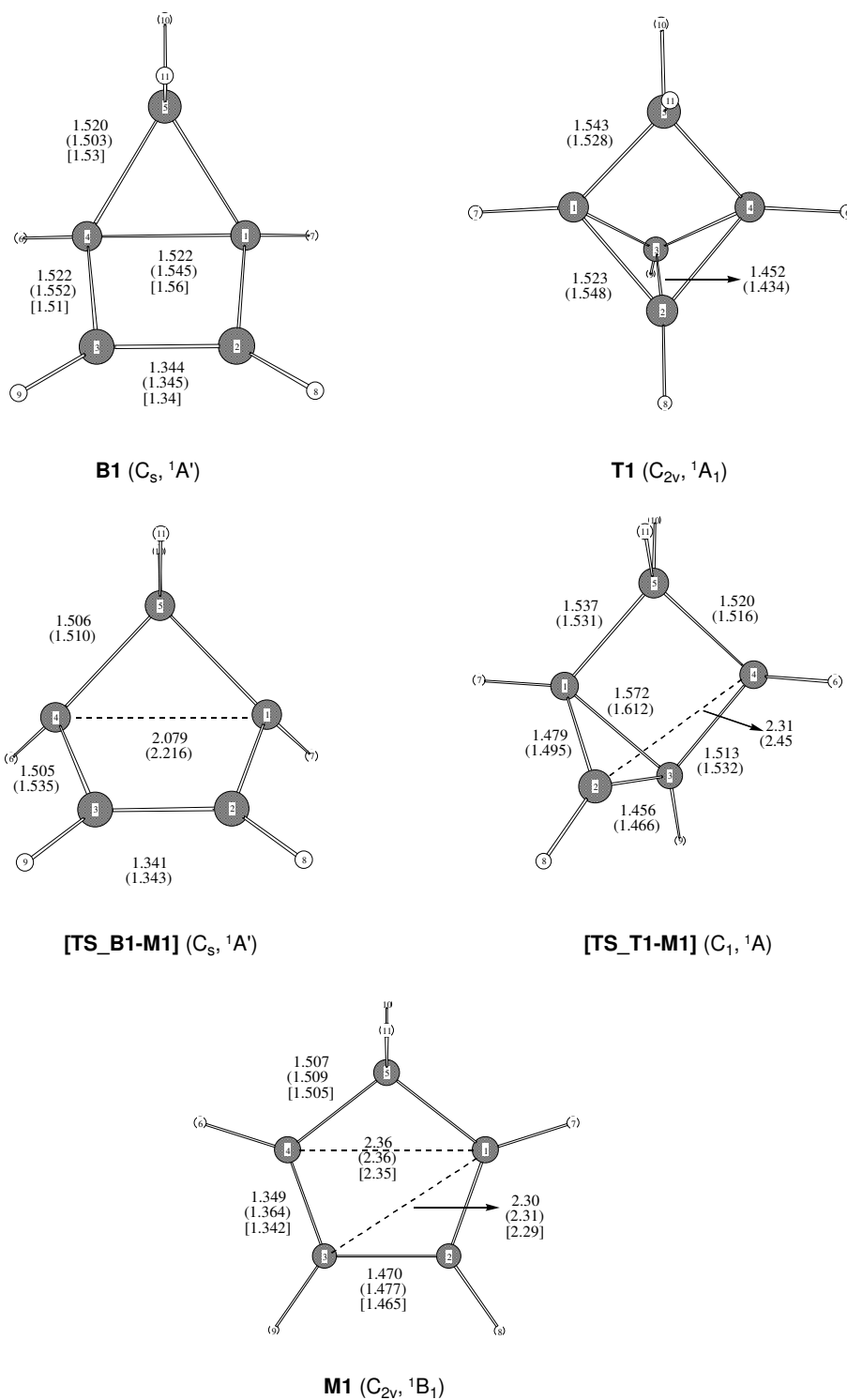


Figure 3.12 Selected interatomic distances (Å), points groups and electronic states shown in Figure 3.11. The uppermost values refer to UB3LYP geometry. The corresponding CAS88 values are indicated in parentheses, and the experimental values (when available) are shown in square brackets (ref [39] for **B1**, ref [163] for **M1**).

First, we will explore the stable species **M1**, **B1** and **T1**. Since CASSCF and DFT geometries of these molecules agree with each other, they are used for coupled cluster (CC) calculations. The CR-CCSD(T) energies of these structures are almost the same (the difference is about 1 kcal/mol), therefore only the results obtained at DFT optimized geometries are presented in Table 3.7. The CR-CCSD(T) energies are going to be used as the reference in the evaluation of relative energy of a given method. The relative energies of **B1** and **T1** obtained by B3LYP method are closest values to the reference within 1 kcal/mol, thus the stable structures were excellently calculated by this method. The other DFT method, BPW91, underestimates the relative energy of **B1** and **T1** by 2.4 and 6.2 kcal/mol, respectively. There was no spin contamination problem in either B3LYP or BPW91 methods, leading to their stability toward spin-symmetry breaking ($\langle S^2 \rangle = 0$). The CAS44 and CAS88 methods significantly overestimate the relative energies of **B1** and **T1** comparing with CC values. Although CAS88 is much more flexible due to having large number of CSFs, its results is worse than that of CAS44 in the case of **B1**. On the other hand, the CASSCF-MP2 method brings both CASSCF energies within a few kcal/mol of the CC values. This clearly indicates that inclusion of dynamical electron correlation is more important than enlargement of the active space.

The correlation energy of species i recovered by a given method m is defined as the difference in the calculated energy from that using the RHF method, $E_{\text{corr},i}(m) = E_i(m) - E_i(\text{RHF})$. This definition will be used below to compare the performance of the ab initio methods. To include the DFT methods into the comparison, we choose a reference molecule and define a relative correlation energy by $\Delta E_{\text{corr},i}(m) = E_{\text{corr},i}(m) - E_{\text{corr},\text{ref}}(m)$. The reference used in our calculations was the cyclopentadiene molecule. A biradical [164] is a molecule in which the unpaired electrons are localized at atomic centers separated by a relatively long distance. The two spins are only weakly coupled with the consequence that the singlet and triplet states of the system are nearly degenerate. Thus, the singlet-triplet (S-T) energy gap, or $\langle S^2 \rangle$ value obtained by a spin-unrestricted method may be used as qualitative measures of biradical character in a molecule.

The total correlation energies ($E_{\text{corr},i}(m)$) of all five species as predicted by the ab initio methods are given in Table 3.8. Calculations in each row of the table were

performed at the (U)B3LYP optimized geometry of the related species. The last column of the table gives the CC values in kcal/mol that will be used as reference data. As affirmed before, these three stable species have similar correlation energies, with **B1** and **T1** having slightly more (3.7 and 2.25 kcal/mol, respectively) than in **M1**. On the average, the CASSCF methods recovered only 9.5% and 16% of the correlation energy with CAS44 and CAS88, respectively. CASSCF-MP2 performed much better since it recovered the correlation energy up to 92%. A severe problem related to CASSCF is its uneven recovery of the correlation energy. Thus, even though **M1**, **B1**, and **T1** have similar CC correlation energies with the first species having the least amount, CASSCF predicts **M1** to have the largest correlation energy among the three. Consequences of such behavior are quantified in Table 3.9 which gives the relative correlation energies ($\Delta E_{\text{corr},i}(m)$) in kcal/mol as predicted by all methods considered in this part of the thesis. It will be observed that the CAS88 predictions for the relative correlation energies in **B1** and **T1** are in error by about 12 and 16 kcal/mol, respectively. It should also be noted that the B3LYP and CAS88-MP2 predictions for these two species are in satisfactory agreement with the CC values.

Table 3.8 Correlation energies of various species at (U)B3LYP/6-3G(d) optimized structures as predicted by the ab initio methods^a

| | CAS44 | CAS44-MP2 | CAS88 | CAS88-MP2 | CR-CCSD(T) ^b |
|------------|--------|-----------|--------|-----------|-------------------------|
| M1 | 8.00% | 92.50% | 15.50% | 91.40% | -436.89 |
| B1 | 6.90% | 91.80% | 13.50% | 91.40% | -440.59 |
| T1 | 5.10% | 91.00% | 12.30% | 90.80% | -439.14 |
| [TS_B1-M1] | 13.20% | 94.20% | 18.90% | 93.70% | -457.7 |
| [TS_T1-M1] | 14.30% | 94.10% | 20.10% | 93.70% | -467.07 |
| Average | 9.50% | 92.70% | 16.10% | 92.20% | -448.28 |

^aCASSCF and CASSCF-MP2 values are given as percentages of those in the CR-CCSD(T) column.

^bCR-CCSD(T) values are in kcal/mol.

Table 3.9 Relative^a correlation energies (kcal/mol) of various species at (U)B3LYP/6-31G(d) optimized geometries predicted by different methods

| | (U)B3LYP | (U)BPW91 | CAS44 | CAS44-MP2 | CAS88 | CAS88-MP2 | CR-CCSD(T) |
|------------|----------|----------|--------|-----------|--------|-----------|------------|
| B1 | -2.53 | -6.14 | 4.67 | -0.17 | 8.56 | -3.58 | -3.7 |
| T1 | -2.17 | -8.5 | 12.76 | 4.69 | 13.77 | 0.45 | -2.25 |
| [TS_B1-M1] | -21.54 | -23.93 | -25.47 | -26.82 | -18.62 | -29.37 | -20.81 |
| [TS_T1-M1] | -38.74 | -42.96 | -31.98 | -34.96 | -25.96 | -38.2 | -30.18 |

^a $\Delta E_{\text{corr},i}(m)$ relative to **M1**

The reaction enthalpies at 0 K calculated by various methods for the rearrangements of **B1** and **T1** into **M1** are collected in Table 3.10 and Table 3.11, respectively, which also include the activation energies to be discussed in the sequel. As stated above, the experimental value for the conversion of **B1** into **M1** at 25 °C is −47.8 kcal/mol. The predictions by RHF, B3LYP, CC, CAS44-MP2, and CAS88-MP2 methods are within roughly 1.5 kcal/mol of the experimental value, and they all may be considered as equally good (Table 3.10). No experimental quantitative data is available for the conversion of **T1** into **M1**. Assuming that the CC prediction ($\Delta H_0 = -63.8$ kcal/mol) is nearest to the actual one, RHF, B3LYP, and CAS88-MP2 perform reasonably well, being within 3 kcal/mol of the CC value, with B3LYP nearest to CC (Table 3.11).

Table 3.10 Activation and reaction energies (kcal/mol) for the rearrangement of **B1** into **M1** at 0 K at different levels of theory using the 6-31G(d) basis set

| | UB3LYP | UBPW91 | RHF ^a | CR-CCSD(T) ^a | CAS44 | CAS44-MP2 ^b | CAS88 | CAS88-MP2 ^c | exp. |
|-----------------------|--------|--------|------------------|-------------------------|--------|------------------------|--------|------------------------|--------------------|
| ΔH_0^\ddagger | 23.3 | 24.9 | 42.31 | 25.21 | 13.23 | 20.01 | 16.5 | 20.04 | 26 ^d |
| ΔH_0 | -47.69 | -44.13 | -50.22 | -46.52 | -55.04 | -50.2 | -58.23 | -46.89 | -47.8 ^e |

^aCalculated at the (U)B3LYP optimized geometries and (U)B3LYP ZPVEs are used. ^bCalculated at the CAS44 optimized geometries and CAS44 ZPVEs are used. ^cCalculated at the CAS88 optimized geometries and CAS88 ZPVEs are used. ^dref 4,5. ^eref 15,16.

Table 3.11 Activation and reaction energies (kcal/mol) for the rearrangement of **T1** into **M1** at 0 K at different levels of theory using the 6-31G(d) basis set

| | UB3LYP | UBPW91 | RHF ^a | CR-CCSD(T) ^a | CAS44 | CAS44-MP2 ^b | CAS88 | CAS88-MP2 ^c |
|-----------------------|--------|--------|------------------|-------------------------|--------|------------------------|--------|------------------------|
| ΔH_0^\ddagger | 39.52 | 41.98 | 76.1 | 48.16 | 32.54 | 39.5 | 38.9 | 40.37 |
| ΔH_0 | -63.85 | -57.61 | -66.01 | -63.77 | -80.44 | -72.26 | -79.69 | -67.11 |

^aCalculated at the (U)B3LYP optimized geometries and (U)B3LYP ZPVEs are used. ^bCalculated at the CAS44 optimized geometries and CAS44 ZPVEs are used. ^cCalculated at the CAS88 optimized geometries and CAS88 ZPVEs are used.

Turning now to the activation enthalpies; for the rearrangement of **B1** into **M1** (Table 3.10), the experimental ΔH^\ddagger is 26 kcal/mol. The CC prediction is 25.2 kcal/mol with the UB3LYP, UBPW91 values of 23.3 and 24.9 kcal/mol, respectively, nearly paralleling CC in accuracy while the CASSCF-MP2 value is

20.0 kcal/mol for both CAS44-MP2 and CAS88-MP2, being about 5 kcal/mol too low relative to CC. The good performance of the broken symmetry spin-unrestricted DFT in [TS_B1-M1] comes as a surprise since there is a significant amount of biradical character in this species by all measures mentioned above. The vertical S-T gaps in [TS_B1-M1] as calculated by various methods are given in the first row of Table 3.12. For the DFT methods, $\langle S^2 \rangle$ values are also shown in parentheses. It should be noted that each method in the table employed its own optimized geometry of the singlet biradical at which the S-T gap was computed. All methods predict the ground state of [TS_B1-M1] to be a singlet. At the UB3LYP geometry, the S-T gap is a small 10.95 kcal/mol with a high spin contamination of $\langle S^2 \rangle = 0.68$ in the singlet. The singlet RB3LYP energy at UB3LYP geometry was calculated to be 5.55 kcal/mol above the spin-unrestricted energy. The CASSCF characterization of the biradical is similar (Table 3.13). Thus, Jensen's [37] BR = 0.31 and Staroverov-Davidson's [85, 86] 'number of effectively unpaired electrons' at each carbon of the breaking bond is 0.54 at the CAS88//UB3LYP level. The corresponding values at the CAS88 optimized geometry are 0.59 and 0.80 for BR and number of free spins, respectively. The latter values strikingly illustrate the overestimation of the biradical character by CASSCF methods. This behavior of CASSCF is also reflected in its prediction of TS geometry. Thus, referring to Figure 3.11, one sees that the C1-C4 distance in the CAS88 [TS_B1-M1] is 0.14 Å longer than that predicted by UB3LYP. More bond-breaking at TS is predicted by CASSCF which in turn implies more localized spins. Due to the longer distance between the radical centers, the spins in the CASSCF TS have a weaker coupling than in UB3LYP with the result that the S-T gap at the CASSCF geometry is smaller (Table 3.13).

Table 3.12 Vertical singlet-triplet splitting energies^a in kcal/mol, and spin contaminations ($\langle S^2 \rangle$ for singlets in parentheses) in DFT methods of the transition structures

| | UB3LYP ^b | UBPW91 ^c | CAS44 ^d | CAS44-MP2 ^d | CAS88 ^e | CAS88-MP2 ^e |
|------------|---------------------|---------------------|--------------------|------------------------|--------------------|------------------------|
| [TS_B1-M1] | 10.95 (0.684) | 6.94 (0.741) | 6.3 | 4.53 | 6.24 | 4.85 |
| [TS_T1-M1] | 2.65 (0.889) | 3.12 (0.935) | -1.49 | -3.42 | -2.32 | -3.02 |

^a $\Delta E = E_{\text{triplet}} - E_{\text{singlet}}$, using the 6-31G(d) basis set and not including ZPVEs. ^bCalculated at the UB3LYP optimized singlet geometries. ^cCalculated at the UBPW91 optimized singlet geometries. ^dCalculated at the CAS44 optimized singlet structures. ^eCalculated at the CAS88 optimized singlet structures.

Ring opening of the C_{2v} -symmetric **T1** into the transition structure, **[TS_T1-M1]**, takes place in the following manner (see the numbering in Figure 3.11 and Figure 3.12). One of the two equivalent carbons at positions 1 or 4 rotates around the C_2 axis. Taking C4 as the moving carbon (together with its hydrogen), its rotation continues until it becomes approximately coplanar with C1, C3, and C5. In the meantime, C2 rotates around the C1-C3 bond outward so that the C2-C3-C1-C5 torsion angle increases by 21.2° at the UB3LYP level (23.8° at CAS88) when **[TS_T1-M1]** is reached. The net effect is the breakage of the C2-C4 bond while the length of the C1-C3 bond increases by a minor 0.05 \AA (0.1 \AA at CAS88). The C1-C3 bond is broken on the **M1** side of the reaction path, accompanied by the formation of the two π bonds.

Table 3.13 CAS88^a Mulliken Effectively Unpaired Electron Populations and Biradical Indices^{b,c}

| | M1 | | B1 | | T1 | | [TS_B1-M1] | | [TS_T1-M1] | |
|----|-----------|--------|-----------|--------|-----------|--------|-------------------|--------|-------------------|--------|
| C1 | 0.18 | (0.19) | 0.10 | (0.11) | 0.10 | (0.11) | 0.54 | (0.80) | 0.13 | (0.16) |
| C2 | 0.17 | (0.18) | 0.21 | (0.22) | 0.11 | (0.12) | 0.19 | (0.27) | 0.80 | (0.94) |
| C3 | 0.17 | (0.18) | 0.21 | (0.22) | 0.11 | (0.12) | 0.19 | (0.27) | 0.11 | (0.16) |
| C4 | 0.18 | (0.19) | 0.10 | (0.11) | 0.10 | (0.11) | 0.54 | (0.80) | 0.82 | (0.98) |
| C5 | 0.00 | (0.00) | 0.00 | (0.00) | 0.00 | (0.00) | 0.10 | (0.02) | 0.00 | (0.01) |
| BR | 0.06 | (0.10) | 0.03 | (0.09) | 0.02 | (0.04) | 0.31 | (0.59) | 0.56 | (0.98) |

^a6-31G(d) basis set. See Scheme 1 for the numbering of carbon atoms. ^bIn each pair of numbers in the table, the first one refers to the spin population calculated at the UB3LYP optimized geometry, and the second one, shown in parenthesis, is the corresponding value at the CAS88 optimized geometry. ^cFor comparison, the net spin population on each carbon in benzene is 0.16, and BR=0.10 (with CAS66 employing the 6 π MOs).

Assessing the performance of various methods in predicting the relative energy of **[TS_T1-M1]** is not easy. The UDFT methods predict geometries at which the ground state is a singlet whereas CASSCF predicts just the opposite (Table 3.12). The PESs belonging to the two spin states are nearly degenerate in the vicinity of **[TS_T1-M1]**, and it is certain that they cross between the UDFT and CASSCF structures (Figure 3.13). Indeed, the UB3LYP IRC quickly crosses into the triplet surface at a reaction coordinate (rxn) value of $0.4 \text{ amu}^{1/2} \text{ bohr}$ on the **M1** side of the TS, and crosses out of it at rxn= $1.7 \text{ amu}^{1/2} \text{ bohr}$. The minimum of the nearby triplet surface is calculated to be about 3 kcal/mol below the singlet saddle point at both the

UB3LYP and CAS88-MP2 levels. Structure of the molecule at the triplet minimum is quite similar to [TS_T1-M1]. At the singlet UB3LYP saddle point where the triplet lies higher in energy, the S-T gap is calculated to be 2.65 and 3.79 kcal/mol by the UB3LYP and CAS88-MP2 methods, respectively. The latter value should be trustworthier as CASSCF-MP2 preserves the spin symmetry. As expected, the spin contamination, $\langle S^2 \rangle = 0.89$, in UB3LYP is higher than that in [TS_B1-M1]. At CAS88//UB3LYP level, the biradical index, BR = 0.56, and number of free spins at the radical centers C2 and C4 are 0.80 and 0.82, respectively (Table 3.13). It appears that the biradical character in UB3LYP [TS_T1-M1] is almost identical to that in CAS88 [TS_B1-M1]. The CAS88 optimized [TS_T1-M1] has a longer C2-C4 distance (Figure 3.12), and consequently, has more biradical character: BR = 0.98, and the number of unpaired electrons is nearly one at each radical center (0.94 and 0.98 at C2 and C4, respectively).

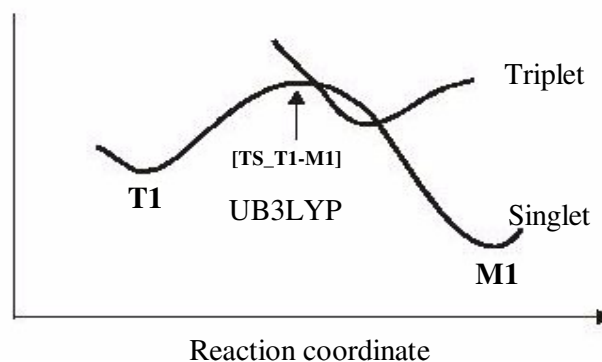


Figure 3.13 Qualitative behavior of the minimum energy path in the isomerization of **T1**, showing the intersystem crossing.

The heat of formation of [TS_T1-M1] relative to that of **T1** (i.e. the activation enthalpy) calculated at different levels of theory is given in the first row of Table 3.11. Lack of experimental data makes it difficult to judge the reliability of these values. The UB3LYP and CASSCF-MP2 predictions are in close agreement with each other, and the UBPW91 estimate is within 2 kcal/mol of the former values. Shall we trust the UB3LYP result, especially considering its unexpected success in the case of [TS_B1-M1]? The answer appears to be no. Reference to Table 3.7

shows that the agreement among UB3LYP, UBPW91, and CASSCFMP2 is due to fortuitous cancellations. While success of computational chemistry is largely dependent on systematic cancellation of errors, there are inconsistencies in our case. The high level CC calculations employing the same geometries as in UB3LYP predict an activation enthalpy that is 8 kcal/mol higher. Of course it is possible that the CC calculations are in error as the CR-CCSD(T) method we used is based on the RHF determinant, and hence it may be unable to handle the multireference nature of the wave function in **[TS_T1-M1]**. However, the TS under consideration effectively contains one broken bond, and as mentioned before, CR-CCSD(T) has been shown to be successful even in the case of two broken bonds. Further evidence supporting CC comes from the data in Table 3.8 and Table 3.9. It is seen from Table 3.9 that the CAS88-MP2 method overestimates the correlation energy of **[TS_B1-M1]** relative to that in **M1** by 8.5 kcal/mol. At this geometry CR-CCSD(T) method (also UB3LYP) works excellently. Assuming that CAS88-MP2 overestimates the relative correlation energy of the **[TS_T1-M1]** structure by the same amount, an assumption supported by the data in Table 3.8 (93.7% recovery in both TSs), we conclude that CC results are probably correct, and that the UB3LYP method is also suffering from the overestimation problem.

If energies of **[TS_T1-M1]** predicted by UB3LYP and CASSCF are both unreliable, then what is the correct geometry of this TS? The CR-CCSD(T) energy of the UB3LYP optimized structure differs significantly from the corresponding CC energy of the CAS88 optimized structure; the UB3LYP **[TS_T1-M1]** was lower in energy by 11.80 kcal/mol (the analogous difference in **[TS_B1-M1]** was 7.04 kcal/mol). There are indications that the UB3LYP geometry is more plausible. The distance between C2 and C4 (one of the two broken bonds) is 2.30 Å in the product, **M1** (Figure 3.12). In the TS, according to UB3LYP, the breakup of this bond is completed (C2-C4=2.31 Å in **[TS_T1-M1]**) whereas CAS88 predicts it to be 0.14 Å longer. This behavior of CASSCF, predicting the length of a breaking bond exceeding its ultimate value at some intermediate point along the reaction path is not sensible on chemical grounds. It appears that the UB3LYP structure should be closer to the actual one. Our estimate of the activation enthalpy in the rearrangement, **T1** to **M1**, is then < 48 kcal/mol at the CR-CCSD(T) level of theory (Table 3.11).

3.2.2. 1,5-Sigmatropic Hydrogen Shift Reaction of Cyclopentadiene (M1)

The interest on thermal [1,j]-sigmatropic rearrangements [165] has considerably increased since the description of elementary theoretical framework governing [1,j]-sigmatropic migration by Woodward and Hoffmann in 1970 [166]. Hydrogen migration can be considered as the interaction of the hydrogen atom with the HOMO of a polyene radical. [1,5]-sigmatropic hydrogen shift reaction in cyclopentadiene (Figure 3.14) is an important reaction among the thermal sigmatropic rearrangements because of being a representative example of such type of reactions in cyclic molecules. This reaction is a suprafacial, thermally allowed rearrangement and the existence of the conjugated π molecular orbitals in cyclopentadiene molecule allows the facile occurrence of this migration. Obviously, it is a “degenerate” reaction as the reactant and product are the same, cyclopentadiene, itself.

In 1964, Roth [167] conducted several gas phase experiments on 1,5-H shift in cyclopentadiene to obtain the thermodynamics of the reaction and determined the activation energy, E_a , being 24.3 ± 0.5 kcal/mol for the temperature range 45 – 65°C. The geometry and electronic structure of the transition state structure as well as the activation enthalpy of the reaction have been determined at different levels of theory in several computational studies [168-172]. Furthermore, it is predicted that several metal cation (Li^+ , Na^+ , Mg^{2+} etc.) complexations accelerate 1,5-H shifts in cyclopentadiene by inducing electrostatic field [173, 174].

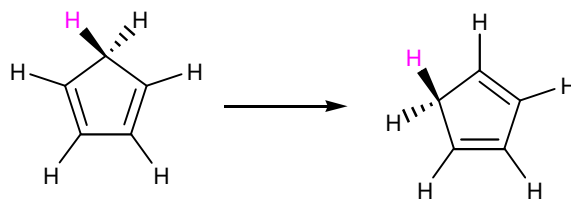


Figure 3.14 1,5-sigmatropic hydrogen shift in cyclopentadiene

In this part, mostly the performance of B3LYP functionals with various basis sets on 1,5-sigmatropic hydrogen shift reaction in cyclopentadiene was investigated. Specifically, cyclopentadiene (**M1**) and transition state geometry (**[TS_M1-M1]**) of this rearrangement were optimized by RB3LYP method with 6-31G(d), 6-31G(d,p), cc-pVTZ basis sets. Then, single point RCCSD(T)/6-31G(d,p) and RCCSD(T)/6-311G(d,p) calculations performed on RB3LYP/cc-pVTZ level optimized geometries were used to compare the performance of B3LYP with CCSD(T), which is known as giving accurate energies. Electronic and zero point vibrational energies (kcal/mol) of the species relative to **M1** are given in Table 3.14 while activation enthalpies (ΔH_0^\ddagger) at various levels are shown in Table 3.15. The **[TS_M1-M1]** geometry and the selected geometrical parameters are given in Figure 3.15.

Table 3.14 Electronic^a and zero-point vibrational energies^b (kcal/mol) of the species involved in the 1,5-H shift reaction relative to **M1**.

| Level | M1 | [TS_M1-M1] | |
|---|---------------------|-------------------|---------|
| RB3LYP/6-31G(d) | -194.101058 (58.29) | 28.92 | (-2.06) |
| RB3LYP/6-31G(d,p) | -194.110691 (58.17) | 27.82 | (-2.04) |
| RB3LYP/cc-pVTZ | -194.174117 (57.93) | 27.32 | (-2.08) |
| RCCSD(T)/6-31G(d,p)^c | -193.543980 | 31.97 | |
| RCCSD(T)/6-311G(d,p)^c | -193.616853 | 30.86 | |

^aElectronic energies for the reference **M1** molecule are in hartrees.

^bZPVEs in kcal/mol are shown in parentheses.

^cRB3LYP/cc-pVTZ level optimized geometries are used.

Table 3.15 Activation and reaction enthalpies (kcal/mol) of the 1,5-H shift reaction of cyclopentadiene. Electronic^a and zero-point vibrational energies^b (kcal/mol) of the species involved in the 1,5-H shift reaction relative to **M1**.

| | RB3LYP | | | RCCSD(T)^a | | Exp |
|-----------------------|-----------------|-------------------|----------------|-------------------------------|--------------------------------|-------------------|
| | 6-31G(d) | 6-31G(d,p) | cc-pVTZ | 6-31G(d,p)^b | 6-311G(d,p)^b | |
| ΔH_0^\ddagger | 26.86 | 25.78 | 25.24 | 29.89 | 28.78 | 23.6 ^c |

^aRB3LYP/cc-pVTZ level optimized geometries are used.

^bThese parameters are corrected with ZPVEs of RB3LYP/cc-pVTZ level

^cThe activation enthalpy at 328 K given in ref [167]

We have successfully located **[TS_M1-M1]** for 1,5-hydrogen shift reaction in cyclopentadiene by using B3LYP functionals with several basis sets. It has a C_s symmetric geometry having the C \cdots H distances of 1.310 Å and the H \cdots C \cdots H angle of

69.2° as well as the C1-C5 bond length of 1.486 Å at RB3LYP/cc-pVTZ level. It is important to be aware of that the carbon skeleton of the [TS_M1-M1] is positioned almost in the same plane with distances whose values are very close to each other (1.4 – 1.5 Å), leading to an aromatic-like TS structure. Probably, this brings about the stability of TS and being a facile reaction due to low activation barrier.

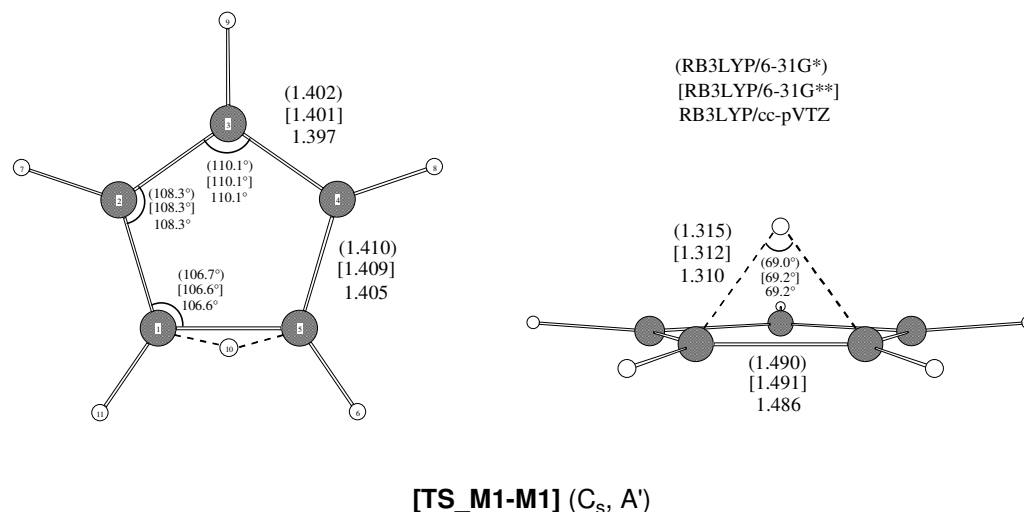


Figure 3.15 Selected geometrical parameters of [TS_M1-M1] optimized by RB3LYP method.

All three basis sets give very similar [TS_M1-M1] geometries. In the bond lengths, usage of large basis set brings only ~0.005 Å improvements to the TS geometry, and it has almost no effect on the angles. On the other hand, using more flexible basis set produces considerable advance in electronic energy of the TS structure. Experimental activation enthalpy for the 1,5-hydrogen migration reaction was found to be 23.6 kcal/mol. As expected, B3LYP method has a great performance even in standard basis set. Overall basis set improvement to activation enthalpy is 1.62 kcal/mol (from 26.86 to 25.24 kcal/mol). It is interesting that while the addition of polarization functions on hydrogen atoms with the 6-31G(d,p) basis set brings about 1 kcal/mol improvement, usage of very large basis set, cc-pVTZ, causes only ~0.5 kcal/mol better activation enthalpy. Hence, it is concluded that especially in hydrogen shift reactions basis set used should contain polarization functions on hydrogens to get better energy values.

Coupled cluster method was used to determine the electronic energies of RB3LYP/cc-pVTZ level optimized **M1** and **[TS_M1-M1]** structures and these energies were corrected with ZPVEs of the optimization level. The activation barrier calculated at RCCSD(T)/6-31G(d,p) level is approximately 6 kcal/mol above the empirical value, and usage of triple zeta basis set, 6-311G(d,p), overestimates it by 5 kcal/mol. If the DFT geometries are accepted as the correct ones, it can be supposed that B3LYP method has better performance than CC method, at least for this reaction, due to providing more consistent results with the experiment.

3.2.3. 1,2-Hydrogen Shift Reactions of 3-cyclopentenylidene (**M4**) and 2-cyclopentenylidene (**M5**) yielding cyclopentadiene (**M1**)

It has been reported [175] that reactions of 1,1-dibromo-2-vinylcyclopropane with methyllithium yield cyclopentadiene as the main product together with small amounts of allenic compounds as shown Figure 3.16.

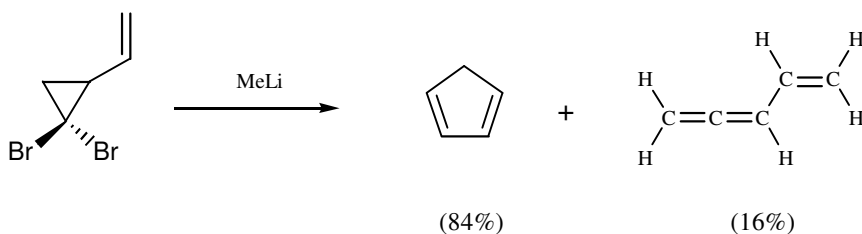


Figure 3.16 Reaction of 1,1-dibromo-2-vinyl-cyclopropane with methyllithium yielding cyclopenta-1,3-diene and penta-1,2,4-triene.

For the formation of cyclopentadiene, Holm and Skattebol [176] devised two reaction paths that differ essentially in the mode of ring opening of the initially formed substituted cyclopropylidene (Figure 3.17).

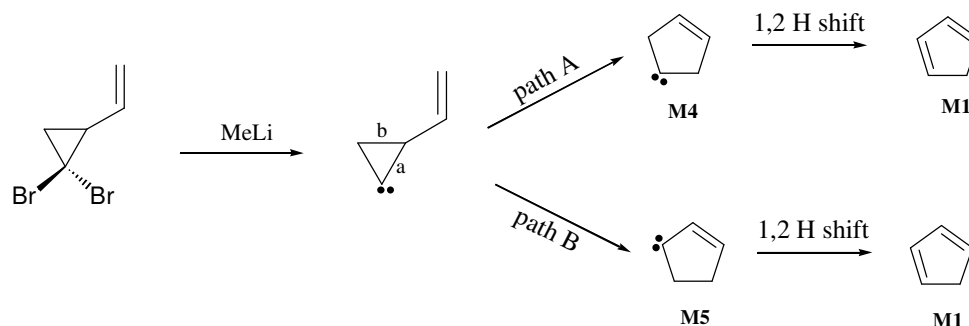


Figure 3.17 Reaction of 1,1-dibromo-2-vinyl-cyclopropane with methyllithium yielding cyclopenta-1,3-diene via (path A) **M4** and (path B) **M5** intermediates.

The cleavage of bond **a** (path A) should lead to 3-cyclopentenylidene (**M4**) while 2-cyclopentenylidene (**M5**) should be formed by the rupture of bond **b** (path B). Subsequently, both cyclic carbenes (**M4** and **M5**) are converted into cyclopentadiene (**M1**) via 1,2-H shift reactions. In order to distinguish the paths, labeling experiments [176] have been performed, as a result, it is found that the substituted cyclopropylidene rearrange to the corresponding cyclopentadiene from the path A to the extent of at least 95%.

As indicated Figure 3.17, isomers **M4** and **M5** are converted into **M1** by migration of hydrogen atom to the neighboring carbon. In the literature, we could not come across any kinetic study related to these reactions to be able to compare our findings. On the other hand, we expect that they should have rather small activation barriers because not only the experiments performed before imply so but also carbenes are most of the time reactive species that try to complete their valences. Recently, Nicolaides *et al.* [177] have computationally investigated the ground state rearrangements of conjugated cycloalkenylidenes involving 1,2-H shift in **M5**. Additionally, Olivella and his colleagues [178] have studied thermal rearrangements of 2-vinylcyclopropylidene whose path includes hydrogen migration in **M4**. All of the optimizations have been performed at B3LYP/6-31G(d) level in both of these studies. In present study, we carried out calculations on these two hydrogen transfer reactions with again using hybrid B3LYP functionals to obtain their TSs, activation barriers as well as reaction enthalpies. Our main aim is to obtain better geometries for the species involved in the reactions if possible. For this reason the cc-pVTZ basis set, which is pretty larger than 6-31G(d), was employed throughout the calculations. In order to get better thermodynamical parameters, single point

RCCSD(T)/6-31G(d,p) level calculations were done using the new geometries obtained by (U)B3LYP/cc-pVTZ level.

Table 3.16 Electronic and zero point vibrational energies (kcal/mol) of **M4**, **M5**, [**TS_M4-M1**] and [**TS_M5-M1**] relative to the energy (Hartrees) and ZPVE of **M1** calculated at different levels of theory. ZPVEs are given in parenthesis.

| Level | M1 | M4 | M5 | [TS_M4-M1] | [TS_M5-M1] |
|---------------------|---------------------|---------------|---------------|---------------|---------------|
| (U)B3LYP/6-31G(d) | -194.101058 (58.29) | 71.36 (-2.28) | 61.44 (-1.42) | 76.46 (-3.34) | 76.05 (-3.17) |
| (U)B3LYP/cc-pVTZ | -194.174117 (57.93) | 71.48 (-2.50) | 61.96 (-1.49) | 75.11 (-3.38) | 74.23 (-3.19) |
| RCCSD(T)/6-31G(d,p) | -193.543980 | 73.79 | 65.54 | 77.79 | 77.36 |

Electronic and zero point vibrational energies (kcal/mol) of the reactant **M4**, **M5** molecules as well as the [**TS_M4-M1**] and [**TS_M5-M1**] species relative to the energy of the product (**M1**) are given in Table 3.16. The calculated activation barriers and reaction enthalpies at 0 K for the species involved in the reactions are shown in Table 3.17. The selected geometrical parameters of (U)B3LYP/6-31G(d) and (U)B3LYP/cc-pVTZ level optimized geometries are illustrated in Figure 3.18.

Table 3.17 Activation barriers and reaction enthalpies at absolute zero for 1,2-hydrogen shift reactions of **M4** and **M5** calculated with DFT and RCCSD(T) methods.

| Reaction | | (U)B3LYP | | RCCSD(T) | |
|----------------|-----------------------|----------|---------|------------|----------------------|
| | | 6-31G(d) | cc-pVTZ | 6-31G(d,p) | |
| M4 - M1 | ΔH_0^\ddagger | 4.04 | 2.75 | 3.13 | (2.0) ^a |
| | ΔH_0 | -69.08 | -68.98 | -71.28 | (-69.1) ^a |
| M5 - M1 | ΔH_0^\ddagger | 12.87 | 10.58 | 10.12 | (8.0) ^b |
| | ΔH_0 | -60.02 | -60.46 | -64.05 | (-63.4) ^b |

^aRef. 177 ^bRef. 178.

In Table 3.17, the values in parentheses indicate the results of high level ab initio calculations calculated at B3LYP/6-31G(d) level optimized geometries. Alternatively, we chose much larger basis set for the optimizations, namely cc-pVTZ, since both reactions investigated includes migrations of hydrogen atoms whose electronic structure must be calculated precisely. As stated, these geometries were employed for single point CC calculations. The activation barriers of hydrogen

shifts in **M4** and **M5** are 3.13 and 10.12 kcal/mol, respectively. These values can be accepted as reasonable due to their closeness to the previous estimations. The similar or even better results were obtained for their exothermicity. The enthalpies of the former and the latter reactions are found to be -71.28 and -64.05 kcal/mol, respectively, and they agree with the previous results within 2 kcal/mol. As a result, 1,2-hydrogen shift in **M4** is not only more facile but also more exothermic compared to hydrogen migration reaction of **M5**. The B3LYP method works rather well for predicting both parameters of the former reaction, as well as the activation barrier of the latter. However, it underestimates the reaction enthalpy of the **M5** to **M1** conversion by ~ 4 kcal/mol. Additionally, it is important to note that basis set enlargement for DFT calculations has almost no improvement on the reaction enthalpy of the **M5** to **M1** conversion, while it enhances the accuracy of the other three parameters up to 2 kcal/mol.

The relative energies of **M4** and **M5** are 72.79 and 65.54 kcal/mol, respectively. Even though both reactant molecules **M4** and **M5** are the carbene structures of five-membered ring alkenes, they have significant difference in their stabilities. Specifically, **M5** has greater thermodynamic stability than **M4**. What is the underlying reason of the **M5**'s stability? To answer this question, it is necessary to compare their geometries. The carbene carbon and the C1-C2 double bond in isomer **M4** are not neighbors as the corresponding structures are conjugated in isomer **M5**. Therefore, :C-C=C unit of **M5** lets the delocalization of p-electrons of three carbon atoms and increases the stability relative to the non-conjugated arrangement of **M4**. This argument is really consistent with the related geometrical parameters. For the :C-C=C unit of **M5**, the double bond (1.356 \AA) is slightly longer than a typical double bond (1.34 \AA) as the :C-C bond (1.441 \AA) is considerably smaller than corresponding bonds ($\sim 1.5 \text{ \AA}$) in **M4**, showing the electron delocalization in :C-C=C unit.

It is important to know whether the usage of large basis set in the DFT optimizations improve the geometries of the species or not. It is hard to say that the basis set enlargement brings about a considerable improvement for the stable structures. Only prominent difference is observed in :C-C bond lengths of **M4** and **M5** such that they both decrease by 0.01 \AA as the basis set becomes larger. In fact,

we are expecting considerable variations in the transition state geometries, especially in the locations where hydrogen migrations take place. The [TS_M4-M1] structure satisfies our expectations since the basis set extension affects its geometry. The deviations in bond distances reach up to 0.01 Å, and more significantly the C[⋯]H[⋯]C angle diverge almost 4° in going from small to large basis. On the contrary, the [TS_M5-M1] structure is not affected from the basis change as much as [TS_M4-M1] does. Especially in the reaction site the geometry of 6-31G(d) is almost the same as the one found by cc-pVTZ

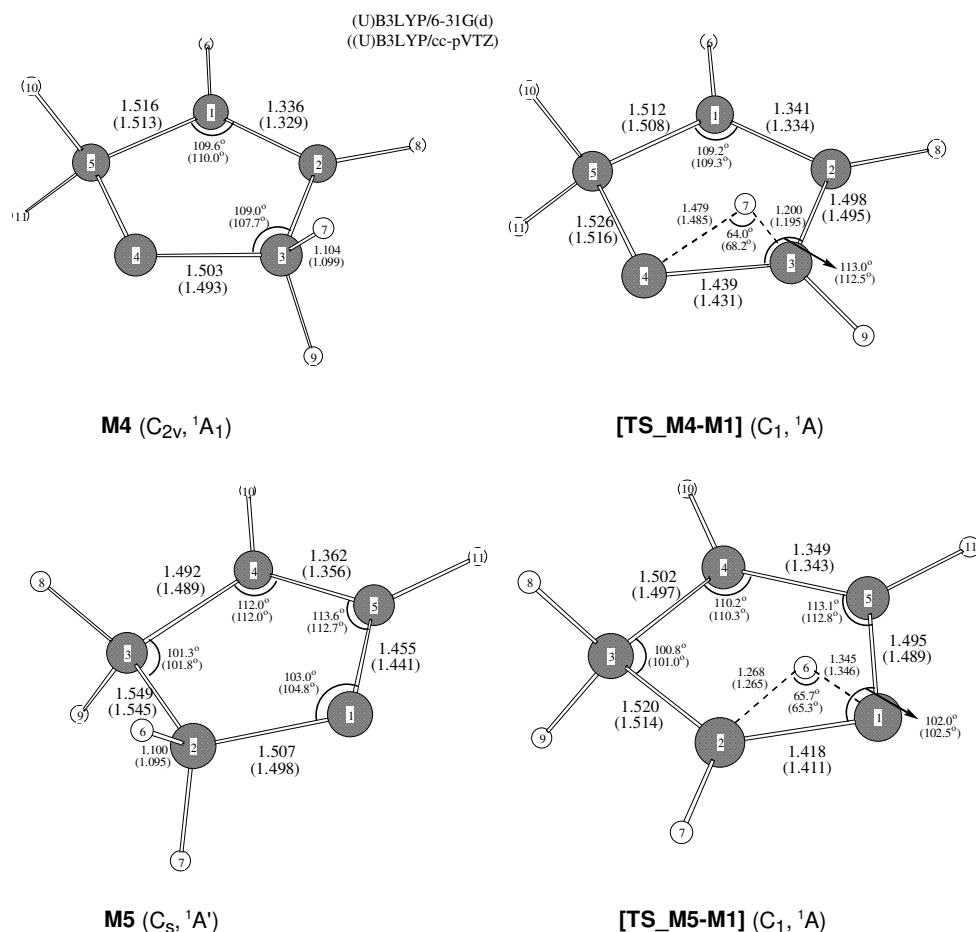


Figure 3.18 Selected geometrical parameters of M4, [TS_M4-M1], M5 and [TS_M5-M1] obtained by DFT optimizations.

Another interesting point is that the relative energies of [TS_M4-M1] and [TS_M5-M1] are very close to each other. At this time, we will try to interrogate the

relation of this degeneracy with the geometries of the TSs. Both of them, to some extent, resemble bicyclic systems made from a three-membered ring with the “elongated” bonds and a fused five -membered cycloalkene. First of all, let us try to consider each of these structures in two divisions: first part is the three-membered rings and the remaining C_3H_4 unit constitutes the second part. As shown in the Figure 3.18, the C_3H_4 units of both TSs are almost the same in terms of the arrangement in space and all the geometrical parameters of them are similar, as well. Qualitatively, the only difference in the three membered rings is that the spectator hydrogen atoms (the one that does not migrate) are bound to different carbon atoms. If these structures are examined carefully, it can easily be realized that they are approximately mirror images of each other that have the same energy. Although these three membered rings are quantitatively (in terms of geometrical parameters) somewhat different, all calculations predicted that they are more or less energetically degenerate. Hence, such variations in geometrical parameters may not cause huge deviations in energy, at least for this case. Owing to the degeneracy of TSs, the difference in their activation barriers is totally originated from the stability difference between the reactant molecules.

3.2.4. Formation of Cyclopentyne (**M3**) from cyclobutylidenemethylene (**M7**)

Small-ring cyclic alkynes are of considerable interest due to their high strain and reactivity. Cyclooctyne [179] is the smallest isolable cyclic alkyne. Seven-, six-, and five-member ring alkynes exist only as short-lived intermediates in low temperature matrices [180-187]. Although a metal complex containing the ligand cyclobutynes [188] has been synthesized, unencumbered (free) alkynes with three- and four-member rings have not been experimentally observed. Furthermore, Kitamura *et al.* [189] reported that they had synthesized a bicyclic alkyne, namely bicyclo[2.2.1]hept-2-en-5-yne, being more strained than **M3**, based on the results of ab initio calculations. Consequently, cyclopentyne (**M3**) is the smallest and one of the most strained free (uncomplexed) cyclic alkyne whose existence was proven experimentally.

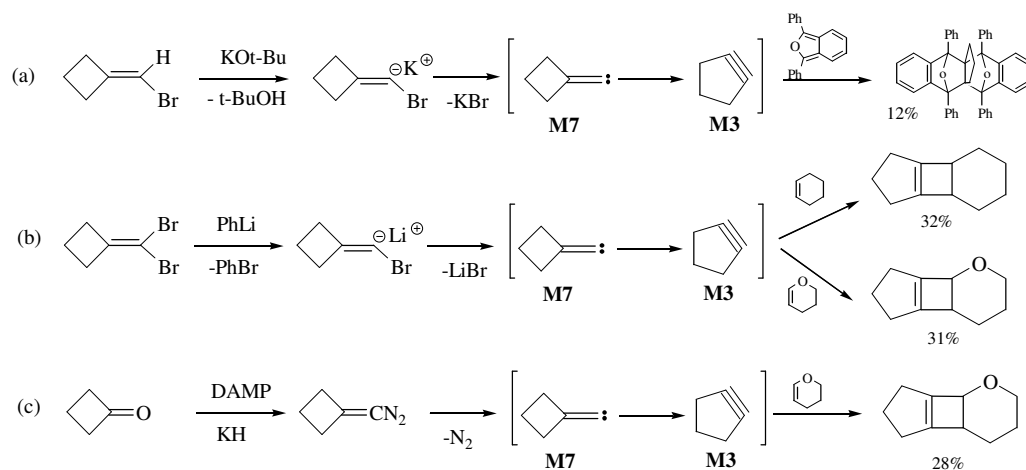


Figure 3.19 The proposed synthesis mechanism of cyclopentyne from different cyclobutane derivatives

The existence of **M3** as a reaction intermediate was first suggested by Favorskii [190] in 1936 when the metallic sodium is reacted with 1,2-dibromopentane. Later, **M3** was obtained from the reactions of (a) Mg with 1,2-dibromocyclopentene in tetrahydrofuran, (b) 1,2-cyclopentanedione dihydrazone with HgO in C₆H₆, conducted by Wittig *et al.* [191]. Montgomery *et al.* [192] performed ¹⁴C experiments by coupling of phenyllithium with 1-chlorocyclopentene, proving the existence of **M3** intermediate. In all these reactions, cyclopentene derivatives were used for synthesis of **M3**. In 1965, Erickson *et al.* [193] firstly used the ring enlargement of carbene to alkyne pathway by reacting bromomethylenecyclobutane with KO-*tert*-Bu and trapped **M3** in 12% yield (Figure 3.19a). Fitjer *et al.* [184] increased the **M3** yield to 32% by reacting 1,1-dibromocyclobutane with phenyllithium (Figure 3.19b). A new precursor of **M7**, diazomethylene-cyclobutane [182], was also reported in the base-promoted (KH) reaction of cyclobutanone with dialkyl (diazomethyl)phosphonates (DAMP) producing **M3** (Figure 3.19c). The common feature of these three reactions is the formation of **M3** via isomerization of cyclobutylidene methylene (**M7**), which is called cycloalkylidene to cycloalkyne rearrangement.

The first suggestion related to the electronic structure of cyclopentyne has been made by Fitjer and Modaressi [183] because of unusual [2+2]-cycloaddition reactions of **M3** to a variety of olefins. Their statement is that the cyclopentyne (**M3**) has an antisymmetrical singlet ground state having biradical character.

Unfortunately, the term they had used for the ground state of **M3** was conceptually erroneous. In fact, they mean that **M3** has a singlet ground state with antisymmetric HOMO. After their proposal, the ground state geometry, electronic structure and biradical character of **M3** have been theoretically obtained by Olivella *et al.* [31]. According to their calculations, **M3** has a slightly puckered ring structure with C_s symmetry, a considerable biradical character and an electronic state of $^1A'$. Moreover, GVB calculations showed that acetylenic in plane π and π^* natural orbitals have occupation numbers of 1.71 and 0.29, respectively. In the present study, we have also calculated that this structure has a 20% biradical character (Section 3.1.1). The existence of electron density in π^* MO, antisymmetric with respect to C_s symmetry plane, may explain this odd behavior of cyclopentyne. Gilbert and Kirshner [194, 195] also have also tried to explain the stated stereospecificity of **M3** and introduced a new concept, “lumomer”, the product of a pericyclic process in which conversion of reactant into an isomeric product requires a HOMO-LUMO orbital crossing according to orbital isomerism theory of Dewar [196-198]. For supporting their hypothesis, they performed semi-empirical AM1 calculations with 3x3 configuration interaction on the ring expansion of **M7** to **M3**. These calculations resulted a structure resembling **M3** but it was geometrically distinct and energetically different isomer, so they named this isomer as the cyclopentyne lumomer. On the other hand, MP2 and MCSCF calculations by Johnson *et al.* [199] showed that there is no stationary point on the **M7**→**M3** reaction pathway referring to the lumomer. Hence, they assessed the lumomer being an artifact of AM1 methodology, which incorrectly predicts the reaction enthalpy for this reaction. Very recently, Gilbert and his colleagues [200] have performed DFT calculations on addition of **M3** to ethylene and they proposed a new computationally supported addition mechanism, in which ethylene adds **M3** from one of the acetylenic carbons forming an intermediate carbene. The carbene then rearranges to form the final [2+2]-cycloadduct.

Alkylidenecarbenes can easily be trapped by alkenes giving alkylidenecyclopropane derivatives as adducts. Their generation methods [201] and reactions with alkenes [202] have already been reviewed in detail. Although methylenecyclopentane and methylenecyclohexane (higher ring analogs of **M7**) were trapped by cyclic alkenes in good yields [203], all attempts for trapping of

methylidenecyclobutane (**M7**) failed [184, 203] and only the adducts from cyclopentyne trapping were observed. The results of these experiments imply that either **M7** is a shallow minimum [199] on PES of C₅H₆ with a small barrier for conversion to **M3** or the barrier for addition of **M7** to double bond is high relative to that of **M7** → **M3** rearrangement.

In the light of this knowledge, we decided to explore **M7** to **M3** reaction pathway with the high-level quantum chemical methods. Specifically, the geometries and energies of all stationary points on this path have been determined by (U)B3LYP method with 6-31G(d), 6-311G(d,p) and cc-pVTZ basis sets, as well as CASSCF(6,6)/6-31G(d) level. The full reaction pathway was investigated by IRC calculations at UB3LYP/6-31G(d) and CASSCF(6,6)/6-31G(d) level. The active space orbitals the CASSCF calculations are chosen so as to include σ and σ^* orbitals formed and broken bonds with in-plane π and π^* orbitals of cyclopentyne. In order to get more accurate energies of the species, single point RCCSD(T)/6-31G(d,p) and CASSCF-MP2/6-31G(d) calculations were performed on the (U)B3LYP/cc-pVTZ and CASSCF(6,6)/6-31G(d) level optimized geometries, respectively.

The schematic representations of the reaction pathway drawn with respect to the results of DFT and CAS66 methods are given in Figure 3.20 and Figure 3.21, respectively. Electronic and zero point vibrational energies of the TS structures and the product, **M3**, relative to the reactant, **M7**, calculated by (U)B3LYP, CAS66, CAS66-MP2 and CC methods are listed in Table 3.18, while the thermodynamic parameters (ΔH_0^\ddagger and ΔH_0) of the reaction are given in Table 3.19. Furthermore, the crucial geometrical parameters all species obtained at CASSCF(6,6)/6-31G(d) and (U)B3LYP/cc-pVTZ levels are depicted in Figure 3.22 and Figure 3.23, respectively.

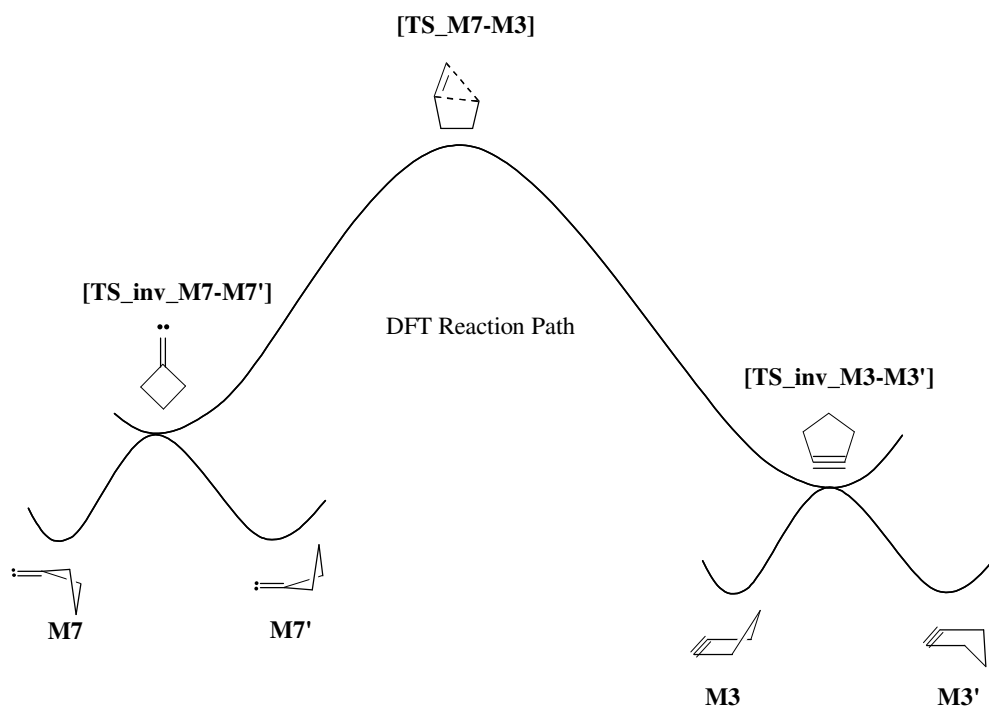


Figure 3.20 Schematic representation of **M7** to **M3** path resulted in UB3LYP method.

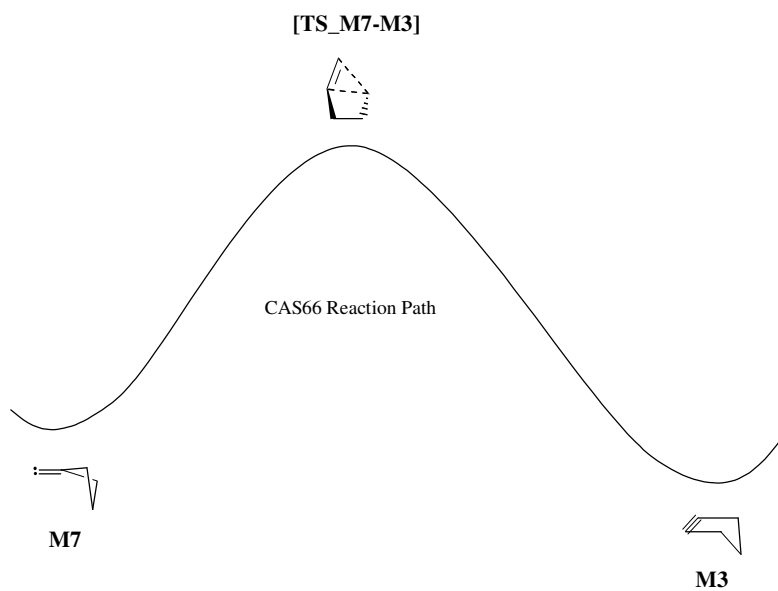


Figure 3.21 Schematic representation of **M7** to **M3** path resulted in CAS66 method.

Table 3.18 Electronic and zero point vibrational energies (kcal/mol) of **M3**, [TS_M7-M3], [TS_inv_M7-M7'] and [TS_inv_M3-M3'] relative to the energy (Hartrees) and ZPVE of **M7** calculated at different levels of theory. ZPVEs are given in parenthesis.

| Method | Basis set | M7 | M3 | [TS_inv_M7-M7'] | [TS_M7-M3] | [TS_inv_M3-M3'] |
|-----------|-------------|---------------------|--------------|------------------|---------------|------------------|
| UB3LYP | 6-31G(d) | -193.964813 (56.96) | -0.35 (0.58) | 0.24 (-0.20) | 2.98 (0.03) | -0.06 (0.41) |
| | 6-311G(d,p) | -194.015996 (56.41) | -1.38 (0.53) | 0.22 (-0.18) | 3.22 (0.02) | -1.09 (0.36) |
| | cc-pVTZ | -194.035640 (56.48) | -1.15 (0.46) | 0.23 (-0.19) | 3.02 (-0.02) | -0.95 (0.31) |
| CAS66 | 6-31G(d) | -192.725704 (60.73) | -1.40 (1.25) | | 13.79 (-0.10) | |
| CAS66-MP2 | 6-31G(d) | -193.271533 | -4.53 | | 6.30 | |
| RCCSD(T) | 6-31G(d) | -193.357259 | -6.01 | 0.41 | 3.54 | -5.44 |
| | 6-31G(d,p) | -193.407214 | -6.18 | 0.50 | 3.68 | -5.58 |

The vertical S - T energy gaps and $\langle S^2 \rangle$ values calculated by UB3LYP method are given in Table 3.20. The activation barrier and reaction enthalpy predicted by the CC method are 3.65 and -5.72 kcal/mol, correspondingly (Table 3.19). These estimations indicate that the reaction path is rather shallow as expected from experimental findings. The UB3LYP method had a good performance in the determination of the activation barrier because it predicted the value only 0.65 kcal/mol less than the CC barrier, even with small basis set. The CAS66 method, on the other hand, has rather poor performance in view of the fact that its guess is more than quadruple size of the barrier predicted by the CC method. In the reaction heat estimation, the DFT and CAS66 methods result in the values that are far away from the CC values, but they are in agreement with each other. In other words, **M3** is predicted as slightly stable (< 1 kcal/mol) than the corresponding carbene, **M7**, according to these methods. The CAS66 method underestimated the stability of cyclopentyne due to inability of recovering dynamic electron correlation. The CAS66-MP2 method predicted the cyclopentyne stability and activation barrier better than CAS66, as expected, since it includes the dynamic electron correlation. The B3LYP method shows similar behavior with the CASSCF i.e. it predicts an energy difference between the reactant and the product less than 1 kcal/mol. What is the reason behind producing such weak results for reaction heat while it gives excellent prediction of the barrier? It is seen from the Table 3.20, cyclopentyne contains an appreciable amount of spin contamination whereas there is no such problem in **M7** and [TS_M7-M3] whose energy difference gives the activation

barrier. Thus, the reason behind the low performance of DFT in determination of reaction heat is likely due to the inability of B3LYP functionals in the prediction of reasonable energy value for cyclopentyne molecule due to spin contamination. In order to understand the effect of spin contamination on this reaction, it is necessary to find out that how close the triplet state PES to the singlet reaction path. The triplet state of the reactant is approximately 43 kcal/mol above the singlet state. Similarly, [TS_M7-M3] has a triplet state energy of 121 kcal/mol relative to singlet one. These explain the zero $\langle S^2 \rangle$ values for the species, hence the good performance of B3LYP. However, the triplet state of cyclopentyne is located only 25 kcal/mol above its singlet state and, as previously stated, this molecule has 20% biradical character requiring a multiconfigurational wave function. These features of cyclopentyne obstruct the performance of B3LYP functionals even though unrestricted formalism is employed. Furthermore, the cyclopentyne lumomer introduced by semiempirical methods might be originated from this kind of structural features of cyclopentyne. In other words, the approach of triplet state on the product side of the reaction pathway probably produces such type of spurious stationary point when the methods based on single determinantal wave function is used.

Table 3.19 Activation barriers and reaction enthalpies at absolute zero for the **M7** to **M3** rearrangement calculated at various levels of theory.

| | UB3LYP | | | CAS66 | CAS66-MP2 ^a | RCCSD(T) ^b | |
|-----------------------|----------|-------------|---------|----------|------------------------|-----------------------|------------|
| | 6-31G(d) | 6-311G(d,p) | cc-pVTZ | 6-31G(d) | 6-31G(d) | 6-31G(d) | 6-31G(d,p) |
| ΔH_0^\ddagger | 3.01 | 3.25 | 3.00 | 13.69 | 6.19 | 3.52 | 3.65 |
| ΔH_0 | 0.24 | -0.84 | -0.69 | -0.16 | -3.28 | -5.55 | -5.72 |

^a CASSCF(6,6)/6-31G(d) level optimized geometries and their ZPVEs were used.

^b UB3LYP/cc-pVTZ level optimized geometries and their ZPVEs were used

The reactant and the product have extremely small inversion barriers whose values are less than 1 kcal/mol according to CC calculations. This shows the way that their geometries instantaneously invert back and forth. Accordingly, we can predict that there may be severe difficulties in the experimental determination of their ground state geometrical parameters.

Table 3.20 Vertical S – T energy differences, ΔE_{S-T}^{ver} , and $\langle S^2 \rangle$ values (in parenthesis) obtained from UB3LYP calculations for all species involved in the reaction.

| | (U)B3LYP | | | | | |
|------------------|----------|---------|-------------|---------|---------|---------|
| | 6-31G(d) | | 6-311G(d,p) | | cc-pVTZ | |
| M7 | 41.45 | (0.000) | 42.46 | (0.000) | 43.16 | (0.000) |
| M3 | 40.97 | (0.000) | 42.02 | (0.000) | 42.73 | (0.000) |
| [TS_inv_M7-M7'] | 121.34 | (0.000) | 121.97 | (0.000) | 121.21 | (0.000) |
| [TS_M7-M3] | 21.81 | (0.427) | 25.41 | (0.311) | 25.57 | (0.294) |
| [TS_inv_M3-M3'] | 22.06 | (0.418) | 25.60 | (0.305) | 25.80 | (0.287) |

The cyclopentyne and its precursor carbene, cyclobutylidene methylene, both have C_s symmetry with slightly puckered ring structures. The B3LYP and CAS66 methods predict distinct geometries for the TS structure connecting these minima, [TS_M7-M3]. While the one optimized by DFT method has a planar geometry of C_s symmetry, the TS of CAS66 is asymmetric with a tilted geometry so as to form directly C_s symmetric reactant and the product geometries. Due to that distinction in TS geometries, the predicted reaction paths seem to be different from each other. The IRC calculations at (U)B3LYP/6-31G(d) level indicate that there are five stationary points on this path. As going down from [TS_M7-M3] in both directions, the path passes from C_{2v} symmetric inversion TSs, [TS_inv_M7-M7'] and [TS_inv_M3-M3'] before reaching **M7** and **M3** whilst the IRC path of CAS66 method directly connects the two minima. Energetically, the inversion transition state structures are extremely close to the corresponding minima. Moreover, the TS modes of [TS_inv_M7-M7'] and [TS_inv_M3-M3'] have values of 74i and 94i cm^{-1} predicted at (U)B3LYP/cc-pVTZ level, pointing out that their curvatures are rather smooth. Toward minima, there must be an inflection point since the curvature will change its sign. Since the PES of the reaction is a hyper surface, these inflection points may constitute another path and within reaction the molecule may go down to minimum via this path before reaching the inversion TSs. Then, the attitude of molecule on the DFT pathway becomes very similar to that on the CASSCF route. As a result, the path predicted by the CASSCF method can be accepted as more plausible.

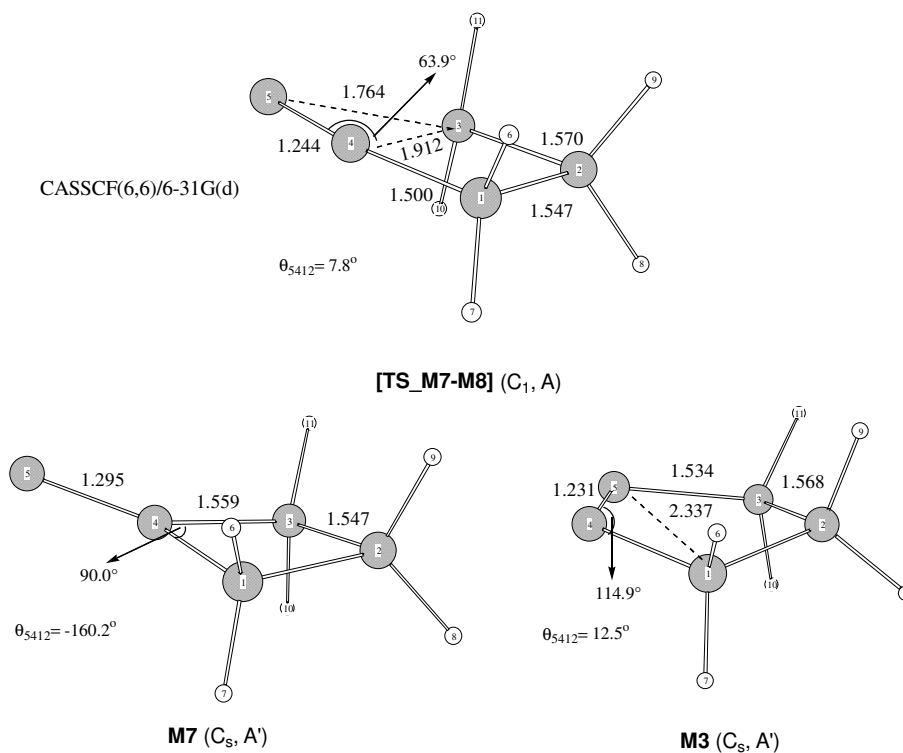


Figure 3.22 Selected geometrical parameters of all stationary points on **M7** to **M3** path optimized by CASSCF/6-31G(d) level.

The geometry of **[TS_M7-M3]** was predicted differently by the employed methods, as expressed. The elementary difference is that all carbon atoms of the TS are found to be planar ($\theta_{5412} = 0^\circ$) at DFT level as the CAS66 geometry is a bit tilted ($\theta_{5412} = 7.8^\circ$). Both methods agree with each other in the prediction of all the C-C single bonds and the C=C: bond lengths, but they give considerably different distances at the reaction site where the bond breakage and formation occurs. In the CAS66 geometry the broken bond is 0.151 Å longer and the formed bond is 0.153 Å smaller compared to the DFT geometry. For the reactant, **M7**, and the product, **M3**, molecules, the geometry predicted by CAS66 and DFT methods convincingly confirm each other within a deviation of 0.03 Å, at most. Moreover, the both methods are completely consistent with each other in that the C4-C5 bond distance continuously decreases from 1.29 Å to 1.23 Å as the reaction proceeds.

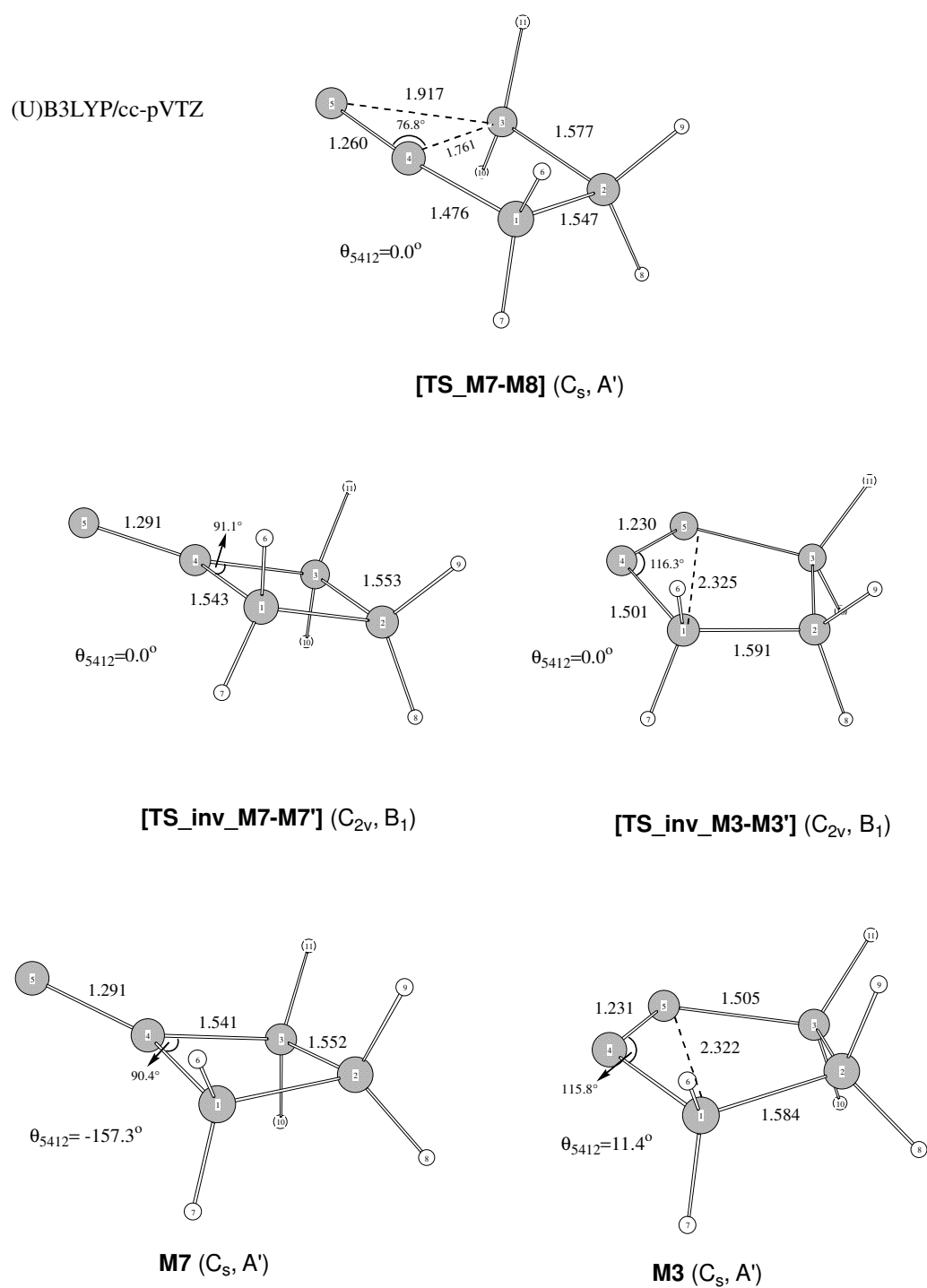


Figure 3.23 Selected geometrical parameters of all stationary points on **M7** to **M3** path optimized by (U)B3LYP/6-31G(d) level.

3.2.5. Triplet State Isomerization of Bicyclo[2.1.0]pent-5-ylidene (³B5) to cyclopenta-1,2-diene (³M2)

Cyclopenta-1,2-diene (**M2**), a five-membered ring allene (Figure 3.24), is an elusive compound since it has not been isolated or trapped, yet. First study for synthesis of **M2** was performed by Favorskii [190] in 1936. In his treatment, 1,2-dibromo-cyclopentene was reacted with metallic sodium, but the isolated product was **M3**, instead. Recently, fluoride ion-promoted elimination of a β -halogenosilane [204] to (2-Bromo-cyclopent-2-enyl)-trimethyl-silane and zinc catalysed elimination [205] of 1,5-dibromo-cyclopentene have been applied by Ceylan *et al.* [206] to generate this highly strained cyclic allene. However, isomeric Wurtz-like condensation products were obtained in both reactions. There were some other attempts for synthesis of **M2**, but unfortunately, none of them resulted with success [207, 208]. Finally, Algi *et al.* [22] has recently reported that one of its derivatives, namely 2-dehydro-3a,4,5,6a-pentahydropentalene, were firstly generated and trapped with furan by addition of fluorobromocarbene to a suitable bicyclic alkene (bicyclo[3.2.0]hept-6-ene) in ether containing methyllithium. Besides these experimental studies, Angus *et al.* [15] have computationally investigated the geometry and electronic structure of this compound. Their prediction was that the ground state geometry of **M2** is a chiral allenic structure in singlet state with an inversion barrier of 2-5 kcal/mol.

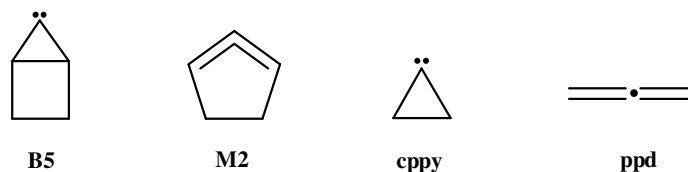


Figure 3.24 The structures of bicyclo[2.1.0]pent-5-ylidene (**B5**), 1,2-cyclopentadiene (**M2**), cyclopropylidene (**cppy**) and 1,2-propadiene (**ppd**).

Doering-Moore-Skattebol [209-211] method, which involves the ring opening of substituted cyclopropylidenes, is a convenient way for synthesis of allenes. From the beginning of 1960s, a large number of allenes has been produced

by this method. The ring opening of cyclopropylidene, (**cppy**), the simplest cyclic carbene, to 1,2-propadiene, (**ppd**) is called “cyclopropylidene to allene rearrangement”, the subject of many studies [212-216]. This thermal isomerization reaction must occur very quickly because **cppy** has never been isolated [217]. The ab initio calculations [218-222], convincingly show that the ground state of **cppy** is singlet and the conversion to **ppd** proceeds on a singlet potential energy surface with an activation barrier of only 3 - 6 kcal/mol [216], consistent with the experiments. This reaction can be considered as a prototype, which provides insight for the reactions involving ring opening of substituted cyclopropylidenes.

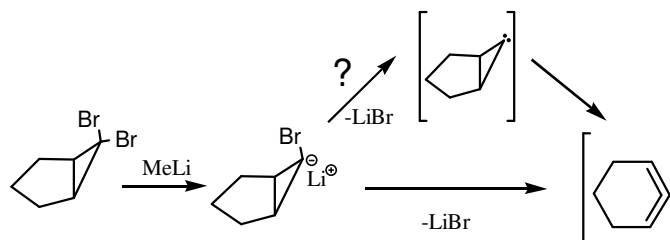


Figure 3.25 The proposed mechanism for synthesis of 1,2-cyclohexadiene.

Six membered ring analogue of **M2**, cyclohexa-1,2-diene, can be synthesized by the reaction 6,6-dibromobicyclo[3.1.0]hexane, a cyclopropylidene carbenoid, with methyllithium. The proposed mechanism [223] for this reaction is depicted in Figure 3.25. The formation of six membered ring allene in this mechanism is believed to occur via rearrangement of bicyclo[3.1.0]hex-6-ylidene. According to the high level ab initio calculations [216], it also has extremely small cyclopropylidene ring opening barrier that can be easily overcome at even very low temperatures. The synthesis of **M2** might be possible in a similar fashion with six-membered ring allene i.e. via isomerization of bicyclo[2.1.0]pent-5-ylidene (**B5**). Up to our knowledge, there is no information related to the existence of **B5**. On the other hand, seven- [224-227] and six- [209, 215, 228] membered ring homologues of this structure have been studied several times in the past. The cyclopropylidene ring opening barriers of these two bicyclic carbenes (bicyclo[4.1.0]hept-7-ylidene and bicyclo[3.1.0]hex-6-ylidene) were predicted computationally as 14.6 and 0.5 kcal/mol [215], respectively. These results indicate that the activation barriers for the ring opening decrease as the

ring size diminishes. Isomer **B5** has much more strain than those structures due to having smaller ring. Accordingly, it is reasonable to expect that there should be no activation barrier for singlet state conversion of **B5** to **M2**, and therefore, **B5** cannot be a minimum on singlet PES of C₅H₆. As explained in section 3.1.1, the singlet state of **B5** is not a stable structure. On the contrary, ³**B5** is a local minimum on the triplet PES of C₅H₆ in every level employed, so it must be a stable molecule. In the light of the given information, the **B5** to **M2** rearrangement on the singlet PES seems impossible to occur via cyclopropylidene to allene rearrangement. On the other hand, the same rearrangement taking place on the triplet PES most probably occurs via cyclopropylidene to allene rearrangement. As stated previously, the ³**B5** isomer may be achieved by the reaction of atomic carbon with cyclobutene. Hence, we report here the results of computational study employing DFT and high-level ab initio methods on bicyclo[2.1.0]pent-5-ylidene (³**B5**) to cyclopenta-1,2-diene (³**M2**) isomerization that is the main reaction to be presented, as well as the parent cyclopropylidene (³**cppy**) to 1,2-propadiene (³**ppd**) rearrangement [229] for comparison purpose.

Initially, the stationary points of ³**B5** to ³**M2** reaction have been obtained and identified by UB3LYP and CASSCF level optimizations. In order to introduce dynamic electron correlation into the CASSCF energies, single point CAS44-MP2 calculations, implemented in GAUSSIAN 98 package, were also performed at CAS44 optimized geometries. Single point UCCSD(T)/6-31G(d,p) level calculations were done on UB3LYP/cc-pVTZ optimized geometries to attain more accurate energies, as well. Species of the parent rearrangement, ³**cppy**, ³**ppd** and ³[**TS_cppy-ppd**], were optimized by UB3LYP method with 6-31G(d), 6-311G(d,p) and cc-pVTZ basis sets and then UCCSD(T) energy was obtained for each UB3LYP/cc-pVTZ level optimized geometries.

Electronic and zero point vibrational energies (kcal/mol) of the ³**B5** to ³**M2** reaction and the parent rearrangement are given in Table 3.21 and Table 3.22, respectively. While the activation barrier and reaction enthalpy (at 0 K) of the former reaction are shown in Table 3.23, those of the latter reaction are given in Table 3.24. The geometries and important geometrical parameters of these triplet state reactions are depicted in Figure 3.26 and Figure 3.27.

Table 3.21 Electronic and zero point vibrational energies (kcal/mol) of $^3\text{M2}$, $^3[\text{TS_B5-M2}]$ relative to the energy (Hartrees) and ZPVE of $^3\text{B2}$ calculated at different levels of theory. ZPVEs are given in parenthesis.

| Method | Basis set | $^3\text{B5}$ | $^3[\text{TS_B5-M2}]$ | $^3\text{M2}$ |
|-----------|-------------------------|---------------------|------------------------|----------------|
| UB3LYP | 6-31G(d) | -193.919417 (57.01) | 7.70 (-1.20) | -46.83 (-0.34) |
| | 6-31G(d,p) | -193.928092 (56.84) | 7.67 (-1.21) | -46.99 (-0.35) |
| | cc-pVTZ | -193.987559 (56.48) | 6.45 (-1.18) | -48.28 (-0.24) |
| CAS44 | 6-31G(d) | -192.653227 (61.37) | 6.65 (-1.72) | -52.41 (-1.30) |
| | 6-31G(d,p) | -192.663015 (61.07) | 6.63 (-1.74) | -52.53 (-1.29) |
| CAS44-MP2 | 6-31G(d) ^a | -193.231349 | 7.56 | -49.54 |
| | 6-31G(d,p) ^b | -193.280533 | 7.63 | -49.59 |
| UCCSD(T) | 6-31G(d,p) ^c | -193.360113 | 9.30 | -44.40 |

^aCASSCF(4,4)/6-31G(d) level, ^bCASSCF(4,4)/6-31G(d,p) level, ^cUB3LYP/cc-pVTZ level optimized geometries were used.

There is no experimentally obtained quantitative (thermodynamic, kinetic or spectroscopic) data available on the triplet state ring expansion of $^3\text{B5}$ to $^3\text{M3}$. Therefore, the UB3LYP/cc-pVTZ level optimized geometries are assumed the most accurate geometries and the activation and reaction enthalpies of the rearrangement calculated by CC method will constitute the base of our assessment on the results.

Table 3.22 Electronic and zero point vibrational energies (kcal/mol) of ^3ppd and $^3[\text{TS_cppy-ppd}]$ relative to the energy (Hartrees) and ZPVE of $^3\text{cppy}$ calculated at different levels of theory. ZPVEs are given in parenthesis.

| | | $^3\text{cppy}$ | $^3[\text{TS_cppy-ppd}]$ | ^3ppd |
|-----------------------|-------------|---------------------|---------------------------|----------------|
| UB3LYP | 6-31G(d) | -116.529368 (34.66) | 16.97 (-2.80) | -31.51 (-1.67) |
| | 6-311G(d,p) | -116.561118 (34.28) | 14.99 (-3.10) | -33.36 (-1.61) |
| | cc-pVTZ | -116.573310 (34.31) | 14.45 (-2.95) | -33.97 (-1.55) |
| UCCSD(T) ^a | 6-31G(d) | -116.189551 | 19.35 | -27.14 |
| | 6-311G(d,p) | -116.229875 | 17.99 | -27.12 |
| | cc-pVTZ | -116.303345 | 16.99 | -28.73 |

^a UB3LYP/cc-pVTZ level optimized geometries were used.

Table 3.23 Activation barriers and reaction enthalpies at absolute zero for the $^3\text{B5}$ to $^3\text{M2}$ rearrangement calculated with various methods.

| | UB3LYP | | | CAS44 | | CAS44-MP2 | | UCCSD(T) |
|-----------------------|----------|------------|---------|----------|------------|-----------------------|-------------------------|-------------------------|
| | 6-31G(d) | 6-31G(d,p) | cc-pVTZ | 6-31G(d) | 6-31G(d,p) | 6-31G(d) ^a | 6-31G(d,p) ^b | 6-31G(d,p) ^c |
| ΔH_0^\ddagger | 6.50 | 6.45 | 5.28 | 4.92 | 4.90 | 5.84 | 5.89 | 8.12 |
| ΔH_0 | -47.18 | -47.34 | -48.52 | -53.71 | -53.81 | -50.84 | -50.88 | -44.63 |

^aCASSCF(4,4)/6-31G(d) level, ^bCASSCF(4,4)/6-31G(d,p) level, ^cUB3LYP/cc-pVTZ level optimized geometries and their ZPVEs were used.

Table 3.24 Activation barriers and reaction enthalpies at absolute zero for the $^3\text{cppy}$ to ^3ppd rearrangement calculated with DFT and CCSD(T) methods.

| | UB3LYP | | | UCCSD(T) | | |
|-----------------------|----------|-------------|---------|----------|-------------|---------|
| | 6-31G(d) | 6-311G(d,p) | cc-pVTZ | 6-31G(d) | 6-311G(d,p) | cc-pVTZ |
| ΔH_0^\ddagger | 14.16 | 11.89 | 11.50 | 16.55 | 14.89 | 14.04 |
| ΔH_0 | -33.19 | -34.97 | -35.53 | -28.81 | -28.73 | -30.28 |

^a UB3LYP/cc-pVTZ level optimized geometries and their ZPVEs were used.

The UCCSD(T) method estimates a moderate enthalpic barrier whose value is 8.12 kcal/mol for the isomerization of $^3\text{B5}$. The values obtained by larger basis sets for the same method are expected to be more accurate. Accordingly, the best UB3LYP value for the barrier should be 5.28 kcal/mol found with cc-pVTZ basis set, even though the usage of larger basis decreases the barrier height and takes the value away from the reference. CAS44 method predicted the barrier height of 4.90 kcal/mol, which is in the order of UB3LYP. The CAS44-MP2 method estimated the best activation energy (5.89 kcal/mol) that is 2.2 kcal/mol lower than the reference. For the overall performance of the activation enthalpy predictions of all three methods, it is concluded that they agree with each other within 1 kcal/mol while they underestimate the barrier by 2-3 kcal/mol.

It is certain that the reaction is exothermic with the reaction enthalpy of -44.63 kcal/mol by UCCSD(T) method. The best method for ΔH_0 prediction among the three is UB3LYP that overestimates the reaction exothermicity by only ~4 kcal/mol. The CAS44-MP2 method works better than the CAS44 method because it predicted the ΔH_0 value is around 6 kcal/mol more negative than the reference, while CAS44 estimation is ~9 kcal/mol below the CC value.

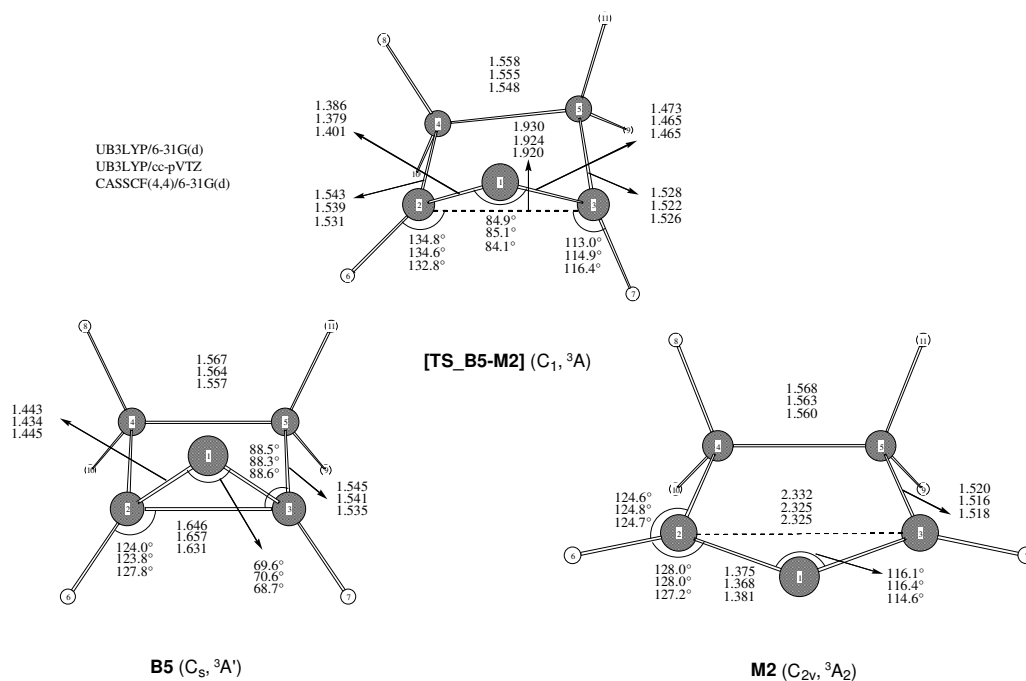


Figure 3.26 Selected geometrical parameters for 3B5 , 3M2 and $^3[TS_B5-M2]$ geometries optimized by DFT and CASSCF methods.

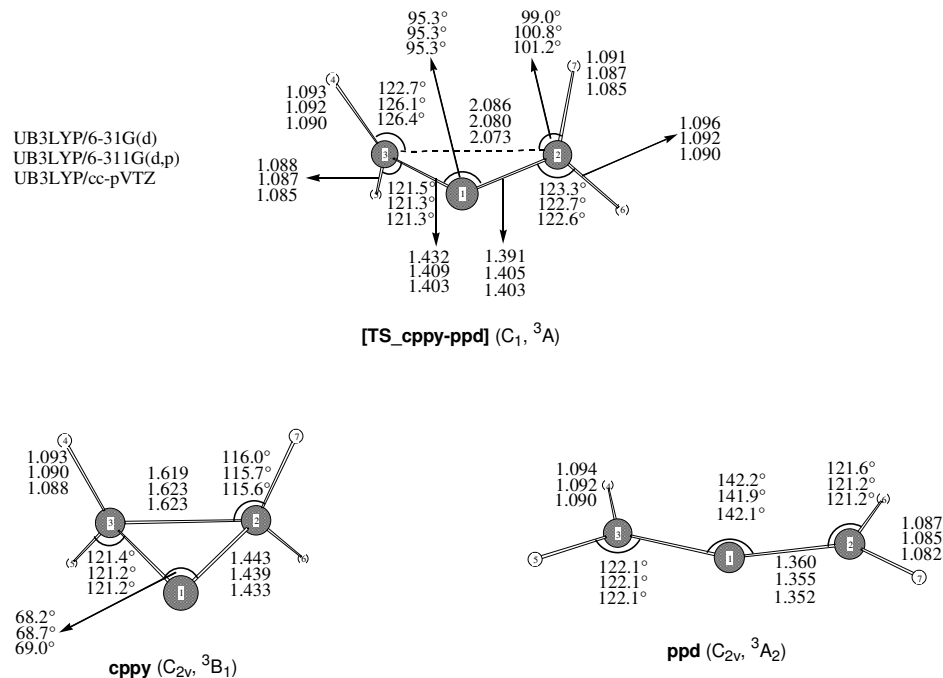


Figure 3.27 Selected geometrical parameters for 3ccpy , 3ppd and $^3[TS_ccpy-ppd]$ geometries optimized by UB3LYP method.

The isomerization of $^3\text{cppy}$ to ^3ppd is also exothermic with heat of reaction (ΔH_0) about -30 kcal/mol and its calculated barrier height is 14 kcal/mol. Compared to the $^3\text{B5}$ isomerization, the parent reaction is both less exothermic and less facile one owing to its lower reaction heat and higher enthalpic barrier. The main reaction has an activation energy which is ~ 6 kcal/mol lower than that of parent reaction. UB3LYP method predicts the activation energy of the parent reaction pretty good since the deviation between these values is only ~ 2 kcal/mol. On the other hand, it overestimates the reaction enthalpy by ~ 5 kcal/mol resembling to the case in the main reaction.

The activation barriers and exothermicity of these highly correlated reactions are considerably different from each other. In other words, the exothermicity of $^3\text{B5}$ isomerization is higher than that of the parent one while its activation barrier is lower. This feature of the main reaction should be originated from the strain on the $^3\text{B5}$, which is higher than that of $^3\text{cppy}$. It is known that $^3\text{B5}$ contains a cyclopropylidene unit in its structure. When the geometries of parent $^3\text{cppy}$ and cyclopropylidene unit of $^3\text{B5}$ are compared, it is seen that the carbene angle, C1-C2, C1-C3 and C2-C3 bond lengths have rather similar values. On the other hand, these structures have several geometrical parameters that are considerably different from each other. As the $^3\text{cppy}$ molecule has four CCH angles (C2-C3-H4, C3-C2-H7, C2-C3-H5 and C3-C2-H6) whose predicted values are 116° , $^3\text{B5}$ has two CCH and two CCC angles corresponding to the CCH angles of $^3\text{cppy}$. The CCC angles of $^3\text{B5}$ are around 88° , which is 28° lower than the corresponding CCH angles of parent cyclopropylidene due to the constraints imposed by the four-membered ring. The HCC angles in $^3\text{B5}$ are 124° , which are 8° more than the corresponding angles in $^3\text{cppy}$. This 8° increase cannot relax the strain caused by the four-membered ring. In summary, the ring constraints in $^3\text{B5}$ make this structure very strained, leading to an increase in both reactivity of the molecule and exothermicity of the reaction. Furthermore, instability of the $^1\text{B5}$ structure is most probably due to this huge strain exerted by four-membered ring.

The reactant, $^3\text{B5}$, is a C_s symmetric molecule with $^3A'$ electronic state. The geometries of $^3\text{B5}$ predicted by DFT and CAS44 methods almost fully agree with

each other within the deviations less than 0.03 Å in distances and 2° in angles. The product, $^3\mathbf{M2}$, is found to be a C_{2v} symmetric planar allene structure with 3A_2 electronic state by all four methods. These findings exactly matches the triplet planar five membered cyclic allene found by Angus *et al.*[15]. Unfortunately, we could not compare the geometrical parameters of their triplet allene with our geometries since they did not present any geometry data related to this molecule. Therefore, geometry of the product will be compared with that of 1,2-propadiene ($^3\mathbf{ppd}$) obtained at UB3LYP/cc-pVTZ level. Whereas the C1-C2 and C1-C3 bond lengths are almost equal for both molecules, the allenic angle of $^3\mathbf{M2}$ is $\sim 25^\circ$ smaller than that of $^3\mathbf{ppd}$. Evidently, this is an expected situation because $^3\mathbf{M2}$ is a cyclic molecule and the ring constraints make the angle narrow.

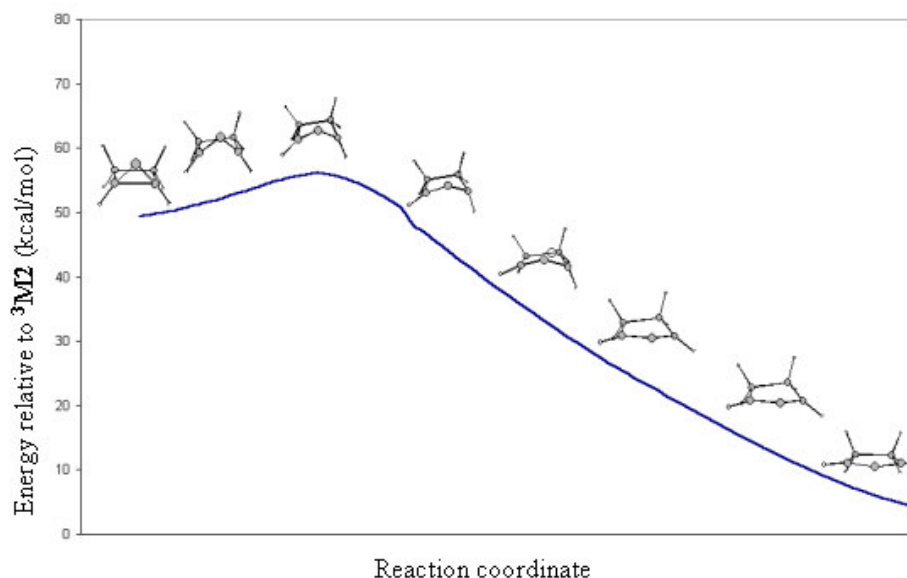


Figure 3.28 IRC pathway of $^3\mathbf{B5}$ to $^3\mathbf{M2}$ isomerization calculated at UB3LYP/6-31G(d) level

$^3[\mathbf{TS_B5-M2}]$ has an asymmetric structure whose C2-C3 bond, ~ 1.92 Å, is broken. When its cyclopropylidene unit is taken into account, it resembles the TS of the parent reaction, $^3[\mathbf{TS_cppy-ppd}]$. At the outset, it is important to note that the C2-C3 bond breakages in both structures occur in a way that the C_s symmetry planes of both reactants are removed somewhere until the TSs are reached. Although the corresponding C1-C2 and C1-C3 bond distances have similar value, all of the

geometrical parameters of $^3[\text{TS_B5-M2}]$ are more strained than those of $^3[\text{TS_cppy-ppd}]$. The most prominent parameter in which this feature arises is the allenic (C2-C1-C3) angle. This angle has a value of 95° in TS of parent reaction while its value drops to 85° in $^3[\text{TS_B5-M2}]$. It is clear that $^3[\text{TS_B5-M2}]$ being more strained is attributable to the constraints exposed by its five-membered ring structure.

Conrotatory opening of cyclopropylidene ring in $^3\text{B5}$ would lead to enormously strained trans-substituted cyclic allene, therefore, this type opening is impossible. Accordingly, $^3\text{B5}$ must open disrotatorily. The transition state structure $^3[\text{TS_B5-M2}]$ is not symmetrical, leading to an unsymmetrical disrotatory ring opening. Similar situation arises in the ring opening reaction of $^3\text{cppy}$ as revealed in Rauk's study [222]. This unsymmetrical disrotatory motion of $^3[\text{TS_B5-M2}]$ has been verified by intrinsic reaction coordinate (IRC) calculations at UB3LYP/6-31G(d) and CASSCF(4,4)/6-31G(d) levels of theory. Figure 3.28 illustrates not only the full IRC pathway calculated at UB3LYP/6-31G(d) level but also the geometries at several IRC points including reactant, TS and product. It is very prominent that one side of the molecule ($^3\text{B5}$) opens faster than the other part and it removes the C_s symmetry plane on the path by letting an asymmetric TS geometry. After completion of the movement of the faster part, the slower part starts to move and forms the product, $^3\text{M2}$.

CHAPTER IV

CONCLUSION

In the present study, computational stabilities of eighteen cyclic C_5H_6 isomers have been explored both on singlet and triplet state PESs, and seven unimolecular isomerization reactions occurring among several of these molecules have been investigated computationally by ab initio quantum chemical methods. The results discussed above can be summarized as follows;

- (1) All of the isomers have singlet ground states except for bicyclo[2.1.0]pent-5-ylidene (**B5**) that has no stable geometry on the singlet C_5H_6 PES. Thermodynamically, cyclopenta-1,3-diene (**M1**) is the most stable cyclic C_5H_6 isomer while cyclopent-1,4-diylidene (**M6**) is the least stable one among all. Cyclopenta-1,2-diene (**M2**) and cyclopentyne (**M3**) have biradical characters of 46.9 and 21.5%, respectively, in their ground states. All of the remaining isomers are closed shell structures.
- (2) For the conversions of bicyclo[2.1.0]pent-2-ene (**B1**) and tricyclo[2.1.0.0^{2,5}]-pentane (**T1**) into 1,3-cyclopentadiene (**M1**); both processes are concerted, and the paths pass through transition states with a high degree of biradical character. In both reactions the π bonds of cyclopentadiene are formed after TSs, on the **M1** side of the paths. Geometries of the stable species predicted by the DFT and CASSCF methods were equally good. CC and B3LYP methods predicted the reaction enthalpies excellently (-47.7 vs. exp = -47.8 kcal/mol for **B1**, and -63.8 kcal/mol for **T1**, at the B3LYP level) whereas the MCSCF method did not perform as well. The activation enthalpy for the ring opening of **B1** was calculated by the CR-CCSD(T) method to be 25.2 kcal/mole, in good agreement

with experiment. The value obtained by the UB3LYP method was a satisfactory 23.3 kcal/mol even though there was a high spin contamination ($\langle S^2 \rangle = 0.68$) in the singlet biradical transition state. It appears that the B3LYP functional is quite resistant to the possible consequences of spin contamination. The performance of CAS88-MP2 was poorer, predicting the activation enthalpy too low by 6 kcal/mol. The low activation energies given by CASSCF-MP2 were rationalized by showing that the method overestimated the correlation energy of biradical structures, a problem shared by UB3LYP when spin contamination is too high. CASSCF also overestimated the biradical character by predicting unrealistically long distances between the radical centers. The transition structure, [TS_T1-M1], was found to be nearly degenerate with the triplet state causing a reliable assessment of its properties very difficult. We argued that the energy obtained by the UB3LYP method for this structure was probably too low as in CAS88-MP2, but that the geometry was more plausible than that predicted by the CAS88 method. Using the UB3LYP structure, the activation enthalpy for the ring opening of **T1** was obtained by the CRCCSD(T) method to be 48.2 kcal/mol.

- (3) 1,5-sigmatropic hydrogen shift in cyclopentadiene is a facile, concerted reaction with an aromatic-like TS. The activation barrier estimations of B3LYP and CC methods are 25.24 and 28.78 kcal/mol, correspondingly. As these values are compared with the experimental barrier having the value of 23.6 kcal/mol, it is seen that the B3LYP method has better performance with an overestimation of only ~2 kcal/mol. Furthermore, especially in hydrogen shift reactions, basis set to be used for DFT calculations should contain polarization functions on hydrogen atoms to reach better energy values. In this reaction addition of polarization functions on hydrogens improved the calculated activation enthalpy value by 1 kcal/mol.
- (4) 1,2-hydrogen shift reactions of 3-cyclopentenylidene (**M4**) and 2-cyclopentenylidene (**M5**) are easily occurring reactions having rather high exothermicity. RCCSD(T)/6-31G(d,p) level single point calculations performed

on (U)B3LYP/cc-pVTZ level optimized geometries predicted the activation barriers of 3.13 and 10.12 kcal/mol, as well as, the reaction enthalpy values of -71.28 and -64.05 kcal/mol, respectively. These values are consistent with the results of the previous studies. 1,2-hydrogen shift in **M4** is not only more facile but also more exothermic compared to hydrogen migration reaction of **M5**. The B3LYP method worked rather well for predicting both parameters of the former reaction, as well as the activation barrier of the latter. However, it underestimated the reaction enthalpy of the **M5** to **M1** conversion by ~4 kcal/mol. Additionally, the basis set enlargement for DFT calculations had almost no improvement on the reaction enthalpy of the **M5** to **M1** conversion, while it enhanced the accuracy of the other three parameters up to 2 kcal/mol. The reason of **M5** being more stable than **M4** is due to the conjugation of the carbene carbon and the double bond in **M5**. The TS structures of both reactions are both structurally and energetically degenerate, hence the difference in their activation barriers is totally originated from the stability difference between the reactant molecules.

- (5) The reaction path of cyclobutylidene methylene (**M7**) to cyclopentyne (**M3**) rearrangement is rather shallow as expected from the experimental findings. The activation barrier and reaction enthalpy predicted by the RCCSD(T) method 3.65 and -5.72 kcal/mol, respectively. The B3LYP method calculated the energies of **M7** and [TS_**M7-M3**] accurately and hence produced very reasonable reaction barrier value, which is very close to that of the CC method. On the other hand, its reaction enthalpy prediction was rather poor, probably caused by the inability of these functionals in the prediction of the cyclopentyne energy due to its biradical character requiring multi configurational methods. As expected, the CAS66 method had worse performance in the quantitative estimations and it overestimated the barrier height while it predicted more plausible path and TS structure for the reaction. CAS66-MP2 method had better performance in the quantitative estimations because it includes the dynamic electron correlation, which is not sufficiently recovered by the CAS66 method.

Furthermore, the CC methods predicted that **M7** and **M3** have extremely small inversion barriers of approximately 0.5 kcal/mol.

- (6) Triplet state isomerization of bicyclo[2.1.0]pent-5-ylidene (**³B5**) to cyclopenta-1,2-diene (**³M2**), as well as, its parent reaction, cyclopropylidene (**³cppy**) to 1,2-propadiene (**³ppd**) were investigated at several levels of theory including DFT, CASSCF and CC methods. The UCCSD(T) method estimated a moderate activation barrier whose value is 8.12 kcal/mol for the isomerization of **³B5** with the reaction enthalpy of -44.63 kcal/mol. The isomerization of **³cppy** to **³ppd** is also exothermic with the heat of reaction about -30 kcal/mol and its calculated barrier height is 14 kcal/mol. The **³B5** isomerization is more reactive (with lower barrier) and more exothermic than the parent reaction due to the strain on the reactant imposed by the four-membered ring. Corresponding bond lengths and allenic angles in the reactants, the TSs and the products of both reactions were found to be similar to some extent, indicating the resemblance, but some critical geometrical parameters reflected the cyclic constraints for the reaction of **³B5**. Finally, the IRC calculations of UB3LYP and CAS44 methods verified that **³B5** has an unsymmetrical disrotatory ring opening as the asymmetrical geometry of **³[TS_B5-M2]** implies.

REFERENCES

- [1] Keenan M. J., "Cyclopentadiene and Dicyclopentadiene", Exxon Chemical Company, Kirk-Othmer Encyclopedia of Chemical Technology.
- [2] Roscoe, H. E. *Ann.*, **1886**, 232, 348.
- [3] Wilson, P. J.; Wells J. H. *Chem. Rev.*, **1944**, 34, 1, and references therein.
- [4] Erker, G. *Pure and Applied Chemistry* 1989, 61, 1715.
- [5] Dias, A. R.; Simoes, J. A. M. *Polyhedron* 1988, 7, 1531.
- [6] Kumar, A. *Chem. Rev.*, **2001**, 101, 1.
- [7] Kagan, H. B.; Riant, O. *Chem. Rev.*, **1992**, 92, 1007.
- [8] Li, C. J. *Chem. Rev.*, **1993**, 93, 2023.
- [9] Branchadell, V. *Int. J. Quan. Chem.*, **1997**, 61, 381.
- [10] Jursic B. S. *Theochem*, **1995**, 358, 139.
- [11] Pedley, J. B. *The Thermochemical Data and Structures of Organic Compounds; TRC Data Series*; TRC: Texas, **1994**; Vol. I.
- [12] Taylor, D. R. *Chem. Rev.*, **1966**, 66, 317.
- [13] R. P. Johnson; *Chem. Rev.*, **1989**, 89, 1111.
- [14] Balci, M., Taskesenligil, Y.; "Recent Development in Strained Cyclic Allenes In Strained and Interesting Organic Molecules" Edited by B. Halton, JAI Press Inc., Stamford, Connecticut, **2000**.
- [15] Angus, R.O.; Schmidt, M. W.; Johnson, R. P. *J. Am. Chem. Soc.*, **1985**, 107, 532.
- [16] Blomquist, A. T.; Burger, R. E., Jr.; Liu, L. H.; Bohrer, J. C.; Sucsy, A. C.; Kleis J. J. *J. Am. Chem. Soc.*, **1951**, 73, 5510.
- [17] Ball, W. J.; Landor, S. R. *J. Chem. Soc.* **1962**, 2298.
- [18] Wittig, G.; Meske-Schuller, J. *Justus Liebigs Ann. Chem.* **1968**, 711, 76.

- [19] Visser, J. P.; Ramakers, J. E. *J. Chem. Soc., Chem. Commun.* **1972**, 178.
- [20] Wittig, G.; Fritze, P. *Angew. Chem., Int. Ed. Engl.* **1966**, 5, 846.
- [21] Balci, M.; Jones, W. M. *J. Am. Chem. Soc.* **1980**, 102, 7607.
- [22] Algi, F.; Özen, R.; Balci, M. *Tetrahedron Lett.* **2002**, 43, 3129.
- [23] Skell, P. S.; Wescott, L. D.; Golstein, J. P.; Engel, R. R. *J. Am. Chem. Soc.* **1965**, 87, 2829.
- [24] Strauss, C. E. M.; Kable, S. H.; Chawla, G. K.; Houston, P. L. *J. Chem. Phys.*, **1991**, 94, 1837.
- [25] Skell, P. S.; Klabunde, K. J.; Plonka, J. H.; Roberts, J. S.; William-Smith, D. L. *J. Am. Chem. Soc.*, **1973**, 95, 1547.
- [26] McKee, M. L.; Paul, G. C.; Shevlin, P. B. *J. Am. Chem. Soc.*, **1990**, 112, 3374.
- [27] Emanuel, C. J. ; Shevlin, P. B. *J. Am. Chem. Soc.*, **1994**, 116, 5991.
- [28] Armstrong, B. M.; Zheng, F.; Shevlin, P. B. *J. Am. Chem. Soc.*, **1998**, 120, 6007.
- [29] Xu, G.; Chang, T. M.; Zhou, J.; McKee, M. L.; Paul, G. C.; Shevlin, P. B. *J. Am. Chem. Soc.*, **1999**, 121, 7150.
- [30] Kaiser, R. I.; Lee, Y. T.; Suits, A. G. *J. Chem. Phys.*, **1996**, 105, 8705.
- [31] Olivella, S.; Pericas, M. A.; Riera, A.; Sole, A. *J. Am. Chem. Soc.*, **1986**, 108, 6884.
- [32] Skattebol, L. *Chem. Ind. London.*, **1962**, 2146.
- [33] Wiberg, K. B.; Walker, F. H., *J. Am. Chem. Soc.*, **1982**, 104, 5239.
- [34] Rogers, D. W.; McLafferty, F. J.; Podosenin A. V. *J. Phys. Chem. A*, **1988**, 102, 1209.
- [35] Clarck, T.; Wilhelm, D.; Schleyer P. v. R. *Tet. Lett.*, **1982**, 23, 3547.
- [36] Brauman, J. I.; Ellis, L. E.; Tamalen, E. E., *J. Am. Chem. Soc.*, **1966**, 88, 846.
- [37] Jensen, F., *J. Am. Chem. Soc.*, **1989**, 111, 4643.
- [38] Brauman, J. I.; Golden, D. M., *J. Am. Chem. Soc.*, **1968**, 90, 1920.
- [39] Golden, D. M.; Brauman, J. I., *Trans. Faraday Soc.*, **1969**, 65, 464.
- [40] Andrews, G. D.; Baldwin, J. E., *J. Am. Chem. Soc.*, **1977**, 99, 4853.
- [41] Woodward, R. B.; Hoffmann, R., *Angew. Chem. Int. Ed. Engl.*, **1969**, 8, 781.
- [42] Wagner, H. U.; Szeimies, G.; Chandrasekhar, J; Schleyer, P. v. R.; Pople, J. A. *J. Am. Chem. Soc.*, **1978**, 100, 1210.

- [43] Harnisch, J.; Baumgartel, O.; Szeimies, G.; Meerssche, M.; Germain, G.; Declercq, J. *J. Am. Chem. Soc.*, **1979**, 101, 3370.
- [44] Wiberg, K. B.; Artis, D. R.; Bonneville, G. *J. Am. Chem. Soc.*, **1991**, 113, 7969.
- [45] Maier, W. F.; Schleyer, P. v. R., *J. Am. Chem. Soc.*, **1981**, 133, 1891.
- [46] Jones, W.M.; Stowe, M. E., *Tetrahedron Lett.*, **1964**, 5, 3459.
- [47] Bloch, R.; Denis, J., *Angew. Chem.*, **1980**, 92, 969.
- [48] Dodziuk, H.; Leszczynski, J.; Jacowski, K., *Tetrahedron*, **2001**, 57, 5509.
- [49] Doering, W. V. E.; Pomerantz, M.; *Tetrahedron Lett.*, **1964**, 961.
- [50] Masamune, S. J., *Am. Chem. Soc.*, **1964**, 86, 735.
- [51] Andrews, G. D.; Baldwin, J. E. *J. Am. Chem. Soc.* **1977**, 99, 4851.
- [52] Levin, M. D.; Kaszynski, P.; Michl, J., *Chem. Rev.*, **2000**, 100, 169.
- [53] M. D. Newton, J. M. Schulman, M. M. Manus; *J. Am. Chem. Soc.*, **1974**, 96, 17.
- [54] K. B. Wiberg, R. F. W. Bader, C. D. H. Lau; *J. Am. Chem. Soc.*, **1987**, 109, 1001.
- [55] Wiberg, K. B. *Angew. Chem., Int. Ed. Engl.*, **1986**, 25, 312.
- [56] Semmler, K.; Szeimies, G.; Belzner, J. *J. Am. Chem. Soc.*, **1985**, 107, 6410.
- [57] Wiberg, K. B. *Chem. Rev.*, **1989**, 89, 975.
- [58] K. B. Wiberg, S. T. Wadell; *Tetrahedron Letters*, **1987**, 28, 151.
- [59] K. B. Wiberg, S. T. Wadell, K. Laidig; *Tetrahedron Letters*, **1986**, 27, 1553.
- [60] A. Sella, H. Basch, S. Hoz; *Tetrahedron Letters*, **1996**, 37, 5573.
- [61] K. B. Wiberg, N. McMurdie, J. V. McClusky, C. M. Hadad; *J. Am. Chem. Soc.*, **1993**, 115, 10653.
- [62] K. B. Wiberg, J. V. McClusky; *Tetrahedron Letters*, **1987**, 28, 5411.
- [63] E. Schrödinger, *Ann. Physik.*, **1926**, 79, 361.
- [64] M. Born, J. R. Oppenheimer, *Ann. Physik.*, **1927**, 84, 457.
- [65] J. C. Slater, *Phys. Rev.*, **1930**, 35, 210.
- [66] Hartree, D. R. *Proc. Camb. Phil. Soc.* **1928**, 24, 89.
- [67] Fock. V. *Z. Phys.* **1930**, 61, 161.
- [68] Pople, J. A.; Nesbet, R. K. *J. Chem. Phys.*, **1954**, 22, 571.
- [69] F. Jensen, "Introduction to Computational Chemistry", John Wiley & Sons, Denmark, **1999**, 150.
- [70] Roothaan, C. C. J. *Rev. Mod. Phys.* **1951**, 23, 69.

- [71] Hall, G. G. *Proc. Roy. Soc. London*, **1951**, A205, 541.
- [72] Hehre, W. J.; Stewart, R. F., Pople, J. A. *J. Chem. Phys.*, **1969**, 51, 2657.
- [73] J. S. Binkley, J. A. Pople and W. J. Hehre, *J. Amer. Chem. Soc.*, **1980**, 102, 939.
- [74] W. J. Hehre, R. Ditchfield and J. A. Pople, *J. Chem. Phys.*, **1972**, 56, 2257.
- [75] Frisch, M. J.; Pople, J. A.; Binkley, J. S. *J. Chem. Phys.*, **1984**, 80, 3265.
- [76] D. E. Woon and T. H. Dunning Jr., *J. Chem. Phys.*, **1993**, 98, 1358.
- [77] R. A. Kendall, T. H. Dunning Jr. and R. J. Harrison, *J. Chem. Phys.*, **1992**, 96, 6796.
- [78] T. H. Dunning Jr., *J. Chem. Phys.*, **1989**, 90, 1007.
- [79] S. F. Boys, *Proc. Roy. Soc. (London)*, **1950**, A201, 125.
- [80] J. A. Pople, J. S. Binkley, R. Seeger, *Int. J. Quant. Chem. Symp.*, **1976**, 10, 1.
- [81] L. Brillouin, *Actualities Sci. Ind.*, **1934**, 71, 159.
- [82] J. A. Pople, R. Seeger and R. Krishnan, *Int. J. Quant. Chem. Symp.*, **1977**, 11, 149.
- [83] R. Krishnan, H. B. Schlegel and J. A. Pople, *J. Chem. Phys.*, **1980**, 72, 4654.
- [84] K. Raghavachari and J. A. Pople, *Int. J. Quant. Chem.*, **1981**, 20, 167.
- [85] Staroverov, V. N.; Davidson, E. R. *J. Am. Chem. Soc.* **2000**, 122, 7377.
- [86] Staroverov, V. N.; Davidson, E. R. *J. Mol. Struct. (Theochem)*, **2001**, 573, 81.
- [87] Møller, C.; Plesset, M. S. *Phys. Rev.* **1934**, 46, 618.
- [88] M. Springborg, “*Methods of Electronic-Structure Calculations*”, John Wiley & Sons, England, **2000**.
- [89] A. R. Leach, “*Molecular Modeling*”, Longman, England, **1996**.
- [90] J. J. McDouall, K. Peasley and M. A. Robb, *Chem. Phys. Lett.*, **1988**, 148, 183.
- [91] K. Wollinski, H. L. Sellers, P. Pulay, *Chem. Phys. Lett.*, **1987**, 140, 255.
- [92] K. Andersson, P. Malmqvist, B.O. Roos, A. J. Sadlej, K. Wollinski, *J. Phys. Chem.*, **1990**, 94, 5483.
- [93] K. Andersson, P. Malmqvist, B.O. Roos, *J. Phys. Chem.*, **1992**, 96, 1218.
- [94] Nakano, H. *J. Chem. Phys.*, **1993**, 99, 7983.
- [95] Hirao, K. *Chem. Phys. Lett.*, **1993**, 201, 59.
- [96] Cizek, J. *J. Chem. Phys.*, **1966**, 45, 4256.
- [97] Cizek, J. *Adv. Chem. Phys.* **1969**, 14, 35.
- [98] Bartlett, R. J. *J. Phys. Chem.* **1989**, 93, 1697.

- [99] J. A. Pople, R. Krishnan, H. B. Schlegel and J. S. Binkley, *Int. J. Quant. Chem.*, **1978**, 14, 545.
- [100] G. D. Purvis and R. J. Bartlett, *J. Chem. Phys.*, **1982**, 76, 1910.
- [101] G. E. Scuseria, C. L. Janssen and H. F. Schaefer, III, *J. Chem. Phys.*, **1988**, 89, 7382.
- [102] G. E. Scuseria and H. F. Schaefer, III, *J. Chem. Phys.*, **1989**, 90, 3700.
- [103] J. A. Pople, M. Head-Gordon and K. Raghavachari, *J. Chem. Phys.*, **1987**, 87, 5968.
- [104] Frisch, M. J.; Trucks, G. W.; Schlegel, H. B.; Scuseria, G. E.; Robb, M. A.; Cheeseman, J. R.; Zakrzewski, V. G.; Montgomery, J. A., Jr.; Stratmann, R. E.; Burant, J. C.; Dapprich, S.; Millam, J. M.; Daniels, A. D.; Kudin, K. N.; Strain, M. C.; Farkas, O.; Tomasi, J.; Barone, V.; Cossi, M.; Cammi, R.; Mennucci, B.; Pomelli, C.; Adamo, C.; Clifford, S.; Ochterski, J.; Petersson, G. A.; Ayala, P. Y.; Cui, Q.; Morokuma, K.; Malick, D. K.; Rabuck, A. D.; Raghavachari, K.; Foresman, J. B.; Cioslowski, J.; Ortiz, J. V.; Baboul, A. G.; Stefanov, B. B.; Liu, G.; Liashenko, A.; Piskorz, P.; Komaromi, I.; Gomperts, R.; Martin, R. L.; Fox, D. J.; Keith, T.; Al-Laham, M. A.; Peng, C. Y.; Nanayakkara, A.; Challacombe, M.; Gill, P. M. W.; Johnson, B.; Chen, W.; Wong, M. W.; Andres, J. L.; Gonzalez, C.; Head-Gordon, M.; Replogle, E. S.; Pople, J. A., Gaussian 98 (Rev. A.9), Gaussian, Inc., Pittsburgh PA, **1998**.
- [105] Piecuch, P.; Kucharski, S.A.; Kowalski, K.; Musial, M. *Comput. Phys. Comm.*, **2002**, 149, 71.
- [106] Schmidt, M.W.; Baldridge, K.K.; Boatz, J.A.; Elbert, S.T.; Gordon, M.S.; Jensen, J.H.; Koseki, S.; Matsunaga, N.; Nguyen, K.A.; Su, S.; Windus, T.L.; Dupuis, M.; Montgomery, J.A. *J. Comput. Chem.*, **1993**, 14, 1347.
- [107] Thomas, L. H. *Proc. Camb. Phil. Soc.*, **1927**, 23, 542.
- [108] Fermi, E. *Rend. Accad. Lincei.*, **1927**, 6, 602.
- [109] Hohenberg, P. ; Kohn, W. *Phys. Rev. B.*, **1964**, 136, 864.
- [110] W. Kohn, L. J. Sham, *Phys. Rev.*, **1965**, 140, A1133.
- [111] P. A. M. Dirac, *Proc. Camb. Phil. Soc.* **1930**, 26, 376.
- [112] S.J. Vosko, L. Wilk, M. Nusair, *Can. J. Phys.*, **1980**, 58, 1200.
- [113] A. D. Becke, *Phys. Rev. A*, **1988**, 38, 3098.

- [114] C. Lee, W. Yang and R. G. Parr, *Phys. Rev. B*, **1988**, 37, 785.
- [115] J. P. Perdew, Y. Wang, *Phys. Rev. B*, **1986**, 33, 8800.
- [116] J. P. Perdew, *Phys. Rev. B*, **1986**, 33, 8822.
- [117] J. P. Perdew, Y. Wang, *Phys. Rev. B*, **1992**, 45, 13244.
- [118] J. P. Perdew, J. A. Chevary, S. H. Vosko, K. A. Jackson, M. R. Pederson, D. J. Singh, C. Fiolhais, *Phys. Rev. B*, **1992**, 46, 6671
- [119] Perdew, J. P.; Burke, K.; Wang, Y. *Phys. Rev. B*, **1996**, 54, 16533.
- [120] A. D. Becke, *J. Chem. Phys.*, **1996**, 104, 1040.
- [121] A. D. Becke, *J. Chem. Phys.*, **1993**, 98, 5648.
- [122] Dupuis, M.; Marquez, A.; Davidson, E. R. HONDO 8.5; IBM Corp.: Neighborhood Road, Kingston, NY 12401; **1994**.
- [123] Özkan, İ., Unpublished.
- [124] Ishida, K.; Morokuma, K.; Komornicki, A. *J. Chem. Phys.*, **1977**, 66, 2153.
- [125] Fukui, K. *Acc. Chem. Res.*, **1981**, 14, 363.
- [126] Andrews, G. D.; Baldwin, J. E.; Gilbert, K. E.; *J. Org. Chem.*, **1980**, 45, 1523.
- [127] Wiberg, K. B.; Dailey, W. P.; Walker, F. H.; Waddell, S. T.; Crocker, L. S.; Newton, M. *J. Am. Chem. Soc.*, **1985**, 107, 7247.
- [128] Schafer, O.; Allan, M.; Szeimies, G.; Sanktjohanser, M. *J. Am. Chem. Soc.*, **1992**, 114, 8180.
- [129] Hedberg, L.; Hedberg K. *J. Am. Chem. Soc.*, **1985**, 107, 7257.
- [130] Kao, J.; Radom, L. *J. Am. Chem. Soc.*, **1978**, 100, 706.
- [131] Rogers, D.; McLafferty, F. J.; Podosenin A. V. *J. Phys. Chem. A* , **1997**, 101, 4776.
- [132] Wiberg, B. K.; Snoonian, J. R. *J. Org. Chem.*, **1998**, 63, 1390.
- [133] Hehre, W. J.; Radom, L.; Schleyer, P. v. R.; Pople, J. A. *Ab Initio Molecular Orbital Theory*; Wiley: New York, **1986**; p 298.
- [134] Freeman, P. K.; Dacres, J. E. *J. Org. Chem.*, **2003**, 68, 1386.
- [135] Bunker, P. R.; Jensen, P.; Kraemer, W. P.; Beardsworth, R. J., *J. Chem. Phys.*, **1986**, 85, 3724.
- [136] Baldwin, J. E.; Pinschmidt, R. K. *J. Am. Chem. Soc.* **1970**, 92, 5247.
- [137] Baldwin, J. E.; Pinschmidt, R. K.; Andrist, A. H. *J. Am. Chem. Soc.* **1970**, 92, 5249.

- [138] Hsu, S. L.; Andrist, A. H.; Gierke, T. D.; Benson, R. C.; Flygare, W. H.; Baldwin, J. E. *J. Am. Chem. Soc.* **1970**, 92, 5250.
- [139] Gajewski, J. J. *Hydrocarbon Thermal Isomerizations*; Academic Press: New York, **1981**; p 75-77.
- [140] Altmann, J. A.; Tee, O. S.; Yates, K. *J. Am. Chem. Soc.* **1976**, 98, 7132.
- [141] Roth, W. R.; Klerner, F. G.; Lennartz, H. W. *Chem. Ber.* **1980**, 113, 1818.
- [142] Roth, W. R.; Rekowski, V.; Börner, S.; Quast, M. *Liebigs Ann.* **1996**, 3, 409.
- [143] Dewar, M. J. S.; Kirschner, S. J. *Chem. Soc. Chem. Commun.* **1975**, 461.
- [144] Bofill, J. M.; Gomez, J.; Olivella, S. *J. Mol. Struct. (Theochem)*, **1988**, 163, 285.
- [145] Olivella, S.; Salvador, J. *J. Comput. Chem.* **1991**, 12, 792.
- [146] Skancke, P. N.; Yamashita, K.; Morokuma, K. *J. Am. Chem. Soc.* **1987**, 109, 4157.
- [147] Hosokawa, T.; Morinati, I. *J. Chem. Soc., Chem. Commun.* **1970**, 905.
- [148] Zeller, K. P. *Angew. Chem., Int. Ed. Engl.* **1982**, 21, 440.
- [149] Dowd, P.; Irngartinger, H. *Chem. Rev.* **1989**, 89, 985.
- [150] Dowd, P.; Garner, P.; Schappert, R. *J. Org. Chem.* **1982**, 47, 4240.
- [151] Dowd, P.; Schappert, R.; Garner, P.; Go C. L. *J. Org. Chem.* **1985**, 50, 44.
- [152] Dowd, P.; Schappert, R.; Garner, P. *Tetrahedron Lett.* **1982**, 23, 3.
- [153] Irngartinger, H.; Jahn, R.; Rodewald, H. *J. Am. Chem. Soc.* **1987**, 109, 6547.
- [154] Gleiter, R.; Haider, R.; Bischof, P. *J. Org. Chem.* **1984**, 49, 375.
- [155] Ona, H.; Yamaguchi, H.; Masamune, S. *J. Am. Chem. Soc.* **1970**, 92, 7495.
- [156] Pomerantz, M.; Wilke, R. N. *Tetrahedron Lett.* **1969**, 10, 463.
- [157] J. P. Chesick, *J. Phys. Chem.*, **1964**, 68, 2033.
- [158] R. Srinivasan, A. A. Levi, I. Haller, *J. Phys. Chem.*, **1965**, 69, 1775.
- [159] G. L. Closs, P. E. Pfeffer, *J. Am. Chem. Soc.*, **1968**, 90, 2452.
- [160] M. J. S. Dewar, S. Kirschner, *J. Am. Chem. Soc.*, **1974**, 97, 2931.
- [161] P. B. Shevlin, M. L. McKee, *J. Am. Chem. Soc.*, **1988**, 110, 1666.
- [162] K. A. Nguyen, M. S. Gordon, *J. Am. Chem. Soc.*, **1995**, 117, 3835.
- [163] Damiani, D.; Ferreti, L.; Gallinella, E. *Chem. Phys. Lett.*, **1976**, 37, 265.
- [164] Minkin, V. I. *Pure Appl. Chem.* **1999**, 71, 1919.
- [165] Spangler, C. W. *Chem. Rev.* **1976**, 76, 187.

- [166] Woodward, R. B.; Hoffmann, R., “*The Conservation of Orbital Symmetry*”, Verlag Chemie, Academic Press, Weinheim, **1970**, p. 114.
- [167] Roth W.R., *Tet. Lett.* **1964**, 1009.
- [168] Rondan, N. G.; Houk, K. N. *Tet. Lett.* **1984**, 25, 2519.
- [169] Bachrach, S. M. *J. Org. Chem.* **1993**, 58, 5414.
- [170] Alkorta, I; Elguero, J. *J. Chem. Soc., Perkin Trans. 2*, **1998**, 2497.
- [171] Okajima, T.; Imafuku, K. *J. Org. Chem.*, **2002**, 67, 625.
- [172] Guner, V.; Khuong, K. S.; Leach, A. G.; Lee, P. S.; Bartberger, M. D.; Houk, K. N. *J. Phys. Chem. A*, **2003**, 107, 11445.
- [173] Jiao, H.; Schleyer, P. v. R. *J. Chem. Soc. Faraday Trans.*, **1994**, 90, 1559.
- [174] Jiao, H.; Schleyer, P. v. R. *J. Am. Chem. Soc.*, **1995**, 117, 11529.
- [175] Skattebol, L. *Tetrahedron*, **1967**, 23, 1107.
- [176] Holm, K. H.; Skattebol, L. *Tetrahedron Lett.*, **1977**, 2347.
- [177] Nicolaidis, A.; Matsushi, T.; Tomioka, H. *J. Org. Chem*, **1999**, 64, 3299.
- [178] Olivella, S.; Lopez, N. *Chem. Eur. J.*, **2001**, 7, 3951-3960.
- [179] Blomquist, A. T.; Liu, L. H. *J. Am. Chem. Soc.* **1953**, 75, 2153.
- [180] Gilbert, J. C.; Hou, D.-R.; Grimme, J. W. *J. Org. Chem.* **1999**, 64, 1529.
- [181] Gilbert, J. C.; McKinley, E. G.; Hou, D.-R. *Tetrahedron* **1997**, 53, 9891.
- [182] Gilbert, J. C.; Baze, M. E. *J. Am. Chem. Soc.* **1983**, 105, 664.
- [183] Fitjier, L.; Modaressi, S. *Tetrahedron Lett.* **1983**, 24, 5495.
- [184] Fitjier, L.; Kliebisch, V.; Wehle, D.; Modaressi, S. *Tetrahedron Lett.* **1982**, 23, 1661.
- [185] Wentrup, C.; Blanch, R.; Briehl, H.; Gross, G. *J. Am. Chem. Soc.* **1988**, 110, 1874.
- [186] Bottini, A. T.; Frost, K. A., II; Anderson, B. R.; Dev, V. *Tetrahedron* **1973**, 29, 1975.
- [187] Montgomery, L. K.; Applegate, L. E. *J. Am. Chem. Soc.* **1967**, 89, 5305.
- [188] Adams, R. D.; Chen, G.; Qu, X.; Wu, W.; Yamamoto, J. H. *Organometallics* **1993**, 12, 3029.
- [189] Kitamura T., Kotani M., Yokoyama T., Fujiwara Y., *J. Org. Chem.* **1999**, 64, 680.
- [190] Favorskii A. E.; *J. Gen. Chem USSR (Engl. Transl.)*, **1936**, 6, 720.

- [191] Wittig, G.; Krebs, A.; Pohlke, R. *Angew. Chem.* **1960**, 72, 324.
- [192] Montgomery, L. K.; Roberts, J. D. *J. Am. Chem. Soc.* **1960**, 82, 4750.
- [193] Erickson, K.L., Wolinsky J., *J. Am. Chem. Soc.* **1965**, 87, 1142.
- [194] Gilbert, J. C.; Kirschner, S. *Tet. Lett.*, **1993**, 34, 599.
- [195] Gilbert, J. C.; Kirschner, S. *Tet. Lett.*, **1993**, 34, 603.
- [196] Dewar, M. J. S.; Kirschner, S. *J. Am. Chem. Soc.*, **1974**, 96, 5246.
- [197] Dewar, M. J. S.; Kirschner, S.; Kollmar, H. W. *J. Am. Chem. Soc.*, **1974**, 96, 5240.
- [198] Dewar, M. J. S.; Kirschner, S. *J. Am. Chem. Soc.* **1974**, 96, 5244.
- [199] Johnson, R. P.; Daoust, K. J. *J. Am. Chem. Soc.*, **1995**, 117, 362.
- [200] S. M. Bachrach, J. C. Gilbert, D. W. Laird, *J. Am. Chem. Soc.*, **2001**, 123, 6706.
- [201] Stang, P. J. *Chem. Rev.*, **1978**, 78, 383.
- [202] A. Brandi, A. Goti, *Chem. Rev.*, **1998**, 98, 589.
- [203] Xu L.X., Lin G.Y., Tao F.G., Brinker U. H. *Acta Chem. Scand.*, **1992**, 46, 650.
- [204] Sütbeyaz Y.; Ceylan M.; Secen H., *J. Chem. Research (S)*, **1993**, 70.
- [205] Taskesenligil Y.; Tumer F.; Balci M., *Turk. J. Chem.*, **1995**, 19, 305.
- [206] Ceylan M.; Secen H.; Sütbeyaz Y., *J. Chem. Research (S)*, **1997**, 293.
- [207] Tolbert M. L.; Islam M. N.; Johnson R. P.; Loisella P. M.; Shakespeare W. C., *J. Am. Chem. Soc.*, **1990**, 112, 6416.
- [208] Tolbert M. L., Siddiqui S., *J. Am. Chem. Soc.*, **1984**, 106, 5538.
- [209] Doering, W. v. E.; LaFlamme, P. M. *Tetrahedron*, **1958**, 2, 75.
- [210] Moore, W. R.; Ward, H. R. *J. Org. Chem.*, **1960**, 25, 2073.
- [211] Skattebøl, L. *Acta Chem. Scand.*, **1963**, 17, 1683.
- [212] Valtazanos, P.; Elbert, S.T.; Xantheas, S.; Ruedenberg, K. *Theor. Chim. Acta*, **1991**, 78, 287.
- [213] Xantheas, S.; Valtazanos, P.; Ruedenberg, K. *Theor. Chim. Acta*, **1991**, 78, 327.
- [214] Xantheas, S.; Elbert, S.T.; Ruedenberg, K. *Theor. Chim. Acta*, **1991**, 78, 365.
- [215] Bettinger, H.F.; Schleyer, P.R.; Schreiner, P.R.; Schaefer, H.F. *J. Org. Chem.*, **1997**, 62, 9267.

- [216] Bettinger, H.F.; Schleyer, P.R.; Schreiner, P.R.; Schaefer, H.F. *J. Phys. Chem.*, **1996**, 100, 16147.
- [217] Chapman O. L., *Pure Appl. Chem.*, **1974**, 40, 511.
- [218] Stierman, T. J.; Johnson, R. P. *J. Am. Chem. Soc.*, **1985**, 107, 3971.
- [219] Honjou, N.; Pacansky, J.; Yoshimine, M. *J. Am. Chem. Soc.*, **1985**, 107, 5332.
- [220] Yoshimine, M.; Pacansky, J.; Honjou, N. *J. Am. Chem. Soc.*, **1989**, 111, 4198.
- [221] Cramer, C. J.; Worthington, S. E. *J. Phys. Chem.*, **1995**, 99, 1462.
- [222] Rauk A., Bouma, W. J., Radom L., *J. Am. Chem. Soc.*, **1985**, 107, 3780.
- [223] Balci M., Jones W. M., *J. Am. Chem. Soc.*, **1980**, 102, 7608.
- [224] Köbrich, G.; Goyert, W. *Tetrahedron*, **1968**, 24, 4327.
- [225] Warner, P. M.; Herold, R. D. *J. Org. Chem.*, **1983**, 48, 5411.
- [226] Warner, P. M.; Herold, R. D.; Chu, I.; Lessman, J. *J. Org. Chem.*, **1988**, 53, 942.
- [227] Kirmse, W.; Jendralla, H. *Chem. Ber.*, **1978**, 111, 1857.
- [228] Moore, W. R.; Moser, W. R. *J. Am. Chem. Soc.*, **1970**, 92, 5469.
- [229] Le T. N., Lee H., Mebel A. M., Kaiser R. I. *J. Phys. Chem. A*, **2001**, 105, 1847.

APPENDIX A

ELECTRONIC ENERGIES OF ALL STABLE AND TRANSITION STATE STRUCTURES

Stable Isomers

The singlet and triplet state electronic energies (in Hartree units) of all stable structures calculated at (U)B3LYP/cc-pVTZ and CASSCF(4,4)/6-31G(d,p) levels of theory are given in Tables A1 and A2, respectively.

Table A1. Singlet state electronic energies (in Hartree units) of all stable isomers

| Isomers | (U)B3LYP/cc-pVTZ | CASSCF(4,4)/6-31G(d) |
|---------|------------------|----------------------|
| M1 | -194.174116 | -192.846625 |
| M2 | -194.067288 | -192.749158 |
| M3 | -194.037477 | -192.736017 |
| M4 | -194.060201 | -192.737597 |
| M5 | -194.075378 | -192.747096 |
| M6 | -193.949203 | -192.628796 |
| M7 | -194.035640 | -192.723658 |
| M8 | -194.131398 | -192.802407 |
| B1 | -194.094962 | -192.758953 |
| B2 | -194.019772 | -192.693273 |
| B3 | -194.030535 | -192.697003 |
| B4 | -194.028018 | -192.697712 |
| B5 | - | - |
| B6 | -194.038240 | -192.698074 |
| B7 | -194.066310 | -192.735767 |
| T1 | -194.067106 | -192.706996 |
| T2 | -194.076456 | -192.722164 |
| T3 | -194.025524 | -192.678826 |

Table A2. Triplet state electronic energies (in Hartree units) of all stable isomers

| Stable Isomers | UB3LYP/cc-pVTZ | CASSCF(4,4)/6-31G(d) |
|-----------------|----------------|----------------------|
| ³ M1 | -194.083222 | -192.753619 |
| ³ M2 | -194.064496 | -192.736749 |
| ³ M3 | -194.008689 | -192.696684 |
| ³ M4 | -194.048590 | -192.737797 |
| ³ M5 | -194.068375 | -192.748312 |
| ³ M6 | -193.944506 | -192.629014 |
| ³ M7 | -193.968822 | -192.663238 |
| ³ M8 | -194.035194 | -192.707064 |
| ³ B1 | - | -192.666272 |
| ³ B2 | -193.978336 | -192.643009 |
| ³ B3 | -193.995475 | -192.658881 |
| ³ B4 | -193.993602 | -192.642874 |
| ³ B5 | -193.987559 | -192.635201 |
| ³ B6 | -193.998846 | -192.670440 |
| ³ B7 | -193.981531 | -192.641601 |
| ³ T1 | -193.970316 | -192.620893 |
| ³ T2 | -193.928661 | -192.584760 |
| ³ T3 | -193.997683 | -192.659547 |

Transition State Structures

Electronic energies of the transition state structures belonging to the reactions investigated throughout the thesis at different levels of theory are given in Tables A3 – A8.

Table A3. Electronic energies of the [TS_B1-M1] and [TS_T1-M1] species at several levels

| | [TS_B1-M1] | [TS_T1-M1] |
|----------------------------|-------------|-------------|
| UB3LYP/6-31G(d) | -193.983215 | -193.931126 |
| UBPW91/6-31G(d) | -193.957095 | -193.908152 |
| RHF/6-31G(d) | -192.638003 | -192.558514 |
| CR-CCSD(T)/6-31G(d) | -193.367379 | -193.302838 |
| CAS44/6-31G(d) | -192.734580 | -192.663397 |
| CAS44-MP2/6-31G(d) | -193.318811 | -193.252677 |
| CAS88/6-31G(d) | -192.776220 | -192.706597 |
| CAS88-MP2/6-31G(d) | -193.315494 | -193.251160 |

Table A4. Electronic energies of the [TS_M1-M1] species calculated by DFT and CC methods

| | [TS_M1-M1] |
|-----------------------------|-------------|
| RB3LYP/6-31G(d) | -194.054966 |
| RB3LYP/6-31G(d,p) | -194.066360 |
| RB3LYP/cc-pVTZ | -194.130576 |
| RCCSD(T)/6-31G(d,p) | -193.493033 |
| RCCSD(T)/6-311G(d,p) | -193.567667 |

Table A5. Electronic energies of the [TS_B1-M1] and [TS_T1-M1] species calculated by DFT and CC methods

| | [TS_M4-M1] | [TS_M5-M1] |
|----------------------------|-------------|-------------|
| RB3LYP/6-31G(d) | -193.979210 | -193.979866 |
| RB3LYP/cc-pVTZ | -194.054427 | -194.055818 |
| RCCSD(T)/6-31G(d,p) | -193.426392 | -193.439530 |

Table A6. Electronic energies of the [TS_M7-M7'], [TS_M3-M3'] and [TS_M7-M3] species at several levels

| | [TS_M7-M7'] | [TS_M7-M3] | [TS_M3-M3'] |
|---------------------|--------------|--------------|--------------|
| UB3LYP/6-31G(d) | -193.964428 | -193.960069 | -193.964903 |
| UB3LYP/6-311G(d,p) | -194.015652 | -194.010862 | -194.017741 |
| UB3LYP/cc-pVTZ | -194.035277 | -194.030825 | -194.037154 |
| RCCSD(T)/6-31G(d) | -193.356606 | -193.351617 | -193.365920 |
| RCCSD(T)/6-31G(d,p) | -193.406416 | -193.401355 | -193.416107 |
| CAS66/6-31G(d) | - | -192.7037270 | - |
| CAS66-MP2/6-31G(d) | - | -193.2615011 | - |

Table A7. Electronic energies of the ³[TS_B5-M2] species at several levels of theory

| | ³ [TS_B5-M2] |
|----------------------|-------------------------|
| UB3LYP/6-31G(d) | -193.907147 |
| UB3LYP/6-31G(d,p) | -193.915873 |
| UB3LYP/cc-pVTZ | -193.977277 |
| CAS44/6-31G(d) | -192.642634 |
| CAS44/6-31G(d,p) | -192.652445 |
| CAS44-MP2/6-31G(d) | -193.219303 |
| CAS44-MP2/6-31G(d,p) | -193.268373 |
| UCCSD(T)/6-31G(d,p) | -193.345298 |

Table A8. Electronic energies of the ³[TS_cppy-ppd] species at several levels of theory

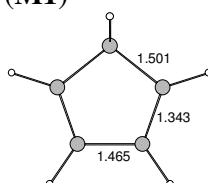
| | ³ [TS_cppy-ppd] |
|----------------------|----------------------------|
| UB3LYP/6-31G(d) | -116.502329 |
| UB3LYP/6-311G(d,p) | -116.537227 |
| UB3LYP/cc-pVTZ | -116.550282 |
| UCCSD(T)/6-31G(d,p) | -116.158709 |
| UCCSD(T)/6-311G(d,p) | -116.201209 |
| UCCSD(T)cc-pVTZ | -116.276265 |

APPENDIX B

CARTESIAN COORDINATES OF ALL STABLE ISOMERS

The cartesian coordinates of singlet state geometries of all stable isomers calculated at (U)B3LYP/cc-pVTZ

Cyclopenta-1,3-diene (M1)

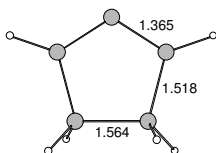
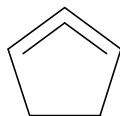


Standard orientation:

| Center Number | Atomic Number | Atomic Type | Coordinates (Angstroms) | | |
|------------------|------------------|----------------|-------------------------|-----------|-----------|
| | | | X | Y | Z |
| 1 | 6 | 0 | 0.000000 | 0.000000 | 1.213180 |
| 2 | 6 | 0 | 0.000000 | 1.176521 | 0.280342 |
| 3 | 6 | 0 | 0.000000 | -1.176521 | 0.280342 |
| 4 | 6 | 0 | 0.000000 | 0.732622 | -0.987395 |
| 5 | 6 | 0 | 0.000000 | -0.732622 | -0.987395 |
| 6 | 1 | 0 | 0.000000 | 2.205077 | 0.606387 |
| 7 | 1 | 0 | 0.000000 | -2.205077 | 0.606387 |
| 8 | 1 | 0 | 0.000000 | 1.344367 | -1.877736 |
| 9 | 1 | 0 | 0.000000 | -1.344367 | -1.877736 |
| 10 | 1 | 0 | -0.874474 | 0.000000 | 1.874125 |
| 11 | 1 | 0 | 0.874474 | 0.000000 | 1.874125 |

E = -194.1741156 a.u. ZPVE = 57.92838 kcal/mol

Cyclopenta-1,2-diene (M2)

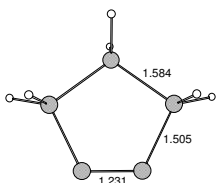
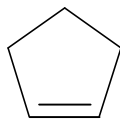


Standard orientation:

| Center Number | Atomic Number | Atomic Type | Coordinates (Angstroms) | | |
|------------------|------------------|----------------|-------------------------|-----------|-----------|
| | | | X | Y | Z |
| 1 | 6 | 0 | 0.000000 | 0.000000 | 1.299172 |
| 2 | 6 | 0 | 0.000000 | 1.149794 | 0.563371 |
| 3 | 6 | 0 | 0.000000 | -1.149794 | 0.563371 |
| 4 | 6 | 0 | 0.153056 | 0.766769 | -0.897155 |
| 5 | 6 | 0 | -0.153056 | -0.766769 | -0.897155 |
| 6 | 1 | 0 | -0.209842 | 2.150649 | 0.908824 |
| 7 | 1 | 0 | 0.209842 | -2.150649 | 0.908824 |
| 8 | 1 | 0 | 1.160899 | 0.960851 | -1.281032 |
| 9 | 1 | 0 | 0.534708 | -1.339252 | -1.522601 |
| 10 | 1 | 0 | -0.534708 | 1.339252 | -1.522601 |
| 11 | 1 | 0 | -1.160899 | -0.960851 | -1.281032 |

E = -194.0672878 a.u. ZPVE = 56.08248 kcal/mol

Cyclopentyne (M3)

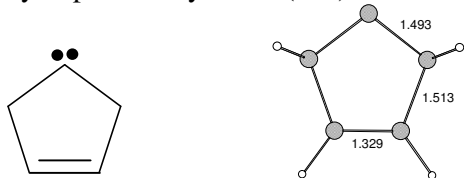


Standard orientation:

| Center Number | Atomic Number | Atomic Type | Coordinates (Angstroms) | | |
|------------------|------------------|----------------|-------------------------|-----------|-----------|
| | | | X | Y | Z |
| 1 | 6 | 0 | -0.238179 | 1.095754 | 0.000000 |
| 2 | 6 | 0 | 0.070152 | 0.200252 | 1.269683 |
| 3 | 6 | 0 | 0.070152 | 0.200252 | -1.269683 |
| 4 | 6 | 0 | 0.070152 | -1.154673 | 0.615419 |
| 5 | 6 | 0 | 0.070152 | -1.154673 | -0.615419 |
| 6 | 1 | 0 | -0.677322 | 0.326823 | 2.051500 |
| 7 | 1 | 0 | -0.677322 | 0.326823 | -2.051500 |
| 8 | 1 | 0 | 1.044437 | 0.420427 | 1.708902 |
| 9 | 1 | 0 | 1.044437 | 0.420427 | -1.708902 |
| 10 | 1 | 0 | 0.310816 | 2.039346 | 0.000000 |
| 11 | 1 | 0 | -1.299623 | 1.344678 | 0.000000 |

E = -194.0374767 a.u. ZPVE = 56.94335 kcal/mol

Cyclopent-3-enylidene (M4)

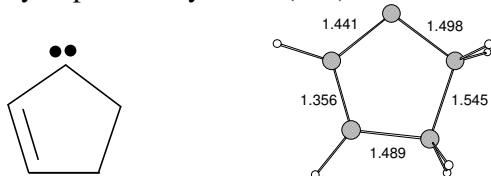


Standard orientation:

| Center Number | Atomic Number | Atomic Type | Coordinates (Angstroms) | | |
|------------------|------------------|----------------|-------------------------|-----------|-----------|
| | | | X | Y | Z |
| 1 | 6 | 0 | 0.000000 | 0.000000 | 1.334471 |
| 2 | 6 | 0 | 0.000000 | 1.181790 | 0.421357 |
| 3 | 6 | 0 | 0.000000 | -1.181790 | 0.421357 |
| 4 | 6 | 0 | 0.000000 | 0.664690 | -1.000266 |
| 5 | 6 | 0 | 0.000000 | -0.664690 | -1.000266 |
| 6 | 1 | 0 | 0.860934 | 1.816494 | 0.673995 |
| 7 | 1 | 0 | -0.860934 | -1.816494 | 0.673995 |
| 8 | 1 | 0 | 0.000000 | 1.296591 | -1.877944 |
| 9 | 1 | 0 | 0.000000 | -1.296591 | -1.877944 |
| 10 | 1 | 0 | -0.860934 | 1.816494 | 0.673995 |
| 11 | 1 | 0 | 0.860934 | -1.816494 | 0.673995 |

E = -194.0602011 a.u. ZPVE = 55.42627 kcal/mol

Cyclopent-2-enylidene (M5)

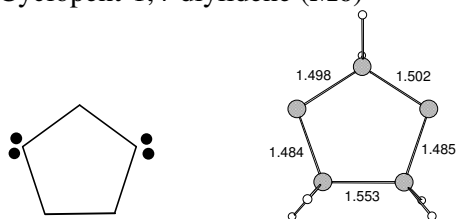


Standard orientation:

| Center Number | Atomic Number | Atomic Type | Coordinates (Angstroms) | | |
|------------------|------------------|----------------|-------------------------|-----------|-----------|
| | | | X | Y | Z |
| 1 | 6 | 0 | -0.486529 | -1.125260 | 0.000000 |
| 2 | 6 | 0 | -1.171200 | 0.260109 | 0.000000 |
| 3 | 6 | 0 | 0.997932 | -0.924814 | 0.000000 |
| 4 | 6 | 0 | 0.000000 | 1.179525 | 0.000000 |
| 5 | 6 | 0 | 1.176569 | 0.504592 | 0.000000 |
| 6 | 1 | 0 | -1.809249 | 0.431643 | 0.872954 |
| 7 | 1 | 0 | -0.104933 | 2.259382 | 0.000000 |
| 8 | 1 | 0 | 2.146035 | 0.985597 | 0.000000 |
| 9 | 1 | 0 | -1.809249 | 0.431643 | -0.872954 |
| 10 | 1 | 0 | -0.761617 | -1.736590 | -0.865503 |
| 11 | 1 | 0 | -0.761617 | -1.736590 | 0.865503 |

E = -194.0753778 a.u. ZPVE = 56.43422 kcal/mol

Cyclopent-1,4-diylidene (M6)

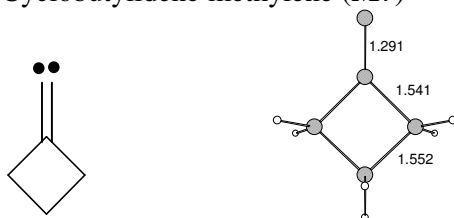


Standard orientation:

| Center Number | Atomic Number | Atomic Type | Coordinates (Angstroms) | | |
|------------------|------------------|----------------|-------------------------|-----------|-----------|
| | | | X | Y | Z |
| 1 | 6 | 0 | 0.951648 | -0.762802 | 0.055661 |
| 2 | 6 | 0 | 0.924839 | 0.788012 | -0.016782 |
| 3 | 6 | 0 | -0.433542 | -1.251589 | -0.159068 |
| 4 | 6 | 0 | -0.485786 | 1.249411 | -0.025073 |
| 5 | 6 | 0 | -1.276884 | -0.022107 | 0.019309 |
| 6 | 1 | 0 | 1.319486 | 1.135479 | -0.983872 |
| 7 | 1 | 0 | 1.523787 | 1.337663 | 0.715479 |
| 8 | 1 | 0 | 1.231266 | -1.150051 | 1.048870 |
| 9 | 1 | 0 | 1.661498 | -1.242436 | -0.622117 |
| 10 | 1 | 0 | -1.575743 | -0.075192 | 1.089450 |
| 11 | 1 | 0 | -2.241943 | -0.011017 | -0.492096 |

E = -193.9492033 a.u. ZPVE = 52.83319 kcal/mol

Cyclobutylidene methylene (M7)

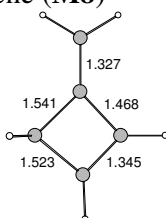
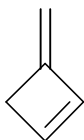


Standard orientation:

| Center Number | Atomic Number | Atomic Type | Coordinates (Angstroms) | | |
|------------------|------------------|----------------|-------------------------|-----------|-----------|
| | | | X | Y | Z |
| 1 | 6 | 0 | 0.197546 | -0.262192 | 1.093687 |
| 2 | 6 | 0 | 0.197546 | -1.363516 | 0.000000 |
| 3 | 6 | 0 | 0.197546 | -0.262192 | -1.093687 |
| 4 | 6 | 0 | -0.154038 | 0.764548 | 0.000000 |
| 5 | 6 | 0 | -0.712523 | 1.928218 | 0.000000 |
| 6 | 1 | 0 | 1.187200 | -0.069355 | 1.506524 |
| 7 | 1 | 0 | -0.522103 | -0.351351 | 1.902805 |
| 8 | 1 | 0 | -0.727086 | -1.936799 | 0.000000 |
| 9 | 1 | 0 | 1.040432 | -2.050978 | 0.000000 |
| 10 | 1 | 0 | -0.522103 | -0.351351 | -1.902805 |
| 11 | 1 | 0 | 1.187200 | -0.069355 | -1.506524 |

E = -194.0356398 a.u. ZPVE = 56.48323 kcal/mol

3-Methylenecyclobutene (M8)

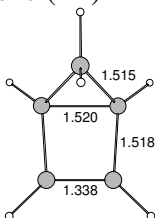
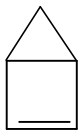


Standard orientation:

| Center Number | Atomic Number | Atomic Type | Coordinates (Angstroms) | | |
|------------------|------------------|----------------|-------------------------|-----------|-----------|
| | | | X | Y | Z |
| 1 | 6 | 0 | 0.000000 | 0.551899 | 0.000000 |
| 2 | 6 | 0 | 1.023157 | -0.600915 | 0.000000 |
| 3 | 6 | 0 | -0.218555 | -1.483544 | 0.000000 |
| 4 | 6 | 0 | -1.075412 | -0.447287 | 0.000000 |
| 5 | 6 | 0 | 0.092401 | 1.875232 | 0.000000 |
| 6 | 1 | 0 | 1.653410 | -0.661323 | 0.889487 |
| 7 | 1 | 0 | 1.653410 | -0.661323 | -0.889487 |
| 8 | 1 | 0 | -0.346611 | -2.556232 | 0.000000 |
| 9 | 1 | 0 | -2.153521 | -0.367897 | 0.000000 |
| 10 | 1 | 0 | 1.053485 | 2.372060 | 0.000000 |
| 11 | 1 | 0 | -0.789716 | 2.502414 | 0.000000 |

E = -194.131398 a.u. ZPVE = 57.11020 kcal/mol

Bicyclo[2.1.0]pent-2-ene (B1)

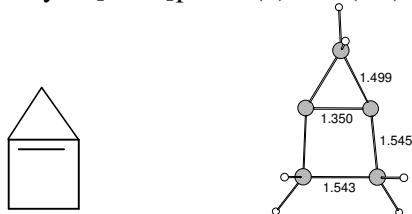


Standard orientation:

| Center Number | Atomic Number | Atomic Type | Coordinates (Angstroms) | | |
|------------------|------------------|----------------|-------------------------|-----------|-----------|
| | | | X | Y | Z |
| 1 | 6 | 0 | 0.922315 | -1.012427 | 0.000000 |
| 2 | 6 | 0 | -0.266233 | -0.460251 | 0.759876 |
| 3 | 6 | 0 | -0.266233 | -0.460251 | -0.759876 |
| 4 | 6 | 0 | -0.266233 | 1.055391 | 0.668883 |
| 5 | 6 | 0 | -0.266233 | 1.055391 | -0.668883 |
| 6 | 1 | 0 | -0.878896 | -1.079494 | -1.396999 |
| 7 | 1 | 0 | 1.025445 | -2.092692 | 0.000000 |
| 8 | 1 | 0 | 1.856312 | -0.463942 | 0.000000 |
| 9 | 1 | 0 | -0.878896 | -1.079494 | 1.396999 |
| 10 | 1 | 0 | -0.134137 | 1.824251 | 1.417494 |
| 11 | 1 | 0 | -0.134137 | 1.824251 | -1.417494 |

E = -194.0949618 a.u. ZPVE = 57.43848 kcal/mol

Bicyclo[2.1.0]pent-1(4)-ene (B2)

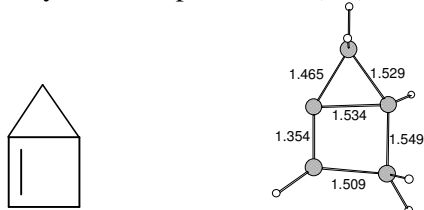


Standard orientation:

| Center Number | Atomic Number | Atomic Type | Coordinates (Angstroms) | | |
|------------------|------------------|----------------|-------------------------|-----------|-----------|
| | | | X | Y | Z |
| 1 | 6 | 0 | 0.762926 | 1.387347 | 0.000000 |
| 2 | 6 | 0 | -0.251230 | 0.513306 | 0.674956 |
| 3 | 6 | 0 | -0.251230 | 0.513306 | -0.674956 |
| 4 | 6 | 0 | -0.251230 | -1.028856 | 0.771753 |
| 5 | 6 | 0 | -0.251230 | -1.028856 | -0.771753 |
| 6 | 1 | 0 | 1.827195 | 1.148220 | 0.000000 |
| 7 | 1 | 0 | 0.550669 | 2.446685 | 0.000000 |
| 8 | 1 | 0 | -1.117637 | -1.445831 | 1.279016 |
| 9 | 1 | 0 | 0.654680 | -1.420361 | -1.234745 |
| 10 | 1 | 0 | 0.654680 | -1.420361 | 1.234745 |
| 11 | 1 | 0 | -1.117637 | -1.445831 | -1.279016 |

E = -194.0197721 a.u. ZPVE = 56.66284 kcal/mol

Bicyclo[2.1.0]pent-1-ene (B3)

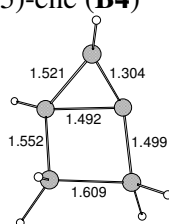
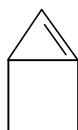


Standard orientation:

| Center Number | Atomic Number | Atomic Type | Coordinates (Angstroms) | | |
|------------------|------------------|----------------|-------------------------|-----------|-----------|
| | | | X | Y | Z |
| 1 | 6 | 0 | 1.443747 | 0.095647 | 0.310068 |
| 2 | 6 | 0 | 0.330358 | -0.813790 | -0.210739 |
| 3 | 6 | 0 | 0.345954 | 0.701422 | -0.447220 |
| 4 | 6 | 0 | -1.144675 | -0.604970 | 0.215012 |
| 5 | 6 | 0 | -0.946118 | 0.862871 | -0.075409 |
| 6 | 1 | 0 | 2.381804 | -0.093214 | -0.197255 |
| 7 | 1 | 0 | 1.557789 | 0.368620 | 1.355238 |
| 8 | 1 | 0 | -1.374085 | -0.791462 | 1.270538 |
| 9 | 1 | 0 | -1.847902 | -1.173526 | -0.396236 |
| 10 | 1 | 0 | -1.498899 | 1.750145 | 0.211458 |
| 11 | 1 | 0 | 0.605693 | -1.507643 | -0.994018 |

E = -194.0949618 a.u. ZPVE = 57.43848 kcal/mol

Bicyclo[2.1.0]pent-1(5)-ene (**B4**)

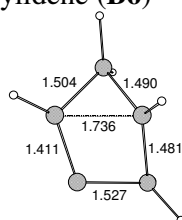
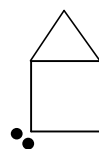


Standard orientation:

| Center Number | Atomic Number | Atomic Type | Coordinates (Angstroms) | | |
|------------------|------------------|----------------|-------------------------|-----------|-----------|
| | | | X | Y | Z |
| 1 | 6 | 0 | 1.461287 | -0.224008 | 0.267835 |
| 2 | 6 | 0 | 0.505569 | 0.781802 | -0.354151 |
| 3 | 6 | 0 | 0.422142 | -0.708093 | -0.353903 |
| 4 | 6 | 0 | -0.888071 | 0.772628 | 0.327641 |
| 5 | 6 | 0 | -1.044218 | -0.782841 | -0.053979 |
| 6 | 1 | 0 | 0.747936 | 1.401498 | -1.207050 |
| 7 | 1 | 0 | -1.643002 | 1.419635 | -0.118732 |
| 8 | 1 | 0 | -1.670455 | -0.881028 | -0.939061 |
| 9 | 1 | 0 | -0.873729 | 0.918473 | 1.410279 |
| 10 | 1 | 0 | -1.366600 | -1.494234 | 0.707468 |
| 11 | 1 | 0 | 2.065594 | -0.401268 | 1.146434 |

E = -194.0280174 a.u. ZPVE = 56.43554 kcal/mol

Bicyclo[2.1.0]pent-2-ylidene (**B6**)

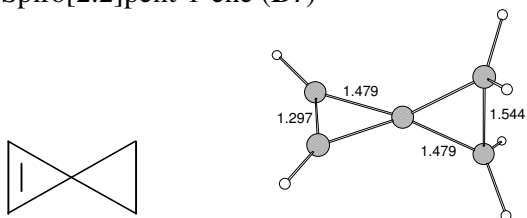


Standard orientation:

| Center Number | Atomic Number | Atomic Type | Coordinates (Angstroms) | | |
|------------------|------------------|----------------|-------------------------|-----------|-----------|
| | | | X | Y | Z |
| 1 | 6 | 0 | 0.669048 | 0.860058 | -0.087756 |
| 2 | 6 | 0 | 1.185871 | -0.542775 | -0.252608 |
| 3 | 6 | 0 | -0.040695 | -0.570599 | 0.592416 |
| 4 | 6 | 0 | -0.731601 | 1.022226 | -0.038396 |
| 5 | 6 | 0 | -1.267227 | -0.395793 | -0.219128 |
| 6 | 1 | 0 | 2.134065 | -0.734537 | 0.236242 |
| 7 | 1 | 0 | 1.091220 | -1.035780 | -1.215751 |
| 8 | 1 | 0 | -0.011188 | -0.674150 | 1.664671 |
| 9 | 1 | 0 | 1.327183 | 1.629517 | 0.304450 |
| 10 | 1 | 0 | -2.236858 | -0.549577 | 0.238808 |
| 11 | 1 | 0 | -1.196797 | -0.874176 | -1.195590 |

E = -194.0382397 a.u. ZPVE = 56.83930 kcal/mol

Spiro[2.2]pent-1-ene (**B7**)

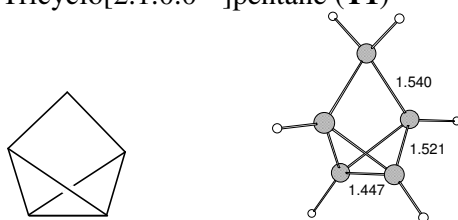


Standard orientation:

| Center Number | Atomic Number | Atomic Type | Coordinates (Angstroms) | | |
|------------------|------------------|----------------|-------------------------|-----------|-----------|
| | | | X | Y | Z |
| 1 | 6 | 0 | -0.772098 | 0.000000 | -1.213259 |
| 2 | 6 | 0 | 0.772098 | 0.000000 | -1.213259 |
| 3 | 6 | 0 | 0.000000 | 0.000000 | 0.047889 |
| 4 | 6 | 0 | 0.000000 | 0.648465 | 1.377641 |
| 5 | 6 | 0 | 0.000000 | -0.648465 | 1.377641 |
| 6 | 1 | 0 | -1.267884 | -0.909045 | -1.531649 |
| 7 | 1 | 0 | -1.267884 | 0.909045 | -1.531649 |
| 8 | 1 | 0 | 1.267884 | 0.909045 | -1.531649 |
| 9 | 1 | 0 | 1.267884 | -0.909045 | -1.531649 |
| 10 | 1 | 0 | 0.000000 | 1.569041 | 1.933343 |
| 11 | 1 | 0 | 0.000000 | -1.569041 | 1.933343 |

E = -194.0663098 a.u. ZPVE = 55.99370 kcal/mol

Tricyclo[2.1.0.0^{2,5}]pentane (**T1**)

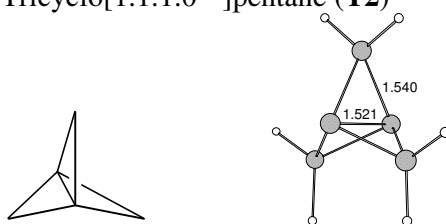


Standard orientation:

| Center Number | Atomic Number | Atomic Type | Coordinates (Angstroms) | | |
|------------------|------------------|----------------|-------------------------|-----------|-----------|
| | | | X | Y | Z |
| 1 | 6 | 0 | 0.000000 | 0.723759 | -0.813370 |
| 2 | 6 | 0 | 0.000000 | -0.723759 | -0.813370 |
| 3 | 6 | 0 | -0.976235 | 0.000000 | 0.100754 |
| 4 | 6 | 0 | 0.976235 | 0.000000 | 0.100754 |
| 5 | 6 | 0 | 0.000000 | 0.000000 | 1.291203 |
| 6 | 1 | 0 | 2.054782 | 0.000000 | 0.038319 |
| 7 | 1 | 0 | 0.000000 | -0.899834 | 1.910799 |
| 8 | 1 | 0 | 0.000000 | 0.899834 | 1.910799 |
| 9 | 1 | 0 | -2.054782 | 0.000000 | 0.038319 |
| 10 | 1 | 0 | 0.000000 | -1.507039 | -1.547028 |
| 11 | 1 | 0 | 0.000000 | 1.507039 | -1.547028 |

E = -194.0671055 a.u. ZPVE = 57.25519 kcal/mol

Tricyclo[1.1.1.0^{1,3}]pentane (**T2**)

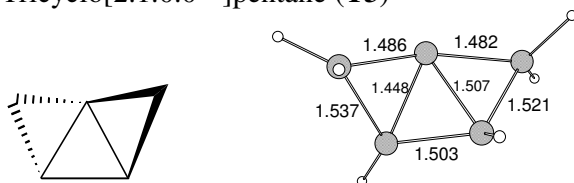


Standard orientation:

| Center Number | Atomic Number | Atomic Type | Coordinates (Angstroms) | | |
|------------------|------------------|----------------|-------------------------|-----------|-----------|
| | | | X | Y | Z |
| 1 | 6 | 0 | -0.784343 | 0.000000 | -0.000113 |
| 2 | 6 | 0 | 0.000000 | 0.000000 | 1.296940 |
| 3 | 6 | 0 | 0.784343 | 0.000000 | -0.000113 |
| 4 | 6 | 0 | 0.000000 | 1.123205 | -0.648385 |
| 5 | 6 | 0 | 0.000000 | -1.123205 | -0.648385 |
| 6 | 1 | 0 | 0.000000 | -0.912693 | 1.877699 |
| 7 | 1 | 0 | 0.000000 | 0.912693 | 1.877699 |
| 8 | 1 | 0 | 0.000000 | 2.082498 | -0.148322 |
| 9 | 1 | 0 | 0.000000 | 1.170032 | -1.729211 |
| 10 | 1 | 0 | 0.000000 | -1.170032 | -1.729211 |
| 11 | 1 | 0 | 0.000000 | -2.082498 | -0.148322 |

E = -194.0764567 a.u. ZPVE = 58.35411 kcal/mol

Tricyclo[2.1.0.0^{1,3}]pentane (**T3**)



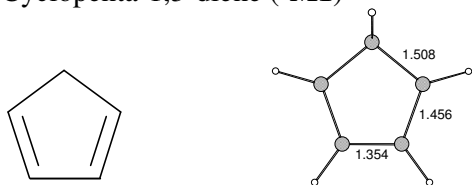
Standard orientation:

| Center Number | Atomic Number | Atomic Type | Coordinates (Angstroms) | | |
|------------------|------------------|----------------|-------------------------|-----------|-----------|
| | | | X | Y | Z |
| 1 | 6 | 0 | 1.440481 | -0.428440 | 0.150726 |
| 2 | 6 | 0 | 0.604428 | 0.743016 | -0.388884 |
| 3 | 6 | 0 | -0.005266 | -0.551190 | -0.168004 |
| 4 | 6 | 0 | -0.579890 | 0.654052 | 0.531736 |
| 5 | 6 | 0 | -1.473487 | -0.353217 | -0.174978 |
| 6 | 1 | 0 | 0.723554 | 1.283403 | -1.318108 |
| 7 | 1 | 0 | -0.522555 | 0.714285 | 1.611440 |
| 8 | 1 | 0 | -2.083561 | -0.994380 | 0.454421 |
| 9 | 1 | 0 | 1.764922 | -0.394629 | 1.187833 |
| 10 | 1 | 0 | 2.144337 | -0.909717 | -0.522281 |
| 11 | 1 | 0 | -1.944291 | -0.084284 | -1.116878 |

E = -194.0255241 a.u. ZPVE = 56.84171 kcal/mol

*The cartesian coordinates of triplet state geometries of all stable isomers calculated
at (U)B3LYP/cc-pVTZ*

Cyclopenta-1,3-diene (³M1)



Standard orientation:

| Center Number | Atomic Number | Atomic Type | Coordinates (Angstroms) | | |
|------------------|------------------|----------------|-------------------------|-----------|-----------|
| | | | X | Y | Z |
| 1 | 6 | 0 | 0.000000 | 0.000000 | 1.273915 |
| 2 | 6 | 0 | 0.000000 | 1.163658 | 0.315190 |
| 3 | 6 | 0 | 0.000000 | -1.163658 | 0.315190 |
| 4 | 6 | 0 | 0.000000 | 0.676978 | -1.056936 |
| 5 | 6 | 0 | 0.000000 | -0.676978 | -1.056936 |
| 6 | 1 | 0 | 0.000000 | 2.201998 | 0.608200 |
| 7 | 1 | 0 | 0.000000 | -2.201998 | 0.608200 |
| 8 | 1 | 0 | 0.000000 | 1.311880 | -1.929558 |
| 9 | 1 | 0 | 0.000000 | -1.311880 | -1.929558 |
| 10 | 1 | 0 | -0.871783 | 0.000000 | 1.950089 |
| 11 | 1 | 0 | 0.871783 | 0.000000 | 1.950089 |

E = -194.0832217 a.u. ZPVE = 55.07721 kcal/mol

Cyclopenta-1,2-diene (³M2)

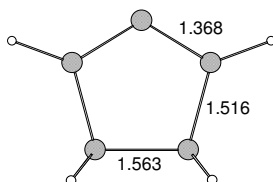
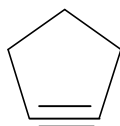


Standard orientation:

| Center Number | Atomic Number | Atomic Type | Coordinates (Angstroms) | | |
|------------------|------------------|----------------|-------------------------|-----------|-----------|
| | | | X | Y | Z |
| 1 | 6 | 0 | 0.000000 | 0.000000 | 1.288965 |
| 2 | 6 | 0 | 0.000000 | 1.162562 | 0.568788 |
| 3 | 6 | 0 | 0.000000 | -1.162562 | 0.568788 |
| 4 | 6 | 0 | 0.000000 | 0.781471 | -0.898446 |
| 5 | 6 | 0 | 0.000000 | -0.781471 | -0.898446 |
| 6 | 1 | 0 | 0.000000 | 2.173840 | 0.941542 |
| 7 | 1 | 0 | 0.000000 | -2.173840 | 0.941542 |
| 8 | 1 | 0 | 0.875215 | 1.185336 | -1.415246 |
| 9 | 1 | 0 | 0.875215 | -1.185336 | -1.415246 |
| 10 | 1 | 0 | -0.875215 | 1.185336 | -1.415246 |
| 11 | 1 | 0 | -0.875215 | -1.185336 | -1.415246 |

E = -194.0644954 a.u. ZPVE = 56.24158 kcal/mol

Cyclopentyne (³M3)

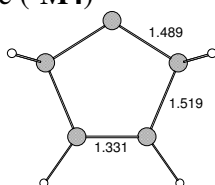
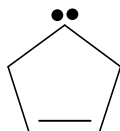


Standard orientation:

| Center Number | Atomic Number | Atomic Type | Coordinates (Angstroms) | | |
|------------------|------------------|----------------|-------------------------|-----------|-----------|
| | | | X | Y | Z |
| 1 | 6 | 0 | 0.200305 | -1.091517 | 0.000000 |
| 2 | 6 | 0 | -0.058372 | -0.205009 | 1.269872 |
| 3 | 6 | 0 | -0.058372 | -0.205009 | -1.269872 |
| 4 | 6 | 0 | -0.058372 | 1.162074 | 0.662795 |
| 5 | 6 | 0 | -0.058372 | 1.162074 | -0.662795 |
| 6 | 1 | 0 | 0.716558 | -0.344007 | 2.023967 |
| 7 | 1 | 0 | -1.020487 | -0.429632 | -1.736927 |
| 8 | 1 | 0 | -0.432935 | -1.976597 | 0.000000 |
| 9 | 1 | 0 | 1.239894 | -1.411802 | 0.000000 |
| 10 | 1 | 0 | -1.020487 | -0.429632 | 1.736927 |
| 11 | 1 | 0 | 0.716558 | -0.344007 | -2.023967 |

E = -194.0086886 a.u. ZPVE = 57.41060 kcal/mol

Cyclopent-3-enylidene (³M4)

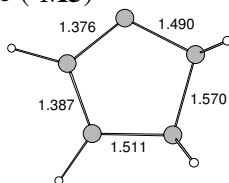
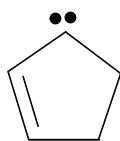


Standard orientation:

| Center Number | Atomic Number | Atomic Type | Coordinates (Angstroms) | | |
|------------------|------------------|----------------|-------------------------|-----------|-----------|
| | | | X | Y | Z |
| 1 | 6 | 0 | 0.000000 | 0.000000 | 1.241148 |
| 2 | 6 | 0 | 0.000000 | 1.254708 | 0.440356 |
| 3 | 6 | 0 | 0.000000 | -1.254708 | 0.440356 |
| 4 | 6 | 0 | 0.000000 | 0.665612 | -0.959895 |
| 5 | 6 | 0 | 0.000000 | -0.665612 | -0.959895 |
| 6 | 1 | 0 | 0.876438 | 1.891223 | 0.620194 |
| 7 | 1 | 0 | -0.876438 | -1.891223 | 0.620194 |
| 8 | 1 | 0 | 0.000000 | 1.285580 | -1.846592 |
| 9 | 1 | 0 | 0.000000 | -1.285580 | -1.846592 |
| 10 | 1 | 0 | -0.876438 | 1.891223 | 0.620194 |
| 11 | 1 | 0 | 0.876438 | -1.891223 | 0.620194 |

E = -194.0485903 a.u. ZPVE = 56.68006 kcal/mol

Cyclopent-2-enylidene (³M5)

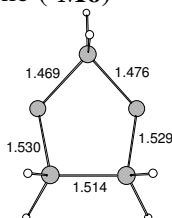
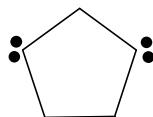


Standard orientation:

| Center Number | Atomic Number | Atomic Type | Coordinates (Angstroms) | | |
|------------------|------------------|----------------|-------------------------|-----------|-----------|
| | | | X | Y | Z |
| 1 | 6 | 0 | -1.263428 | 0.249115 | 0.000000 |
| 2 | 6 | 0 | 0.000000 | 1.181431 | 0.000000 |
| 3 | 6 | 0 | -0.629751 | -1.099260 | 0.000000 |
| 4 | 6 | 0 | 1.176938 | 0.234182 | 0.000000 |
| 5 | 6 | 0 | 0.745869 | -1.083634 | 0.000000 |
| 6 | 1 | 0 | 0.007129 | 1.836701 | 0.875409 |
| 7 | 1 | 0 | 2.206648 | 0.559614 | 0.000000 |
| 8 | 1 | 0 | 1.388616 | -1.951594 | 0.000000 |
| 9 | 1 | 0 | 0.007129 | 1.836701 | -0.875409 |
| 10 | 1 | 0 | -1.893647 | 0.413789 | -0.876990 |
| 11 | 1 | 0 | -1.893647 | 0.413789 | 0.876990 |

E = -194.0683747 a.u. ZPVE = 56.74689 kcal/mol

Cyclopent-1,4-diyldene (³M6)

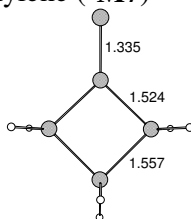
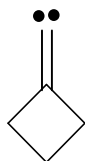


Standard orientation:

| Center Number | Atomic Number | Atomic Type | Coordinates (Angstroms) | | |
|------------------|------------------|----------------|-------------------------|-----------|-----------|
| | | | X | Y | Z |
| 1 | 6 | 0 | -1.007907 | 0.757432 | 0.073040 |
| 2 | 6 | 0 | -1.009467 | -0.756855 | 0.072262 |
| 3 | 6 | 0 | 0.455136 | 0.982112 | -0.314933 |
| 4 | 6 | 0 | 0.452904 | -0.980763 | -0.315167 |
| 5 | 6 | 0 | 1.421415 | -0.001591 | 0.190394 |
| 6 | 1 | 0 | -1.680248 | -1.207360 | -0.656697 |
| 7 | 1 | 0 | -1.220330 | -1.238645 | 1.034678 |
| 8 | 1 | 0 | -1.218264 | 1.238542 | 1.035911 |
| 9 | 1 | 0 | -1.678070 | 1.209681 | -0.655449 |
| 10 | 1 | 0 | 1.526743 | -0.002159 | 1.289840 |
| 11 | 1 | 0 | 2.397687 | -0.002070 | -0.281862 |

E = -193.9445067 a.u. ZPVE = 54.82703 kcal/mol

Cyclobutylidene methylene (³M7)

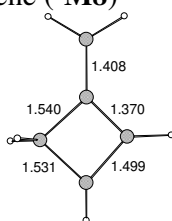
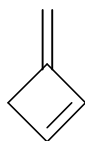


Standard orientation:

| Center Number | Atomic Number | Atomic Type | Coordinates (Angstroms) | | |
|------------------|------------------|----------------|-------------------------|-----------|-----------|
| | | | X | Y | Z |
| 1 | 6 | 0 | 0.149418 | -0.279495 | 1.095490 |
| 2 | 6 | 0 | 0.149418 | -1.385664 | 0.000000 |
| 3 | 6 | 0 | 0.149418 | -0.279495 | -1.095490 |
| 4 | 6 | 0 | -0.198104 | 0.721489 | 0.000000 |
| 5 | 6 | 0 | -0.479603 | 2.046865 | 0.000000 |
| 6 | 1 | 0 | 1.142002 | -0.109626 | 1.516947 |
| 7 | 1 | 0 | -0.565626 | -0.347822 | 1.915576 |
| 8 | 1 | 0 | -0.773391 | -1.961684 | 0.000000 |
| 9 | 1 | 0 | 0.997351 | -2.065623 | 0.000000 |
| 10 | 1 | 0 | -0.565626 | -0.347822 | -1.915576 |
| 11 | 1 | 0 | 1.142002 | -0.109626 | -1.516947 |

E = -193.9688218 a.u. ZPVE = 55.21648 kcal/mol

3-Methylenecyclobutene (³M8)

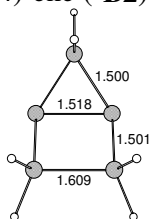


Standard orientation:

| Center Number | Atomic Number | Atomic Type | Coordinates (Angstroms) | | |
|------------------|------------------|----------------|-------------------------|-----------|-----------|
| | | | X | Y | Z |
| 1 | 6 | 0 | -0.505351 | 0.043022 | -0.017668 |
| 2 | 6 | 0 | 0.595779 | -1.032204 | 0.039808 |
| 3 | 6 | 0 | 1.573743 | 0.145763 | 0.045136 |
| 4 | 6 | 0 | 0.396261 | 1.073008 | 0.041360 |
| 5 | 6 | 0 | -1.910027 | -0.044547 | -0.043415 |
| 6 | 1 | 0 | 0.667942 | -1.701955 | -0.819753 |
| 7 | 1 | 0 | 0.587648 | -1.630430 | 0.952609 |
| 8 | 1 | 0 | 2.478886 | 0.228567 | -0.545849 |
| 9 | 1 | 0 | 0.292946 | 2.148206 | 0.065466 |
| 10 | 1 | 0 | -2.410829 | -1.001190 | -0.061117 |
| 11 | 1 | 0 | -2.519023 | 0.846542 | 0.017317 |

E = -194.0351937 a.u. ZPVE = 54.17986 kcal/mol

Bicyclo[2.1.0]pent-1(4)-ene (³B2)

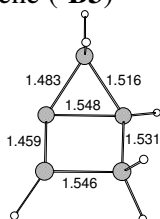
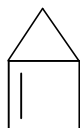


Standard orientation:

| Center Number | Atomic Number | Atomic Type | Coordinates (Angstroms) | | |
|------------------|------------------|----------------|-------------------------|-----------|-----------|
| | | | X | Y | Z |
| 1 | 6 | 0 | 0.881832 | 1.136150 | 0.000000 |
| 2 | 6 | 0 | -0.285316 | 0.576896 | 0.759044 |
| 3 | 6 | 0 | -0.285316 | 0.576896 | -0.759044 |
| 4 | 6 | 0 | -0.285316 | -0.923854 | 0.804293 |
| 5 | 6 | 0 | -0.285316 | -0.923854 | -0.804293 |
| 6 | 1 | 0 | 1.860154 | 0.656893 | 0.000000 |
| 7 | 1 | 0 | 0.907449 | 2.220898 | 0.000000 |
| 8 | 1 | 0 | -1.197655 | -1.368132 | 1.193848 |
| 9 | 1 | 0 | 0.592153 | -1.397464 | -1.250509 |
| 10 | 1 | 0 | 0.592153 | -1.397464 | 1.250509 |
| 11 | 1 | 0 | -1.197655 | -1.368132 | -1.193848 |

E = -193.9783358 a.u. ZPVE = 56.43442 kcal/mol

Bicyclo[2.1.0]pent-1-ene (³B3)

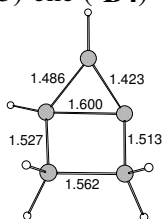
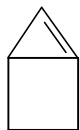


Standard orientation:

| Center Number | Atomic Number | Atomic Type | Coordinates (Angstroms) | | |
|------------------|------------------|----------------|-------------------------|-----------|-----------|
| | | | X | Y | Z |
| 1 | 6 | 0 | -1.353216 | -0.099039 | 0.378807 |
| 2 | 6 | 0 | -0.369105 | 0.730700 | -0.422452 |
| 3 | 6 | 0 | -0.348261 | -0.816735 | -0.441687 |
| 4 | 6 | 0 | 1.012854 | 0.692983 | 0.235036 |
| 5 | 6 | 0 | 1.002654 | -0.847895 | 0.108981 |
| 6 | 1 | 0 | -2.354973 | -0.092476 | -0.033924 |
| 7 | 1 | 0 | -1.307737 | -0.111465 | 1.464263 |
| 8 | 1 | 0 | 1.056142 | 1.091313 | 1.252002 |
| 9 | 1 | 0 | 1.796587 | 1.151868 | -0.368311 |
| 10 | 1 | 0 | 1.830703 | -1.423288 | -0.279447 |
| 11 | 1 | 0 | -0.690281 | 1.423956 | -1.186693 |

E = -193.9954755 a.u. ZPVE = 55.77435 kcal/mol

Bicyclo[2.1.0]pent-1(5)-ene (³B4)

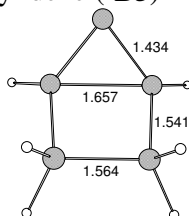


Standard orientation:

| Center Number | Atomic Number | Atomic Type | Coordinates (Angstroms) | | |
|------------------|------------------|----------------|-------------------------|-----------|-----------|
| | | | X | Y | Z |
| 1 | 6 | 0 | 1.368715 | -0.260813 | 0.442312 |
| 2 | 6 | 0 | 0.561902 | 0.774819 | -0.254747 |
| 3 | 6 | 0 | 0.386841 | -0.805404 | -0.431959 |
| 4 | 6 | 0 | -0.896905 | 0.798656 | 0.193982 |
| 5 | 6 | 0 | -1.058324 | -0.744710 | 0.011660 |
| 6 | 1 | 0 | 1.025675 | 1.535628 | -0.868930 |
| 7 | 1 | 0 | -1.536334 | 1.372810 | -0.471731 |
| 8 | 1 | 0 | -1.765219 | -0.982233 | -0.780082 |
| 9 | 1 | 0 | -1.030764 | 1.144813 | 1.220796 |
| 10 | 1 | 0 | -1.295882 | -1.328154 | 0.900950 |
| 11 | 1 | 0 | 2.429160 | -0.318157 | 0.231508 |

E = -193.993602 a.u. ZPVE = 56.24470 kcal/mol

Bicyclo[2.1.0]pent-5-ylidene (³B5)

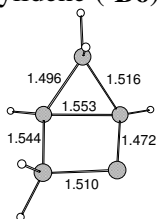
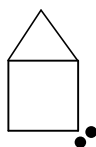


Standard orientation:

| Center Number | Atomic Number | Atomic Type | Coordinates (Angstroms) | | |
|------------------|------------------|----------------|-------------------------|-----------|-----------|
| | | | X | Y | Z |
| 1 | 6 | 0 | 0.901574 | -1.161793 | 0.000000 |
| 2 | 6 | 0 | -0.131331 | -0.610558 | 0.828468 |
| 3 | 6 | 0 | -0.131331 | -0.610558 | -0.828468 |
| 4 | 6 | 0 | -0.131331 | 0.929323 | 0.781933 |
| 5 | 6 | 0 | -0.131331 | 0.929323 | -0.781933 |
| 6 | 1 | 0 | -0.824877 | -1.185995 | 1.431648 |
| 7 | 1 | 0 | -0.824877 | -1.185995 | -1.431648 |
| 8 | 1 | 0 | 0.733768 | 1.395462 | 1.253309 |
| 9 | 1 | 0 | -1.037645 | 1.363326 | -1.201354 |
| 10 | 1 | 0 | -1.037645 | 1.363326 | 1.201354 |
| 11 | 1 | 0 | 0.733768 | 1.395462 | -1.253309 |

E = -193.9875584 a.u. ZPVE = 56.47997 kcal/mol

Bicyclo[2.1.0]pent-2-ylidene (³B6)

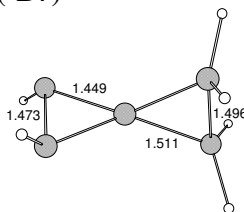
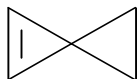


Standard orientation:

| Center Number | Atomic Number | Atomic Type | Coordinates (Angstroms) | | |
|------------------|------------------|----------------|-------------------------|-----------|-----------|
| | | | X | Y | Z |
| 1 | 6 | 0 | -0.557668 | 0.795550 | -0.293955 |
| 2 | 6 | 0 | -1.228930 | -0.341514 | 0.450313 |
| 3 | 6 | 0 | -0.110829 | -0.679659 | -0.483880 |
| 4 | 6 | 0 | 0.783075 | 1.014792 | 0.272967 |
| 5 | 6 | 0 | 1.285201 | -0.400322 | 0.114198 |
| 6 | 1 | 0 | -2.222416 | -0.600846 | 0.105828 |
| 7 | 1 | 0 | -1.079965 | -0.435621 | 1.519018 |
| 8 | 1 | 0 | -0.259640 | -1.251216 | -1.389686 |
| 9 | 1 | 0 | -1.101169 | 1.422051 | -0.985741 |
| 10 | 1 | 0 | 2.083012 | -0.515090 | -0.623912 |
| 11 | 1 | 0 | 1.555085 | -0.952360 | 1.016636 |

E = -193.9988455 a.u. ZPVE = 56.63318 kcal/mol

Spiro[2.2]pent-1-ene (³B7)

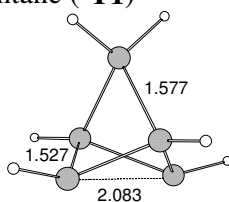
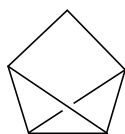


Standard orientation:

| Center Number | Atomic Number | Atomic Type | Coordinates (Angstroms) | | |
|------------------|------------------|----------------|-------------------------|-----------|-----------|
| | | | X | Y | Z |
| 1 | 6 | 0 | 0.000000 | 0.747724 | -1.205468 |
| 2 | 6 | 0 | 0.000000 | -0.747724 | -1.205468 |
| 3 | 6 | 0 | 0.000000 | 0.000000 | 0.107620 |
| 4 | 6 | 0 | 0.728454 | 0.107326 | 1.355682 |
| 5 | 6 | 0 | -0.728454 | -0.107326 | 1.355682 |
| 6 | 1 | 0 | -0.918969 | 1.260256 | -1.458959 |
| 7 | 1 | 0 | 0.910236 | 1.266580 | -1.471337 |
| 8 | 1 | 0 | 0.918969 | -1.260256 | -1.458959 |
| 9 | 1 | 0 | -0.910236 | -1.266580 | -1.471337 |
| 10 | 1 | 0 | 1.277983 | 0.973228 | 1.706152 |
| 11 | 1 | 0 | -1.277983 | -0.973228 | 1.706152 |

E = -193.9815312 a.u. ZPVE = 54.72528 kcal/mol

Tricyclo[2.1.0.0^{2,5}]pentane (³T1)

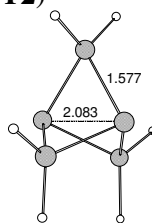


Standard orientation:

| Center Number | Atomic Number | Atomic Type | Coordinates (Angstroms) | | |
|------------------|------------------|----------------|-------------------------|-----------|-----------|
| | | | X | Y | Z |
| 1 | 6 | 0 | 0.000000 | 1.041542 | -0.672488 |
| 2 | 6 | 0 | 0.000000 | -1.041542 | -0.672488 |
| 3 | 6 | 0 | -0.959181 | 0.000000 | -0.099862 |
| 4 | 6 | 0 | 0.959181 | 0.000000 | -0.099862 |
| 5 | 6 | 0 | 0.000000 | 0.000000 | 1.152292 |
| 6 | 1 | 0 | 2.043706 | 0.000000 | -0.097713 |
| 7 | 1 | 0 | 0.000000 | -0.906800 | 1.761149 |
| 8 | 1 | 0 | 0.000000 | 0.906800 | 1.761149 |
| 9 | 1 | 0 | -2.043706 | 0.000000 | -0.097713 |
| 10 | 1 | 0 | 0.000000 | -2.111507 | -0.486209 |
| 11 | 1 | 0 | 0.000000 | 2.111507 | -0.486209 |

E = -193.9703158 a.u. ZPVE = 55.76836 kcal/mol

Tricyclo[1.1.1.0^{1,3}]pentane (³T2)

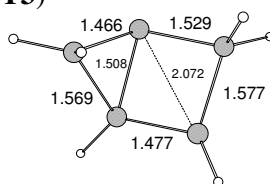


Standard orientation:

| Center Number | Atomic Number | Atomic Type | Coordinates (Angstroms) | | |
|------------------|------------------|----------------|-------------------------|-----------|-----------|
| | | | X | Y | Z |
| 1 | 6 | 0 | 0.000000 | 0.000000 | 0.901425 |
| 2 | 6 | 0 | 0.000000 | 1.269744 | 0.000000 |
| 3 | 6 | 0 | 0.000000 | 0.000000 | -0.901425 |
| 4 | 6 | 0 | -1.099631 | -0.634872 | 0.000000 |
| 5 | 6 | 0 | 1.099631 | -0.634872 | 0.000000 |
| 6 | 1 | 0 | 0.906024 | 1.869691 | 0.000000 |
| 7 | 1 | 0 | -0.906024 | 1.869691 | 0.000000 |
| 8 | 1 | 0 | -2.072212 | -0.150206 | 0.000000 |
| 9 | 1 | 0 | -1.166188 | -1.719485 | 0.000000 |
| 10 | 1 | 0 | 1.166188 | -1.719485 | 0.000000 |
| 11 | 1 | 0 | 2.072212 | -0.150206 | 0.000000 |

E = -193.9286613 a.u. ZPVE = 57.16251 kcal/mol

Tricyclo[2.1.0.0^{1,3}]pentane (**³T3**)



Standard orientation:

| Center Number | Atomic Number | Atomic Type | Coordinates (Angstroms) | | |
|------------------|------------------|----------------|-------------------------|-----------|-----------|
| | | | X | Y | Z |
| 1 | 6 | 0 | 1.323908 | -0.313938 | 0.392657 |
| 2 | 6 | 0 | 0.474986 | 0.779954 | -0.346018 |
| 3 | 6 | 0 | 0.262738 | -0.700210 | -0.541480 |
| 4 | 6 | 0 | -0.883648 | 0.842713 | 0.231095 |
| 5 | 6 | 0 | -1.166041 | -0.633840 | -0.001632 |
| 6 | 1 | 0 | 0.990400 | 1.525761 | -0.935105 |
| 7 | 1 | 0 | -1.302558 | 1.520510 | 0.967064 |
| 8 | 1 | 0 | -1.404073 | -1.267725 | 0.856947 |
| 9 | 1 | 0 | 1.223718 | -0.452495 | 1.464448 |
| 10 | 1 | 0 | 2.338259 | -0.375931 | 0.016947 |
| 11 | 1 | 0 | -1.917400 | -0.798193 | -0.778031 |

E = -193.9976827 a.u. ZPVE = 55.60712 kcal/mol

The cartesian coordinates of singlet state geometries of all stable isomers calculated
at CASSCF(4,4)/6-31G(d) level

Cyclopenta-1,3-diene (**M1**)

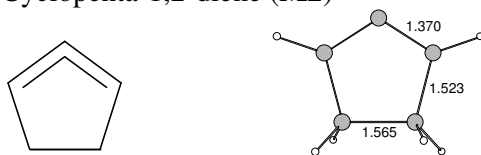


Standard orientation:

| Center Number | Atomic Number | Atomic Type | Coordinates (Angstroms) | | |
|------------------|------------------|----------------|-------------------------|-----------|-----------|
| | | | X | Y | Z |
| 1 | 6 | 0 | 0.000000 | 0.000000 | 1.226624 |
| 2 | 6 | 0 | 0.000000 | 1.177607 | 0.280560 |
| 3 | 6 | 0 | 0.000000 | -1.177607 | 0.280560 |
| 4 | 6 | 0 | 0.000000 | 0.738565 | -0.994070 |
| 5 | 6 | 0 | 0.000000 | -0.738565 | -0.994070 |
| 6 | 1 | 0 | 0.000000 | 2.200972 | 0.604172 |
| 7 | 1 | 0 | 0.000000 | -2.200972 | 0.604172 |
| 8 | 1 | 0 | 0.000000 | 1.348154 | -1.877938 |
| 9 | 1 | 0 | 0.000000 | -1.348154 | -1.877938 |
| 10 | 1 | 0 | -0.873912 | 0.000000 | 1.874957 |
| 11 | 1 | 0 | 0.873912 | 0.000000 | 1.874957 |

E = -192.8466247 a.u. ZPVE = 61.29763 kcal/mol

Cyclopenta-1,2-diene (**M2**)

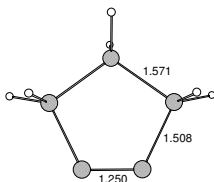
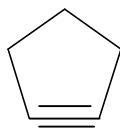


Standard orientation:

| Center Number | Atomic Number | Atomic Type | Coordinates (Angstroms) | | |
|------------------|------------------|----------------|-------------------------|-----------|-----------|
| | | | X | Y | Z |
| 1 | 6 | 0 | 0.000000 | 0.000000 | 1.310715 |
| 2 | 6 | 0 | 0.000000 | 1.142642 | 0.554535 |
| 3 | 6 | 0 | 0.000000 | -1.142642 | 0.554535 |
| 4 | 6 | 0 | 0.247411 | 0.742282 | -0.893820 |
| 5 | 6 | 0 | -0.247411 | -0.742282 | -0.893820 |
| 6 | 1 | 0 | -0.340496 | 2.113451 | 0.860074 |
| 7 | 1 | 0 | 0.340496 | -2.113451 | 0.860074 |
| 8 | 1 | 0 | 1.297082 | 0.793253 | -1.173608 |
| 9 | 1 | 0 | 0.301658 | -1.376016 | -1.582904 |
| 10 | 1 | 0 | -0.301658 | 1.376016 | -1.582904 |
| 11 | 1 | 0 | -1.297082 | -0.793253 | -1.173608 |

E = -192.7491575 a.u. ZPVE = 60.79479 kcal/mol

Cyclopentyne (M3)

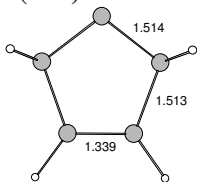
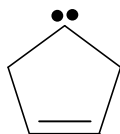


Standard orientation:

| Center Number | Atomic Number | Atomic Type | Coordinates (Angstroms) | | |
|------------------|------------------|----------------|-------------------------|-----------|-----------|
| | | | X | Y | Z |
| 1 | 6 | 0 | -0.261618 | 1.084892 | 0.000000 |
| 2 | 1 | 0 | 0.248833 | 2.043163 | 0.000000 |
| 3 | 1 | 0 | -1.326277 | 1.293996 | 0.000000 |
| 4 | 6 | 0 | 0.076735 | 0.208788 | 1.259335 |
| 5 | 6 | 0 | 0.076735 | 0.208788 | -1.259335 |
| 6 | 6 | 0 | 0.076735 | -1.159199 | 0.624944 |
| 7 | 6 | 0 | 0.076735 | -1.159199 | -0.624944 |
| 8 | 1 | 0 | -0.649921 | 0.336406 | 2.051781 |
| 9 | 1 | 0 | -0.649921 | 0.336406 | -2.051781 |
| 10 | 1 | 0 | 1.052676 | 0.442805 | 1.670202 |
| 11 | 1 | 0 | 1.052676 | 0.442805 | -1.670202 |

E = -192.7360166 a.u. ZPVE = 62.12507 kcal/mol

Cyclopent-3-enylidene (M4)

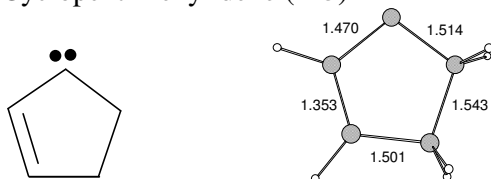


Standard orientation:

| Center Number | Atomic Number | Atomic Type | Coordinates (Angstroms) | | |
|------------------|------------------|----------------|-------------------------|-----------|-----------|
| | | | X | Y | Z |
| 1 | 6 | 0 | 0.000000 | 0.000000 | 1.350552 |
| 2 | 6 | 0 | 0.000000 | 1.192785 | 0.418786 |
| 3 | 6 | 0 | 0.000000 | -1.192785 | 0.418786 |
| 4 | 6 | 0 | 0.000000 | 0.669375 | -1.001227 |
| 5 | 6 | 0 | 0.000000 | -0.669375 | -1.001227 |
| 6 | 1 | 0 | 0.864739 | 1.812489 | 0.657476 |
| 7 | 1 | 0 | -0.864739 | -1.812489 | 0.657476 |
| 8 | 1 | 0 | 0.000000 | 1.299485 | -1.871961 |
| 9 | 1 | 0 | 0.000000 | -1.299485 | -1.871961 |
| 10 | 1 | 0 | -0.864739 | 1.812489 | 0.657476 |
| 11 | 1 | 0 | 0.864739 | -1.812489 | 0.657476 |

E = -192.7375968 a.u. ZPVE = 59.83688 kcal/mol

Cyclopent-2-enylidene (M5)

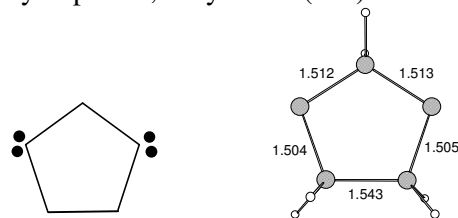


Standard orientation:

| Center Number | Atomic Number | Atomic Type | Coordinates (Angstroms) | | |
|------------------|------------------|----------------|-------------------------|-----------|-----------|
| | | | X | Y | Z |
| 1 | 6 | 0 | -0.490997 | -1.122022 | 0.000000 |
| 2 | 6 | 0 | -1.180034 | 0.258900 | 0.000000 |
| 3 | 6 | 0 | 1.012330 | -0.945313 | 0.000000 |
| 4 | 6 | 0 | 0.000000 | 1.186910 | 0.000000 |
| 5 | 6 | 0 | 1.174667 | 0.515383 | 0.000000 |
| 6 | 1 | 0 | -1.808716 | 0.418263 | 0.872045 |
| 7 | 1 | 0 | -0.101610 | 2.258649 | 0.000000 |
| 8 | 1 | 0 | 2.139058 | 0.991514 | 0.000000 |
| 9 | 1 | 0 | -1.808716 | 0.418263 | -0.872045 |
| 10 | 1 | 0 | -0.757906 | -1.724917 | -0.865034 |
| 11 | 1 | 0 | -0.757906 | -1.724917 | 0.865034 |

E = -192.7470962 a.u. ZPVE = 60.78559 kcal/mol

Cyclopent-1,4-diyldiene (M6)

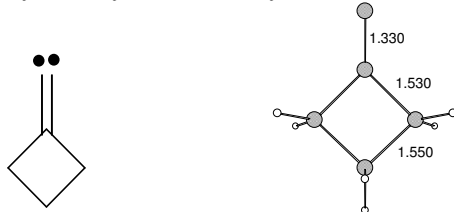


Standard orientation:

| Center Number | Atomic Number | Atomic Type | Coordinates (Angstroms) | | |
|------------------|------------------|----------------|-------------------------|-----------|-----------|
| | | | X | Y | Z |
| 1 | 6 | 0 | 0.939823 | -0.773447 | 0.074177 |
| 2 | 6 | 0 | 0.950954 | 0.765120 | -0.047351 |
| 3 | 6 | 0 | -0.462933 | -1.260171 | -0.168764 |
| 4 | 6 | 0 | -0.461986 | 1.275409 | 0.024378 |
| 5 | 6 | 0 | -1.276865 | 0.001872 | 0.018126 |
| 6 | 1 | 0 | 1.282290 | 1.073066 | -1.042539 |
| 7 | 1 | 0 | 1.605023 | 1.286667 | 0.644579 |
| 8 | 1 | 0 | 1.156503 | -1.102183 | 1.094464 |
| 9 | 1 | 0 | 1.661992 | -1.284822 | -0.553486 |
| 10 | 1 | 0 | -1.664889 | -0.080548 | 1.044084 |
| 11 | 1 | 0 | -2.174881 | 0.055123 | -0.590499 |

E = -192.6287958 a.u. ZPVE = 61.70891 kcal/mol

Cyclobutylidene methylene (M7)

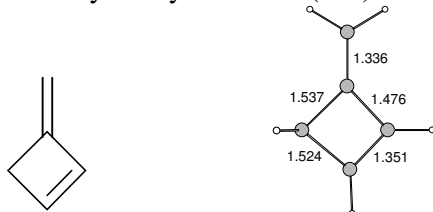


Standard orientation:

| Center Number | Atomic Number | Atomic Type | Coordinates (Angstroms) | | |
|------------------|------------------|----------------|-------------------------|-----------|-----------|
| | | | X | Y | Z |
| 1 | 6 | 0 | 0.173028 | -0.271715 | 1.096174 |
| 2 | 6 | 0 | 0.173028 | -1.368237 | 0.000000 |
| 3 | 6 | 0 | 0.173028 | -0.271715 | -1.096174 |
| 4 | 6 | 0 | -0.133034 | 0.750153 | 0.000000 |
| 5 | 6 | 0 | -0.626361 | 1.985848 | 0.000000 |
| 6 | 1 | 0 | 1.148254 | -0.110532 | 1.540094 |
| 7 | 1 | 0 | -0.563312 | -0.364593 | 1.883224 |
| 8 | 1 | 0 | -0.742590 | -1.946453 | 0.000000 |
| 9 | 1 | 0 | 1.014567 | -2.049306 | 0.000000 |
| 10 | 1 | 0 | -0.563312 | -0.364593 | -1.883224 |
| 11 | 1 | 0 | 1.148254 | -0.110532 | -1.540094 |

E = -192.7236582 a.u. ZPVE = 60.73443 kcal/mol

3-Methylenecyclobutene (M8)

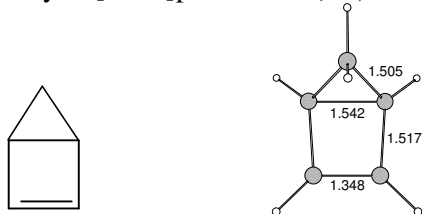


Standard orientation:

| Center Number | Atomic Number | Atomic Type | Coordinates (Angstroms) | | |
|------------------|------------------|----------------|-------------------------|-----------|-----------|
| | | | X | Y | Z |
| 1 | 6 | 0 | 0.000000 | 0.551100 | 0.000000 |
| 2 | 6 | 0 | 1.024704 | -0.594344 | 0.000000 |
| 3 | 6 | 0 | -0.208060 | -1.490897 | 0.000000 |
| 4 | 6 | 0 | -1.077975 | -0.457686 | 0.000000 |
| 5 | 6 | 0 | 0.083379 | 1.884691 | 0.000000 |
| 6 | 1 | 0 | 1.651114 | -0.652152 | 0.884191 |
| 7 | 1 | 0 | 1.651114 | -0.652152 | -0.884191 |
| 8 | 1 | 0 | -0.322698 | -2.557881 | 0.000000 |
| 9 | 1 | 0 | -2.149586 | -0.384136 | 0.000000 |
| 10 | 1 | 0 | 1.034672 | 2.386170 | 0.000000 |
| 11 | 1 | 0 | -0.796901 | 2.502970 | 0.000000 |

E = -192.8024075 a.u. ZPVE = 60.36835 kcal/mol

Bicyclo[2.1.0]pent-2-ene (B1)

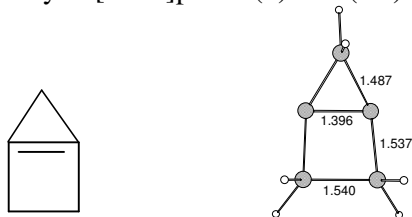


Standard orientation:

| Center Number | Atomic Number | Atomic Type | Coordinates (Angstroms) | | |
|------------------|------------------|----------------|-------------------------|-----------|-----------|
| | | | X | Y | Z |
| 1 | 6 | 0 | 0.905996 | -1.008434 | 0.000000 |
| 2 | 6 | 0 | -0.265273 | -0.460670 | 0.770888 |
| 3 | 6 | 0 | -0.265273 | -0.460670 | -0.770888 |
| 4 | 6 | 0 | -0.265273 | 1.053612 | 0.674076 |
| 5 | 6 | 0 | -0.265273 | 1.053612 | -0.674076 |
| 6 | 1 | 0 | -0.866457 | -1.066182 | -1.423339 |
| 7 | 1 | 0 | 1.006554 | -2.083197 | 0.000000 |
| 8 | 1 | 0 | 1.843756 | -0.477649 | 0.000000 |
| 9 | 1 | 0 | -0.866457 | -1.066182 | 1.423339 |
| 10 | 1 | 0 | -0.093408 | 1.814252 | 1.413097 |
| 11 | 1 | 0 | -0.093408 | 1.814252 | -1.413097 |

E = -192.7589525 a.u. ZPVE = 61.32302 kcal/mol

Bicyclo[2.1.0]pent-1(4)-ene (B2)

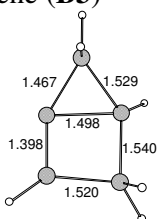


Standard orientation:

| Center Number | Atomic Number | Atomic Type | Coordinates (Angstroms) | | |
|------------------|------------------|----------------|-------------------------|-----------|-----------|
| | | | X | Y | Z |
| 1 | 6 | 0 | 0.783747 | 1.329289 | 0.000000 |
| 2 | 6 | 0 | -0.256418 | 0.528915 | 0.698156 |
| 3 | 6 | 0 | -0.256418 | 0.528915 | -0.698156 |
| 4 | 6 | 0 | -0.256418 | -1.006720 | 0.770195 |
| 5 | 6 | 0 | -0.256418 | -1.006720 | -0.770195 |
| 6 | 1 | 0 | 1.826434 | 1.036880 | 0.000000 |
| 7 | 1 | 0 | 0.630162 | 2.392218 | 0.000000 |
| 8 | 1 | 0 | -1.133064 | -1.417541 | 1.252165 |
| 9 | 1 | 0 | 0.630534 | -1.418048 | -1.237420 |
| 10 | 1 | 0 | 0.630534 | -1.418048 | 1.237420 |
| 11 | 1 | 0 | -1.133064 | -1.417541 | -1.252165 |

E = -192.6932731 a.u. ZPVE = 61.50723 kcal/mol

Bicyclo[2.1.0]pent-1-ene (**B3**)

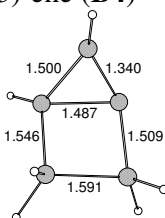
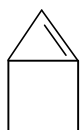


Standard orientation:

| Center Number | Atomic Number | Atomic Type | Coordinates (Angstroms) | | |
|------------------|------------------|----------------|-------------------------|-----------|-----------|
| | | | X | Y | Z |
| 1 | 6 | 0 | 1.411033 | 0.102840 | 0.345447 |
| 2 | 6 | 0 | 0.323910 | -0.798611 | -0.240899 |
| 3 | 6 | 0 | 0.368995 | 0.673341 | -0.514443 |
| 4 | 6 | 0 | -1.130896 | -0.605287 | 0.224441 |
| 5 | 6 | 0 | -0.943758 | 0.872533 | -0.076123 |
| 6 | 1 | 0 | 2.380088 | -0.084038 | -0.084427 |
| 7 | 1 | 0 | 1.440085 | 0.373255 | 1.388980 |
| 8 | 1 | 0 | -1.331930 | -0.792572 | 1.277004 |
| 9 | 1 | 0 | -1.850243 | -1.154026 | -0.373254 |
| 10 | 1 | 0 | -1.441445 | 1.750633 | 0.296557 |
| 11 | 1 | 0 | 0.627747 | -1.562139 | -0.935389 |

E = -192.6970036 a.u. ZPVE = 60.89936 kcal/mol

Bicyclo[2.1.0]pent-1(5)-ene (**B4**)

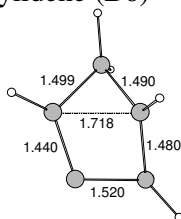
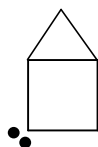


Standard orientation:

| Center Number | Atomic Number | Atomic Type | Coordinates (Angstroms) | | |
|------------------|------------------|----------------|-------------------------|-----------|-----------|
| | | | X | Y | Z |
| 1 | 6 | 0 | 1.436728 | -0.230200 | 0.300910 |
| 2 | 6 | 0 | 0.520996 | 0.754589 | -0.365050 |
| 3 | 6 | 0 | 0.414424 | -0.723480 | -0.410633 |
| 4 | 6 | 0 | -0.869198 | 0.781071 | 0.310889 |
| 5 | 6 | 0 | -1.046127 | -0.762081 | -0.032236 |
| 6 | 1 | 0 | 0.818088 | 1.411313 | -1.162934 |
| 7 | 1 | 0 | -1.602701 | 1.427976 | -0.156740 |
| 8 | 1 | 0 | -1.706077 | -0.897768 | -0.879271 |
| 9 | 1 | 0 | -0.860710 | 0.971825 | 1.380725 |
| 10 | 1 | 0 | -1.336929 | -1.437883 | 0.763997 |
| 11 | 1 | 0 | 1.947387 | -0.394856 | 1.230946 |

E = -192.6977121 a.u. ZPVE = 60.89936 kcal/mol

Bicyclo[2.1.0]pent-2-ylidene (B6)

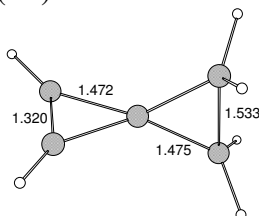
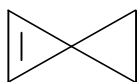


Standard orientation:

| Center Number | Atomic Number | Atomic Type | Coordinates (Angstroms) | | |
|------------------|------------------|----------------|-------------------------|-----------|-----------|
| | | | X | Y | Z |
| 1 | 6 | 0 | -1.256181 | -0.412853 | -0.215026 |
| 2 | 6 | 0 | -0.026401 | -0.544498 | 0.597444 |
| 3 | 6 | 0 | -0.761936 | 1.014138 | -0.046255 |
| 4 | 6 | 0 | 0.668350 | 0.861233 | -0.105158 |
| 5 | 6 | 0 | 1.185621 | -0.538533 | -0.248956 |
| 6 | 1 | 0 | -2.210090 | -0.590665 | 0.253208 |
| 7 | 1 | 0 | -1.181836 | -0.901673 | -1.177260 |
| 8 | 1 | 0 | 0.002627 | -0.649483 | 1.663141 |
| 9 | 1 | 0 | 1.302170 | 1.616021 | 0.327741 |
| 10 | 1 | 0 | 1.100501 | -1.041067 | -1.199912 |
| 11 | 1 | 0 | 2.129907 | -0.710054 | 0.240785 |

E = -192.6980735 a.u. ZPVE = 61.40025 kcal/mol

Spiro[2.2]pent-1-ene (B7)

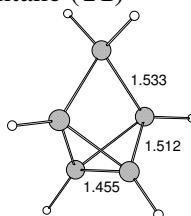
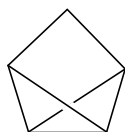


Standard orientation:

| Center Number | Atomic Number | Atomic Type | Coordinates (Angstroms) | | |
|------------------|------------------|----------------|-------------------------|-----------|-----------|
| | | | X | Y | Z |
| 1 | 6 | 0 | -0.766404 | 0.000000 | -1.206153 |
| 2 | 6 | 0 | 0.766404 | 0.000000 | -1.206153 |
| 3 | 6 | 0 | 0.000000 | 0.000000 | 0.053873 |
| 4 | 6 | 0 | 0.000000 | 0.660010 | 1.369994 |
| 5 | 6 | 0 | 0.000000 | -0.660010 | 1.369994 |
| 6 | 1 | 0 | -1.262528 | -0.903721 | -1.521042 |
| 7 | 1 | 0 | -1.262528 | 0.903721 | -1.521042 |
| 8 | 1 | 0 | 1.262528 | 0.903721 | -1.521042 |
| 9 | 1 | 0 | 1.262528 | -0.903721 | -1.521042 |
| 10 | 1 | 0 | 0.000000 | 1.589196 | 1.897421 |
| 11 | 1 | 0 | 0.000000 | -1.589196 | 1.897421 |

E = -192.7357677 a.u. ZPVE = 59.93248 kcal/mol

Tricyclo[2.1.0.0^{2,5}]pentane (T1)

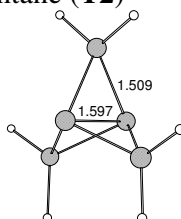


Standard orientation:

| Center Number | Atomic Number | Atomic Type | Coordinates (Angstroms) | | |
|------------------|------------------|----------------|-------------------------|-----------|-----------|
| | | | X | Y | Z |
| 1 | 6 | 0 | 0.000000 | 0.727586 | -0.810142 |
| 2 | 6 | 0 | 0.000000 | -0.727586 | -0.810142 |
| 3 | 6 | 0 | -0.968341 | 0.000000 | 0.095708 |
| 4 | 6 | 0 | 0.968341 | 0.000000 | 0.095708 |
| 5 | 6 | 0 | 0.000000 | 0.000000 | 1.284170 |
| 6 | 1 | 0 | 2.042106 | 0.000000 | 0.040422 |
| 7 | 1 | 0 | 0.000000 | -0.893402 | 1.902462 |
| 8 | 1 | 0 | 0.000000 | 0.893402 | 1.902462 |
| 9 | 1 | 0 | -2.042106 | 0.000000 | 0.040422 |
| 10 | 1 | 0 | 0.000000 | -1.535724 | -1.508789 |
| 11 | 1 | 0 | 0.000000 | 1.535724 | -1.508789 |

E = -192.7069962 a.u. ZPVE = 61.70891 kcal/mol

Tricyclo[1.1.1.0^{1,3}]pentane (T2)

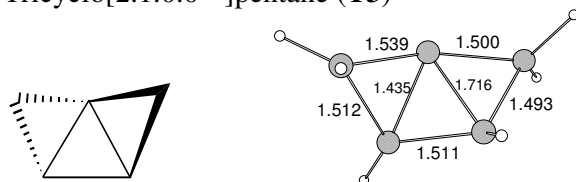


Standard orientation:

| Center Number | Atomic Number | Atomic Type | Coordinates (Angstroms) | | |
|------------------|------------------|----------------|-------------------------|-----------|-----------|
| | | | X | Y | Z |
| 1 | 6 | 0 | 0.000000 | 0.000000 | 0.798419 |
| 2 | 6 | 0 | 0.000000 | 1.280769 | 0.000000 |
| 3 | 6 | 0 | 0.000000 | 0.000000 | -0.798419 |
| 4 | 6 | 0 | -1.109179 | -0.640385 | 0.000000 |
| 5 | 6 | 0 | 1.109179 | -0.640385 | 0.000000 |
| 6 | 1 | 0 | 0.903964 | 1.866825 | 0.000000 |
| 7 | 1 | 0 | -0.903964 | 1.866825 | 0.000000 |
| 8 | 1 | 0 | -2.068700 | -0.150557 | 0.000000 |
| 9 | 1 | 0 | -1.164736 | -1.716268 | 0.000000 |
| 10 | 1 | 0 | 1.164736 | -1.716268 | 0.000000 |
| 11 | 1 | 0 | 2.068700 | -0.150557 | 0.000000 |

E = -192.7221643 a.u. ZPVE = 63.10438 kcal/mol

Tricyclo[2.1.0.0^{1,3}]pentane (**T3**)



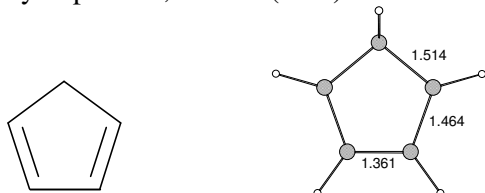
Standard orientation:

| Center Number | Atomic Number | Atomic Type | Coordinates (Angstroms) | | |
|------------------|------------------|----------------|-------------------------|-----------|-----------|
| | | | X | Y | Z |
| 1 | 6 | 0 | 1.394455 | -0.406537 | 0.246703 |
| 2 | 6 | 0 | 0.601409 | 0.686253 | -0.433815 |
| 3 | 6 | 0 | 0.002425 | -0.616529 | -0.374732 |
| 4 | 6 | 0 | -0.592415 | 0.739933 | 0.491029 |
| 5 | 6 | 0 | -1.444149 | -0.342221 | -0.085275 |
| 6 | 1 | 0 | 0.852285 | 1.341156 | -1.247061 |
| 7 | 1 | 0 | -0.380890 | 0.621818 | 1.541998 |
| 8 | 1 | 0 | -1.983785 | -0.971963 | 0.606304 |
| 9 | 1 | 0 | 1.566056 | -0.334655 | 1.308931 |
| 10 | 1 | 0 | 2.186731 | -0.897192 | -0.296519 |
| 11 | 1 | 0 | -2.010742 | -0.124559 | -0.977111 |

E = -192.678826 a.u. ZPVE = 61.47195 kcal/mol

*The cartesian coordinates of triplet state geometries of all stable isomers calculated
at CASSCF(4,4)/6-31G(d)*

Cyclopenta-1,3-diene (³M1)

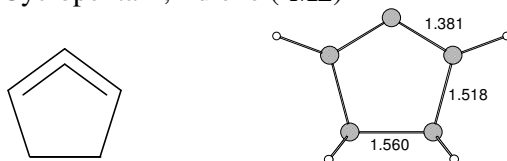


Standard orientation:

| Center Number | Atomic Number | Atomic Type | Coordinates (Angstroms) | | |
|------------------|------------------|----------------|-------------------------|-----------|-----------|
| | | | X | Y | Z |
| 1 | 6 | 0 | -1.276302 | -0.000006 | -0.000404 |
| 2 | 6 | 0 | -0.318545 | 1.172658 | -0.029482 |
| 3 | 6 | 0 | -0.318534 | -1.172662 | -0.029483 |
| 4 | 6 | 0 | 1.059359 | 0.680451 | 0.003091 |
| 5 | 6 | 0 | 1.059365 | -0.680442 | 0.003084 |
| 6 | 1 | 0 | -0.609686 | 2.192430 | 0.128437 |
| 7 | 1 | 0 | -0.609659 | -2.192427 | 0.128512 |
| 8 | 1 | 0 | 1.926533 | 1.312206 | 0.009516 |
| 9 | 1 | 0 | 1.926546 | -1.312188 | 0.009437 |
| 10 | 1 | 0 | -1.960872 | -0.000024 | -0.849099 |
| 11 | 1 | 0 | -1.904913 | 0.000006 | 0.892359 |

E = -192.7536192 a.u. ZPVE = 58.41178 kcal/mol

Cyclopenta-1,2-diene (³M2)

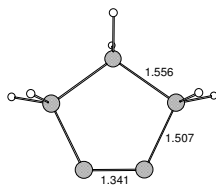
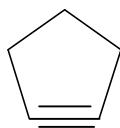


Standard orientation:

| Center Number | Atomic Number | Atomic Type | Coordinates (Angstroms) | | |
|------------------|------------------|----------------|-------------------------|-----------|-----------|
| | | | X | Y | Z |
| 1 | 6 | 0 | 0.000000 | 0.000000 | 1.311096 |
| 2 | 6 | 0 | 0.000000 | 1.162593 | 0.564824 |
| 3 | 6 | 0 | 0.000000 | -1.162593 | 0.564824 |
| 4 | 6 | 0 | 0.000000 | 0.780039 | -0.904007 |
| 5 | 6 | 0 | 0.000000 | -0.780039 | -0.904007 |
| 6 | 1 | 0 | 0.000000 | 2.168683 | 0.932579 |
| 7 | 1 | 0 | 0.000000 | -2.168683 | 0.932579 |
| 8 | 1 | 0 | 0.871518 | 1.178481 | -1.415386 |
| 9 | 1 | 0 | 0.871518 | -1.178481 | -1.415386 |
| 10 | 1 | 0 | -0.871518 | 1.178481 | -1.415386 |
| 11 | 1 | 0 | -0.871518 | -1.178481 | -1.415386 |

E = -192.7367486 a.u. ZPVE = 60.06577 kcal/mol

Cyclopentyne (³M3)

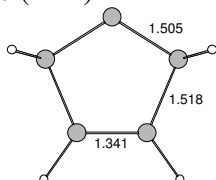
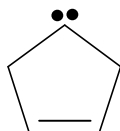


Standard orientation:

| Center Number | Atomic Number | Atomic Type | Coordinates (Angstroms) | | |
|------------------|------------------|----------------|-------------------------|-----------|-----------|
| | | | X | Y | Z |
| 1 | 6 | 0 | 0.257194 | -1.080610 | 0.000000 |
| 2 | 6 | 0 | -0.074880 | -0.218418 | 1.252142 |
| 3 | 6 | 0 | -0.074880 | -0.218418 | -1.252142 |
| 4 | 6 | 0 | -0.074880 | 1.171758 | 0.670720 |
| 5 | 6 | 0 | -0.074880 | 1.171758 | -0.670720 |
| 6 | 1 | 0 | 0.657402 | -0.349817 | 2.040377 |
| 7 | 1 | 0 | -1.048371 | -0.463320 | -1.667013 |
| 8 | 1 | 0 | -0.280618 | -2.020923 | 0.000000 |
| 9 | 1 | 0 | 1.316514 | -1.309220 | 0.000000 |
| 10 | 1 | 0 | -1.048371 | -0.463320 | 1.667013 |
| 11 | 1 | 0 | 0.657402 | -0.349817 | -2.040377 |

E = -192.6966844 a.u. ZPVE = 62.02130 kcal/mol

Cyclopent-3-enylidene (³M4)

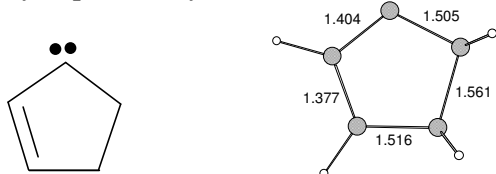


Standard orientation:

| Center Number | Atomic Number | Atomic Type | Coordinates (Angstroms) | | |
|------------------|------------------|----------------|-------------------------|-----------|-----------|
| | | | X | Y | Z |
| 1 | 6 | 0 | 0.000000 | 0.000000 | 1.258952 |
| 2 | 6 | 0 | 0.000000 | 1.259546 | 0.435966 |
| 3 | 6 | 0 | 0.000000 | -1.259546 | 0.435966 |
| 4 | 6 | 0 | 0.000000 | 0.670714 | -0.963363 |
| 5 | 6 | 0 | 0.000000 | -0.670714 | -0.963363 |
| 6 | 1 | 0 | 0.874135 | 1.882015 | 0.616486 |
| 7 | 1 | 0 | -0.874135 | -1.882015 | 0.616486 |
| 8 | 1 | 0 | 0.000000 | 1.285244 | -1.845448 |
| 9 | 1 | 0 | 0.000000 | -1.285244 | -1.845448 |
| 10 | 1 | 0 | -0.874135 | 1.882015 | 0.616486 |
| 11 | 1 | 0 | 0.874135 | -1.882015 | 0.616486 |

E = -192.7377978 a.u. ZPVE = 61.03935 kcal/mol

Cyclopent-2-enylidene (³M5)

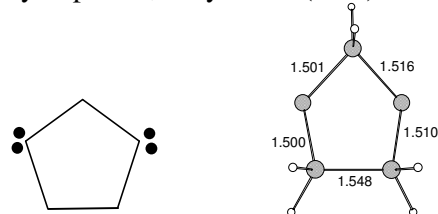


Standard orientation:

| Center Number | Atomic Number | Atomic Type | Coordinates (Angstroms) | | |
|---------------|---------------|-------------|-------------------------|-----------|-----------|
| | | | X | Y | Z |
| 1 | 6 | 0 | -1.259212 | 0.261403 | 0.000000 |
| 2 | 6 | 0 | 0.000000 | 1.184390 | 0.000000 |
| 3 | 6 | 0 | -0.649487 | -1.114540 | 0.000000 |
| 4 | 6 | 0 | 1.176827 | 0.228525 | 0.000000 |
| 5 | 6 | 0 | 0.754613 | -1.082219 | 0.000000 |
| 6 | 1 | 0 | 0.016760 | 1.832573 | 0.871382 |
| 7 | 1 | 0 | 2.199311 | 0.555616 | 0.000000 |
| 8 | 1 | 0 | 1.393759 | -1.944337 | 0.000000 |
| 9 | 1 | 0 | 0.016760 | 1.832573 | -0.871382 |
| 10 | 1 | 0 | -1.881518 | 0.429113 | -0.872983 |
| 11 | 1 | 0 | -1.881518 | 0.429113 | 0.872983 |

E = -192.7483118 a.u. ZPVE = 60.92161 kcal/mol

Cyclopent-1,4-diylidene (³M6)

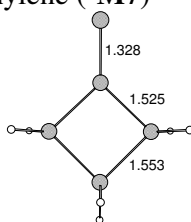
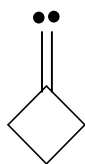


Standard orientation:

| Center Number | Atomic Number | Atomic Type | Coordinates (Angstroms) | | |
|---------------|---------------|-------------|-------------------------|-----------|-----------|
| | | | X | Y | Z |
| 1 | 6 | 0 | -0.812908 | 0.869874 | 0.064198 |
| 2 | 6 | 0 | -1.124992 | -0.640722 | -0.071924 |
| 3 | 6 | 0 | 0.660762 | 1.148829 | -0.112073 |
| 4 | 6 | 0 | 0.243309 | -1.232426 | 0.092142 |
| 5 | 6 | 0 | 1.333824 | -0.204720 | 0.001178 |
| 6 | 1 | 0 | -1.548903 | -0.866928 | -1.048021 |
| 7 | 1 | 0 | -1.833217 | -0.991095 | 0.671540 |
| 8 | 1 | 0 | -0.984300 | 1.206900 | 1.091010 |
| 9 | 1 | 0 | -1.423232 | 1.515107 | -0.558422 |
| 10 | 1 | 0 | 2.000294 | -0.178660 | 0.863618 |
| 11 | 1 | 0 | 1.989388 | -0.330337 | -0.860845 |

E = -192.6290146 a.u. ZPVE = 59.43611 kcal/mol

Cyclobutylidene methylene (³M7)

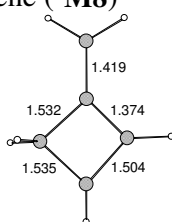
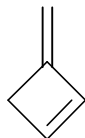


Standard orientation:

| Center Number | Atomic Number | Atomic Type | Coordinates (Angstroms) | | |
|------------------|------------------|----------------|-------------------------|-----------|-----------|
| | | | X | Y | Z |
| 1 | 6 | 0 | 0.056041 | -0.292624 | 1.102590 |
| 2 | 6 | 0 | 0.056041 | -1.386333 | 0.000000 |
| 3 | 6 | 0 | 0.056041 | -0.292624 | -1.102590 |
| 4 | 6 | 0 | -0.049778 | 0.755360 | 0.000000 |
| 5 | 6 | 0 | -0.198245 | 2.074964 | 0.000000 |
| 6 | 1 | 0 | 0.975401 | -0.234601 | 1.675298 |
| 7 | 1 | 0 | -0.778290 | -0.322390 | 1.794116 |
| 8 | 1 | 0 | -0.835890 | -2.000747 | 0.000000 |
| 9 | 1 | 0 | 0.921060 | -2.037738 | 0.000000 |
| 10 | 1 | 0 | -0.778290 | -0.322390 | -1.794116 |
| 11 | 1 | 0 | 0.975401 | -0.234601 | -1.675298 |

E = -192.6632381 a.u. ZPVE = 60.77037 kcal/mol

3-Methylenecyclobutene (³M8)

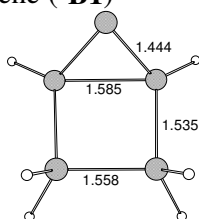
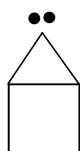


Standard orientation:

| Center Number | Atomic Number | Atomic Type | Coordinates (Angstroms) | | |
|------------------|------------------|----------------|-------------------------|-----------|-----------|
| | | | X | Y | Z |
| 1 | 6 | 0 | -0.501828 | 0.043264 | -0.009079 |
| 2 | 6 | 0 | 0.588898 | -1.031367 | 0.033634 |
| 3 | 6 | 0 | 1.582464 | 0.138992 | 0.058736 |
| 4 | 6 | 0 | 0.404369 | 1.074364 | 0.039589 |
| 5 | 6 | 0 | -1.917671 | -0.040399 | -0.041983 |
| 6 | 1 | 0 | 0.652597 | -1.674877 | -0.838555 |
| 7 | 1 | 0 | 0.588763 | -1.648828 | 0.925949 |
| 8 | 1 | 0 | 2.448374 | 0.213549 | -0.579121 |
| 9 | 1 | 0 | 0.311325 | 2.143580 | 0.055313 |
| 10 | 1 | 0 | -2.417477 | -0.989815 | -0.035373 |
| 11 | 1 | 0 | -2.520976 | 0.847268 | -0.013596 |

E = -192.7070638 a.u. ZPVE = 57.88477 kcal/mol

Bicyclo[2.1.0]pent-2-ene (³B1)

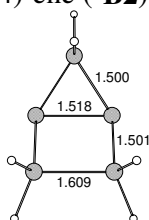
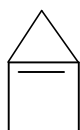


Standard orientation:

| Center Number | Atomic Number | Atomic Type | Coordinates (Angstroms) | | |
|------------------|------------------|----------------|-------------------------|-----------|-----------|
| | | | X | Y | Z |
| 1 | 6 | 0 | 1.241047 | -0.048003 | 0.476202 |
| 2 | 6 | 0 | 0.334077 | -0.701706 | -0.524185 |
| 3 | 6 | 0 | 0.308450 | 0.859433 | -0.252819 |
| 4 | 6 | 0 | -1.039521 | -0.802709 | 0.059207 |
| 5 | 6 | 0 | -1.092940 | 0.708833 | 0.247502 |
| 6 | 1 | 0 | 0.667444 | 1.665615 | -0.866547 |
| 7 | 1 | 0 | 2.272341 | 0.026408 | 0.173235 |
| 8 | 1 | 0 | 1.110967 | -0.234269 | 1.529864 |
| 9 | 1 | 0 | 0.715335 | -1.250365 | -1.367159 |
| 10 | 1 | 0 | -1.390276 | -1.566986 | 0.731769 |
| 11 | 1 | 0 | -1.882497 | 1.264516 | -0.236606 |

E = -192.6593239 a.u. ZPVE = 59.85002 kcal/mol

Bicyclo[2.1.0]pent-1(4)-ene (³B2)

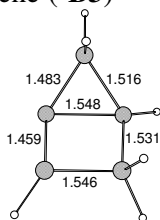


Standard orientation:

| Center Number | Atomic Number | Atomic Type | Coordinates (Angstroms) | | |
|------------------|------------------|----------------|-------------------------|-----------|-----------|
| | | | X | Y | Z |
| 1 | 6 | 0 | 0.873803 | 1.137352 | 0.000000 |
| 2 | 6 | 0 | -0.282252 | 0.581744 | 0.766585 |
| 3 | 6 | 0 | -0.282252 | 0.581744 | -0.766585 |
| 4 | 6 | 0 | -0.282252 | -0.929800 | 0.790476 |
| 5 | 6 | 0 | -0.282252 | -0.929800 | -0.790476 |
| 6 | 1 | 0 | 1.841302 | 0.654057 | 0.000000 |
| 7 | 1 | 0 | 0.918546 | 2.214902 | 0.000000 |
| 8 | 1 | 0 | -1.191193 | -1.361021 | 1.188281 |
| 9 | 1 | 0 | 0.576889 | -1.397177 | -1.260222 |
| 10 | 1 | 0 | 0.576889 | -1.397177 | 1.260222 |
| 11 | 1 | 0 | -1.191193 | -1.361021 | -1.188281 |

E = -192.643009 a.u. ZPVE = 61.47934 kcal/mol

Bicyclo[2.1.0]pent-1-ene (³B3)

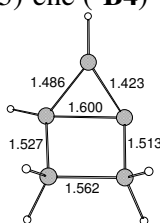
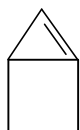


Standard orientation:

| Center Number | Atomic Number | Atomic Type | Coordinates (Angstroms) | | |
|------------------|------------------|----------------|-------------------------|-----------|-----------|
| | | | X | Y | Z |
| 1 | 6 | 0 | -1.340610 | -0.090523 | 0.384931 |
| 2 | 6 | 0 | -0.370246 | 0.725387 | -0.428581 |
| 3 | 6 | 0 | -0.363674 | -0.822747 | -0.453842 |
| 4 | 6 | 0 | 1.012932 | 0.688350 | 0.230064 |
| 5 | 6 | 0 | 1.002532 | -0.848474 | 0.125989 |
| 6 | 1 | 0 | -2.348508 | -0.085704 | 0.003806 |
| 7 | 1 | 0 | -1.277305 | -0.112244 | 1.462457 |
| 8 | 1 | 0 | 1.065919 | 1.105315 | 1.230760 |
| 9 | 1 | 0 | 1.791585 | 1.132954 | -0.379700 |
| 10 | 1 | 0 | 1.818853 | -1.396078 | -0.309870 |
| 11 | 1 | 0 | -0.696148 | 1.443798 | -1.158823 |

E = -192.6588803 a.u. ZPVE = 60.69180 kcal/mol

Bicyclo[2.1.0]pent-1(5)-ene (³B4)

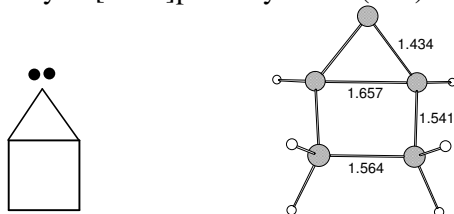


Standard orientation:

| Center Number | Atomic Number | Atomic Type | Coordinates (Angstroms) | | |
|------------------|------------------|----------------|-------------------------|-----------|-----------|
| | | | X | Y | Z |
| 1 | 6 | 0 | 1.412009 | -0.273209 | 0.369099 |
| 2 | 6 | 0 | 0.577433 | 0.705661 | -0.368047 |
| 3 | 6 | 0 | 0.345151 | -0.775395 | -0.560858 |
| 4 | 6 | 0 | -0.821377 | 0.816691 | 0.259482 |
| 5 | 6 | 0 | -1.051952 | -0.709942 | 0.034297 |
| 6 | 1 | 0 | 1.022671 | 1.447447 | -1.008205 |
| 7 | 1 | 0 | -1.496198 | 1.427101 | -0.327124 |
| 8 | 1 | 0 | -1.833056 | -0.901701 | -0.690443 |
| 9 | 1 | 0 | -0.843242 | 1.156511 | 1.289425 |
| 10 | 1 | 0 | -1.226871 | -1.322973 | 0.911546 |
| 11 | 1 | 0 | 1.609121 | -0.389223 | 1.420965 |

E = -192.642874 a.u. ZPVE = 60.67384 kcal/mol

Bicyclo[2.1.0]pent-5-ylidene (³B5)

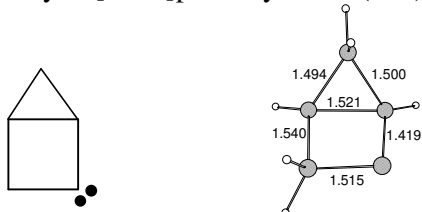


Standard orientation:

| Center Number | Atomic Number | Atomic Type | Coordinates (Angstroms) | | |
|------------------|------------------|----------------|-------------------------|-----------|-----------|
| | | | X | Y | Z |
| 1 | 6 | 0 | 0.947152 | -1.127844 | 0.000000 |
| 2 | 6 | 0 | -0.144147 | -0.612434 | 0.792465 |
| 3 | 6 | 0 | -0.144147 | -0.612434 | -0.792465 |
| 4 | 6 | 0 | -0.144147 | 0.922870 | 0.778806 |
| 5 | 6 | 0 | -0.144147 | 0.922870 | -0.778806 |
| 6 | 1 | 0 | -0.760759 | -1.215121 | 1.436638 |
| 7 | 1 | 0 | -0.760759 | -1.215121 | -1.436638 |
| 8 | 1 | 0 | 0.703758 | 1.392530 | 1.264035 |
| 9 | 1 | 0 | -1.054696 | 1.343505 | -1.188331 |
| 10 | 1 | 0 | -1.054696 | 1.343505 | 1.188331 |
| 11 | 1 | 0 | 0.703758 | 1.392530 | -1.264035 |

E = -192.635201 a.u. ZPVE = 61.77176 kcal/mol

Bicyclo[2.1.0]pent-2-ylidene (³B6)

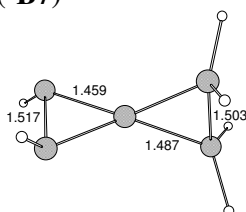
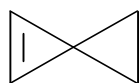


Standard orientation:

| Center Number | Atomic Number | Atomic Type | Coordinates (Angstroms) | | |
|------------------|------------------|----------------|-------------------------|-----------|-----------|
| | | | X | Y | Z |
| 1 | 6 | 0 | -0.555916 | 0.776318 | -0.322596 |
| 2 | 6 | 0 | -1.222120 | -0.309934 | 0.467993 |
| 3 | 6 | 0 | -0.128947 | -0.674885 | -0.482802 |
| 4 | 6 | 0 | 0.818982 | 1.020112 | 0.275405 |
| 5 | 6 | 0 | 1.269035 | -0.417316 | 0.109068 |
| 6 | 1 | 0 | -2.217510 | -0.572469 | 0.151412 |
| 7 | 1 | 0 | -1.064008 | -0.379068 | 1.531692 |
| 8 | 1 | 0 | -0.306701 | -1.305261 | -1.335495 |
| 9 | 1 | 0 | -1.083608 | 1.403009 | -1.016672 |
| 10 | 1 | 0 | 2.063843 | -0.539576 | -0.619569 |
| 11 | 1 | 0 | 1.521779 | -0.972409 | 1.006219 |

E = -192.6704398 a.u. ZPVE = 61.58768 kcal/mol

Spiro[2.2]pent-1-ene (³B7)

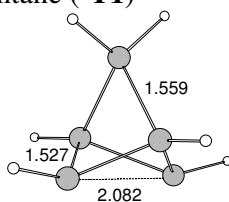
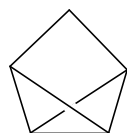


Standard orientation:

| Center Number | Atomic Number | Atomic Type | Coordinates (Angstroms) | | |
|------------------|------------------|----------------|-------------------------|-----------|-----------|
| | | | X | Y | Z |
| 1 | 6 | 0 | 0.000000 | 0.751270 | -1.185573 |
| 2 | 6 | 0 | 0.000000 | -0.751270 | -1.185573 |
| 3 | 6 | 0 | 0.000000 | 0.000000 | 0.097724 |
| 4 | 6 | 0 | 0.756530 | 0.055321 | 1.343689 |
| 5 | 6 | 0 | -0.756530 | -0.055321 | 1.343689 |
| 6 | 1 | 0 | -0.907636 | 1.257225 | -1.465091 |
| 7 | 1 | 0 | 0.905060 | 1.259399 | -1.468872 |
| 8 | 1 | 0 | 0.907636 | -1.257225 | -1.465091 |
| 9 | 1 | 0 | -0.905060 | -1.259399 | -1.468872 |
| 10 | 1 | 0 | 1.327467 | 0.897818 | 1.692091 |
| 11 | 1 | 0 | -1.327467 | -0.897818 | 1.692091 |

E = -192.6416015 a.u. ZPVE = 59.61478 kcal/mol

Tricyclo[2.1.0.0^{2,5}]pentane (³T1)

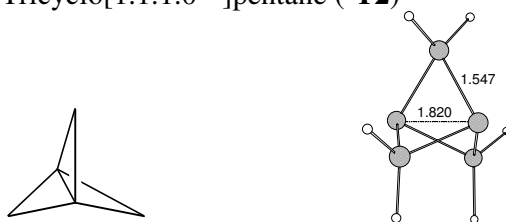


Standard orientation:

| Center Number | Atomic Number | Atomic Type | Coordinates (Angstroms) | | |
|------------------|------------------|----------------|-------------------------|-----------|-----------|
| | | | X | Y | Z |
| 1 | 6 | 0 | 0.000000 | 1.040889 | -0.681719 |
| 2 | 6 | 0 | 0.000000 | -1.040889 | -0.681719 |
| 3 | 6 | 0 | -0.950100 | 0.000000 | -0.093856 |
| 4 | 6 | 0 | 0.950100 | 0.000000 | -0.093856 |
| 5 | 6 | 0 | 0.000000 | 0.000000 | 1.141846 |
| 6 | 1 | 0 | 2.029740 | 0.000000 | -0.092945 |
| 7 | 1 | 0 | 0.000000 | -0.895428 | 1.754969 |
| 8 | 1 | 0 | 0.000000 | 0.895428 | 1.754969 |
| 9 | 1 | 0 | -2.029740 | 0.000000 | -0.092945 |
| 10 | 1 | 0 | 0.000000 | -2.092457 | -0.434114 |
| 11 | 1 | 0 | 0.000000 | 2.092457 | -0.434114 |

E = -192.620893 a.u. ZPVE = 61.16634 kcal/mol

Tricyclo[1.1.1.0^{1,3}]pentane (³T2)

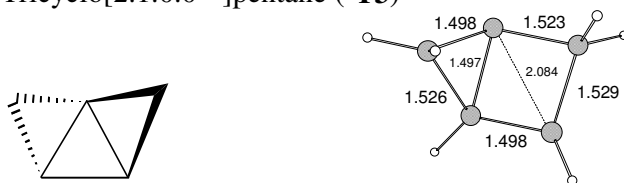


Standard orientation:

| Center Number | Atomic Number | Atomic Type | Coordinates (Angstroms) | | |
|------------------|------------------|----------------|-------------------------|-----------|-----------|
| | | | X | Y | Z |
| 1 | 6 | 0 | 0.000000 | 0.000000 | 0.909822 |
| 2 | 6 | 0 | 0.000000 | 1.250855 | 0.000000 |
| 3 | 6 | 0 | 0.000000 | 0.000000 | -0.909822 |
| 4 | 6 | 0 | -1.083272 | -0.625428 | 0.000000 |
| 5 | 6 | 0 | 1.083272 | -0.625428 | 0.000000 |
| 6 | 1 | 0 | 0.896397 | 1.857228 | 0.000000 |
| 7 | 1 | 0 | -0.896397 | 1.857228 | 0.000000 |
| 8 | 1 | 0 | -2.056606 | -0.152311 | 0.000000 |
| 9 | 1 | 0 | -1.160208 | -1.704917 | 0.000000 |
| 10 | 1 | 0 | 1.160208 | -1.704917 | 0.000000 |
| 11 | 1 | 0 | 2.056606 | -0.152311 | 0.000000 |

E = -192.5847598 a.u. ZPVE = 62.53761 kcal/mol

Tricyclo[2.1.0.0^{1,3}]pentane (³T3)



Standard orientation:

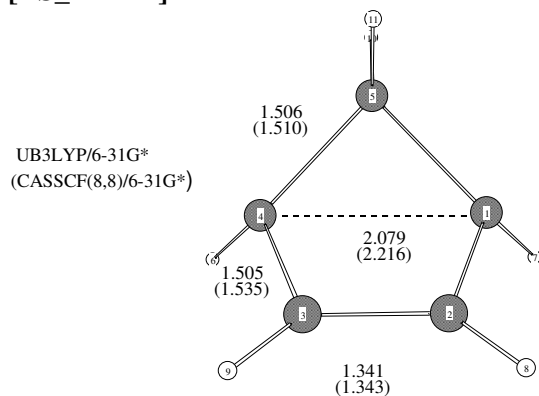
| Center Number | Atomic Number | Atomic Type | Coordinates (Angstroms) | | |
|------------------|------------------|----------------|-------------------------|-----------|-----------|
| | | | X | Y | Z |
| 1 | 6 | 0 | 1.305861 | -0.302968 | 0.410675 |
| 2 | 6 | 0 | 0.507538 | 0.737734 | -0.369548 |
| 3 | 6 | 0 | 0.234840 | -0.723429 | -0.549049 |
| 4 | 6 | 0 | -0.866210 | 0.874341 | 0.210906 |
| 5 | 6 | 0 | -1.176859 | -0.609763 | 0.011942 |
| 6 | 1 | 0 | 1.003673 | 1.447898 | -1.005923 |
| 7 | 1 | 0 | -1.183787 | 1.513164 | 1.018679 |
| 8 | 1 | 0 | -1.400347 | -1.210733 | 0.888295 |
| 9 | 1 | 0 | 1.181906 | -0.411930 | 1.477319 |
| 10 | 1 | 0 | 2.318403 | -0.425022 | 0.063732 |
| 11 | 1 | 0 | -1.950868 | -0.768864 | -0.731660 |

E = -192.659547 a.u. ZPVE = 60.56736 kcal/mol

APPENDIX C

CARTESIAN COORDINATES OF TS STRUCTURES

[TS_B1-M1]



Standard orientation:

| Center Number | Atomic Number | Atomic Type | Coordinates (Angstroms) | | |
|------------------|------------------|----------------|-------------------------|-----------|-----------|
| | | | X | Y | Z |
| 1 | 6 | 0 | 0.574404 | -1.176561 | 0.000000 |
| 2 | 6 | 0 | -0.176736 | -0.385780 | 1.038886 |
| 3 | 6 | 0 | -0.176736 | -0.385780 | -1.038886 |
| 4 | 6 | 0 | -0.122198 | 1.071931 | 0.670687 |
| 5 | 6 | 0 | -0.122198 | 1.071931 | -0.670687 |
| 6 | 1 | 0 | -1.080868 | -0.807048 | 1.479497 |
| 7 | 1 | 0 | -1.080868 | -0.807048 | -1.479497 |
| 8 | 1 | 0 | -0.073141 | 1.903353 | 1.367949 |
| 9 | 1 | 0 | -0.073140 | 1.903353 | -1.367949 |
| 10 | 1 | 0 | 0.353693 | -2.246232 | 0.000000 |
| 11 | 1 | 0 | 1.657845 | -1.004163 | 0.000000 |

$E^{\text{B3LYP/6-31G(d)}} = -193.983213526$ a.u. ZPVE = 55.3265 kcal/mol

One imaginary frequency: **653.1650i** cm^{-1}

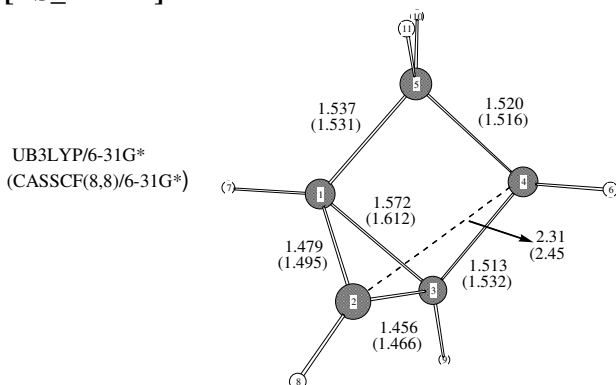
Standard orientation:

| Center Number | Atomic Number | Atomic Type | Coordinates (Angstroms) | | |
|------------------|------------------|----------------|-------------------------|-----------|-----------|
| | | | X | Y | Z |
| 1 | 6 | 0 | 1.292638 | 0.364113 | 0.000004 |
| 2 | 6 | 0 | 0.403750 | -0.147222 | -1.108184 |
| 3 | 6 | 0 | 0.403752 | -0.147220 | 1.108192 |
| 4 | 1 | 0 | 2.284430 | -0.068953 | 0.000002 |
| 5 | 1 | 0 | 1.371746 | 1.445598 | 0.000006 |
| 6 | 6 | 0 | -1.043191 | 0.119890 | -0.671582 |
| 7 | 6 | 0 | -1.043189 | 0.119923 | 0.671591 |
| 8 | 1 | 0 | 0.624143 | -1.102085 | -1.560798 |
| 9 | 1 | 0 | 0.624122 | -1.102109 | 1.560760 |
| 10 | 1 | 0 | -1.871506 | 0.262658 | -1.339449 |
| 11 | 1 | 0 | -1.871502 | 0.262706 | 1.339457 |

$E^{\text{CASSCF}(8,8)/6-31\text{G}(\text{d,p})} = -192.7762195688$ a.u. ZPVE = 58.66919 kcal/mol

One imaginary frequency: **609.4599i** cm^{-1}

[TS_T1-M1]



Standard orientation:

| Center Number | Atomic Number | Atomic Type | Coordinates (Angstroms) | | |
|------------------|------------------|----------------|-------------------------|-----------|-----------|
| | | | X | Y | Z |
| 1 | 6 | 0 | 1.185560 | -0.508169 | -0.097314 |
| 2 | 6 | 0 | -0.262737 | -0.860181 | 0.279341 |
| 3 | 6 | 0 | 0.775418 | 0.955882 | -0.084069 |
| 4 | 6 | 0 | -0.602311 | 0.662838 | 0.468641 |
| 5 | 6 | 0 | -1.195108 | -0.125176 | -0.603097 |
| 6 | 1 | 0 | -0.574220 | -1.688968 | 0.911643 |
| 7 | 1 | 0 | 1.051139 | 1.748193 | -0.777186 |
| 8 | 1 | 0 | -1.118354 | 1.167594 | 1.282134 |
| 9 | 1 | 0 | -2.229443 | -0.303235 | -0.869830 |
| 10 | 1 | 0 | 1.562859 | -0.937187 | -1.033343 |
| 11 | 1 | 0 | 1.903090 | -0.737567 | 0.705570 |

$E^{\text{B3LYP}/6-31\text{G}(\text{d})} = -193.931126202$ a.u. ZPVE = 55.02637 kcal/mol

One imaginary frequency: **322.8792i** cm^{-1}

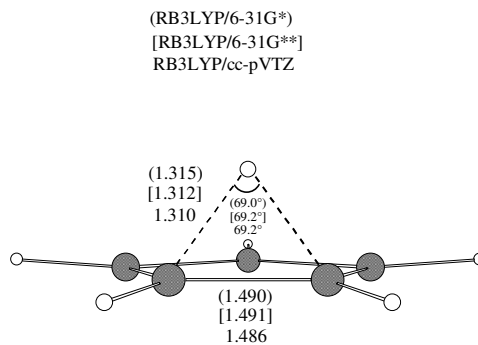
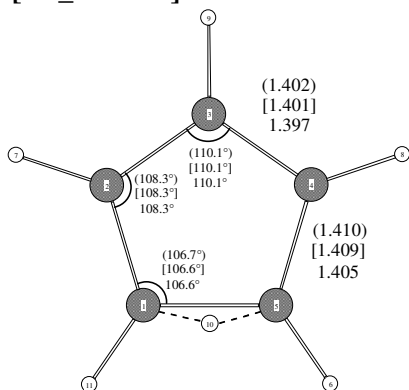
Standard orientation:

| Center Number | Atomic Number | Atomic Type | Coordinates (Angstroms) | | |
|------------------|------------------|----------------|-------------------------|-----------|-----------|
| | | | X | Y | Z |
| 1 | 6 | 0 | 1.179055 | -0.499602 | -0.095825 |
| 2 | 6 | 0 | -0.261540 | -0.863231 | 0.274360 |
| 3 | 6 | 0 | 0.836889 | 0.973574 | 0.002053 |
| 4 | 6 | 0 | -0.626096 | 0.703955 | 0.369959 |
| 5 | 6 | 0 | -1.234852 | -0.178046 | -0.630132 |
| 6 | 1 | 0 | -0.546242 | -1.664229 | 0.932897 |
| 7 | 1 | 0 | 1.209932 | 1.787907 | -0.594405 |
| 8 | 1 | 0 | -1.192497 | 1.237325 | 1.113298 |
| 9 | 1 | 0 | -2.281853 | -0.417462 | -0.645199 |
| 10 | 1 | 0 | 1.520739 | -0.868315 | -1.057979 |
| 11 | 1 | 0 | 1.895293 | -0.802792 | 0.662126 |

$E^{\text{CASSCF}(8,8)/6-31\text{G}(\text{d,p})} = -192.7065965215$ a.u. ZPVE = 58.8479 kcal/mol

One imaginary frequency: **397.4616i** cm^{-1}

[TS_M1-M1]



Standard orientation:

| Center Number | Atomic Number | Atomic Type | Coordinates (Angstroms) | | |
|------------------|------------------|----------------|-------------------------|-----------|-----------|
| | | | X | Y | Z |
| 1 | 6 | 0 | -0.025289 | -0.937951 | 0.745084 |
| 2 | 6 | 0 | -0.025289 | -0.937951 | -0.745084 |
| 3 | 6 | 0 | -0.025289 | 0.412557 | 1.149127 |
| 4 | 6 | 0 | -0.025289 | 0.412557 | -1.149127 |
| 5 | 6 | 0 | -0.028121 | 1.215175 | 0.000000 |
| 6 | 1 | 0 | -0.162157 | -1.823466 | -1.353892 |
| 7 | 1 | 0 | 0.019054 | 0.756940 | 2.174747 |
| 8 | 1 | 0 | 0.019054 | 0.756940 | -2.174747 |
| 9 | 1 | 0 | 0.024891 | 2.298920 | 0.000000 |
| 10 | 1 | 0 | 1.036971 | -1.152183 | 0.000000 |
| 11 | 1 | 0 | -0.162157 | -1.823466 | 1.353892 |

$E^{\text{B3LYP}/6-31\text{G}(\text{d})} = -194.0549665$ a.u. ZPVE = 56.23743 kcal/mol

One imaginary frequency: **1243.1555i** cm^{-1}

Standard orientation:

| Center Number | Atomic Number | Atomic Type | Coordinates (Angstroms) | | |
|------------------|------------------|----------------|-------------------------|-----------|-----------|
| | | | X | Y | Z |
| 1 | 6 | 0 | -0.025451 | -0.938175 | 0.745543 |
| 2 | 6 | 0 | -0.025451 | -0.938175 | -0.745543 |
| 3 | 6 | 0 | -0.025451 | 0.412341 | 1.148749 |
| 4 | 6 | 0 | -0.025451 | 0.412341 | -1.148749 |
| 5 | 6 | 0 | -0.028143 | 1.214918 | 0.000000 |
| 6 | 1 | 0 | -0.159306 | -1.823026 | -1.354465 |
| 7 | 1 | 0 | 0.019612 | 0.756440 | 2.173620 |
| 8 | 1 | 0 | 0.019612 | 0.756440 | -2.173620 |
| 9 | 1 | 0 | 0.025060 | 2.297824 | 0.000000 |
| 10 | 1 | 0 | 1.034000 | -1.144159 | 0.000000 |
| 11 | 1 | 0 | -0.159306 | -1.823026 | 1.354465 |

$E^{\text{B3LYP/6-31G(d,p)}} = -194.06636$ a.u. ZPVE = 56.13083 kcal/mol

One imaginary frequency: **1222.9235i** cm^{-1}

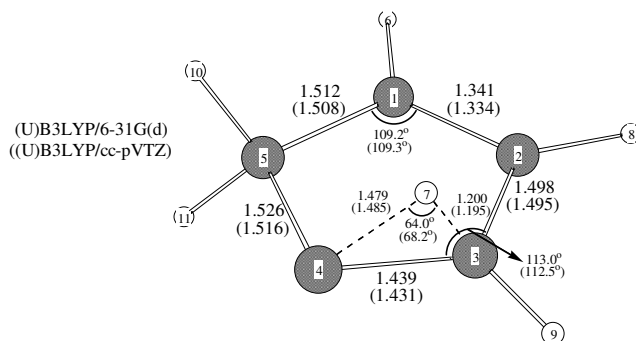
Standard orientation:

| Center Number | Atomic Number | Atomic Type | Coordinates (Angstroms) | | |
|------------------|------------------|----------------|-------------------------|-----------|-----------|
| | | | X | Y | Z |
| 1 | 6 | 0 | -0.024988 | -0.935354 | 0.743235 |
| 2 | 6 | 0 | -0.024988 | -0.935354 | -0.743235 |
| 3 | 6 | 0 | -0.024988 | 0.410835 | 1.144778 |
| 4 | 6 | 0 | -0.024988 | 0.410835 | -1.144778 |
| 5 | 6 | 0 | -0.028346 | 1.211149 | 0.000000 |
| 6 | 1 | 0 | -0.156617 | -1.816292 | -1.349990 |
| 7 | 1 | 0 | 0.014392 | 0.753836 | 2.165696 |
| 8 | 1 | 0 | 0.014392 | 0.753836 | -2.165696 |
| 9 | 1 | 0 | 0.020182 | 2.289849 | 0.000000 |
| 10 | 1 | 0 | 1.034048 | -1.137609 | 0.000000 |
| 11 | 1 | 0 | -0.156617 | -1.816292 | 1.349990 |

$E^{\text{B3LYP/cc-pVTZ}} = -194.1305755$ a.u. ZPVE = 55.84809 kcal/mol

One imaginary frequency: **1195.2597i** cm^{-1}

[TS_M4-M1]



Standard orientation:

| Center Number | Atomic Number | Atomic Type | Coordinates (Angstroms) | | |
|------------------|------------------|----------------|-------------------------|-----------|-----------|
| | | | X | Y | Z |
| 1 | 6 | 0 | -1.098030 | -0.539471 | 0.005934 |
| 2 | 6 | 0 | -0.765192 | 0.936015 | 0.008160 |
| 3 | 6 | 0 | 0.204146 | -1.330856 | -0.103268 |
| 4 | 6 | 0 | 0.567236 | 1.088781 | -0.013921 |
| 5 | 6 | 0 | 1.177113 | -0.278274 | -0.030266 |
| 6 | 1 | 0 | -1.500372 | 1.735328 | 0.023166 |
| 7 | 1 | 0 | 1.034106 | -0.885053 | 1.007993 |
| 8 | 1 | 0 | 1.122989 | 2.020763 | -0.010548 |
| 9 | 1 | 0 | 2.236601 | -0.441738 | -0.236001 |
| 10 | 1 | 0 | -1.715570 | -0.826718 | -0.861118 |
| 11 | 1 | 0 | -1.689390 | -0.859754 | 0.876679 |

$E^{\text{B3LYP/6-31G(d)}} = -193.9792102$ a.u. ZPVE = 54.95150 kcal/mol

One imaginary frequency: **719.4558i** cm^{-1}

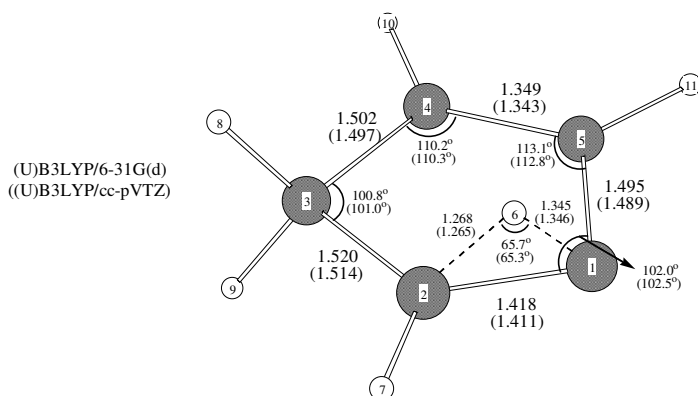
Standard orientation:

| Center Number | Atomic Number | Atomic Type | Coordinates (Angstroms) | | |
|------------------|------------------|----------------|-------------------------|-----------|-----------|
| | | | X | Y | Z |
| 1 | 6 | 0 | -1.105283 | -0.519206 | 0.006268 |
| 2 | 6 | 0 | -0.744965 | 0.944925 | 0.007904 |
| 3 | 6 | 0 | 0.174563 | -1.324014 | -0.101186 |
| 4 | 6 | 0 | 0.582771 | 1.072701 | -0.015369 |
| 5 | 6 | 0 | 1.172351 | -0.301014 | -0.028147 |
| 6 | 1 | 0 | -1.460709 | 1.754813 | 0.025198 |
| 7 | 1 | 0 | 1.041198 | -0.867962 | 1.015861 |
| 8 | 1 | 0 | 1.148943 | 1.992548 | -0.015051 |
| 9 | 1 | 0 | 2.217485 | -0.487837 | -0.255092 |
| 10 | 1 | 0 | -1.721983 | -0.799766 | -0.857595 |
| 11 | 1 | 0 | -1.701552 | -0.832140 | 0.869860 |

$E^{\text{B3LYP/cc-pVTZ}} = -194.054427$ a.u. ZPVE = 54.54862 kcal/mol

One imaginary frequency: **636.6856i** cm^{-1}

[TS_M5-M1]



| Standard orientation: | | | | | |
|-----------------------|------------------|----------------|-------------------------|-----------|-----------|
| Center Number | Atomic Number | Atomic Type | Coordinates (Angstroms) | | |
| | | | X | Y | Z |
| 1 | 6 | 0 | -0.523255 | 1.095985 | -0.003667 |
| 2 | 6 | 0 | -1.146072 | -0.291159 | -0.025075 |
| 3 | 6 | 0 | 0.939073 | 0.748467 | 0.007307 |
| 4 | 6 | 0 | -0.194015 | -1.335548 | -0.114224 |
| 5 | 6 | 0 | 1.098560 | -0.591121 | 0.001184 |
| 6 | 1 | 0 | -2.214893 | -0.440930 | -0.178281 |
| 7 | 1 | 0 | 1.725466 | 1.497928 | 0.038780 |
| 8 | 1 | 0 | -0.963316 | -1.085905 | 0.956010 |
| 9 | 1 | 0 | 2.058128 | -1.099538 | 0.030535 |
| 10 | 1 | 0 | -0.827136 | 1.706594 | 0.858491 |
| 11 | 1 | 0 | -0.824001 | 1.662108 | -0.898682 |

$E^{\text{B3LYP/6-31G(d)}} = -193.979866$ a.u. ZPVE = 55.12820 kcal/mol

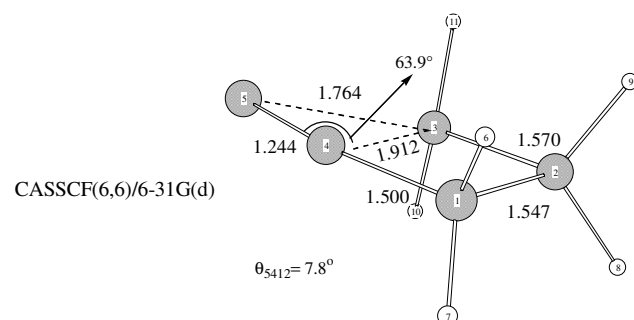
One imaginary frequency: **1148.7497i** cm^{-1}

| Standard orientation: | | | | | |
|-----------------------|------------------|----------------|-------------------------|-----------|-----------|
| Center Number | Atomic Number | Atomic Type | Coordinates (Angstroms) | | |
| | | | X | Y | Z |
| 1 | 6 | 0 | -0.530763 | 1.084373 | -0.003854 |
| 2 | 6 | 0 | -1.143042 | -0.300025 | -0.026595 |
| 3 | 6 | 0 | 0.928861 | 0.751663 | 0.006826 |
| 4 | 6 | 0 | -0.180401 | -1.327912 | -0.111789 |
| 5 | 6 | 0 | 1.102176 | -0.579730 | 0.001079 |
| 6 | 1 | 0 | -2.203650 | -0.464069 | -0.181772 |
| 7 | 1 | 0 | 1.705748 | 1.503783 | 0.039276 |
| 8 | 1 | 0 | -0.955030 | -1.071293 | 0.958190 |
| 9 | 1 | 0 | 2.060788 | -1.077962 | 0.027914 |
| 10 | 1 | 0 | -0.835688 | 1.689952 | 0.855282 |
| 11 | 1 | 0 | -0.833153 | 1.649372 | -0.892898 |

$E^{\text{B3LYP/cc-pVTZ}} = -194.0558183$ a.u. ZPVE = 54.73751 kcal/mol

One imaginary frequency: **1052.8158i** cm^{-1}

[TS_M7-M3]

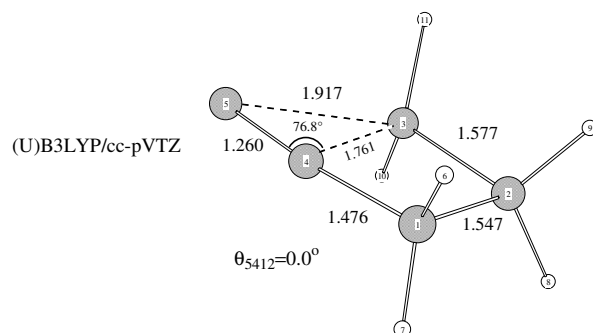


Standard orientation:

| Center Number | Atomic Number | Atomic Type | Coordinates (Angstroms) | | |
|------------------|------------------|----------------|-------------------------|-----------|-----------|
| | | | X | Y | Z |
| 1 | 6 | 0 | -0.900620 | 0.788919 | -0.055973 |
| 2 | 6 | 0 | -1.092673 | -0.743079 | 0.042110 |
| 3 | 6 | 0 | 0.658125 | 0.944171 | 0.053863 |
| 4 | 6 | 0 | 0.391351 | -0.947302 | -0.026597 |
| 5 | 6 | 0 | 1.573874 | -0.560127 | -0.038672 |
| 6 | 1 | 0 | -1.637716 | -1.181300 | -0.782200 |
| 7 | 1 | 0 | 1.073603 | 1.517792 | -0.757418 |
| 8 | 1 | 0 | -1.520150 | -1.078643 | 0.977816 |
| 9 | 1 | 0 | 0.969580 | 1.352826 | 1.000980 |
| 10 | 1 | 0 | -1.417381 | 1.334042 | 0.723561 |
| 11 | 1 | 0 | -1.248281 | 1.159790 | -1.011121 |

$E^{\text{CASSCF}(6,6)/6-31\text{G(d)}} = -192.7037266$ a.u. ZPVE = 60.62778 kcal/mol

One imaginary frequency: **205.8952i** cm^{-1}



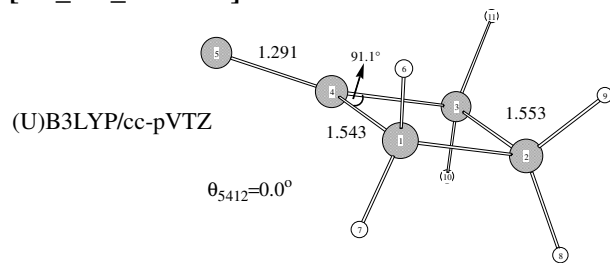
Standard orientation:

| Center Number | Atomic Number | Atomic Type | Coordinates (Angstroms) | | |
|------------------|------------------|----------------|-------------------------|-----------|-----------|
| | | | X | Y | Z |
| 1 | 6 | 0 | -1.279817 | 0.183691 | 0.000000 |
| 2 | 6 | 0 | -0.506489 | -1.155841 | 0.000000 |
| 3 | 6 | 0 | 0.953798 | -0.560768 | 0.000000 |
| 4 | 6 | 0 | 0.000000 | 0.919989 | 0.000000 |
| 5 | 6 | 0 | 1.187152 | 1.342442 | 0.000000 |
| 6 | 1 | 0 | -1.888567 | 0.360376 | 0.885362 |
| 7 | 1 | 0 | -1.888567 | 0.360376 | -0.885362 |
| 8 | 1 | 0 | -0.691820 | -1.760071 | -0.884037 |
| 9 | 1 | 0 | -0.691820 | -1.760071 | 0.884037 |
| 10 | 1 | 0 | 1.516455 | -0.788842 | -0.895015 |
| 11 | 1 | 0 | 1.516455 | -0.788842 | 0.895015 |

$E^{\text{B3LYP/cc-pVTZ}} = -194.0308248$ a.u. ZPVE = 56.46139 kcal/mol

One imaginary frequency: **175.5060i** cm^{-1}

[TS_inv_M7-M7']



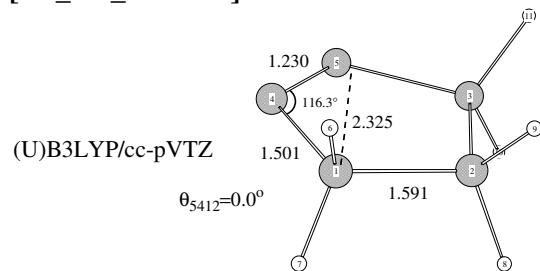
Standard orientation:

| Center Number | Atomic Number | Atomic Type | Coordinates (Angstroms) | | |
|---------------|---------------|-------------|-------------------------|-----------|-----------|
| | | | X | Y | Z |
| 1 | 6 | 0 | 0.000000 | 1.101075 | -0.300050 |
| 2 | 6 | 0 | 0.000000 | 0.000000 | -1.395248 |
| 3 | 6 | 0 | 0.000000 | -1.101075 | -0.300050 |
| 4 | 6 | 0 | 0.000000 | 0.000000 | 0.780834 |
| 5 | 6 | 0 | 0.000000 | 0.000000 | 2.071566 |
| 6 | 1 | 0 | -0.886694 | 1.730515 | -0.270465 |
| 7 | 1 | 0 | 0.886694 | 1.730515 | -0.270465 |
| 8 | 1 | 0 | 0.882839 | 0.000000 | -2.030225 |
| 9 | 1 | 0 | -0.882839 | 0.000000 | -2.030225 |
| 10 | 1 | 0 | 0.886694 | -1.730515 | -0.270465 |
| 11 | 1 | 0 | -0.886694 | -1.730515 | -0.270465 |

$$E^{\text{B3LYP/cc-pVTZ}} = -194.0352771 \text{ a.u. ZPVE} = 56.29630 \text{ kcal/mol}$$

One imaginary frequency: **74.8936i** cm⁻¹

[TS_inv_M3-M3']



Standard orientation:

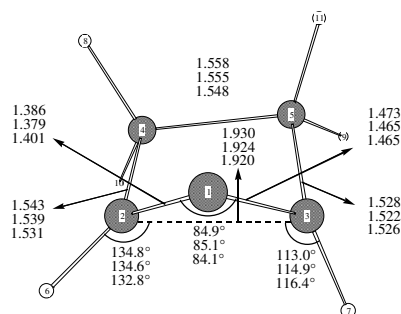
| Center Number | Atomic Number | Atomic Type | Coordinates (Angstroms) | | |
|------------------|------------------|----------------|-------------------------|-----------|-----------|
| | | | X | Y | Z |
| 1 | 6 | 0 | 0.000000 | 1.281305 | 0.185109 |
| 2 | 6 | 0 | 0.000000 | 0.000000 | 1.128364 |
| 3 | 6 | 0 | 0.000000 | -1.281305 | 0.185109 |
| 4 | 6 | 0 | 0.000000 | 0.615087 | -1.160488 |
| 5 | 6 | 0 | 0.000000 | -0.615087 | -1.160488 |
| 6 | 1 | 0 | 0.877715 | 1.907563 | 0.343585 |
| 7 | 1 | 0 | -0.877715 | 1.907563 | 0.343585 |
| 8 | 1 | 0 | -0.874113 | 0.000000 | 1.780009 |
| 9 | 1 | 0 | 0.874113 | 0.000000 | 1.780009 |
| 10 | 1 | 0 | -0.877715 | -1.907563 | 0.343585 |
| 11 | 1 | 0 | 0.877715 | -1.907563 | 0.343585 |

$$E^{\text{B3LYP/cc-pVTZ}} = -194.0371539 \text{ a.u. ZPVE} = 56.79227 \text{ kcal/mol}$$

One imaginary frequency: **94.4373i** cm⁻¹

³[TS_B5-M2]

UB3LYP/6-31G(d)
UB3LYP/cc-pVTZ
CASSCF(4,4)/6-31G(d)



Standard orientation:

| Center Number | Atomic Number | Atomic Type | Coordinates (Angstroms) | | |
|------------------|------------------|----------------|-------------------------|-----------|-----------|
| | | | X | Y | Z |
| 1 | 6 | 0 | 1.317438 | -0.225135 | -0.520099 |
| 2 | 6 | 0 | 0.738625 | 0.844624 | 0.143567 |
| 3 | 6 | 0 | 0.381381 | -1.048093 | 0.264727 |
| 4 | 6 | 0 | -0.796169 | 0.900418 | -0.010265 |
| 5 | 6 | 0 | -1.036310 | -0.635079 | -0.126613 |
| 6 | 1 | 0 | 1.258286 | 1.574018 | 0.775271 |
| 7 | 1 | 0 | 0.600870 | -1.461148 | 1.249055 |
| 8 | 1 | 0 | -1.137340 | 1.522732 | -0.849911 |
| 9 | 1 | 0 | -1.807159 | -1.000616 | 0.557248 |
| 10 | 1 | 0 | -1.251498 | 1.298054 | 0.904177 |
| 11 | 1 | 0 | -1.292949 | -0.953447 | -1.143748 |

$E^{\text{B3LYP/6-31G(d)}} = -193.907147$ a.u. ZPVE = 55.80822 kcal/mol

One imaginary frequency: **857.3381i** cm^{-1}

Standard orientation:

| Center Number | Atomic Number | Atomic Type | Coordinates (Angstroms) | | |
|------------------|------------------|----------------|-------------------------|-----------|-----------|
| | | | X | Y | Z |
| 1 | 6 | 0 | 1.307708 | -0.222364 | -0.519662 |
| 2 | 6 | 0 | 0.739049 | 0.841180 | 0.148782 |
| 3 | 6 | 0 | 0.378197 | -1.045718 | 0.258534 |
| 4 | 6 | 0 | -0.790517 | 0.901213 | -0.011372 |
| 5 | 6 | 0 | -1.035995 | -0.630726 | -0.121767 |
| 6 | 1 | 0 | 1.262817 | 1.558124 | 0.781763 |
| 7 | 1 | 0 | 0.611288 | -1.499455 | 1.214991 |
| 8 | 1 | 0 | -1.118201 | 1.515378 | -0.855168 |
| 9 | 1 | 0 | -1.796601 | -0.988045 | 0.569042 |
| 10 | 1 | 0 | -1.248676 | 1.304077 | 0.892963 |
| 11 | 1 | 0 | -1.301278 | -0.951596 | -1.130682 |

$E^{\text{B3LYP/cc-pVTZ}} = -193.9772773$ a.u. ZPVE = 55.30500 kcal/mol

One imaginary frequency: **847.7686i** cm^{-1}

| Standard orientation: | | | | | |
|-----------------------|------------------|----------------|-------------------------|-----------|-----------|
| Center Number | Atomic Number | Atomic Type | Coordinates (Angstroms) | | |
| | | | X | Y | Z |
| 1 | 6 | 0 | 1.323645 | -0.111984 | -0.533228 |
| 2 | 6 | 0 | 0.659680 | 0.887728 | 0.190060 |
| 3 | 6 | 0 | 0.465969 | -1.022179 | 0.229356 |
| 4 | 6 | 0 | -0.853445 | 0.846472 | -0.038707 |
| 5 | 6 | 0 | -0.989351 | -0.694531 | -0.093746 |
| 6 | 1 | 0 | 1.125888 | 1.590597 | 0.861764 |
| 7 | 1 | 0 | 0.773208 | -1.514795 | 1.132877 |
| 8 | 1 | 0 | -1.178638 | 1.388791 | -0.922124 |
| 9 | 1 | 0 | -1.678877 | -1.070442 | 0.651585 |
| 10 | 1 | 0 | -1.384471 | 1.252335 | 0.814520 |
| 11 | 1 | 0 | -1.296091 | -1.079523 | -1.061030 |

$E^{\text{CASSCF}(4,4)/6-31\text{G(d)}} = -192.642634$ a.u. ZPVE = 59.64744 kcal/mol

One imaginary frequency: **947.3744i** cm^{-1}

CURRICULUM VITAE

Surname : KINAL
Name : Armağan
Date of birth : January 1st, 1973

Education and Degrees Awarded

1986 – 1989 : Ankara 50. Yıl High School
1990 – 1992 : Preparatory School, METU
1992 – 1996 : METU Department of Chemistry, BS in Chemistry

1996 – 1998 : METU Department of Chemistry, M.S. in Chemistry

M.S. Thesis :

“Fragmentation of Small Lennard-Jones Clusters upon Surface Impact”

Supervisor : Prof. Dr. H. Önder PAMUK

Co-advisor : Prof. Dr. Ersin YURTSEVER

1998 – 2004 : METU Department of Chemistry, Ph. D. in Chemistry

Ph.D. Thesis :

“Theoretical Investigation of Unimolecular Reactions of Cyclic C₅H₆ Compounds by

Ab Initio Quantum Chemical Methods”

Supervisor : Prof. Dr. İlker ÖZKAN

Co-advisor : Prof. Dr. Metin BALCI

LIST OF PUBLICATIONS

1. Özkan İ., **Kinal A.**, Balcı M., “*Isomerizations of Bicyclo[2.1.0]pent-2-ene and Tricyclo[2.1.0.02,5]pentane into Cyclopenta-1,3-diene: A Computational Study by DFT and High-Level ab Initio Methods*”, J. Phys. Chem. A., 108 (2004) 507-514.
2. Ceylan M., **Kinal A.**, Sütbeyaz Y., Balcı M., “*Bromination of 1-Cyclopent-1-en-1-ylbenzene and 1-(5-Bromocyclopent-1-en-1-yl)benzene and Theoretical Investigation of the Products*”, Turk. J. Chem., 27 (2003) 287-294.
3. Saraçoğlu N., Menzek A., **Kinal A.**, Balcı M., “*Synthesis of new substituted dihydroheptalene derivatives: SiO₂- and base-catalyzed rearrangement of dimethyl trans-3,8-dihydroheptalene-3,8-dicarboxylate*”, Can. J. Chem., 79 (2001) 35-41.
4. Cheranovskii V. O., Ezerskaya E. V., Zhikol O. A., **Kinal A.**, Pamuk H. O., “*Effect of doping on the ground-state spin of stacked organometallic ferromagnets*” Proceedings of the Regional Conference on Magnetic and Superconducting Materials, 1st, Tehran, Islamic Republic of Iran, Sept. 27-30, 1999 (2000), Meeting Date 1999.
5. Cheranovskii V. O., Ezerskaya E. V., Zhikol O. A., **Kinal A.**, Pamuk H. O., “*Effect of doping on the ground-state spin of stacked organometallic ferromagnets*” Int. J. Quantum. Chem., 73 (1999) 511-517.